Predicting Forest Pests: Generalized models for invasive species establishment, spread, and impacts

Emma J. Hudgins
Biology Department, McGill University, Montreal

September, 2020
A thesis submitted to McGill University in partial fulfillment of the degree of Doctor of Philosophy in Biology

Table of contents

Dedication

To Mack, who keeps me grounded in my values, keeps his distance when that is what I need, and wraps me in a blanket burrito when that's more appropriate.

To my parents, from whom my values were learnt and without whom I would never have gotten the chance to let my curiosity grow to the point of filling these pages.

To my grandparents, who raised my parents to become the wonderful people they are, and whose legacy I hope to honour in all I do.

To my sisters, who have always modelled courage, strength, spontaneity, diligence, adventure, compassion and care.

To my community of family and friends near and far whose smiling faces watched me walk down the aisle, and whose same faces I imagine when I need to remember that I am part of something larger than myself.

To Rachel, for your unconditional love in spite of not believing in it.

..And to Piper, who knew only this kind of love.

Acknowledgements

This work began as a casual discussion between my supervisor, Brian Leung, and my collaborator Andrew Liebhold (Sandy), to build a model for US forest pest spread. Without Brian's persistent striving to create new and better quantitative tools to answer applied questions, and if not for collaborators like Sandy, this thesis would not exist.

I am so grateful for Brian seeing my potential as a 3rd year undergrad in his statistics course. His reaching out to me, and my passion for pursuing applied work that I saw as meaningful, meant that I was able to join his lab full of wonderful, engaged, outside-the-box thinkers. My early to mid-20s forced me to face a variety of challenges and was a time for several important milestones, and Brian's level of understanding and flexibility helped me work through this period of my life and develop all aspects of who I am while continuing to conduct research I was proud of.

I am grateful for the continued oversight of my Supervisory Committee, including Brian Leung, T. Jonathan Davies and Patrick M.A. James. While I may have dreaded some of their early grilling, their ability to force me to push the limits of my knowledge and focus on the big-picture implications of my work has allowed me to produce a far more meaningful end product.

I would like to thank the Leung lab members past and present, including Abbie Gail Jones, Adam Pietrobon, Andrew Sellers, Anthony Sardain, Camille Clement, Charlotte Steeves, Dat Nguyen, Johanna Bradie, Lidia Della Venezia, Natalie Richards, Sarah Chamberland-Fontaine, Shriram Varadarajan, and Victoria Reed. My labmates have always made me feel comfortable sharing my fears, troubles, and joys, and I will be so sad to leave.

Within the McGill Community, the McGill Stats-Bio Exchange was an important avenue for statistical help in the early stages of my project. The Quebec Centre for Biodiversity Science funded my travel to several conferences, and Guillaume Larocque in particular helped me develop the quantitative skills necessary to complete this work.

I have been fortunate enough to work with many inspiring collaborators, including Forest Service employees Andrew M. Liebhold, Laura Blackburn, Frank H. Koch, and Mark J. Ambrose. The close connection to government science throughout this project helped ensure that I was developing tools that can actually be implemented in effective ways by end users.

I am grateful to NSERC for the chance to spend 3 months at the University of Queensland in Winter 2017, where I benefitted from the supervision of Dr. Eve McDonald-Madden. I met so many talented conservation scientists, all the while exploring all of the incredible nature Australia has to offer.

Finally, my loved ones have kept me balanced throughout a project that has the tendency to take over one's life. These include my husband, Mackenzie Doiron, my parents, Joan & Bernie Hudgins, my sweet dog Piper, my sisters and their families: Jill Hudgins & Adam Young, Lauren Hudgins, Ariel Eiberman Malachy Eiberman Hudgins and Hazel Libertad Eiberman Hudgins, my parents-in-law Joe & Michelle Doiron, grandparents-in-law, Roger & Brenda Miller, Judy and Mike Nimigon, Jim and Peggy Moar, and the rest of my extended family.

My community of friends in Montréal and abroad have never been more than a phone call away, including Rachel Nam, Danika Carleton, Angela Yu, Logan James, Dylan DiCicco, Pedro Braga, Gabrielle Généreux, Christina Tadiri, Anna Luz, Erin Wall, Andrew Matheson, Ariel Greiner, Mel Tamporello, Lindsay Potts, Sophie Koch, Prasanna Iyengar, Andrew Balcom, Sydney Lee, Rebecca Suggitt, Isha Berry, Serena McDonnell, Eve Finley, Jordan Kaga, and so many more. You all are such caring, kind souls, and I will never forget the love you continue to show me.

I have built a life I love here in Montréal, and though it is time to move on, I will never forget the parts of my day that kept me going in the hardest times, including the services of McGill Mental Health and the BACA clinic, the community at YMCA Du Parc, the sweet deals at Supermarché PA, and the much needed 24-hour service of Restaurant Arahova.

This work was supported by NSERC CGS-M and CGS-D fellowships.

Abstract

The primary goal of this thesis was to identify largescale generalities across species invasions. Arguably, due to the dominant role of humans, many of the drivers of invasive species establishment, spread, and associated damages should be common among species. However, whether generalized predictive models were possible or whether species must be modelled and fit separately to account for idiosyncrasies remained unanswered. In Chapter 1, I built a single, general model for the spread of all invasive forest pests in the United States that explained more than 75% of the variation in pest distributions. In Chapter 2, I contrasted this general model with more complex single-species models. I also generated semi-generalized models using the general model as a starting point and adding simple species-specific correction factors. I found that single-species models performed 17% better than the general model but underperformed compared to semi-generalized models that incorporated cross-species generalities. In Chapter 3, I tackled pest establishment and its relation to host diversity. Many current hypotheses (e.g., dilution and amplification effects) have been considered in isolation, have heterogeneous support, and can be strongly affected by a range of confounding factors. I developed a general model, which simultaneously integrated processes argued in the literature, to allow a more rigorous, systematic analysis of biodiversity effects on pest occurrence. I measured host diversity as phylogenetic dissimilarity from the focal host community of a particular pest, and modelled it simultaneously with pest spread patterns, host richness, and host density effects. I detected a nonlinear relationship, where positive density dependence emerged for closely related species (amplification), and negative density dependence (dilution) emerged for more distantly related species. In Chapter 4, I projected future damages to urban trees by synthesizing my pest invasion

forecasts with models of urban tree distributions and tree mortality. I projected future urban tree mortality of roughly 385M trees over 30 years (including 8% of all street trees). I provided updated estimates of the economic costs of this mortality, advancing the field by 1) leveraging newly created, more complete datasets, 2) providing increased spatiotemporal resolution, and 3) separating the costs across pest species causes, host tree genera, and urban tree categories: street, residential and community. Taken in sum, these models produce general predictions across invasion stages that can act as inputs to invasive species control programs, and I plan to use them in subsequent work to develop general heuristics for effective pest management.

Résumé

L’objectif principal de cette thèse était d’identifier la présence de tendances générales à grande échelle parmi les invasions biologiques d’espèces de ravageurs forestiers exotiques envahissants. J’ai émis l’hypothèse que plusieurs mécanismes responsables du progrès des ravageurs exotiques envahissants — marqué par leur établissement, leur propagation et leurs dommages associés — sont communs entre différentes espèces en raison des actions humaines. Cependant, il demeurait incertain si de tels modèles généraux étaient possibles ou si les mécanismes idiosyncrasiques de différentes espèces nécessitaient d’être caractérisés et modélisés séparément. Dans mon premier chapitre, j’ai construit un modèle général qui simule la propagation de toutes les espèces de ravageurs forestiers exotiques envahissants aux États-Unis. Ce modèle explique plus de 75 % de la variation présente dans la répartition spatiale des espèces modélisées. Dans mon deuxième chapitre, j’ai mis le modèle général en contraste avec des modèles plus complexes basés sur des espèces uniques. De plus, j’ai produit des modèles semi-généraux en modifiant le modèle général avec des corrections simples pour la modélisation de chaque espèce. Tandis que les modèles à espèce unique tiennent compte de 17 % de variation spatiale additionnelle en comparaison à la performance du modèle général, les modèles semi-généraux offrent une performance supérieure aux deux modèles précédents. Dans mon troisième chapitre, je me suis concentrée sur la relation entre l’établissement des ravageurs envahissantes exotiques et la diversité des espèces d’arbres hôtes. Plusieurs des hypothèses actuelles qui abordent cette relation (p. ex., les effets de la dilution et de l’amplification d’arbres hôtes) ont seulement été considérées en isolation, reçoivent un appui hétérogène de la part des experts, et peuvent être particulièrement affectées par plusieurs variables confusionnelles. J’ai développé un modèle général qui intègre simultanément les processus hypothétiques pour effectuer avec rigueur une évaluation systématique des effets

de la biodiversité sur l'établissement des espèces envahissantes. J'ai quantifié la diversité des arbres hôtes en obtenant une mesure de dissemblance phylogénétique à la communauté d'hôtes focaux de chaque ravageur. En modélisant l'effet de celle-ci simultanément à la propagation prédite des ravageurs ainsi qu'à la richesse et la densité des espèces d'hôtes, j'ai détecté une relation non linéaire, où l'effet de la densité d'arbres hôtes est positif entre hôtes apparentés (amplification), mais négatif entre espèces faiblement apparentées. Dans mon quatrième chapitre, j'ai intégré mes modèles de propagation avec des modèles de distribution et de mortalité d'arbres hôtes pour établir des projections des dommages qui sont anticipés à impacter les arbres en milieu urbain. J'ai prédit un taux de mortalité d'arbres urbains de ~385 millions dans les 30 prochains ans, y compris 8 % de tous les arbres de rue. J'ai fourni de meilleures estimations des coûts totaux associés à cette mortalité, avançant le domaine en : 1) utilisant des ensembles de données plus complets et récents, 2) améliorant la résolution spatiotemporelle de telles prévisions, 3) offrant des estimations de coûts séparant les diverses espèces de ravageurs impliquées, les genres d'arbres hôtes affectés, et les types d'arbres urbains vulnérables (arbres de rue, résidentiels ou communautaires). En résumé, mes modèles ont fourni des prédictions générales pour plusieurs phases des invasions biologiques; ces prédictions pourront être employées par divers programmes de gestion et de contrôle d'espèces envahissantes, et je propose d'en faire usage dans ma recherche subséquente pour développer des règles approximatives robustes qui permettront d'optimiser l'application de la gestion de ravageurs forestiers envahissants exotiques de façon efficace.

List of figures

Figure 1.1 Conceptual framework for model building (main loop) and simulation procedure (expanded yellow box). The model is built by a forward selection procedure, where starting with the intercept-only constant dispersal model, all possible j single term additions are simulated and fit. The best term j* is chosen to be added to the model if it improves the MET score by at least 5 km and the process is repeated, otherwise the model building procedure is halted and the current model is kept as the final model.

Figure 1.2 Predicted versus observed species range sizes for the analogous regression model (top, $R^2_{MSE} = 0.2733$ ($R^2_{MSE} = 0.2900$ for a regression of pest radius instead of area), constant dispersal model (middle, $R^2_{MSE} = 0.6870$) and full GDK model (bottom, $R^2_{MSE} = 0.7774$).

Figure 1.3 Distribution of MET scores across all species expected at random (left, mean = 288.96 km), and modelled for the constant dispersal (centre, mean = 115.74 km), and GDK (right, mean = 47.45 km) models.

Figure 1.4 A selection of model predictions for individual species (a. *Coleophora laricella*, b. *Leucoma salicis*, c. *Nuculaspis tsugae*), showing the true presence data (left column), constant dispersal model predictions (centre column) and GDK predictions (right column) as green areas. These distributions are only a small selection and do not show the full variation in model predictions across species, which are included in Fig. S1.1.7.

Figure 1.5 True observations of pest richness (top panel), predicted pest richness for the constant dispersal (top left) and GDK (bottom left) models, and the Euclidean distance or number of mismatched pest presences in the constant dispersal (top right), and GDK (bottom right) models. For the true observations and predicted richness maps, deeper green indicates higher richness.

For the mismatch maps, deeper green indicates a higher degree of mismatch (false presences + false absences).

Figure 2.1 Historical spread patterns of the three focal species: Gypsy moth (GM), hemlock woolly adelgid (HWA) and beech bark disease (BBD). Older invasions are shown in yellow while more contemporary invasions are shown in blue. Known host distribution is shown in beige.

Figure 2.2 A comparison of the predictive ability of customized (top row), uncorrected GDK (GDK, middle row) and SDK models for gypsy moth (GM, left column), hemlock woolly adelgid (HWA, middle column) and beech bark disease (BBD, right column). Host presence is indicated in beige, predicted distributions after a forecast (5-year) are shown in red, and observed distributions are shown in blue. Areas of overlap between predicted and observed distributions produce a darker red color due to the overlap of the red and blue colors.

Figure 2.3 Forecasted pest species richness from **a.** 2005 (fitting year of SDK) to **b.** 2030 generated by extending simulated spread patterns for each species from the best fitting SDK parameters.

Figure 2.4 Newly predicted local establishments (for existing United States invasive forest pests) between years 2005 and 2030, created by subtracting Fig. 2.3b from Fig. 2.3a. Areas of particular interest are labelled, and dominant mechanisms promoting new invasions are denoted with dashed vs. solid lines. **A**–Seattle, WA region **B**–Northern Idaho and Western Montana (includes Kootenai, Nez Perce-Clearwater, and Flathead National Forests), **C**–Northern Minnesota and Wisconsin (includes Kabetogama state forest), **D**–Chicago, IL region, **E**–Northern New England (Maine, New Hampshire, Vermont and Massachusetts) where blue represents the Boston, MA region, **F**–Pennsylvania and New Jersey, **G**–Chesapeake, VA region,

H–Huntington, WV region, **I**–Saint Louis, MO region, **J**–Monroe, LA region (includes Upper Ouachita National Wildlife Refuge), **K**–Carson and Gila National Forests, NM.

Figure 2.5 Projections of combined SDK uncertainty at 2030 (range of predicted pest richness at each site) arising from two climate change scenarios (rcp2.6 and rcp8.5 BIOCLIM scenarios), two alternative population growth scenarios (SSP3: "Regional Rivalry", SSP: "Fossil-fueled Development), and from a sensitivity analysis of model parameters (see Appendix S2.6).

Figure 3.1 Potential relationships between host tree relatedness (s) and the effect of host density on establishment probabilities ($V_{t,i}$ exponent), where blue indicates dilution and yellow indicates amplification across all plots. Hypothesized mechanisms (Table 3.1a): **a.** linear amplification for closely related species and linear dilution for distantly related species ($c_2>0$, $c_3=0$) **b.** nonlinear amplification for closely related species and nonlinear dilution for distantly related species, ($c_2>0$, $c_3>0$) **c.** nonlinear amplification for closely related species peaking at some maximum relatedness (green), and nonlinear dilution for distantly related species ($c_2>0$,$c_3<0$) **d.** nonlinear dilution for distantly related species, with a minimum at some minimum functional relatedness (purple), and nonlinear amplification for closely related species ($c_2<0$,$c_3>0$). Alternative mechanisms to yield previously published results (Table 3.1b): **e.** Host species richness mediated amplification ($a_2>0$) and dilution ($a_2<0$) (no effect of volume or phylogeny), **f.** Total host volume mediated amplification (no effect of phylogeny)**, g.** Focal host volume mediated amplification.

Figure 3.2 Fitted relationship between the relatedness (s) of trees of a given species *t* to each pest *i* and the effect of increased density of tree species *t* at site *j* ($V_{t,i}$ exponent) in the integrative establishment model. Tree volume contributes positively to establishment for closely related hosts (yellow), while it contributes negatively for distantly related hosts (blue), levelling-off and even slightly increasing for very unrelated hosts (purple), consistent with phylogenetically-based dilution.

Figure 3.3 Relationship between alternative model proxies (see Table 3.1b) and pest infestation levels, including: **a.** Pest species richness and total host species richness, **b.** Pest species richness and log(total host volume), **c.** Pest species richness and log(focal host volume), and **d.** Host species richness and log(focal host volume).

Figure 3.4 Spatial pattern of model residuals, for the spread (**a**) and integrative establishment (**b**) models. Clear opposing patterns are present, indicating a likely benefit with their synthesis. The integrative joint model residuals are shown in (**c**), indicating some persistent spatial patterning, particularly in terms of East-West regionality.

Figure 4.1 Schematic representation of the four subcomponent models we combined to produce refined damage estimates to street trees from invasive US forest pests. Methodology is represented within braces, where GAM= Generalized Additive Model, and BRT= Boosted Regression Tree. The spread model predictions correspond to SDK forecasts from Hudgins et al (2019).

Figure 4.2 Fit of the genus-specific host tree models across all genera and size classes.

Figure 4.3 Model outputs for the first three subcomponent models, including **a.** predicted street tree numbers, **b.** predicted new pest invasions, **c.** predicted street tree exposure levels (number of focal host tree + pest species interactions) from 2020 to 2050, and finally **d.** Predicted total tree mortality from 2020 to 2050 in the best guess mortality debt scenario across space. Top ten most impacted cities are shown in terms of total tree mortality 2020 to 2050 (A =Minneapolis/St. Paul/Bloomington, MN; B=Milwaukee, WI; C=New York City, NY; D=Indianapolis, IN; E=Columbus, OH; F=Chicago/Aurora, IL; G=Seattle, WA).

List of tables

Table 3.1 Hypothesized relationships between predictor variables and probability of establishment when modelled simultaneously (**a**), and alternative model comparisons (**b**).

Table 3.2 Integrative establishment model results. Significance is examined via Type III Likelihood Ratio Tests (comparing the full model to a reduced model without a given parameter). The overall model log-likelihood was 123809.60, while the null (a_1 only) model likelihood was 132000.23, and overall deviance explained was 6.21%. The last column presents the proportional change in deviance explained for the reduced model.

Table 4.1 Predicted annualized cost (in 2019 USD) and tree mortality across invasion scenarios from 2020 to 2050 across all 57 species. "Best Guess" indicates the scenario with expert-elicited mortality debt durations by guild, "Vary" scenarios hold all guilds but the focal guild constant at their best guess scenario, and "All" fix all three guilds at a given mortality debt duration. Mean mortality for best guess = 7.8%, 59M trees, 146M USD annualized (3.3B over the next 30 years).

Table 4.2 Visual representation of the sources of uncertainty and their relative quantification across impact types, where redder hues indicate greater uncertainty. Sources of uncertainty include 1) future climatic variability, 2) spread model uncertainty, 3) host distributional model uncertainty, 4) asymptotic mortality misestimation, 5) mortality debt model misspecification, 6) variability in management behaviour.

Preface

Thesis format and style

This thesis is presented in a manuscript-based format, and consists of four papers. Each chapter focuses on developing general frameworks to forecast invasions, spanning from the establishment and spread phases of invasions in terms of ecological prediction, to frameworks that use ecological predictions to forecast ecological and economic impacts of invasions. The first chapter has been corrected since its original publication with a peer-reviewed corrigendum, which is included as an appendix.

Chapter 1. Hudgins, E. J., Liebhold, A. M., & Leung, B. (2017). Predicting the spread of all invasive forest pests in the United States. *Ecology letters*, 20(4), 426-435.

Chapter 2. Hudgins, E. J., Liebhold, A. M., & Leung, B. (2020). Comparing generalized and customized spread models for nonnative forest pests. *Ecological Applications*, 30(1), e01988.

Chapter 3. Hudgins, E.J., Davies, T.J. & Leung, B. A unifying phylogenetic model of amplification and dilution effects of host biodiversity on pest establishment. *in prep*.

Chapter 4. Hudgins, E. J., Koch, F. H., Ambrose, M. J., & Leung, B. Estimating damage to urban trees from invasive forest pests in the United States. *in prep.*

Contributions of co-authors

This thesis is composed of my original work, and I am the primary author for all chapters. My work has been conducted in close cooperation with my supervisor, Prof. Brian Leung. Additionally, all chapters have benefitted from the contributions additional co-authors, who are specified below.

Chapter 1. Emma J. Hudgins and Brian Leung designed the modelling framework and analyses. Emma J. Hudgins wrote the R scripts and performed all analyses. Andrew M. Liebhold obtained the data and contributed to interpretation of results. Emma J. Hudgins wrote the framework of the manuscript, but received detailed feedback from Brian Leung and Andrew M. Liebhold.

Chapter 2. Emma J. Hudgins and Brian Leung conceived of the ideas and designed the methodology. Emma J. Hudgins performed the analyses. Emma J. Hudgins led the writing of the manuscript, with advice and editing from Brian Leung. Andrew M. Liebhold provided pest expertise and edited the manuscript.

Chapter 3. Emma J. Hudgins and Brian Leung designed the modelling and theoretical validation frameworks. Emma J. Hudgins conducted all analyses, built the phylogenetic tree, and wrote the manuscript with consistent feedback and editing from Brian Leung. T. Jonathan Davies provided expertise on model structures, phylogenetic analyses, first-principles predictions, and edited the manuscript.

Chapter 4. Emma J. Hudgins and Brian Leung conceived of the economic and ecological models. Emma J. Hudgins performed all analyses and wrote the manuscript with advice and editing from Brian Leung. Frank H. Koch provided urban tree and management expertise and edited the manuscript. Mark Ambrose provided access to the urban tree inventory, provided urban tree and management expertise, and edited the manuscript.

Original contributions to knowledge

I have been examining generalities that emerge at large scales across species invasions from the ecological to the applied. These analyses have provided support for the theory that humans are allowing for invasive species distributions, and thus their associated damages, to become broadly predictable across contexts. It is of fundamental interest in ecology to determine whether general rules govern invasions sufficiently to make predictions across species using common models and frameworks. Such general rules also have considerable applied value in allowing potential new pest threats to be predicted and management to be planned before they have even established in a region. The frameworks produced throughout this thesis have immediate value to forest managers, as they can be used to motivate and direct the effective allocation of government funding for invasive species surveillance and management by delineating areas of high future risk and predict potential economic losses if preventative measures are not taken.

In Chapter 1, I developed a general model for the spread of all invasive forest pests presently found in the United States. This fit of this model was extremely strong, and contained very few predictor variables, indicating consistency in the spread process of a diversity of pests at large scales. This has been published in Ecology Letters, which is one of the most visible and prestigious ecology journals. Previous spread models had been built idiosyncratically, and it was not clear a general model could be used effectively to forecast invasion patterns. However, it appears that due to anthropogenically-induced generalities across species, the general pattern of invasive spread is consistent across the entire forest pest community. Since publication, the paper has been cited 29 times. This model can be applied in predictive contexts to identify areas of high future invasion risk. This work formed the foundation of the remainder of my PhD research. In addition to my own extensions, I have shared code with several researchers. I have been working with Prof. Matthew Helmus at Temple University on an extension to a new pest species (spotted lanternfly). Based on the results of the GDK, I first developed the idea of anthropogenic replacement, where natural ecological processes are essentially being overridden by anthropogenic ones, and predictable generalities that operate across entire suites of species arise as a consequence of this.

In Chapter 2, I compared the model built in Chapter 1 with single-species models to determine how much predictive power differs between generalized and customized models. Further, I examined whether an intermediate model, combining a general model with species-specific modifications, could yield predictive advantages. I fit models to three of the most damaging invasive forest pests (gypsy moth, beech bark disease, hemlock woolly adelgid). I found that using the GDK alone, I lost some power compared to customized approaches (57% vs. 74% variation explained). However, by using this generalized model as a backbone that could be modified with simple species-specific corrections (SDK), I attained a mean of 91% of the spatial variation explained. This is the first comparison of general and species-specific ecological spread models' predictive abilities. My results suggest that general models can be effectively synthesized with context-specific information to respond quickly to invasions. I used the models to create spread forecasts for all 63 United States pests in the dataset, which formed the basis of the pest impact models built in Chapter 4.

The plant pathogen literature has promoted of the so-called buffering role of host biodiversity against pests in line with dilution, but support is mixed. For instance, there is a latitudinal biodiversity gradient in pest richness that peaks in the tropics in the same way host biodiversity does, suggesting amplification rather than dilution. The existing literature possesses three main limitations that I believed made previously demonstrated relationships between host biodiversity and pest establishment equivocal and their associated inferences suspect: A sampling effect for host presence, a host density effect, and spurious correlations with pest spread. In Chapter 3, I analyzed the processes involved in establishment simultaneously, explicitly considering their relations to one another in an overarching model. I detected a novel, nonlinear relationship between phylogenetic host dissimilarity and pest establishment, where density-dependent amplification occurs for closely-related pest species, density-dependent dilution occurs for more distantly related pest species, and very distantly related species have negligible effects. These patterns occur in part due to the greater ease of generalist pests to establish, but appear to also be driven by climatic or other factors.

In order to make the most effective pest management decisions, policymakers and managers require information on the most likely spatiotemporal pattern of future pest damages. In Chapter 4, I created a framework to estimate urban tree damages across all United States invasive forest pests in roughly 30,000 US communities. Previous analyses suggest that urban trees are likely to be the dominant component of damages due to forest insect pests (Aukema et al. 2011). Moreover, the importance of urban forestry is only expected to grow. This analysis provided the most comprehensive estimate of pest damages to date, which was previously impossible: damages were predicted at the city level for each urban tree genus across three tree types (street, residential, community). Moreover, impacts were separated by pest species cause, in part due to the high resolution spatiotemporal spread predictions from Chapter 2. I showed that these pests will likely kill 5-12% of all street trees from 2020 to 2050, and could have total damages on the order of tens of billions of dollars. While these are rough estimates subject to many sources of uncertainty, they illustrate the gravity of pest infestations in urban areas. The creation of finescale spatiotemporal cost estimates also allows for the prioritization of future management efforts. This can allow for predictive impact modelling for future invaders, thereby allowing managers to be better prepared for future threats.

Throughout this thesis, I have demonstrated support for my anthropogenic replacement hypothesis, where humans are making systems easier to predict at large scales, and have used this to my advantage to create higher resolution forecasts of future pest establishment, spread, and associated damage for forest pests. Across chapters, I have used general models that borrow power across contexts to help overcome limited data, whether this was with the GDK and SDK, the integrative joint spread-establishment model, or the urban tree and host mortality components of my economic analysis. Along the way, I have uncovered a more nuanced role of host biodiversity on forest pest infestation and improved on existing estimates of countrywide damage due to these species. These frameworks will subsequently inform my future postdoctoral research, where I intend to shift to a prescriptive focus, and determine optimal strategies for forest pest management.

General Introduction

0.1 Introduction

The number of invasions by non-indigenous species is increasing worldwide due to growing trends in travel and trade (Drake & Lodge 2004). Species invasions consist of three stages: arrival at a site, establishment at that location, and subsequent spread (Elton 2000). The stages of species invasions, along with their associated impacts, can all be considered components of invasion risk (Leung et al. 2012), where the likelihood of each subsequent stage occurring depends on the probability of all previous stages occurring. Arguably, many of the drivers of these stages should be common among invading species. However, whether generalized predictive models are possible or whether species must be modelled and fit separately to account for idiosyncrasies remained unanswered (Leung et al. 2012). It is of fundamental interest in ecology to determine whether general rules govern invasions sufficiently to quantitatively make predictions across a suite of species using a common model. Invasions at a macroecological scale are particularly relevant, given that there are conflicting opinions as to whether generalities exist across invasions and there have been few largescale studies of potential generalities (Cadotte et al. 2006). Such general rules could also have considerable applied value, allowing invasions to be predicted a priori. Since each of the invasion stages is probabilistic, models of each stage and associated impacts can be combined into a risk assessment framework to predict expected risks and impacts. Current models are typically derived after a pest has already arrived and spread (e.g. Tisseuil et al. 2015; Walter et al. 2015), potentially lessening the efficacy of management, for instance when implementing containment, rapid response and/or eradication efforts of novel species (Lovett et al. 2016).

0.2 Invasions as a driver of global change

Species invasions are a stressor characteristic of the current geologic period, known as the Anthropocene, which gets its name for the role of humans in fundamentally altering biogeochemical processes on Earth (Crutzen 2006). Invasive species are species transported outside of the areas in which they evolved, and make up one dimension of a complex acceleration of interacting ecosystem stressors within the Anthropocene known as the Great Acceleration (Steffen et al. 2015). Increased stress due to growing human populations, rising CO_2 levels, more frequent major climatic events, and higher rates of species extinctions mirror the accelerating pattern of invasive species discovery within this era (Seebens et al. 2017). Since all of these anthropogenic stressors interact, we must try to consider them together when trying to forecast our future. While there are limits to the number of stressors that can feasibly be integrated, a key potential synergy exists between species invasions and patterns of current and future human population growth and movement, since humans are known to drive species invasions at large scales, and our population and its associated activities are growing rapidly (Seebens et al. 2013; Sardain et al. 2019). Notwithstanding potential future accelerations, invasive species are known to already cost hundreds of billions of dollars each year, with insects alone costing tens of billions annually (Bradshaw et al. 2016). This makes the need for effective policy to manage these species where they have invaded and limit future invasions dire.

0.3 Secondary Invasions

The majority of the largescale invasion literature examines the primary invasion process, where species make first contact with an area beyond which they have involved. I have been studying the secondary invasion process of invasive species, after they have successfully established in an area outside of their native range. This secondary invasion process mirrors the primary invasion process at a smaller scale, and can be broken into the same three components: first, arrival at a new site due to unintentional or intentional introduction, second, establishment in that new location defined as having a reproducing population there, and third, subsequent spread to new sites. Invaded sites can experience ecological and economic impacts due to pests at any point after their arrival (Parker et al. 1999). Secondary invasion stages and associated impacts can be similarly modelled probabilistically in order to forecast risk and expected impacts across species, space and time (Leung et al. 2012).

0.4 Secondary Spread

The secondary spread process has been extensively modelled using population ecology models that employ general growth and dispersal equations (Shigesada et al. 1995; Neubert & Parker 2004; Skarpaas & Shea 2007). Such models have been typically parameterized for individual species separately, and have not incorporated moderating variables for habitat invasibility, propagule pressure, and pest life history, which have been highlighted within the invasion biology literature (Leung et al. 2012). Incorporating these factors into a general model could uncover macroecological patterns in secondary spread that could allow it to be predicted a priori.

For instance, invasion biologists have theorized that certain habitat suitability characteristics may allow for greater pest incursion, or greater habitat invasibility (Simberloff 2009). Secondly, pest life history characteristics may be important in determining differential spread rates across species. In addition to these factors, proxies of propagule pressure, or the number of pest individuals introduced, have been associated with higher probabilities of invasion (Lockwood et al. 2005; Bradie et al. 2013). The first two factors are more biotic in their nature (e.g. pest body size, tree density), while propagule pressure proxies are more related to the degree of human activity (e.g. population density, road density).

0.5 Secondary Establishment

Invasive pest propagules may fail to establish, in spite of spreading successfully to new locations (Simberloff & Gibbons 2004). This is true both for the initial introduction through the primary invasion process, and for subsequent secondary spread to new sites within the invaded range. The factors that influence which invaders are among those most successful in this process, and which sites allow for successful expansion are thus important to understand. Rather than proceeding on a case-by-case-basis, the same arguments in support of uncovering generalities in spread equally apply to the secondary establishment phase. Namely, the production of a general establishment model allows for rapid response to both existing and novel invaders (Liebhold 2012; Lovett et al. 2016).

The factors governing pest establishment can be broadly grouped into pest traits, host traits, and site traits. After accounting for the spread process, which is predicted to be driven both by biotic factors and human activity, there may be additional pest biotic factors that improve their success across any site or host relative to other species. Further, there may be site qualities beyond host presence that influence the success of many pest species, such as climatic suitability. However, perhaps the most important factor governing pest success is the presence of an adequate recipient host community at a given site.

Host susceptibility has been shaped by evolutionary history, where evolutionarily naïve hosts are more susceptible than those with a history of co-evolution with a particular pest species (Desurmont et al. 2011). Evolutionarily naïve hosts most closely related to co-evolved hosts are likely those most susceptible, since these hosts are at the greatest risk of pathogen spillover (Gilbert & Webb 2007). Biodiversity, including the evolutionary diversity of host species, has been purported to be important in buffering against human and animal disease (Cardinale et al. 2012; Hooper et al. 2012; Young et al. 2017). In terms of host biodiversity, correlational studies consistently show lower single-pest invasion success in mixed forests compared to monocultures of a preferred host (Jactel & Brockerhoff 2007; Haas et al. 2011). However, there has been literature support for the opposing positive correlation between host diversity and pathogen success. Along these lines, global parasite load follows the latitudinal biodiversity gradient, with a peak in the tropics (Hechinger & Lafferty 2005).

0.6 Associated Impacts of Secondary Invasions

Invasive species produce impacts on a variety of important ecosystem goods and services, from killing or outcompeting species in recipient communities, impeding industrial or agricultural activities, negatively impacting human health, to increasing spending on control and eradication (Bradshaw et al. 2016). Managers must balance the costs of control and eradication with the damages avoided by taking action. Thus, the species, spatial, and temporal variability in invasive species impacts should be examined to prioritize future management (Essl et al. 2019). Invasive species secondary invasion impacts are determined both by secondary spread and establishment patterns, and their per-capita impacts on different ecosystem goods and services (Parker et al. 1999). The expected secondary invasion impacts of a given species can be extracted from a synthesis of probabilistic models accounting for each of these factors (Lovett et al. 2016). This can lead to very different patterns than risk assessments conducted for a single invasion stage, since per-capita impact need not be correlated to establishment or spread risk (Ricciardi & Cohen 2007).

0.7 Specific versus general invasion models

Identification of generalized models that explain and predict species distributions is of fundamental importance to ecologists, and there is a clear need for rapid responses to species invasions. However, to make effective decisions, we need an accurate picture of current and future invasions and associated damages. The challenge with making these predictions to new species or across entire invasion pathways is that within invasion ecology, the focus has been on species-specific models using context-specific information (e.g., Liebhold et al. 1992; Gilbert et al. 2004). Intuitively, models that are based on a particular invasive species' local context should provide better predictions than general models, and should facilitate management. While customized models have undeniably been useful, there have been calls for pathway level analyses, which account for multiple invasive species simultaneously (Lodge et al. 2006; Bradie & Leung 2015). To tackle this, my thesis chapters build off of one another to create a suite of generalized models of secondary invasions. Rather than producing forecasts for single case studies, the scaling up of individual species predictions using general models can produce whole-community predictions. These can be for establishment, spread, or impacts, and potentially even for the best management strategies to limit these impacts.

Although general invasion models are in the minority, the interest in multi-species predictions species invasions arises because of their potential advantages. In order to prepare for and limit invasive species impacts across space, which accrue immense costs (Vilà & Hulme 2017), managers need to know where these species will invade next. Further, the sooner they can take action, the more effective their control measures will be (Lovett et al. 2016). The lower the data requirements of a given model, the sooner it can be implemented to inform management. As such, a highly general model could be rapidly applied to many species, potentially including species that have not yet completed the primary invasion process.

0.8 Anthropogenic generalities

This thesis aims to leverage the role of humans in dominating invaded ecosystems to help make better predictions. I predicted that human influence means that at broad scales, invasions behave in less traditionally ‘ecological’ ways. In other words, heavily human-altered ecosystems are governed more by patterns of human behaviour than ‘intrinsic’ ecological rules of community assembly such as species interactions. By focusing on anthropogenic processes, a model’s management utility can be balanced with a search for general macroecological rules, that is, largescale principles that govern ecosystems in this new era of human dominance (Brown 1999).

For invasive species, one phenomenon that supports such cross-species generality is the dominant role of humans in transporting species via mechanisms that are analogous across entire suites of species invading different spatial locations (e.g., through ballast water transport, Seebens et al. 2013; firewood transport, Haack et al. 2006). This anthropogenic dominance can thus provide general macroecological predictions for the spread of groups of invasive species within a particular transport pathway. In the case of secondary invasions, anthropogenic mechanisms such as transport through road networks may mean that conventional ecological processes governing dispersal, which are more idiosyncratic across species (wind direction, flight ability etc., Aylor 1990; Taylor et al. 2010), are less important for forecasting spread at large scales. Further, species traits relating to association with anthropogenic dispersal vectors may be most important in determining their spread rates.

Pathway-level spread and establishment models facilitate the creation of pathway-level impact estimates. Since humans are known to transport individuals long distances within invaded ranges (Kelly et al. 2003; Haack et al. 2006), and human population density is predictive of invasive secondary spread patterns (Hudgins et al. 2017), humans are likely to be a major driver of future secondary invasion patterns across entire secondary invasion pathways, and therefore of future pathway-level impacts. These estimates demonstrate the severity of whole communities of invasive species, and therefore the extent to which it is important to limit future secondary invasions via these human transport pathways (e.g. through quarantines, highway checkpoints to limit firewood movement etc.).

0.9 Study system: United States invasive forest pests

This thesis expands the field of invasion macroecology through the study of United States (US) invasive forest pests. An invasive pest is a non-native species that has the ability to spread and cause damage to both the environment and human interests (CBD 2006), and forest pests specifically harm forest products. Many of these species exist within the US, and can be grouped into four feeding guilds based on the method with which they predominantly damage their host trees (Aukema et al. 2010). Foliage feeders include insects that feed on leaf or needle tissue. Sap feeders include all species that consume sap, including scale insects and gall-forming species. Phloem- and wood-borers feed on phloem, cambium, or xylem. Pathogens include species of fungi (e.g., chestnut blight, *Cryphonectria parasitica*) and disease complexes (e.g., beech scale, *Cryptococcus fagisuga*, and beech bark disease, *Neonectria faginata* and *N. ditissima*). This set of species comprises multiple kingdoms and spans a large portion of the evolutionary tree. While many pest invasions have been documented within this system, detailed data of invasion patterns exist for only a small subset of the invasive pest community – thereby motivating the search for general models to extrapolate across species.

US invasive forest pests have predominantly arrived via the live plant trade and untreated wood packaging materials (Lovett et al. 2016). Across the contiguous US, the load of pests is particularly high in the northeast and along the west coast, coinciding with areas of high human activity (Liebhold et al. 2013). While they have a range of natural dispersal mechanisms, uptake within the human transport network is possible for all of these species, indicating the potential for a single pathway-level model for invasion patterns via anthropogenically-induced generalities.

While the precise temporal patterns of invasions within this system are largely unknown, the biotic components of the recipient community are well characterized. Thanks to the Federal

Inventory and Analysis program (FIA), US forest volume data has been collected at the tree species level across the country. As such, host biodiversity patterns can be linked to pest spread projections to better understand their role in secondary establishment. While urban forest data is much more scarce, recent advances in synthesizing municipal inventories (Koch et al. 2019) have meant that for the first time, the impact of pest invasion patterns on urban host trees can begin to be understood.

In addition to its suitability as a system to model pathway-level secondary invasions, predicting impacts to US forests from invasive pests is fundamental to preventing the mortality and even extirpation of tree species and limiting associated ecological, economic, and ecosystem service impacts. United States forests deliver many fundamental ecosystem services to residents, including water and air purification, carbon sequestration, timber and fuel wood, wildlife habitat, and recreational space (Campbell & Brown 2012). While US forests are subject to many interacting stressors whose severity is accelerating, invasive forest pests are unique in the speed at which they have extirpated US tree species (Lovett et al. 2016).

Previous analyses suggest that urban trees are likely to be the dominant component of damages due to forest insect pests (Aukema et al. 2011). Urban tree communities tend to include highly susceptible species like ash (*Fraxinus spp.)* that have been decimated in recent years by pests such as emerald ash borer (*Agrilus planipennis,* Kovacs et al. 2010), and dead and dying urban trees pose an immediate threat to resident safety, and thus require management. Moreover, the importance of urban forestry is only expected to grow. Across the world, more people are moving to cities, and while urbanization is already very high in the US (82% in 2018), it has not yet saturated (World Bank, http://data.worldbank.org, UN DESA, http://population.un.org). At the same time, there has been a push for urban 'greening' (i.e., increasing urban forest canopy), both for environmental benefits, as well as to improve urban dwellers' wellbeing. Estimates of forest pest damage have been important in providing support for cutting-edge phytosanitary measures for primary invasive pest establishment such as ISPM15 (IPPC 2002), a wood packing material treatment protocol whose adoption is growing across nations worldwide (Leung et al. 2014). A similar protocol could be motivated by an analogous pathway-level damage estimate for secondary spread.

0.10 Thesis outline

The primary goal of this thesis was to identify largescale generalities across species invasions in this secondary invasion process, for use both in predicting the outcomes of the establishment and spread phases, as well as forecasting associated impacts. In Chapter 1, I built a single model for the spread of all invasive forest pests in the US. In Chapter 2, I contrasted this general model with more complex single-species models. Chapter 3, I built a general, integrative model for invasive forest pest establishment in order to examine its relationship with host biodiversity, and in Chapter 4, I created an updated estimate for the future impacts of invasive forest pests to urban forests. The more complex spread models from Chapter 2 were based on those from Chapter 1, and the spread models from Chapters 1 and 2 were used in the subsequent establishment and impact models to help fill in missing data and make higher resolution predictions.

Chapter 1.

Predicting the spread of all invasive forest pests in the United States

Authors: Emma J. Hudgins, Andrew M. Liehold, Brian Leung

A version of this chapter has been published in the journal Ecology Letters, 08 February 2017, Volume 20, Issue 4, 426-435, with a corrigendum published later in that same year (DOI: 10.1111/ele.12741, See Appendix S1). The two have been condensed into one cohesive thesis chapter with permission from John Wiley & Sons.

1.1 Abstract

We tested whether a general spread model could capture macroecological patterns across all damaging invasive forest pests in the United States. We showed that a common constant dispersal kernel model, simulated from the discovery date, explained 67.94% of the variation in range size across all pests, and had 67.49% accuracy between predicted and observed locational distributions. Further, by making dispersal a function of forested land area, tree density, and human population density, variation explained increased to 77.74%, with 73.85% locational accuracy. These results indicated that a single general dispersal kernel (GDK) model was sufficient to predict the majority of variation in extent and locational distribution across pest species and that proxies of propagule pressure and habitat invasibility – well studied predictors of establishment – should also be applied to the dispersal stage. This model provides a key element to forecast novel invaders and to extend pathway-level risk analyses to include spread.

1.2 Introduction

The number of invasions by non-indigenous forest pests is increasing worldwide due to growing travel and trade (Liebhold 2012). Pest invasions consist of three phases: arrival at a site, establishment at that location, and subsequent spread (Elton 2000). Predictive models of each process allow managers to take targeted actions, decreasing the number of pests completing each phase (Simberloff & Gibbons 2004).

Arguably, many of the drivers of invasion stages should be common among invading species. However, whether a generalized predictive model is possible or whether species must be modelled and fit separately to account for idiosyncrasies remains unanswered (Leung et al. 2012). To this effect, we focus on the third phase, and build a general predictive tool for invasive forest pest spread within the United States. This is of fundamental interest in ecology - to determine whether general rules govern dispersal sufficiently to quantitatively make predictions across a suite of species using a common model. Spread at a macroecological scale is particularly relevant, given that there are conflicting opinions as to whether generalities exist across invasions and there have been few largescale studies of potential generalities (Cadotte et al. 2006). Such general rules could also have considerable applied value, allowing spread to be predicted a priori. Current spread models are typically derived after a pest has already arrived and spread (e.g. Gilbert et al. 2004; Morin et al. 2009; Tisseuil et al. 2015, Walter et al. 2015), potentially lessening the efficacy of management, for instance when implementing containment, rapid response and/or eradication efforts of novel species (Lovett et al. 2016).

The spread process has been extensively modelled using population ecology models that employ general growth and dispersal equations (Shigesada et al. 1995; Neubert & Parker 2004; Skarpaas & Shea 2007). Such models have been typically parameterized for individual species separately, and do not incorporate moderating variables for habitat invasibility, propagule pressure, and pest life history, which have been highlighted within the invasion biology literature, would aid generalization (Leung et al. 2012), but have not been examined in an explicit spread model. For instance, invasion biologists have theorized that certain habitat suitability characteristics may allow for greater establishment success, or greater habitat invasibility (Simberloff 2009). Logically, habitat invasibility could be incorporated into a dispersal kernel model, where certain habitat characteristics accelerate dispersal into or out of cells. In addition to environmental factors, proxies of propagule pressure, or the number of pest individuals introduced, have been associated with higher probabilities of establishment (Lockwood et al. 2005; Bradie et al. 2013). Likewise, higher numbers of individuals dispersed should accelerate secondary spread. Variables such as human population density may moderate propagule pressure, as humans are often vectors for pest spread, especially over long distances (Haack et al. 2010). These factors could also be included in the dispersal kernel to repartition dispersal preferentially into or out of more frequently visited locations. Finally, life history characteristics may be important in determining differential spread rates across species. For instance, the body size of forest pests may be a predictor of their spread rates, as larger species may disperse farther.

Thus, an ideal generalized model of spread would predict invasions across a suite of species using a single model. It would do so both in terms of the extent of invasion as well as the spatial locations of pest occurrences, and would integrate various factors influencing pest invasions. However, the extent to which such a general model is predictive, and which (if any) factors have common influence across an array of pest species remains an open question.

In this study, we developed a Generalized Dispersal Kernel model (GDK) and tested two hypotheses: First, we hypothesized that the spread of biological invaders proceeds following similar processes across species, and so we predicted that a single general model of pest spread can fit well for all forest pests in the United States. Secondly, we hypothesized that pest life history, propagule pressure, and habitat invasibility can be meaningfully integrated into a dispersal kernel, and lead to improved predictions in a general model.

1.3 Material and Methods

1.3.1 Description of data

To build our model of pest spread, we used county-level species occurrence data, habitat suitability factors, and propagule pressure proxies from Liebhold et al. (2013), the Alien Forest Pest Explorer (Liebhold & Blackburn 2012, http://www.nrs.fs.fed.us/tools/afpe/maps), and 27 sources for pest characteristics (Appendix S1.2). Year of each pest species' first detection from Liebhold et al. (2013) was used as a proxy for year of establishment. Pest occurrence data consisted of 75 pest species distributions, comprising insects, mites and tree pathogens. For each species, we did not have time series data, and instead relied on a single snapshot of their distribution in 2008. We modelled each species as an independent unit and we did not consider interactions between species. We did consider additional predictors, consisting of propagule pressure proxies (human population density per decade (km^{-2}), per capita income in 1999 (USD), road length (km)), habitat invasibility proxies (host species richness, tree density (m^3km^{-2}), forested land (km^2), host tree density (m^3km^{-2})), and pest life history traits (taxa: arthropods versus tree pathogens, number of host species, Eurasian versus non-Eurasian native range, maximum body length (mm) (with a separate intercept fit for tree pathogens, as body length was not applicable)) (Table S1.2.1). All predictor variables included had a correlation $r < 0.7$ with other predictors (Appendix S1.4). Our discrete time dispersal model was fit in decadal increments to achieve computational feasibility and because our human population data were decadal (although we examined sensitivity by using 5-year increments, and found that model fit did not differ substantially, Appendix S1.5) Each species' time since detection was rounded down to the nearest decade, and so we limited our analysis to species that had been present in the United States for at least 10 years at the time of data collection ($N = 64$). Years of first detection spanned between 1790 and 1997 (1-21 time steps). None of the variables were fit separately to each species, in keeping with the desire for a single general model.

To avoid issues with spread dynamics across unequal county sizes, we first converted county-level presence/absence data to a 50 x 50 km lattice using distances measured with the United States Equidistant Conic Projection calculated using ArcMap10.2 (ESRI 2011). Environmental variables within each grid cell were calculated using the area-weighted average of the U.S. counties it encompassed. Further, all explanatory variables were centered and scaled to have a mean of zero and variance of one to ease the interpretation of each variable's contribution to dispersal.

This dispersal model was originally fit to 64 pest species. In refitting the model as part of a corrigendum (Appendix S1.1), we found that *Anoplophora glabripennis* (Asian longhorned beetle, ALB) became a strong outlier (Figure S1.1.1), but that the model was able to fit the other 63 species. We believe our model's inability to predict the distribution of ALB is because it has not actually successfully invaded forested areas (it is still under eradication in N. America), while its potential invasible range spans the entire US due to its breadth of suitable hosts. All detected ALB populations occur in rural or semi-rural areas, and most of them have already been successfully extirpated (Trotter & Hull-Sanders 2015).

1.3.2 Generalized Dispersal Kernel model (GDK)

Dispersal kernels estimate the probability of pest dispersal across space based on the distance between source and destination cells. In our model, we tested additional predictors of spread through modifying the dispersal parameter (discussed below). While we recognize that the predictors may influence processes other than dispersal, our focus was explicitly on the dispersal process in this study. We fit a negative exponential dispersal kernel model using discrete time simulations (Fig. 1.1), where at each (decadal) time step, pests dispersed to surrounding patches according to:

$$T_{i,j} = \frac{e^{-d_{i,j}.f(Z)}}{\sum_j e^{-d_{i,j}.f(Z)}} \tag{1.1}$$

$$d_{i,j} = \sqrt{(x_j - x_i)^2 + (y_j - y_i)^2} \tag{1.2}$$

where $T_{i,j}$ is the proportion of pests dispersing from cell i to cell j, normalized such that proportions sum to one across all cells j for a particular species, $d_{i,j}$ is distance, and f(Z) is a combination of species (Z_S) and cell (dispersal into a cell = Z_I, dispersal out of a cell = Z_O) specific predictors and parameter values influencing the dispersal probabilities. As a special case, we tested a constant dispersal model, where $f(Z)$ was a constant ($f(Z) = \alpha$). In our full generalized dispersal kernel model (GDK), $f(Z)$ was calculated using:

$$f(Z) = 2\alpha \frac{e^{Z_S+Z_I+Z_O}}{1+e^{Z_S+Z_I+Z_O}} \tag{1 3}$$

and the equation for Z_S, Z_I and Z_O followed the general formulation:

$$Z_V = \sum_{p=1}^{k} \beta_p X_p \qquad (1.4)$$

where β_p are parameters associated with variables X – either pest life history variables (S) or environmental variables at either destination cells (I) or source cells (O), thereby allowing these variables to influence dispersal both into and out of a cell.

Additionally, species were only able to invade grid cells where their host species was known to be present, as this was the most comprehensive information available, and logically should be important for pest distributions. For each species, we initiated spread in the central grid cell within each pest's known host distribution. This central point was chosen as a reasonable starting point, given 1) the uncertainty around the true origin for most pest species (Siegert et al. 2014), 2) where records of origin exist, they were sometimes found outside of the known host distribution (n = 21, possibly due to the presence of undocumented urban hosts), and hence there was no good way to incorporate these records, and 3) the lack of urban tree information within our host data. Thus, inferences from the model should be limited to spread throughout natural host distributions.

Next, we assumed that dispersal would increase with time since establishment in each source cell *i,* because propagules should increase as populations grow, up to some maximum number of individuals. Because we built the model using presence/absence data, we only modelled "relative propagule pressure". Specifically, the net influx of propagules and growth at each time step was formulated as an integrodifference equation (Kot et al. 1996), where the relative accumulation of propagules (PP) at cell *i* at timestep *t+1* was equal to the relative propagule pressure at time *t*, minus emigration, plus immigration, multiplied by the growth rate δ:

$$PP_{i,t+1} = (PP_{i,t} - \sum_{\boldsymbol{j}} T_{i,j} PP_{i,t} + \sum_{\boldsymbol{k}} T_{k,i} PP_{k,t})\delta \tag{1.5}$$

Our inclusion of dispersal and growth within a single time step is atypical of integrodifference models, but was needed given that our time steps are decadal.

Cells were considered "presences" capable of being a source of propagules above a threshold population size Φ, to prevent immediate dispersal across the entire landscape. Local extirpation was possible if sites dipped back below the threshold. Both δ and Φ were fitted constants. However, the maximum propagule pressure in a cell was set to 1, because the maximum value was arbitrary and relative to the value of Φ (i.e., maximum 1 with threshold = Φ has identical dynamics as maximum 100 with threshold =100*Φ). These equations allowed us to capture some of the important temporal characteristics associated with population growth, but we do not interpret them as demographic rates, as only presence/absence data were available.

1.3.3 Metrics of fit

We used the Minimum Energy Test (MET) as our metric of model fit between predicted versus observed distributions (Aslan & Zech 2005, Appendix S1.6). MET accounts for distances between predicted and true presences, which constitutes a higher information content than exact matches of presence/absence (i.e., mismatch of 50 km is better than 1000 km). Lower MET scores represent models with better goodness-of-fit.

We built our full dispersal model (GDK) using a forward selection procedure (Fig. 1.1). Starting from the intercept-only constant dispersal model, we determined the MET score for every possible two-term model built by adding the remaining 18 terms individually to the intercept-only model. The term producing the largest improvement was then added to the model, and forward selection repeated with higher-term models, until further additions of terms did not improve the MET score by 5 km. 5 km was chosen as an arbitrary threshold to retain biological relevance.

We report two metrics of model performance. First, we compared predicted and observed locational distributions, using MET. We also report locational accuracy, which is defined as the proportion of correctly assigned presences and absences across the number of possible presence sites. As a spatial null comparison model, we also used the observed number of infested cells, but simulated randomized occurrences within the host distribution for each species (random allocation model) and took the mean MET score of 1000 simulated pest distributions for each species. As our second metric, we compared predicted to observed range sizes, to evaluate the ability to predict the extent of invasions, using mean squared error, MSE, as a proportion of the variation in observed range sizes; R^2_{MSE} (discussed in Appendix S1.6).

As a statistical comparison model for the extent of spread, we regressed the area occupied by all pests against the time since they were first discovered in the United States (Liebhold et al. 2013). Though a regression of pest radius and time follows more logically from the invasion literature (Skellam 1951), we wanted to keep predictions comparable across models, and results were very similar between pest radius and pest area (within ~2% variation explained), and did not change our conclusions.

1.4 Results

We found that even our statistical comparison model – a simple regression model of pest range area as a function of time – had substantial predictive ability ($R^2_{MSE} = 0.2837$), suggesting promise for a common predictive model across pest species (Fig. 1.2). Next, we tested a simple dispersal kernel model with a constant dispersal parameter, without consideration of other predictive factors. We found that using a constant dispersal model improved the ability to predict pest range area by more than twofold compared to the simple regression model ($R^2_{MSE} = 0.6870$). The constant dispersal model also performed well comparing the locational predictions against observed infestations (mean MET score = 115.74 km, corresponding to 67.49% locational accuracy) more than halving the MET score expected by chance (298.52 km for random allocation null model). These results suggest that 1) there is considerable similarity in dynamics among pest species, 2) using a process-based dispersal kernel model that accounted for host distribution yielded substantial benefits compared to a purely statistical approach.

Next, we tested for common predictive factors, which could modify the dispersal parameter (GDK) (Table 1.1, Fig. 1.2). Our final model included the following 4 terms: Forested Land Area (increasing dispersal into sites), Tree Density (reducing dispersal out of sites), Human Population Density (both increasing dispersal into sites, and reducing dispersal out of sites,). The inclusion of these terms improved MET scores by 52.63 km (Fig. 1.3), and resulted in a model with 73.85% locational accuracy. Beyond these four, the addition of the other 15 parameters tested improved fit by less than 5 km in terms of MET (Table 1.1). Our model building results suggest that 1) there are general predictive factors of pest spread across species, which included both habitat invasibility variables (forested land, tree density) as well as proxies for propagule pressure (human population density), 2) the examined species traits other than host associations were not important for spread, and 3) relatively simple models explained more than 3/4 of the variation in extent of pest ranges, and roughly 3/4 of the geographical locations across pest species.

When we analyzed individual species' contributions to the aggregate MET scores, fewer species were predicted incorrectly by the GDK than the constant dispersal model (as shown by the reduced outliers, Fig. 1.3). These mismatches occurred for both predicted presences as well as absences (see Fig. 1.4 for examples of individual fit, Fig. 1.5 for aggregated predictions, and Appendix S1.7 for all individual species fits). We also found that MET was inversely related to the extent of spread (r = -0.3406, p = 0.0059).

1.5 Discussion

Currently, most predictions of invasive species spread use species-specific models (Muirhead et al. 2006; Carrasco et al. 2010, Gagnon et al. 2015). Here, we showed that a common dispersal kernel can capture much of the variation in pest extent across all known damaging forest pests in the United States. As such, it appears that generalities are possible. Further, our GDK model has ramifications for invasion biology as a predictive science, including forecasting the spread of new invaders, a demonstration of predictive improvements using semi-mechanistic models, and the incorporation of general predictors identified in the invasion literature (Leung et al. 2012). We discuss each in turn.

1.5.1 Generalities in ecology

Our results suggest that the rules governing the spread of pest species are sufficiently general to obtain strong quantitative macroecological predictions using a common model. As a line of future inquiry, a search for the underlying processes of these common spread patterns could yield fundamental insights into biological invasions and spread ecology. Parallels to such analyses have occurred across other fields of ecology, where predictive relationships have been discovered that transcend idiosyncratic species relationships and are discernable at large scales, such as those within the maximum entropy theory of ecology (Frank 2009) and the metabolic theory of ecology (West & Brown 2004). These relationships form so-called ‘efficient’ theories (Marquet et al. 2014).

It seems likely that over large scales, an efficient theory may exist for the dispersal of invasive species. The strong predictive power of the constant dispersal model was unexpected and interesting; it suggests that dispersal is largely occurring by one or more analogous spread mechanisms. We hypothesize that these analogous mechanisms are the various forms of human transport. It is well known that humans are important vectors of long-distance dispersal, but it appears that the various types of human transport (e.g., live plant trade, firewood movement) are occurring at roughly the same rate over large scales, allowing a constant dispersal parameter to capture the majority of variation in spread. In addition to this constant human transport, there also appears to be a small but important component of preferential pest dispersal to areas of high population density, given that our GDK model predicts discrete patches of spread surrounding metropolitan areas.

Traditionally, dispersal has been conceptualized as the result of natural processes based on life history traits and habitat suitability as it relates to individual species’ constraints. However, if analogous transport mechanisms and preferential pest dispersal to metropolitan areas occur, then human agency may be overshadowing traditional ecological mechanisms, such as natural flight capacity (Taylor et al. 2010), wind-driven dispersal (Aylor 1990), and community assembly mechanisms (e.g. Belyea & Lancaster 1999). More formally, we hypothesize that "anthropogenic replacement" is occurring, wherein certain natural processes are essentially being overridden by anthropogenic ones, and that predictable generalities that operate across entire suites of species arise as a consequence of these processes' broad effects. The lack of explanatory power of life history parameters and preferential dispersal into high human population density areas are arguably controversial findings, and further study is required to test the generality of such anthropogenic replacement. Additionally, we acknowledge that life history parameters are important for other stages of invasion (e.g., establishment, Forsyth et al. 2004; Bradie & Leung 2015), and could be important in different model formulations or components beyond dispersal distances. Nonetheless, these are important ideas, and replacement of natural processes may have ramifications beyond invasive species dispersal to other systems dominated by anthropogenic processes.

1.5.2 Forecasting spread of novel invaders

In concert with models that predict invader establishment in a country (e.g., Bradie & Leung 2015), our complementary analysis suggests that entry locations and host distributions will provide good predictors of pest spread, given that the GDK model explained 77.78% variation in pest range and had 73.85% locational accuracy, and that life history traits did not explain substantial variation in spread. The GDK results also indicate that future invasions to the United States will be characterized by preferential dispersal into areas of high human population density. Such forecasts allow for the refinement of pathway level analyses of invasion risk to include a spread component (e.g., the solid wood packaging materials pathway and introduction of wood borers, Haack 2006; Leung et al. 2014). Pests that have not been studied extensively can be included in these projections, given some knowledge of their host distributions, and information on establishment rates from the pathway in order to join this spread model to an establishment model (e.g., Aukema et al. 2010; Brockerhoff et al. 2014; Leung et al. 2014).

1.5.3 The importance of semi-mechanistic models

Several alternative models are available for predicting spread (Shigesada & Kawasaki 1997; Hastings *et al*. 2005), the simplest being a purely statistical approach, such as a general linear model of area as a function of time (Liebhold et al. 2013). We argue that the additional complexity of the semi-mechanistic dispersal kernel is well worth inclusion for making predictions. Comparing the simplest models in each, a constant dispersal kernel model essentially doubled the variation explained compared to a regression of pest area against time.

Further, our semi-mechanistic approach can easily incorporate spatial predictors of spread in predictive contexts, while it is less clear how general linear models can utilize spatial variables for prediction. One problem is that incorporating additional spatial variables requires the calculation of a single spatial value per pest in fitting (e.g. average human density across pest distribution). In a predictive context, where future distributions are unknown, these spatial predictors change as a pest spreads, which in turn affects their rate of spread, making these models impractical for prediction. Additionally, while regression models can relate time since discovery to the size of pest ranges, they do not predict spatial locations in their parameterizations of spread, thereby providing less information content than the GDK. Since these models have lesser utility, we did not test additional predictors of pest spread beyond time within a regression context.

Additionally, semi-mechanistic models have the potential to better account for issues of spatial autocorrelation and non-stationarity by replicating a spatially-autocorrelated dispersal process and allowing for differential dispersal across different environments. Many statistical modelling approaches are unable to account for spatial autocorrelation and in particular, non-stationarity, where the effect of spatial autocorrelation varies across space (Dormann et al. 2007). Failing to account for these phenomena when present can result in model misspecification and invalid inferences and subsequent predictions relating to spatial data (Miller 2012).

1.5.4 General predictive factors

Invader life history, habitat invasibility, and propagule pressure have been studied extensively in the invasion biology literature (Leung et al. 2012). We have shown here how these factors can be incorporated into an explicit dispersal model, and found that the predictors that were important and the magnitudes of effects were different than previous studies. In their review of the risk assessment literature, Leung et al. (2012) compiled over 200 models of the stages of species invasions used to predict risk. In contrast to our model, the majority of previously published models of the spatial distributions of invasive species have been largely formulated as models of pest establishment success (Inglis et al. 2006; Catford et al. 2011; Compton et al. 2012). Others have been formulated as gravity models (Gertzen et al. 2011; Potapov et al. 2011), while some studies have analyzed the total richness of pests across space (Stohlgren et al. 2006; Liebhold et al. 2013; Iannone et al. 2015).

Although related, these various modelled processes and their patterns are subtly different. We modelled the factors that promote rapid spread of invasive species in general, rather than the factors influencing the establishment success of individual pest species. Further, in contrast to models of pest presence or richness that attempt to determine differential establishment across space, our model allowed predictor variables to modify the probability of dispersal across space and time, thereby influencing the level of propagule pressure reaching each cell based on the level of propagule pressure at surrounding cells and the associated predictor variables.

Given the difference in underlying phenomena modelled, it may not be surprising that the predictors and their magnitudes also differed between our study and previous results. We found that pest life history parameters were not important in our model, though previous models have found factors such as fruit size (Pyšek et al. 2009) and wind dispersal (Gassó et al. 2009) to be predictive of invasive plant distributions. It is unknown whether differences in our findings reflect differences in system (plant versus pest) or differences in invasion stage (establishment success versus spread). Regardless, our model's lack of pest life history traits enforces the importance of spatial factors for spread in this system, although there may be other important life history factors that were not considered.

Across previous studies of establishment, richness, and gravity models, propagule pressure metrics tended to have higher explanatory power than habitat invasibility metrics (Leung & Mandrak 2007; Catford et al. 2011), and these additional factors explained the majority of the variation in pest presences (Inglis et al. 2006; Compton et al. 2012). Conversely, we have found that a constant dispersal kernel model already explained the majority of the variation in pest spread (> 67%), and therefore that the unique explanatory power of habitat and propagule pressure was moderate (9.04% variation explained, 6.36% increase in locational accuracy), with habitat invasibility explaining more of the variation in pest spread than propagule pressure proxies. However, we suggest that our constant dispersal model is not independent of habitat invasibility and propagule pressure processes, but actually incorporates the parts of these processes that are consistent across space and time. As such, the aspects of propagule pressure and habitat invasibility that have constant spatiotemporal influences on dispersal are contained within the intercept in our constant dispersal model. This spatiotemporal invariance may differ depending on the system (cf. Leung & Mandrak 2007; Gertzen et al. 2011; Compton et al. 2012 which examined discrete lakes). Nonetheless, based on the variation explained by the constant dispersal kernel model, it appears as though the majority of their influence is constant across space and time, facilitating future predictions given an initial establishment.

1.5.5 Caveats and future directions

Scale-dependence occurs when a model's driving factors vary with the grain (spatial and/or temporal) at which it is fit (Pauchard & Shea 2006; Fridley et al. 2007). Our results are at the country scale where, importantly, long-distance anthropogenic dispersal may dominate over natural pest dispersal, possibly explaining why life history traits were not predictive. Hence, while we were able to strongly predict spread across counties, and across the United States, predicting local spread within counties requires additional models, where life history traits could potentially dominate the dispersal signal.

Scale-dependence can also occur when a model's driving factors and fit vary with temporal roughness. The observed correlation between MET score and spread extent is potentially consistent with temporal scale-dependence, as shorter spread time would be more affected by discrete decadal time units. However, sensitivity analyses using 5-year units yielded virtually identical results (Appendix S1.5). As an alternative post-hoc explanation, MET was significantly lower (better) for species with introduction locations inside known host range ($t_{0.05(2),62} = 2.793$, $p = 0.0070$), suggesting that our lack of urban tree data is instead responsible for outliers.

The inability to predict pest presences outside of forested areas is a key shortcoming of our model. The positive influence of population density on pest spread further suggests that urban habitats have strong influences on pest dispersal. Clearly the collection of urban tree data at a large scale should be a priority. Additionally, our model structure assumed a single central introduction of each pest, though we know that several pests have had multiple independent introductions to the United States. Initiating spread from the host range centroid and limiting it to the natural host range likely worsens the estimation of early spread rates, as it adds a spatial mismatch in initial spread to the existing temporal mismatch from the date of establishment to that of first detection. Thus, the formulation of a detection model is an important future direction to understand this system more mechanistically and alleviate the latter source of mismatch. Regardless, the strong predictive power of the model indicates robustness to these details.

We used a general negative exponential dispersal kernel in our model, though other dispersal models exist (e.g., “fat-tailed” dispersal kernels Shigesada et al. 1995; Kot et al. 1996). However, several factors suggest that our model is sufficient to describe this system, including its strong predictive ability. Additionally, the breadth of durations of invasion within our dataset (1790-1997) suggests that we are able to capture both recent and longer-term invasion patterns. Finally, moderation of the dispersal kernel parameter provides an alternative formulation of long-distance dispersal. For instance, the inclusion of population density in our full dispersal model allows for urban centers to attract pests from distant locations. This is arguably a more process-driven formulation of long-distance dispersal than using fixed, alternative shapes for dispersal kernels, if we believe that humans are important vectors causing pest spread.

Our model was based on current and historical conditions. However, climate change could alter environmental suitability due to its influence on host tree species and on local abiotic conditions (Hellmann et al. 2008). Climatic variables such as temperature were not parameterized in our model. However, the most important factor for pest persistence is arguably the presence of viable hosts. In some cases, pests are instead limited by temperature, (e.g., hemlock woolly adelgid (*Adelges tsugae*), which has reached its climatic limit, despite the presence of hosts to the north, Paradis et al. 2008), and these cases could contribute to the remaining error in the model. Additionally, climate change may influence human distributions, which, given their inclusion in our model, should also be forecasted. Finally, forest management could also alter the future distribution of tree species (e.g., which species are planted or cut), which will alter invasible host distributions. Likewise, land use change could alter forested land and urbanization patterns, both of which would affect pest spread. In sum, forecasting into the future will require additional considerations and submodels, although the GDK can play a key role.

1.5.6 Conclusions

We have found that a single spread model for all invasive United States forest pests is predictive of both the extent and locational accuracy of pest distributions. This model provides a key element to forecast pest spread, thereby facilitating rapid responses to new pests. On a more fundamental level, the predictability across pest species suggests generality, and advances the possibility of a unified macroecological theory for invasive species spread by suggesting that common mechanisms underlie spread across species, beyond simple identification to the actual quantification of these mechanisms.

1.6 Acknowledgements

EH would like to thank L. Della Venezia, A. Sardain, V. Reed, A. Sellers, J. Bradie, K. Enciso, A. Pietrobon, D. Nguyen, T. J. Davies, P. M. A. James, and the members of the McGill Stats-Bio Exchange group for their helpful discussion, and L. Blackburn for help with acquiring data. This work was supported by an NSERC CGS-M fellowship awarded to EH and an NSERC Discovery grant to BL.

1.7 References

Aslan, B. & Zech, G. (2005). New test for the multivariate two-sample problem based on the concept of minimum energy. *Journal of Statistical Computation and Simulation,* 75(2), 109-119.

Aukema, J. E., McCullough, D. G., Von Holle, B., Liebhold, A. M., Britton, K., & Frankel, S. J. (2010). Historical accumulation of nonindigenous forest pests in the continental United States. *BioScience*, 60(11), 886-897.

Aylor, D. E. (1990). The role of intermittent wind in the dispersal of fungal pathogens. *Annu. Rev. Phytopathology, 28*(1), 73-92.

Belyea, L. R., & Lancaster, J. (1999). Assembly rules within a contingent ecology. *Oikos*, 86, 402-416.

Bradie, J., Chivers, C., & Leung, B. (2013). Importing risk: quantifying the propagule pressure–establishment relationship at the pathway level. *Diversity and Distributions*, 19(8), 1020-1030.

Bradie, J., & Leung, B. (2015). Pathway-level models to predict non-indigenous species establishment using propagule pressure, environmental tolerance and trait data. *Journal of Applied Ecology,* 52, 100-109.

Brockerhoff, E. G., Kimberley, M., Liebhold, A. M., Haack, R. A., & Cavey, J. F. (2014). Predicting how altering propagule pressure changes establishment rates of biological invaders across species pools. *Ecology*, 95(3), 594-601.

Cadotte, M. W., Murray, B. R., & Lovett-Doust, J. (2006). Ecological patterns and biological invasions: using regional species inventories in macroecology. *Biological Invasions*, 8(4), 809-821.

Carrasco, L. R., Mumford, J. D., MacLeod, A., Harwood, T., Grabenweger, G., Leach, … *et al*. (2010). Unveiling human-assisted dispersal mechanisms in invasive alien insects: integration of spatial stochastic simulation and phenology models. *Ecological Modelling*, 221(17), 2068-2075.

Catford, J.A., Vesk, P.A., White, M.D. & Wintle, B.A. (2011). Hotspots of plant invasion predicted by propagule pressure and ecosystem characteristics. *Diversity and Distributions,* 17, 1099-1110.

Compton, T.J., de Winton, M., Leathwick, J.R. & Wadhwa, S. (2012). Predicting spread of invasive macrophytes in New Zealand lakes using indirect measures of human accessibility. *Freshwater Biology,* 57, 938-948.

Dormann, C. F., M McPherson, J., Araújo, M.B., Bivand, R., Bolliger, J., Carl, G., … *et al*. (2007). Methods to account for spatial autocorrelation in the analysis of species distributional data: a review. *Ecography*, 30(5), 609-628.

Elton, C. S. (2000). *The ecology of invasions by animals and plants*, 2. University of Chicago Press, Chicago, United States.

ESRI (2011). *ArcGIS Desktop: Release 10*. Redlands, CA: Environmental Systems Research Institute.

Forsyth D.M., Duncan R.P., Bomford M., & Moore, G. (2004). Climatic suitability, life-history traits, introduction effort, and the establishment and spread of introduced mammals in Australia. *Conservation Biology*, 18, 557-569.

Frank, S. A. (2009). The common patterns of nature. *Journal of Evolutionary Biology,* 22(8), 1563-1585.

Fridley, J. D., Stachowicz, J. J., Naeem, S., Sax, D. F., Seabloom, E. W., Smith, M. D., … *et al*. (2007). The invasion paradox: reconciling pattern and process in species invasions. *Ecology*, 88(1), 3-17.

Gagnon, K., Peacock, S. J., Jin, Y., & Lewis, M. A. (2015). Modelling the spread of the invasive alga *Codium fragile* driven by long-distance dispersal of buoyant propagules. *Ecological Modelling*, 316, 111-121.

Gassó N., Sol, D., Pino, J., Dana, E.D., Lloret, F., Sanz-Elorza, M., … *et al*. (2009). Exploring species attributes and site characteristics to assess plant invasions in Spain. *Diversity and Distributions,* 15, 50-58.

Gertzen, E., Leung, B. & Yan, N. (2011). Propagule pressure, Allee effects and the probability of establishment of an invasive species (*Bythotrephes longimanus*). *Ecosphere*, 2, 1-17.

Gilbert, M., Grégoire, J. C., Freise, J. F., & Heitland, W. (2004). Long-distance dispersal and human population density allow the prediction of invasive patterns in the horse chestnut leafminer *Cameraria ohridella*. *Journal of Animal Ecology,* 73(3), 459-468.

Haack, R. A. (2006). Exotic bark-and wood-boring Coleoptera in the United States: recent establishments and interceptions. *Canadian Journal of Forest Research,* 36(2), 269-288.

Haack, R.A., Petrice, T.R. & Wiedenhoeft, A.C. (2010). Incidence of bark- and wood-boring insects in firewood: a survey at Michigan's Mackinac Bridge. *Journal of Economic Entomolology*, 103, 1682-1692.

Hellmann, J. J., Byers, J. E., Bierwagen, B. G., & Dukes, J. S. (2008). Five potential consequences of climate change for invasive species. *Conservation Biology*, 22(3), 534-543.

Hastings, A., Cuddington, K., Davies, K.F., Dugaw, C.J., Elmendorf, S., Freestone, A., … *et al.* (2005). The spatial spread of invasions: new developments in theory and evidence. *Ecology Letters,* 8, 91-101.

Iannone, B. V., Oswalt, C. M., Liebhold, A. M., Guo, Q., Potter, K. M., Nunez-Mir, G. C., … *et al.* (2015). Region-specific patterns and drivers of macroscale forest plant invasions. *Diversity and Distributions,* 21(10), 1181-1192.

Inglis, G.J., Hurren, H., Oldman, J. & Haskew, R. (2006). Using habitat suitability index and particle dispersion models for early detection of marine invaders. *Ecological Applications,* 16, 1377-1390.

Kot, M., Lewis, M.A., and Van Den Driessche, P. (1996). Dispersal data and the spread of invading organisms. *Ecology,* 77, 2027-2042.

Leung, B. & Mandrak, N.E. (2007). The risk of establishment of aquatic invasive species:

joining invasibility and propagule pressure. *Proceedings of the Royal Society of London. Series B: Biological Sciences,* 274, 2603-2609.

Leung, B., Roura-Pascual, N., Bacher, S., Heikkilä, J., Brotons, L., Burgman, M. A, … *et al*. (2012). TEASIng apart alien species risk assessments: a framework for best practices. *Ecology Letters, 15*(12), 1475-1493.

Leung, B., Springborn, M. R., Turner, J. A., & Brockerhoff, E. G. (2014). Pathway-level risk analysis: the net present value of an invasive species policy in the US. *Frontiers in Ecology and the Environment,* 12(5), 273-279.

Liebhold, A. M. (2012). Forest pest management in a changing world. *International Journal of Pest Management,* 58, 289-295.

Liebhold, A. M., McCullough, D.G., Blackburn, L. M., Frankel, S. J., Von Holle, B. & Aukema, J. E. (2013). A highly aggregated geographical distribution of forest pest invasions in the USA. *Diversity and Distributions,* 19, 1208-1216.

Lockwood, J. L., Cassey, P., & Blackburn, T. (2005). The role of propagule pressure in explaining species invasions. *Trends in Ecology and Evolution,* 20(5), 223-228.

Lovett, G. M., Weiss, M., Liebhold, A. M., Holmes, T. P., Leung, B., Lambert, K. F., … *et al*. (2016). Nonnative forest insects and pathogens in the United States: Impacts and policy options. *Ecological Applications,* 26, 1437-1455.

Marquet, P. A., Allen, A. P., Brown, J. H., Dunne, J. A., Enquist, B. J., Gillooly, J. F., … *et al*. (2014). On theory in ecology. *BioScience,* 64(8), 701-710.

Miller, J. A. (2012). Species distribution models: Spatial autocorrelation and non-stationarity. *Progress in Physical Geography,* 36(5), 681-692

Morin, R. S., Liebhold, A. M., & Gottschalk, K. W. (2009). Anisotropic spread of hemlock woolly adelgid in the eastern United States. *Biological Invasions,* 11(10), 2341-2350.

Muirhead, J. R., Leung, B., Overdijk, C., Kelly, D. W., Nandakumar, K., Marchant, K. R., … *et al*. (2006). Modelling local and long-distance dispersal of invasive emerald ash borer *Agrilus planipennis* (Coleoptera) in North America. *Diversity and Distributions,* 12(1), 71-79.

Neubert, M. G., & Parker, I. M. (2004). Projecting rates of spread for invasive species. *Risk Analysis*, 24(4), 817-831.

Paradis, A., Elkinton, J., Hayhoe, K. & Buonaccorsi, J. (2008). Role of winter temperature and climate change on the survival and future range expansion of the hemlock woolly adelgid *Adelges tsugae*) in eastern North America. *Mitigation and Adaptation Strategies for Global Change*, 13(5), 541-554.

Pauchard, A., & Shea, K. (2006). Integrating the study of non-native plant invasions across spatial scales. *Biological Invasions*, 8(3), 399-413.

Potapov, A., Muirhead, J., Yan, N., Lele, S. & Lewis, M. (2011). Models of lake invasibility by *Bythotrephes longimanus*, a non-indigenous zooplankton. *Biological Invasions,* 13, 2459-2476.

Pyšek P., Krivanek M. & Jarosik V. (2009). Planting intensity, residence time, and species traits determine invasion success of alien woody species. *Ecology,* 90, 2734-2744.

Shigesada, N. & Kawasaki, K. *Biological invasions: theory and practice.* Oxford University Press, UK, 1997.

Shigesada, N., Kawasaki, K. & Y. Takeda. (1995). Modeling stratified diffusion in biological invasions. *American Naturalist,* 146(2), 229-251.

Siegert, N. W., McCullough, D. G., Liebhold, A. M., & Telewski, F. W. (2014). Dendrochronological reconstruction of the epicentre and early spread of emerald ash borer in North America. *Diversity and Distributions,* 20(7), 847-858.

Simberloff, D. (2009). The role of propagule pressure in biological invasions. *Annual Review of Ecology, Evolution, and Systematics,* 40, 81-102.

Simberloff, D. & Gibbons, L. (2004). Now you see them, now you don't! – population crashes of established introduced species. *Biological Invasions,* 6(2), 161-172.

Skarpaas, O., & Shea, K. (2007). Dispersal patterns, dispersal mechanisms, and invasion wave speeds for invasive thistles. *American Naturalist,* 170(3), 421-430.

Skellam, J.G. (1951). Random dispersal in theoretical populations. *Biometrika,* 38, 196-218.

Stohlgren, T.J., Barnett, D., Flather, C., Fuller, P., Peterjohn, B., Kartesz, J. *et al.* (2006). Species richness and patterns of invasion in plants, birds, and fishes in the United States. *Biological Invasions,* 8(3), 427-447.

Taylor, R. A. J., Bauer, L. S., Poland, T. M., & Windell, K. N. (2010). Flight performance of *Agrilus planipennis* (Coleoptera: Buprestidae) on a flight mill and in free flight. *Journal of Insect Behaviour*, 23(2), 128-148.

Tisseuil, C., Gryspeirt, A., Lancelot, R., Pioz, M., Liebhold, A.M., & Gilbert, M. (2015). Evaluating methods to quantify spatial variation in the velocity of biological invasions. *Ecography,* 39, 409-418.

Trotter, R. T., & Hull-Sanders, H. M. (2015). Quantifying dispersal of the Asian longhorned beetle (*Anoplophora glabripennis*, Coleoptera) with incomplete data and behavioral knowledge. *Biological invasions*, 17(12), 3359-3369.

Walter, J. A., Johnson, D. M., Tobin, P. C., & Haynes, K. J. (2015). Population cycles produce periodic range boundary pulses. *Ecography*, 38(12), 1200-1211.

West, G. B., & Brown, J. H. (2004). Life's universal scaling laws. *Physics Today*, 57(9), 36-43.

1.8 Figures and Tables

1.8.1 Figures

Figure 1.1 Conceptual framework for model building (main loop) and simulation procedure (expanded yellow box). The model is built by a forward selection procedure, where starting with the intercept-only constant dispersal model, all possible j single term additions are simulated and fit. The best term j* is chosen to be added to the model if it improves the MET score by at least 5 km and the process is repeated, otherwise the model building procedure is halted and the current model is kept as the final model.

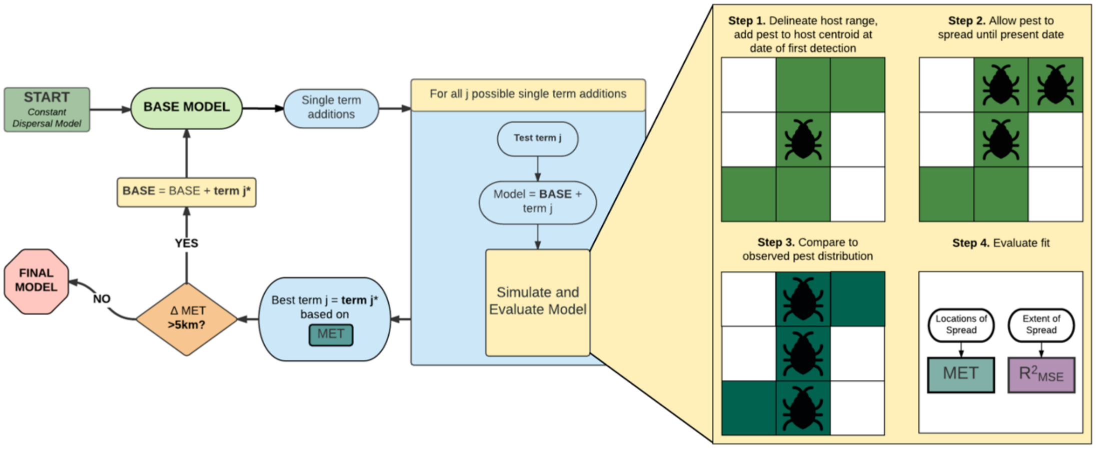

Figure 1.2 Predicted versus observed species range sizes for the analogous regression model (top, $R^2_{MSE} = 0.2733$ ($R^2_{MSE} = 0.2900$ for a regression of pest radius instead of area), constant dispersal model (middle, $R^2_{MSE} = 0.6870$) and full GDK model (bottom, $R^2_{MSE} = 0.7774$).

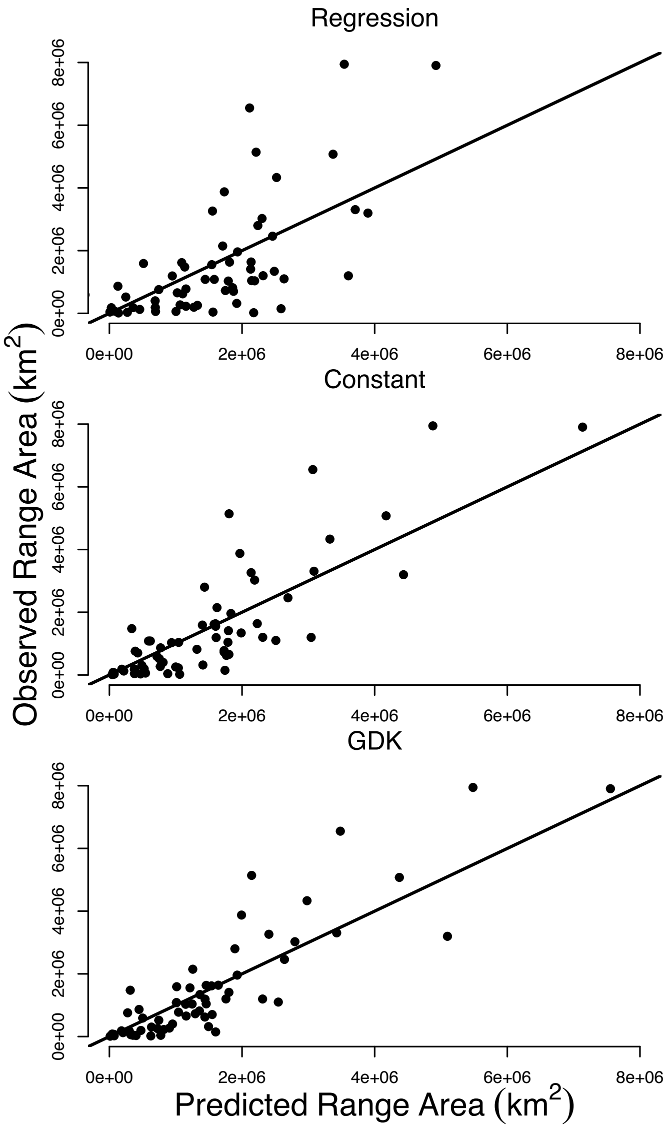

Figure 1.3 Distribution of MET scores across all species expected at random (left, mean = 288.96 km), and modelled for the constant dispersal (centre, mean = 115.74 km), and GDK (right, mean = 47.45 km) models.

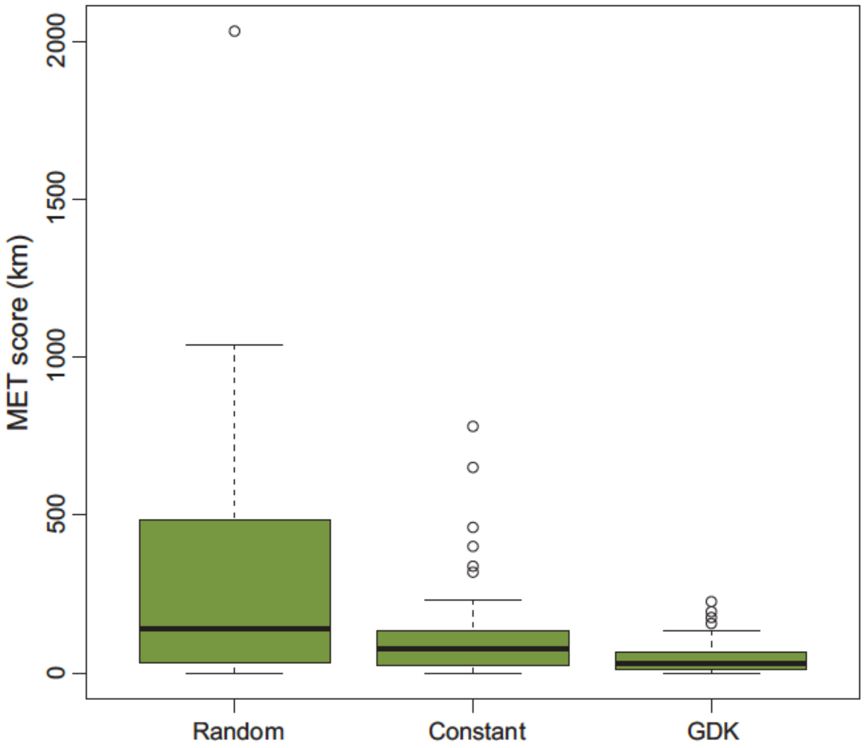

Figure 1.4 A selection of model predictions for individual species (a. *Coleophora laricella*, b. *Leucoma salicis*, c. *Nuculaspis tsugae*), showing the true presence data (left column), constant dispersal model predictions (centre column) and GDK predictions (right column) as green areas. These distributions are only a small selection and do not show the full variation in model predictions across species, which are included in Appendix S1.7.

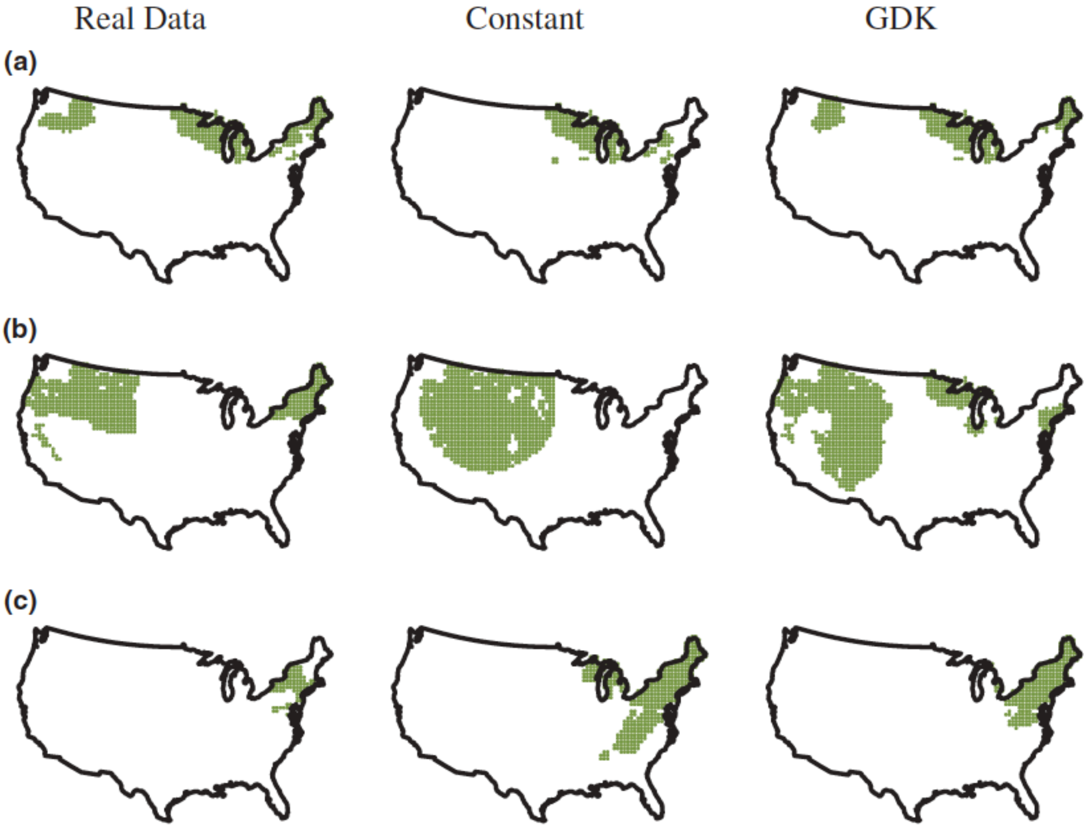

Figure 1.5 True observations of pest richness (top panel), predicted pest richness for the constant dispersal (top left) and GDK (bottom left) models, and the Euclidean distance or number of mismatched pest presences in the constant dispersal (top right), and GDK (bottom right) models. For the true observations and predicted richness maps, deeper green indicates higher richness. For the mismatch maps, deeper green indicates a higher degree of mismatch (false presences + false absences).

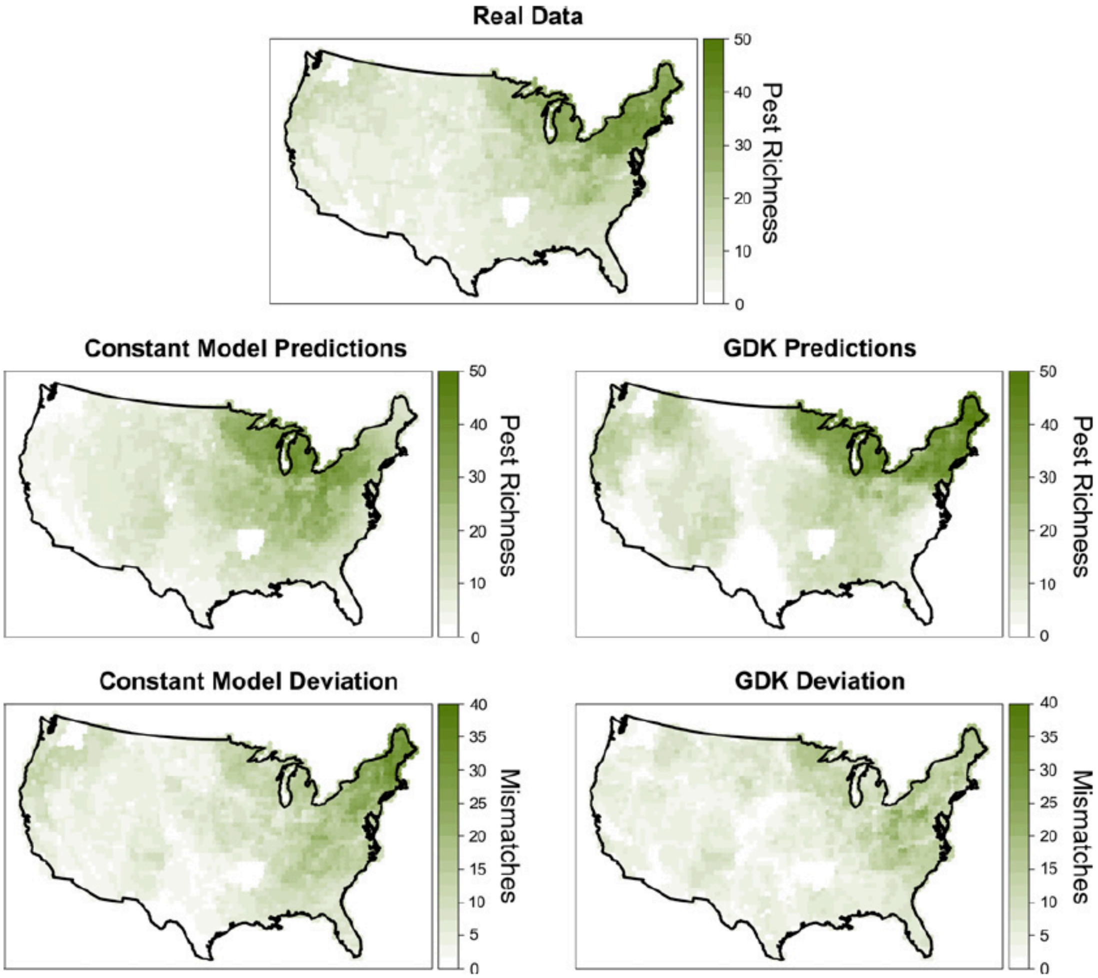

1.8.2 Tables

Table 1.1 Results of stepwise regression for the dispersal kernel model fit to United States data using habitat invasibility (HI), propagule pressure (PP), and pest life history (LH) factors.

Term	**Type**	**Description**	**Entry Order**	**Estimate (β_p)**	**MET score (km)**	**R^2_{MSE}**	**Δ MET score (km)**
Intercept	NA	NA	1	1.4751	115.74	0.6870	NA
Forested land (km^2)[*]	HI	Sum of land area covered by forest	2	-0.5713	70.63	0.7411	-45.11
Tree Density (m^{3}km^{-2})[†]	HI	Total tree volume by grid cell	3	14.1310	60.37	0.8012	-10.26
Human Population (km^{-2})[*]	PP	Current human population density at each time step	4	-0.1660	52.88	0.7311	-7.49
Human Population (km^2)[†]	PP	Current human population density at each time step	5	0.2391	47.45	0.7774	-5.43
Forested land (km^2)[†]	HI	Sum of land area covered by forest	NA	0.0490	47.27	0.7784	-0.18
Host Density (km^{3}km^{-2})[*]	HI	Host tree volume for that particular pest per grid cell	NA	0	47.45	0.7774	0
Host Density (km^{3}km^{-2})[†]	HI	Host tree volume for that particular pest per grid cell	NA	0	47.45	0.7774	0
Host Species Count[*]	HI	Number of tree species that are hosts of any pest present in grid cell	NA	0	47.45	0.7774	0
Host Species Count[†]	HI	Number of tree species that are hosts of any pest present in grid cell	NA	0	47.54	0.7774	0
Tree Density (m^{3}km^{-2})[*]	HI	Total tree volume by grid cell	NA	0	47.54	0.7774	0
Body Size (mm)	LH	Pest body length (separate intercept fit for fungi)	NA	-0.1027; 0.3078	46.36	0.7794	-1.18
Continent of Origin	LH	Continent of native range	NA	0.0018	47.45	0.7774	-0.09
Feeding Guild	LH	Pathogens vs. Arthropods	NA	0.0163	47.22	0.7774	-0.22
Number of Hosts	LH	Number of host species possessed by pest	NA	-0.1105	46.44	0.7802	-1.01
Income (USD)[*]	PP	Per capita income in 1999	NA	0	47.45	0.7774	0

Income (USD)†	PP	Per capita income in 1999	NA	0.0047	47.42	0.7768	-0.13
Road Length (km)*	PP	Total length of all major roads in grid cell	NA	-0.0013	47.40	0.7778	-0.15
Road Length (km)†	PP	Total length of all major roads in grid cell	NA	0	47.54	0.7774	0

* represents parameters influencing the probability of dispersal into a cell (Z_I).
† represents parameters influencing the probability of dispersal out of a cell (Z_O).
Negative estimates indicate positive influences on dispersal and vice versa. Since all variables were standardized, the relative influence of each fitted parameter on dispersal can be determined by its magnitude (magnitude of 'Estimate' in the table). Conversely, the relative importance of each parameter on MET is determined by its entry order in our GDK (See Appendix S1.7). Our best model had $\delta = 1.3155$ and $\Phi = 0.0001254$ with a jackknifed MET score of 47.60 km per species and a jackknifed R^2_{MSE} of 0.7709. Terms with entry order "NA" did not meet our variable importance threshold for inclusion, and their associated data is for their proposed inclusion as a 6th term in our model.

Connecting Statement

In my first chapter, I focused on the spread phase, and built a general model for how all economically damaging forest pests in the US spread, which we call the Generalized Dispersal Kernel (GDK). The GDK is highly predictive, without the need for any species-specific information, and predicts rapid spread influenced by human population. Based on these findings, I first developed the theory of anthropogenic replacement, where natural ecological processes are essentially being overridden by anthropogenic ones, and predictable generalities that operate across entire suites of species arise as a consequence of this. To demonstrate anthropogenic replacement more strongly, I then sought to determine how much predictive power is lost through the creation of a general model, compared to building customized models to individual focal species. This was the focus of Chapter 2, where I built customized spread models for three invasive forest pests based on their individual year-to-year detection records, and compared the predictive power of these models to the GDK. As an intermediate case, I created intermediate models that combined the GDK with simple species-specific corrections. These models leveraged the increased power from the GDK with the greater customizability of species-specific parameters, all the while not requiring time series for individual species.

The more complex spread models from Chapter 2 are fit following the same spatially-explicit simulation framework as those from Chapter 1. The spread model from Chapter 1 is used in the subsequent establishment model in Chapter 3 in order to separate the mechanisms for spread from those for establishment by controlling for spatial autocorrelation in establishment due to the spread process. Fitting an establishment model that controls for spread predictions allows for species, site, and tree-species specific rescaling of establishment probabilities that are previously modelled as being entirely driven due to propagule pressure in the spread model. As an alternative form of rescaling, the Chapter 2 models fit a species-specific spread intercept that allows for accelerated or decelerated spread relative to the global GDK spread rate. These models go on to be used as the best estimate for future invasion patterns in economic damage models within Chapter 2, and allow the creation of higher resolution impact predictions across species, space and time.

Chapter 2.

Comparing generalized and customized spread models for non-native forest pests

Authors: Emma J. Hudgins, Andrew M. Liebhold, Brian Leung

This manuscript was originally published in the journal Ecological Applications, 30 July 2019, Volume 30, Issue 1, e01988, reprinted with permission from John Wiley & Sons.

2.1 Abstract

While generality is often desirable in ecology, customized models for individual species are thought to be more predictive by accounting for context-specificity. However, fully customized models require more information for focal species. We focus on pest spread, and ask: how much does predictive power differ between generalized and customized models? Further, we examine whether an intermediate "semi-generalized" model, combining elements of a general model with species-specific modifications, could yield predictive advantages. We compared predictive power of a generalized model applied to all forest pest species (the Generalized Dispersal Kernel or GDK) to customized spread models for three invasive forest pests (beech bark disease (*Cryptococcus fagisuga*), gypsy moth (*Lymantria dispar),* and hemlock woolly adelgid (*Adelges tsugae*)), for which time-series data exist. We generated Semi-generalized Dispersal Kernel models (SDK) through GDK correction factors based on additional species-specific information. We found that customized models were more predictive than the GDK by an average of 17% for the three species examined, although the GDK still had strong predictive ability (57% spatial variation explained). However, by combining the GDK with simple corrections into the SDK model, we attained a mean of 91% of the spatial variation explained, compared to 74% for the customized models. This is, to our knowledge, the first comparison of general and species-specific ecological spread models' predictive abilities. Our strong predictive results suggest that general models can be effectively synthesized with context-specific information for single species to respond quickly to invasions. We provided SDK forecasts to 2030 for all 63 United States pests in our dataset.

2.2 Introduction

Identification of generalized models that explain and predict species distributions is of fundamental importance to ecologists. However, while general models "potentially inform about phenomena that exist in many systems…", they "…may not necessarily make good predictions about any individual system" (Evans et al. 2013). This tension between generality and context-specificity underlies much of ecology.

The trade-off between generality and ecological prediction also exists within invasion biology, where the focus has been on species-specific models using context-specific information (e.g., Liebhold et al. 1992; Gilbert et al. 2004). For instance, the spread phase, a fundamental part of the invasion process, has typically relied on customized models, accounting for life history, ecological complexity and spatial factors such as dominant wind direction and habitat suitability (Koch & Smith 2008; Kovacs et al. 2011; Liebhold et al. 1992). Intuitively, models that are based on a particular invasive species' local context should provide better predictions than general models, and should facilitate management. For instance, the gypsy moth Slow-the-Spread (STS) project in the United States has reduced spread rates by >70%, since its inception in 2000, (Sharov et al. 2002; Grayson & Johnson 2018; see also Slow Ash Mortality (SLAM) program, McCullough & Mercader 2012).

While customized models have undeniably been useful, there have been calls for pathway level analyses, which account for multiple invasive species simultaneously (Lodge et al. 2006; Bradie & Leung 2015). For invasive species, one phenomenon that supports such cross-species generality is the dominant role of humans in transporting species via mechanisms that are analogous across entire suites of species invading different spatial locations (e.g., through ballast water transport, Seebens et al. 2015; firewood transport, Haack et al. 2006). We hypothesized that across invasions, unique natural dispersal processes are commonly overridden by anthropogenic ones, and that predictable generalities that operate across entire suites of species arise as a consequence of these processes' broad effects (Hudgins et al. 2017). In the case of post-establishment spread, anthropogenic mechanisms such as transport through road networks may mean that conventional ecological processes governing dispersal, which are more idiosyncratic across species (wind direction, flight ability etc., Aylor 1990; Taylor et al. 2010), are less important for forecasting spread at large scales. Further, species traits relating to association with anthropogenic dispersal vectors may be most important in determining their spread rates. This anthropogenic dominance can thus provide us with general macroecological predictions for the spread of groups of invasive species within a particular transport network.

Although general invasion models are in the minority, the interest in multi-species predictions for the spread of invasive species arises because of their potential advantages. In order to prepare for and limit invasive species impacts across space, which accrue immense costs (Vilà & Hulme 2017), managers need to know where these species will invade next. Further, the sooner they can take action, the more effective their control measures will be (Lovett et al. 2016). The lower the data requirements of a given model, the sooner it can be implemented to inform management. As such, a highly general model could be rapidly applied to many species, potentially including species that have not yet established. Thus, in summary, there are potential benefits from using a general model and logical reasons to expect generality in the spread of invasive species.

Applied ecological models can be viewed along a continuum from specific to general. At the specific end of the spectrum, structure, predictors and parameters may all be fit to each separate species (i.e., customized models). At the most general end, a model may be applied to many species, using the same model structure, predictive factors, and parameters. In the middle of the spectrum, parameters can be added or rescaled to different values within a generalized model "backbone" in order to incorporate additional layers of customization (we term these "semi-generalized models"), without the collection of as much species-specific data (e.g., time-series for each species). These intermediate models can be worthwhile to consider, if the reduction in generality is offset by a large gain in predictive ability. Additionally, semi-generalized models that do not rely only on single-species data could conceivably make better predictions relative to customized models, if there are strong commonalities in the spread process across species (e.g., human-mediated vectors), since they are able to "borrow" information from a broad pool of species.

In this paper, we compare a suite of models with varying levels of generality in terms of their ability to predict the spread of invasive forest pests. For context specificity, we designed customized single-species models for three pest species for which time-series data exist (beech bark disease (*Cryptococcus fagisuga*), gypsy moth (*Lymantria dispar*), and hemlock woolly adelgid (*Adelges tsugae*), using species-specific predictors and functional forms (Liebhold et al. 1992; Morin et al. 2007; 2009). These were compared against a general model fit across all forest pest species currently known in the United States, using a previously published "Generalized Dispersal Kernel" (GDK) (Hudgins et al. 2017). At the intermediate level, we examined whether we could use GDK as a starting point, and incorporate species-specific knowledge (semi-generalized models, SDK), and whether doing so improved predictions compared to GDK and customized models.

2.3 Materials and Methods

2.3.1 Dispersal kernel formulation

Dispersal kernels estimate the probability of pest dispersal across space based on the distance, *d,* between source and destination locations (Kot et al. 1996). In the GDK, we moderated dispersal though spatial predictors affecting the dispersal kernel. We fit our model using discrete time simulations, where at each time step, pests dispersed to surrounding patches according to:

$$T_{i,j} = \frac{e^{-d_{i,j,}f(Z)}}{\sum_j e^{-d_{i,j,}f(Z)}} \tag{2.1}$$

$$f(Z) = 2\alpha \frac{e^{Z_S+Z_I+Z_O}}{1+e^{Z_S+Z_I+Z_O}} \tag{2.2}$$

Where $T_{i,j}$ is the proportion of pests dispersing from cell *i* to cell *j,* normalized such that the value of the dispersal kernel across all locations *j* sums to 1 (denominator of eqn. 2.1), $d_{i,j}$ is the distance between sites *i* and *j*, and *f*(*Z*) is a combination of all fitted species (Z_S) and cell (dispersal into a cell = Z_I, dispersal out of a cell = Z_O) specific predictors influencing the dispersal probabilities (described below), scaled to have a mean value of α (i.e. dispersal occurs at rate α for sites with predictor variables at their mean levels). For the GDK, our distributional data were limited to each species' final distribution at the end of the fitting period, plus data on their reported first year of establishment in the United States.

The GDK is made up of both a dispersal and a growth component, where the relative propagule pressure (PP) in cell *i* at timestep *t*+1 is equal to the relative propagule pressure at time *t*, minus emigration to all cells *j*, plus immigration from all cells *k*, multiplied by the growth rate δ:

$$PP_{i,t+1} = (PP_{i,t} - \sum_j T_{i,j} PP_{i,t} + \sum_k T_{k,i} PP_{k,t})\, \delta \tag{2.3}$$

Cells are considered ‘presences’ capable of being a source of propagules when they are above a threshold population size ϕ with a maximum relative propagule pressure in a cell of 1. We assumed that cells which were invaded, remained invaded (extirpation was not possible). Both growth and dispersal were deterministic.

For the GDK, we considered predictors, including propagule pressure proxies, habitat invasibility proxies and pest life history traits (sources fully described in Hudgins et al. 2017). The best-fitting model retained three predictor variables (four terms), wherein sites with greater forested land area and human population density are attractors to invasive pests, and sites with greater tree density and human population density are sinks from which pests do not disperse as much, relative to sites with lower values of these predictors. We modeled 5-year time steps, to achieve finer-scale forecasting (the original model used 10-year steps, but was shown to be robust, Hudgins et al. 2017). Within the GDK, we did not use time series, and fit the same terms to all species.

2.3.2 Allowing context specificity

We designed customized dispersal models for each of three highly damaging invasive forest pests: beech bark disease (BBD), gypsy moth (GM), and hemlock woolly adelgid (HWA) (Fig. 2.1). These were the only species where such a model was possible, because we required detailed time series of detections to fit custimized models. BBD is a disease complex made up of the introduced beech scale insect *C. fagisuga* and (most likely native) fungi (one of two species of *Neonectria*) first detected in Halifax, Nova Scotia in 1890, with potential additional introductions around Boston and New York City (Houston 1994). GM is a highly polyphagous (i.e. having many host tree species) defoliator introduced from France to Medford, MA around 1869 (Liebhold et al. 1989). HWA is a sap-feeding insect that was first detected in 1951 in Richmond, VA (Ward et al. 2004). These species span three of the four feeding guilds of the broader set of 63 species used to fit the GDK (Appendix S2.1, included: pathogens, foliage feeders, sap feeders, missing: borers, Hudgins et al. 2017). While time-series data exist for emerald ash borer (*Agrilus planipennis*), its detection records begin in 2002, which was after our fitting year (2000).

Across the customized models, we tested the inclusion of four additional levels of complexity compared to the GDK: testing additional dispersal kernel shapes, pest entry points, additional species-specific predictor variables, and time-series of pest spread.

Firstly, in addition to the negative exponential dispersal kernel employed in the GDK, a leptokurtic kernel was explored:

$$T_{i,j} = \frac{e^{-\sqrt{d_{i,j}}f(Z)}}{\sum_j e^{-\sqrt{d_{i,j}}f(Z)}} \text{ (\textit{sensu} Kot et al. 1996).} \tag{2.4}$$

Leptokurtic dispersal kernels allow for nonlinear spread rates and increased dispersal to distant locations (Shigesada et al. 1995; Kot et al. 1996). Spatial predictor variables were analogously incorporated via eqn. 2.2, but the leptokurtic kernel has more density in its tails and therefore leads to a higher chance of long-distance dispersal. The dispersal kernel that resulted in the best model fit was selected for each species separately.

Secondly, we simulated the best-known starting location of each pest species (Ward et al. *unpubl. manuscript*) and the host centroid as a starting point for each pest's dispersal. While the use of best-known starting points did not improve the overall fit of the GDK (Hudgins et al.

2017), given that these three species are some of the most well-studied, these starting points are likely more reliable than for other pests. If a starting location was not within our known host range for a given pest (e.g., first detection in an urban area), we chose the closest grid cell in the host range. As with the dispersal kernel, the starting point that resulted in the best model fit was chosen for each species.

Thirdly, we tested additional predictors mined from the literature in our forward selection models. We tested firewood and campground-related variables, which were frequently included in spread models of gypsy moth (Bigsby et al. 2011). We sourced these predictors from the US Census' American Housing Survey (homes fueled by wood, campground density, seasonal homes), and tested for all three pests. Additionally, HWA is known to be highly climatically-limited, with high mortality when exposed to low winter temperatures (Morin et al. 2009; Paradis et al. 2008). We modeled climatic limitation for HWA using minimum temperature of the coldest month (bio6) from WorldClim (Fick & Hijmans 2017; www.worldclim.org) (Appendix S2), and setting the pest density to zero for any patch below a fitted threshold. Any predictor that substantially improved fit was included in the final customized model for a given species.

Finally, the customized models were each fit to time-series of species dispersal patterns, using historical discovery records by county available for the above three species, while the GDK was constructed using only the final distributions (but many more species).

2.3.3 Semi-generalized models (SDK)

For the SDK, we tested the inclusion of three additional layers of species-specific information that went beyond the original GDK, but did not use time series information (in contrast to the customized models), as these data are relatively rare. Firstly, we utilized an "intercept correction" to offset each single-species spread trajectory such that it minimized fitted GDK residuals. Secondly, we tested whether incorporating information on the best-known initial invasion location improved predictive ability for each pest. Thirdly, we tested whether incorporating information on a species' known niche limitations could improve our forecasts.

2.3.4 GDK intercept-correction

The earliest invasive spread model is Skellam's seminal work on reaction-diffusion (RD, 1951). RD uses the physics of diffusion to predict radial spread emanating from a single source, where the size of the invaded range expands uniformly over time (Shigesada et al. 1995), and is a core model in theoretical ecology (Morin et al. 2007; 2009; Skuhravá et al. 2007).

Theoretically, we recognized that the GDK spread intercept (α) is related to the RD diffusion coefficient (D), as it similarly acts to scale the relationship between dispersal distance and probability (Appendix S2.3), and hypothesized that – holding all spatial predictors constant, this intercept could be rescaled to adjust species spread, thereby improving forecasts. Using only the fitted values of the GDK to forecast spread neglects additional information contained in the mismatch between these fitted values and the observed distribution in the fitting year. If GDK residuals reflect constant, unmeasured species-specific factors (such as probability of uptake by humans, fertility rates, etc. that are difficult to obtain for an entire community of species), accounting for these deviations in spread trajectories could improve predictions. We thus refit the spread intercept for each species, but otherwise maintained the proportional relationship with other spatial predictors, and general structure of the GDK previously fit (i.e., eqns. 2.1, 2.2; with dispersal based on forested land area, human population, and tree density as in Hudgins et al. 2017). The data requirements for this adjustment are simply the locations at one time-point in a species' distribution – something that is presently available for all known damaging invasive pests.

2.3.5 GDK starting-point correction

Secondly, as one of the simplest correction factors, we tested whether adding information on our best estimate of a pest's initial invasion site within the United States improved the predictions of our general model, when there is reasonable confidence in those estimates. We note that such estimates may not improve the predictions of all species if the starting point is not well-known, but as we mention above, all three of these species are well-studied. For this correction, we updated our GDK simulation to begin spread from these sites rather than the host range centroid.

2.3.6 Niche limitation correction

Thirdly, we tested the inclusion of species' niche constraints. While the first two correction factors require very little context-specific information, which is likely to be known for any future invader– niche limitations are more idiosyncratic species information. For one of our studied species, HWA, it is clear that climatic limitation plays a strong role in limiting its northward dispersal (see above). Just like in the customized models, we tested the addition of a minimum temperature threshold for HWA persistence (Appendix S2.2).

We chose the SDK corrections for each species that maximized fit. Importantly, all three customizations were added to the basic structure of the GDK, holding all other fitted parameter values constant for all predictor variables in the published model.

2.3.7 Data preparation

For the customized models, historical county-level spread records were assembled for GM, HWA, and BBD. Records of historical GM spread were obtained from the United States Code of Regulations (Title 7, Chapter III, Section 301.45) which annually designates quarantined counties that are part of the "generally infested area". Federal quarantines do not exist in the US for BBD and HWA, however similar county-level records were obtained from other sources (Morin et al. 2007; 2009). County records were overlaid on a 50x50 km grid in order to control for county size, where a detection anywhere in a grid cell was considered a valid presence. Five-year timesteps within historical spread datasets with less than two new detections were not considered in our spread models, because there are inherent delays between the detection of pests in surveys and the incorporation of that information into range databases. These years likely correspond to times where monitoring was not adequately performed (resulting in minimal apparent spread even if new invasions were occurring), and are not a good indicator of the spread trajectory. Once these low-detection years were removed, the number of independent fitting years for each species was 15 for GM, 6 for BBD and 5 for HWA. All three historical spread datasets included data beginning only at the first date of multi-county range for each pest, but dates of initial discovery/introduction are known for each pest, so simulated spread was adjusted to include the period between initial discovery/introduction to the first record of multi-county spread. HWA was adjusted from 1971-2005 to 1950-2005, GM was adjusted from 1902-2005 to 1865-2005, and BBD was adjusted from 1935-2005 to 1890-2005.

2.3.8 Customized model fitting

To maintain consistency with the GDK, a forward selection procedure based on the same metric (MET, Aslan & Zech 2005) and using the same threshold for parameter inclusion (5 km) as in Hudgins et al. (2017) was employed to build the customized models. MET accounts not only for exact spatial matches of predicted and observed presences (similar to measures such as accuracy), but also apportions better scores to 'close' matches than presences predicted very far away from the observed presences (for a further discussion of MET, see Hudgins et al. 2017). Rather than taking the average across 63 species, in the customized models, this 5 km MET threshold was applied on average across all fitting years for a single species. We chose the best single-species forward selection model among the two dispersal kernel shapes and two possible starting locations for each pest species. In the case of HWA, the temperature threshold was applied to all four possible customized models, to remain consistent with the literature on niche limitation and to ensure the methodology was comparable to the fitting of the SDK.

2.3.9 Predictive validation metric

To explore predictive ability with greater ease of interpretation, we derived a novel, simple pseudo R-squared value, based on *optmatch*, an algorithm originally used to match treatment to control subjects in clinical trials (R package *optmatch*, Hansen 2007). The *optmatch* tool uses a global optimization approach to match two sets of points, minimizing the total multivariate distance between the sets. We wished to have a metric that takes its maximum value when two distributions have the same number of points, with the points in the correct spatial locations.

We first used *optmatch* to perform a one to one match between our predicted and observed presence points for a given pest. Next, the leftover points caused by differences in predicted and observed range size were then used to penalize the distance score. To do this, we assigned these leftover points the mean distance between that point and all other points in the opposing distribution. We used the mean of this entire vector of distances (optimal matching mean squared error - *omMSE*) and converted it to a Pseudo R^2 (R^2_{om}) by comparing the observed o*mMSE* value to a spatial null expectation, using 10,000 random points from the host distribution (Appendix S2.4).

2.3.10 Community Forecast

We used the best-fitting SDK to forecast the distribution of all 63 pest species from 2005 to 2030. We used the fitted MET score applied to each individual species' snapshot of dispersal in 2005 in order to determine the SDK layers to include for each species (intercept, starting point, and niche limitation corrections where there was evidence from the literature that they were necessary, see Appendix S2.5). We reset pest distributions to known distributions at 2005 (setting false absences to ϕ, false presences to 0, and maintaining the simulated propagule pressure of true presence sites) before simulating spread using each species' SDK parameters to 2030. We included projected human population estimates from ProximityOne (www.proximityone.com) as an updated human population predictor in the GDK-based models, which all included this term.

To model uncertainty, we considered future climate and human population size projections, and uncertainty in fitted model parameters (see Appendix S2.6 for full details). In brief, for climate change, we used rcp2.6 and rcp8.5 climate scenarios from BIOCLIM, and for population size, we used two scenarios based on the Shared Socioeconomic Pathways: SSP3 or "Regional Rivalry", and SSP5 or "Fossil-Fueled Development" (Hauer 2019), representing the extremes for both climate and population size, respectively. We note that there was only evidence of climate limitations for two species, but we nonetheless considered climate scenarios for completeness (Appendix S2.5). For the parameter uncertainty in the SDK model, we conducted sensitivity analysis, randomly perturbing model parameters, and using the threshold for parameter inclusion in our model fitting process as our criterion to retain parameter sets (i.e., MET within 5 km of the best-fitting model). We examined the combined effect of uncertainty on the range of predicted future pest richness.

2.4 Results

2.4.1 Customized model selection and predictive validation

Customized models were highly predictive on average ($R^2_{om} = 0.74$), though predictions were weakest for HWA ($R^2_{om} = 0.45$). The best-fitting customized model had a very simple functional form for each of the three species (Table 2.1), with fewer predictors than the GDK. For GM, only per capita income was important, showing a negative effect on spread into sites. For BBD, the best model included only an intercept term. In the HWA model, which contained the minimum temperature threshold, human population density displayed the same relationship as it did in the GDK, increasing spread into sites. In all cases, using the hypothesized initial introduction location ("best guess" in Table 2.2) as a starting point led to better fits than using the centroid of the host range. For BBD, the leptokurtic dispersal kernel fit better than the negative exponential kernel, while the negative exponential outperformed the leptokurtic model for HWA and GM.

2.4.2 GDK predictive validation

The strength of the uncorrected model's predictions varied across the three species, from being extremely predictive for GM ($R^2_{om} = 0.87$), to highly predictive for BBD ($R^2_{om} = 0.55$), to more moderately predictive for HWA ($R^2_{om} = 0.30$). The uncorrected GDK overestimated spread for these three species, but predictions were still substantially better than random expectations from our null model, and mean spatial variation explained was $R^2_{om} = 0.57$.

2.4.3 SDK model selection and predictive validation

The R^2_{om} improvement ranged from 0.11 - 0.55 between the uncorrected GDK and the best SDK, and from 0.03-0.40 between the customized model and the best SDK for the validation year (mean SDK $R^2_{om} = 0.91$). The best SDK for BBD and GM included the intercept and starting point corrections, and had $R^2_{om}= 0.89$ and $R^2_{om} = 0.98$, respectively (Table 2.1). HWA required a third level of complexity, where the model with the starting point, intercept and niche limitation corrections resulted in the best fit and had R^2_{om} = 0.85. For GM and BBD, corrected intercepts were larger in magnitude than the uncorrected GDK intercept, consistent with a reduction in spread extent. Conversely, for HWA, SDK had a smaller intercept, indicating a higher spread rate. However, this spread rate was offset by pest mortality upon dispersal into the northernmost parts of its range, thereby leading to a lower extent of spread overall.

2.4.4 Model comparison: spatial details

Although the GDK retained moderate to high predictive power, and performed similarly to the customized model for GM, it was weaker than the customized models for BBD and HWA. For GM, both the customized model and the SDK explained over 92% of spatial variation in pest distributions. However, while the customized model performed well in terms of the R^2_{om}, based on visual inspection, it produced spatial patterning incongruent with the true pest distribution, likely due to its fitted relationship with income (Fig. 2.2, top left panel). The model's leptokurtic kernel and negative relationship with income produce a discrete patch of invaded sites around South Dakota and Nebraska. GM's extensive host range could allow incongruent distributions to have high R^2_{om} if predicted distributions are of approximately the correct range size and close geographically to observed distributions. In contrast, SDK predicted a distribution that overlapped with the observed distribution nearly entirely. Both the SDK and the customized models performed well for BBD, leading to a tight spatial match between its predicted and observed distribution. The HWA customized model explained the lowest amount of spatial variation of the three species (R^2_{om}=0.45), likely due to the increased complexity of this species' spread mechanisms (i.e. climatic limitation), leading to an inability to capture the southernmost part of the range without overpredicting to the north. The customized model's fitted temperature threshold was quite low (~2°C lower than in the SDK), resulting in only a small effect on restricting pest distributions. The GM uncorrected GDK overpredicted spread, producing a distribution that included much of its invaded range, but lacking climatic limitation in northern areas. In contrast, the SDK no longer overpredicted spread in the north, and also did not predict disjointed jumps outside the observed distribution that the customized model predicted (R^2_{om} = 85%), but still did not capture the southernmost distribution.

2.4.5 Forecasts

Using the optimal set of SDK layers for each of the 63 species (see Appendix S3.5 for details of SDK corrections), our simulations project the distribution of pests at 2030 to remain highly aggregated in the northeastern United States, as it was in 2005, but pest species richness to increase (Fig. 2.3a-b). Northern Minnesota and Wisconsin, western Montana and northern Idaho, parts of New Mexico, and northern New England are predicted to have the largest increase in local establishments by 2030 (Fig. 2.4, regions B, C, E, F, K). Some smaller, more concentrated areas of increase are also predicted (Fig. 2.4, regions A, D, G-J). We predict very few new local establishments in the middle of the country. The areas at high risk correspond to high forested land and increasing human population densities. New local establishments are especially high in urban centers close to regions of high forested land area (Fig. 2.4, dashed lines). However, some less populated areas also see large increases in local establishments due to their high amount of forested land (Fig. 2.4, solid lines).

The combination of uncertainties in climate change, future population growth, and model parameters led to strong regional variability across future pest richness predictions (Fig. 2.5). However, the northeastern US typically had the greatest number of relative establishments, indicating a consistent pattern of future spatial risk despite uncertainty. The simulations that produced the fewest novel local establishments were those from the high human population growth scenario, given decreased dispersal out of high population density sites. Scenarios with the highest future spread had increased pest growth rates and less preferential dispersal into high population areas, leading to more even dispersal patterns across space (see Appendix S2.6 for further discussion). The median range of predicted pest load was 5 species, but distinct regional differences were observed. The central portion of the United States had the lowest uncertainty (range of <5 pests), but was consistently predicted to have low numbers of future local establishments. The western US had more moderate levels (~5-10 pests), while the eastern US had the highest levels (~10-20 pests). Some future hotspots were particularly variable (Regions C, D, H in Fig. 2.4). Additionally, many of the high uncertainty patches, which are particularly dense across the eastern US, had not been identified as hotspots (Fig. 2.4), indicating some potential for additional regions of high future pest load that warrant managerial surveillance.

2.5 Discussion

2.5.1 The performance of general versus single-species models

The customized models performed 17% better than the GDK, averaged across our three case studies, with 74% spatial variation explained. While customization showed a marked benefit, notably, the GDK was still able to capture a respectable 57% of spatial variation in spread, for these three species. Moreover, GDK's predictive ability may be substantially higher for most other species: We note that HWA and BBD were much more poorly fit by the uncorrected GDK than the majority of species, while GM was fit better than average, and that the magnitude of over or underprediction in the uncorrected GDK appears to predict forecasting ability (Appendix S2.7). Thus, we expect the GDK's average predictive ability to be between BBD (55%) and GM (87%). While researchers have reasonably focused on customized single-species models for prediction (e.g., Koch & Smith 2008; Kovacs et al. 2011; Liebhold et al. 1992), the GDK yielded useful predictions even without any modification, and will be useful in situations where customized models cannot be built, e.g., in the case of novel invaders.

2.5.2 Comparing predictors in GDK versus customized models

We found different suites of predictors to be important for single-species spread, and that fewer predictors were important compared to the general predictors for all species in the GDK.

The differences in predictors between the GDK and customized models could have arisen due to two processes: 1) species specificity in spread mechanisms, or 2) differences in power across models to detect predictors of spread. While there is likely some species-specificity in the predictors of spread, we also believe that these differences reflect noisiness of single-species data (i.e., power to detect predictors of spread), given that the SDK was more predictive than customized models, and used the same predictors as the GDK. Arguably, the general model could "borrow" power from numerous species, where spread processes are partially consistent across species. The incorporation of multispecies' information has also allowed for recent advances in analogous fields, such as species distribution modeling, improving spatial predictions of individual species occurrences (Fithian et al. 2015; Leung et al. 2019).

2.5.3 Semi-generalized Dispersal Kernel approach

We explored the value of using the GDK as a basic structure upon which to build models, adding context-specific information where it was known. This yielded a 17% average improvement compared to the fully customized model (and 34% improvement compared to GDK). Both GM and BBD customized models were already highly predictive, and SDK yielded modest improvements (3% and 6%, respectively). However, for HWA, by including the three additional corrections to the GDK, SDK yielded a 40% increase in spatial variation explained (from 45% in the customized model to 85% in the SDK). Well-documented biases exist in HWA's spread pattern to support the incorporation of niche limitations (Morin et al. 2009; Paradis et al. 2008). Thus, we recommend integrating such context-specific information into an SDK, following fitting protocols described in this manuscript.

Given that spread models have previously been parameterized using these same time-series data, it was reasonable to expect that customized models would be highly predictive across species. However, the customized model for HWA was only moderately predictive, providing a cautionary tale that even models using the best available data may not produce highly predictive forecasts. It may be that the quality of data is too poor to build single species models, in some cases. On the other hand, it appears that a snapshot of a species distribution, a known initial invasion location, and when necessary, a known niche limitation, synthesized with a semi-generalized model (SDK), can outperform the best-fitting customized model.

2.5.4 Forecasts of future invasion risk

Our simulations suggest future invasions to be even more aggregated in space. Urban centers, areas of high forest cover and tree density appear to be largescale attractors of invasive propagules from all sources (*sensu* Colunga-Garcia et al. 2010; Gaertner et al. 2017). Surprisingly, in the GDK, these attractors do not send out as many propagules as other sites, leading to fewer surrounding invasions than if they were also major sources of propagule pressure. Instead, invaders arrive at these sites (sometimes up to 15-20 new pests in the next 25 years in areas like Chicago, IL and Boston, MA), and remain there, perhaps due to a lack of favorable conditions elsewhere.

While new establishments driven by population density such as Boston, MA and Chicago, IL are relatively unsurprising "hotspots" of future pest load, those driven by forested land, such as Chesapeake, VA, western Montana and northern Idaho, and the national forests of New Mexico, are less obvious. Many of these regions coincide with National and State Forests and National Wildlife Refuges, highlighting the role of forested land in the dispersal model. Moreover, areas such as Northern Minnesota and Wisconsin are projected to be the largest 'hotspot', possibly reflecting historically low numbers of establishments and hence a lack of saturation in comparison to the northeastern United States or the Midwest. These results indicate a high risk of spread into Canada in the Great Lakes region, and may support a management regime that prioritizes limiting propagule entry to these hubs, though an explicit analysis of the consequences of this prioritization requires further study.

We note that while the intercept and niche corrections can only be employed once a species begins spreading and has a substantial enough distribution for these limitations to be fit, the starting-point corrected GDK can be used as a first pass to predict invasion risk of new invaders from likely points of entry, as the only information it requires is an estimated initial introduction location. If the pest does successfully establish, an SDK combining additional corrections based on model fit can more closely hone in on its future trajectory. For species with well-known niche limitations such as HWA, niche limitations can be similarly incorporated by maximizing SDK fit to the observed distribution, once distributional information is available, as we have done here.

2.5.5 Caveats and limitations

As detailed above, even with our best current models, there is substantial uncertainty in future pest distributions, given available data. Intuitively, such uncertainty will commonly occur, and we argue that invasive species models should be validated using temporal data withheld from fitting, where possible.

Our model was based on current and historical conditions. However, climate change could alter environmental suitability either due to its direct influence on the invading species or indirectly via effects on hosts and other species (Hellmann et al. 2008, see Appendix S3.5 for additional species with climatic limitations). However, we note that much of the Northeast, Midwest, and central US is predicted to have colder minimum winter temperatures with climate change, even if mean temperatures are predicted to increase (Appendix S3.3), which will lead to more complex future spread dynamics for temperature-limited species. According to the SDK, HWA will be even more constrained with climate change (Appendix S3.3). Spread could also be affected by conditions becoming hotter or more humid with climate change, potentially affecting GM (Tobin et al. 2014, though these limitations might improve GM forecasts by only 2% based on our analyses). Fortunately, the SDK can easily parameterize any type of spatial limitation for any pest (though these can only be validated using time-series information), and can thus incorporate future knowledge of pest distributional thresholds.

The validation set used in this analysis was not a random selection of species. Instead, it included the three species with time-series data, for which comparative analyses of general versus customized models could be conducted. It was notably useful from an applied perspective, as they represent some of the most damaging invasive forest pests (Aukema et al. 2011). Emerald ash borer has caused more damage than these species, but was not included in this analysis due to its short invasion history. Further, while fine-scale spatiotemporal GM data are available from pheromone trapping, we applied the GDK to new detections at the 50 x 50 km grid scale in 5-year timesteps, which represent a much coarser spatiotemporal dispersal pattern. To account for the finer-resolution dispersal, a second sub-model could be developed for small-scale dispersal and integrated into country-scale model (although such data do not presently exist for species other than GM).

2.5.6 Conclusion

While customizing models for each species based on their ecological context yielded 17% higher predictive power compared to the fully generalized GDK, combining both into the SDK yielded the most powerful approach, outperforming the customized model by an additional 17% of spatial variation explained. These results show that the spread process has a substantial component that is generalizable, and that this generality can be effectively synthesized with context-specific information. The SDK is a strong predictive tool to examine the future distributions of these pests, which we predict are becoming increasingly aggregated at urban centers and are beginning to invade less populated areas with high numbers of trees. These forecasts can aid in estimating future damages due to invasive forest pests, and will be helpful in optimizing future management by highlighting areas of high future pest risk.

2.6 Acknowledgements

EJH and BL conceived of the ideas and designed the methodology. EJH performed the analyses. EJH and BL led the writing of the manuscript. AML provided pest expertise and edited the manuscript. EJH would like to thank Laura Blackburn at the USDA Forest Service for her help in acquiring data, as well as the members of the Leung Lab (L. Della Venezia, D. Nguyen, S. Varadarajan, N. Richards, A. Sellers) for their invaluable feedback on the analysis and manuscript. This work was supported by an NSERC CGS-D fellowship awarded to EJH and an NSERC Discovery Grant to BL.

2.7 Data Accessibility

Model predictions, associated data and code are available at github.com/emmajhudgins/GDK_vs_customized (DOI:10.5281/zenodo.3343027)

2.8 References

Aslan, B., & Zech, G. (2005). New test for the multivariate two-sample problem based on the concept of minimum energy. *Journal of Statistical Computation and Simulation*, 75(2), 109-119.

Aukema, J. E., Leung, B., Kovacs, K., Chivers, C., Britton, K. O., Englin, J., *et al*. (2011). Economic impacts of non-native forest insects in the continental United States. *PLoS One*, 6(9), e24587.

Aylor, D. E. (1990). The role of intermittent wind in the dispersal of fungal pathogens. *Annual Review of Phytopathology,* 28(1), 73-92.

Bigsby, K. M., Tobin, P. C., & Sills, E. O. (2011). Anthropogenic drivers of gypsy moth spread. *Biological Invasions*, 13(9), 2077-2090.

Bradie, J., & Leung, B. (2015). Pathway-level models to predict non-indigenous species establishment using propagule pressure, environmental tolerance and trait data. *Journal of Applied Ecology*, 52(1), 100-109.

Colunga-Garcia, M., Haack, R. A., Magarey, R. A., & Margosian, M. L. (2010). Modeling spatial establishment patterns of exotic forest insects in urban areas in relation to tree cover and propagule pressure. *Journal of Economic Entomology*, 103(1), 108-118.

Evans, M. R., Grimm, V., Johst, K., Knuuttila, T., De Langhe, R., Lessells, C. M., … *et al*. (2013). Do simple models lead to generality in ecology?. *Trends in Ecology and Evolution*, 28(10), 578-583.

Fick, S. E., & Hijmans, R. J. (2017). WorldClim 2: new 1-km spatial resolution climate surfaces for global land areas. *International Journal of Climatology*, 37(12), 4302-4315.

Fithian, W., Elith, J., Hastie, T., & Keith, D. A. (2015). Bias correction in species distribution models: pooling survey and collection data for multiple species. *Methods in Ecology and Evolution,* 6(4), 424-438.

Gaertner, M., Wilson, J. R., Cadotte, M. W., MacIvor, J. S., Zenni, R. D., & Richardson, D. M. (2017). Non-native species in urban environments: patterns, processes, impacts and challenges. *Biological Invasions* 19, 3461–3469.

Gilbert, M., Grégoire, J. C., Freise, J. F., & Heitland, W. (2004). Long-distance dispersal and human population density allow the prediction of invasive patterns in the horse chestnut leafminer *Cameraria ohridella*. *Journal of Animal Ecology*, *73*(3), 459-468.

Grayson, K. L., & Johnson, D. M. (2018). Novel insights on population and range edge dynamics using an unparalleled spatiotemporal record of species invasion. *Journal of Animal Ecology*, 87(3), 581-593.

Haack, R. A. (2006). Exotic bark-and wood-boring Coleoptera in the United States: recent establishments and interceptions. *Canadian Journal of Forest Research*, *36*(2), 269-288.

Hansen, B. B. (2007). Flexible, optimal matching for observational studies. *R News*, *7*, 18-24.

Hellmann, J. J., Byers, J. E., Bierwagen, B. G., & Dukes, J. S. (2008). Five potential consequences of climate change for invasive species. *Conservation Biol*. 22(3), 534-543.

Houston, D. R. (1994). Major new tree disease epidemics: beech bark disease. *Annual Review of Phytopathology*, 32(1), 75-87.

Hudgins, E. J., Liebhold, A. M., & Leung, B. (2017). Predicting the spread of all invasive forest pests in the United States. *Ecology Letters,* 20(4), 426-435.

Koch, F. H., & Smith, W. D. (2008). Spatio-temporal analysis of *Xyleborus glabratus* (Coleoptera: Circulionidae: Scolytinae) invasion in eastern US forests. *Environmental Entomology*, 37(2), 442-452.

Kot, M., Lewis, M. A., & Van Den Driessche, P. (1996). Dispersal data and the spread of invading organisms. *Ecology,* 77, 2027-2042.

Kovacs, K. F., Mercader, R. J., Haight, R. G., Siegert, N. W., McCullough, D. G., & Liebhold, A. M. (2011). The influence of satellite populations of emerald ash borer on projected economic costs in US communities, 2010–2020. *Journal of Environmental Management, 92*(9), 2170-2181.

Leung, B., Hudgins, E. J., Potapova, A., & Ruiz-Jaen, M. (2019). A new baseline for countrywide α-diversity and species distributions: illustration using >6000 plant species in Panama. *Ecological Applications,* 29(3)*, e01866*.

Liebhold, A. M., Halverson, J. A., & Elmes, G. A. (1992). Gypsy moth invasion in North America: a quantitative analysis. *Journal of Biogeography*, 513-520.

Liebhold, A., Mastro, V. & Schaefer, P.W. (1989). Learning from the legacy of Leopold Trouvelot. *Bulletin of the Entomological Society of America,* 35, 20-21.

Liebhold, A. M., McCullough, D. G., Blackburn, L. M., Frankel, S. J., Von Holle, B. & Aukema, J. E. (2013). A highly aggregated geographical distribution of forest pest invasions in the USA. *Diversity and Distributions,* 19, 1208-1216.

Lodge, D. M., Williams, S., MacIsaac, H. J., Hayes, K. R., Leung, B., Reichard, S., … *et al.* (2006). Biological invasions: recommendations for US policy and management. *Ecological Applications*, 16(6), 2035-2054.

Lovett, G. M., Weiss, M., Liebhold, A. M., Holmes, T. P., Leung, B., Lambert, K. F., … *et al*. (2016). Nonnative forest insects and pathogens in the United States: Impacts and policy options. *Ecological Applications,* 26, 1437-1455.

McCullough, D. G., & Mercader, R. J. (2012). Evaluation of potential strategies to SLow Ash Mortality (SLAM) caused by emerald ash borer (Agrilus planipennis): SLAM in an urban forest. *International Journal of Pest Management*, 58(1), 9-23.

Morin, R. S., Liebhold, A. M. & Gottschalk, K. W. (2009). Anisotropic spread of hemlock woolly adelgid in the eastern United States. *Biological Invasions*, 11, 2341–2350.

Morin, R. S., Liebhold, A. M., Tobin, P. C., Gottschalk, K. W., & Luzader, E. (2007). Spread of beech bark disease in the eastern United States and its relationship to regional forest composition. *Canadian Journal of Forest Research,* 37(4), 726-736.

Paradis, A., Elkinton, J., Hayhoe, K. & Buonaccorsi, J. (2008). Role of winter temperature and climate change on the survival and future range expansion of the hemlock woolly adelgid (*Adelges tsugae*) in eastern North America. *Mitigation and Adaptation Strategies for Global Change*, 13(5-6), 541-554.

Seebens, H., Essl, F., Dawson, W., Fuentes, N., Moser, D., Pergl, J., *et al*. (2015). Global trade will accelerate plant invasions in emerging economies under climate change. *Global Change Biology*, 21(11), 4128-4140.

Sharov, A. A., Leonard, D., Liebhold, A. M., Roberts, E. A., & Dickerson, W. (2002). “Slow the spread”: a national program to contain the gypsy moth. *Journal of Forestry,* 100(5), 30-36.

Shigesada, N., Kawasaki, K. & Takeda, Y. (1995). Modeling stratified diffusion in biological invasions. *American Naturalist,* 146(2), 229-251.

Skellam, J. G. (1951). Random dispersal in theoretical populations. *Biometrika*, *38*(1/2), 196-218.

Skuhravá, M., Skuhravý, V., & Csóka, G. (2007). The invasive spread of the gall midge *Obolodiplosis robiniae* in Europe. *Cecidology*, *22*(2), 84-90.

Taylor, R. A. J., Bauer, L. S., Poland, T. M., & Windell, K. N. (2010). Flight performance of *Agrilus planipennis* (Coleoptera: Buprestidae) on a flight mill and in free flight. *Journal of Insect Behaviour*, 23(2), 128-148.

Tobin, P. C., Gray, D. R., & Liebhold, A. M. (2014). Supraoptimal temperatures influence the range dynamics of a non-native insect. *Diversity and Distributions,* 20, 813-823.

Vilà, M., & Hulme, P. E. (Eds.). (2017). *Impact of biological invasions on ecosystem services* (Vol. 12). Cham: Springer.

Ward, J.S., Montgomery, M. E., Cheah C.A.S.-J., Onken, B. P., & Cowles, R. S. (2004). Eastern hemlock forests: guidelines to minimize the impacts of hemlock woolly adelgid. NA-TP-03-04, USDA Forest Service, Northeastern Area State and Private Forestry, Morgantown, 28 pp.

2.9 Figures and Tables

2.9.1 Figures

Figure 2.1 Historical spread patterns of the three focal species: Gypsy moth (GM), hemlock woolly adelgid (HWA) and beech bark disease (BBD). Older invasions are shown in yellow while more contemporary invasions are shown in blue. Known host distribution is shown in beige.

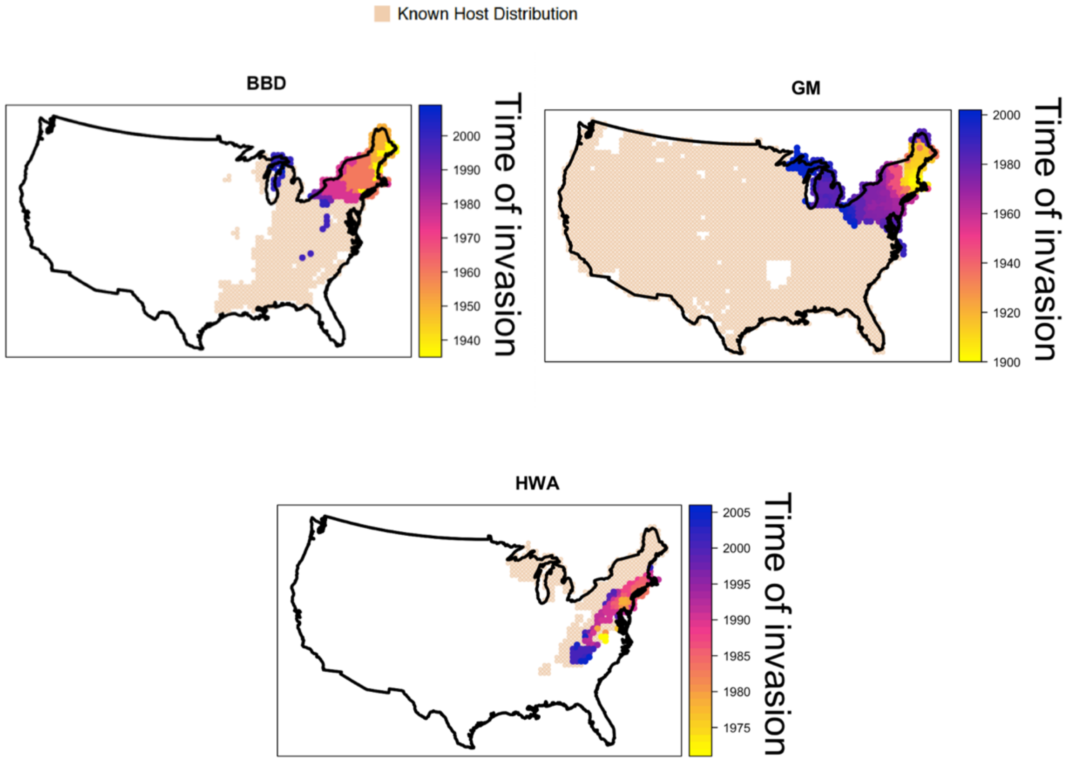

Figure 2.2 A comparison of the predictive ability of customized (top row), uncorrected GDK (GDK, middle row) and SDK models for Gypsy moth (GM, left column), hemlock woolly adelgid (HWA, middle column) and beech bark disease (BBD, right column). Host presence is indicated in beige, predicted distributions after a forecast (5-year) are shown in red, and observed distributions are shown in blue. Areas of overlap between predicted and observed distributions produce a darker red color due to the overlap of the red and blue colors.

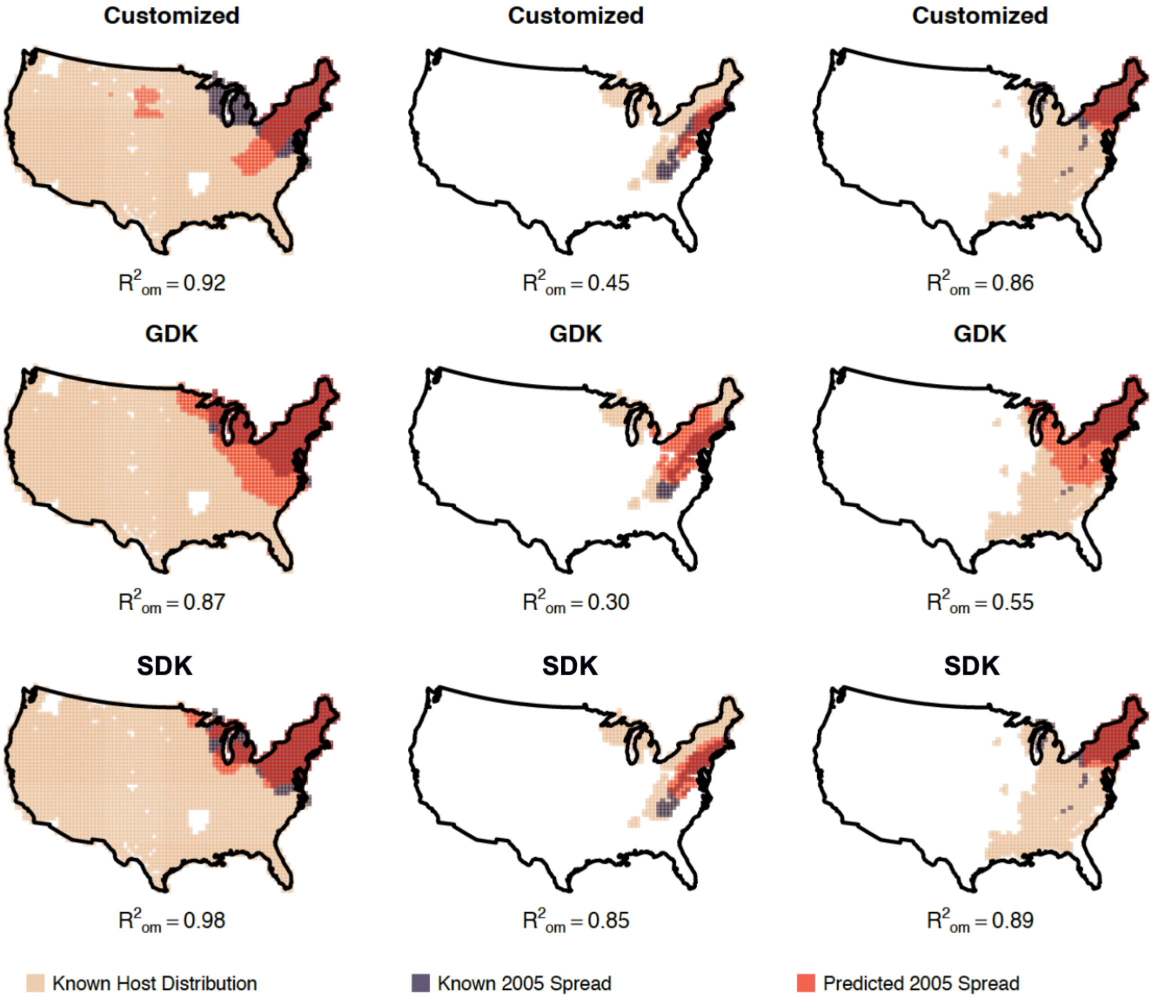

Figure 2.3 Forecasted pest species richness from **a.** 2005 (fitting year of SDK) to **b.** 2030 generated by extending simulated spread patterns for each species from the best fitting SDK parameters.

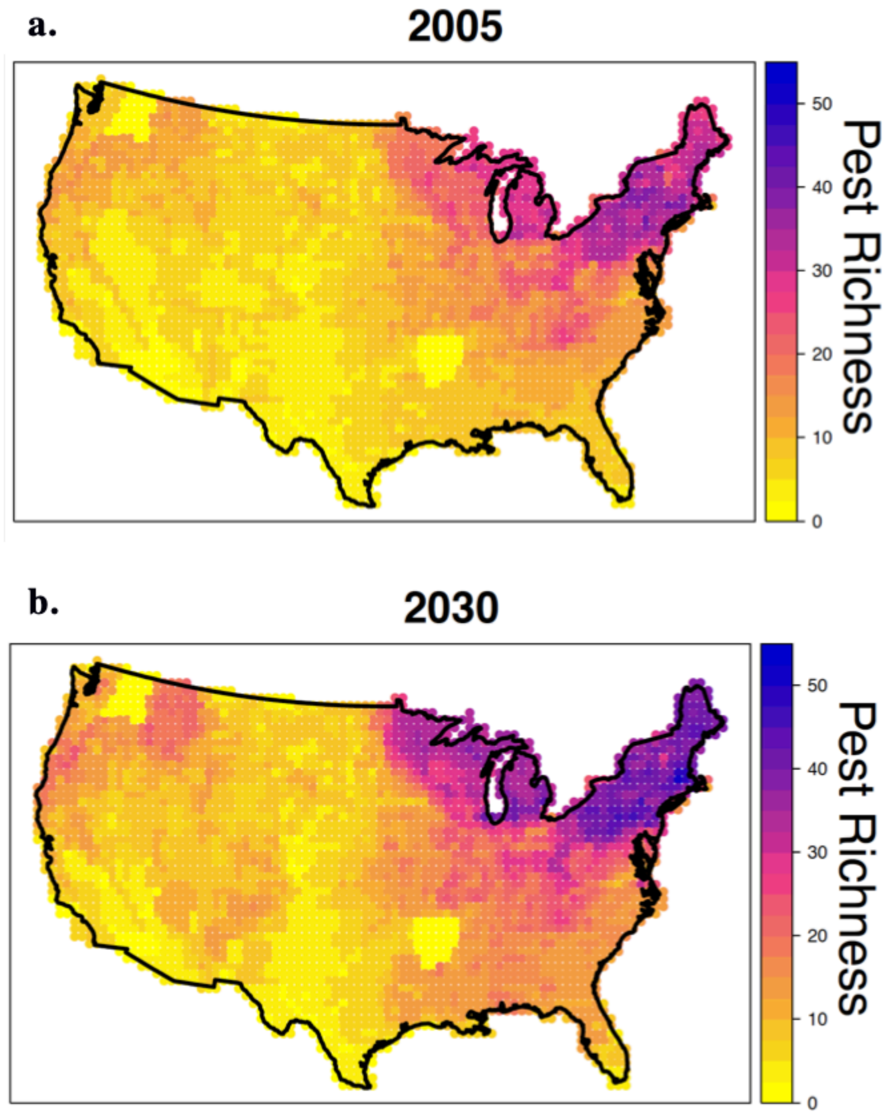

Figure 2.4 Newly predicted local establishments (for existing United States invasive forest pests) between years 2005 and 2030, created by subtracting Fig. 2.3b from Fig. 2.3a. Areas of particular interest are labelled, and dominant mechanisms promoting new invasions are denoted with dashed vs. solid lines. **A**–Seattle, WA region **B**–Northern Idaho and Western Montana (includes Kootenai, Nez Perce-Clearwater, and Flathead National Forests), **C**–Northern Minnesota and Wisconsin (includes Kabetogama state forest), **D**–Chicago, IL region, **E**–Northern New England (Maine, New Hampshire, Vermont and Massachusetts) where blue represents the Boston, MA region, **F**–Pennsylvania and New Jersey, **G**–Chesapeake, VA region, **H**–Huntington, WV region, **I**–Saint Louis, MO region, **J**–Monroe, LA region (includes Upper Ouachita National Wildlife Refuge), **K**–Carson and Gila National Forests, NM

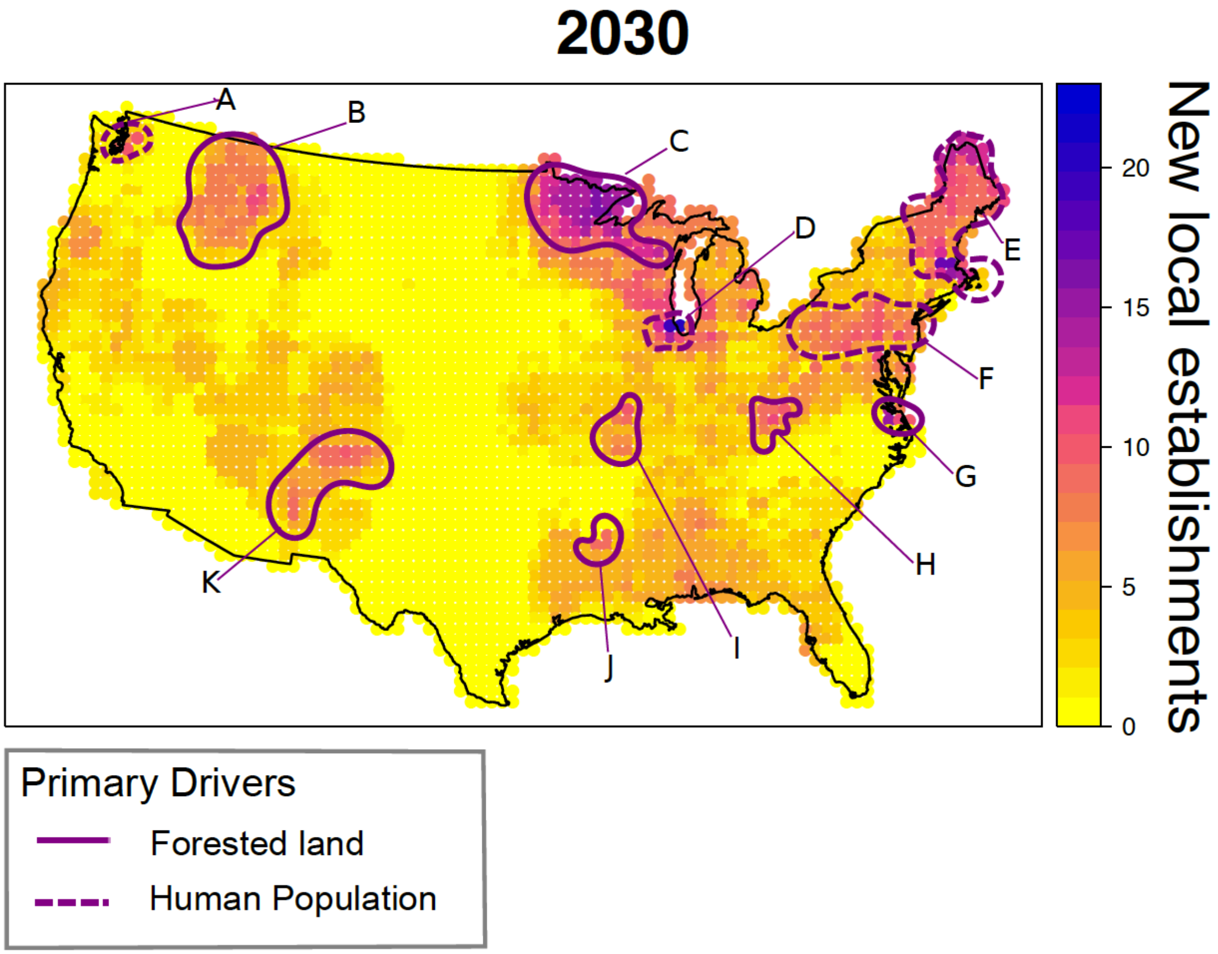

Figure 2.5 Projections of combined SDK uncertainty at 2030 (range of predicted pest richness at each site) arising from two climate change scenarios (rcp2.6 and rcp8.5 BIOCLIM scenarios), two alternative population growth scenarios (SSP3: “Regional Rivalry”, SSP: “Fossil-fueled Development), and from a sensitivity analysis of model parameters (see Appendix S2.6).

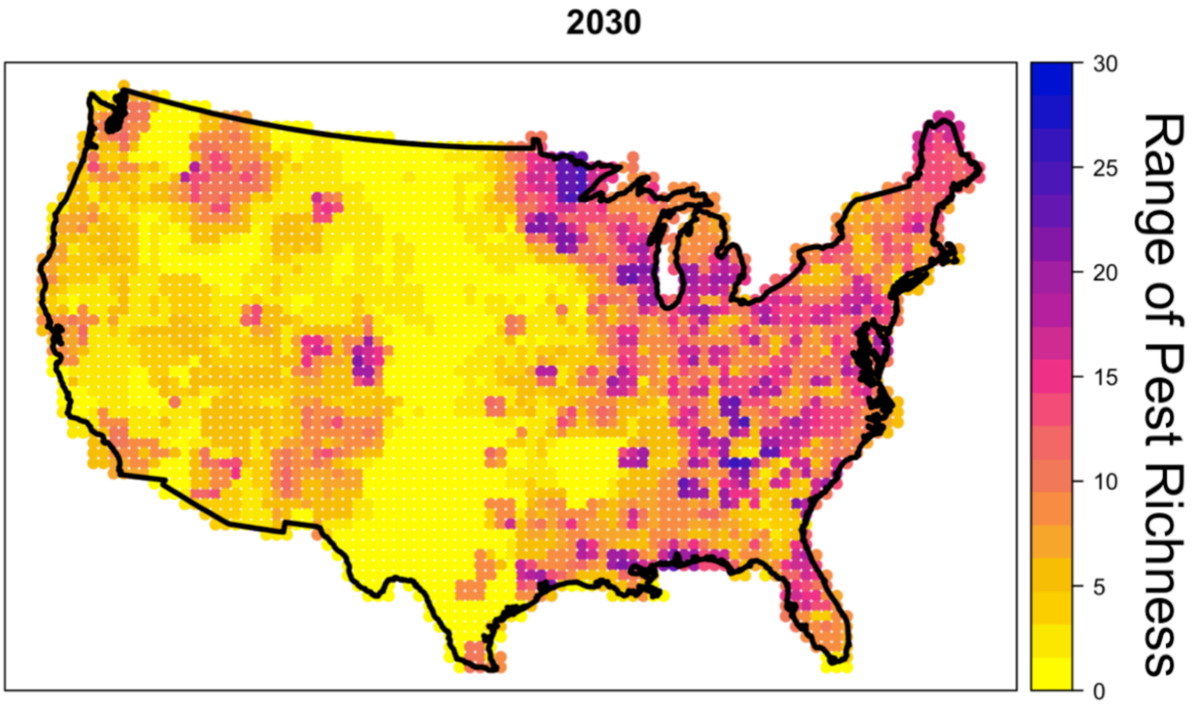

2.9.2 Tables

Table 2.1 The best fitting single-species models for hemlock woolly adelgid (HWA), gypsy moth (GM) and beech bark disease (BBD). Predictor variables labelled “in” represent predictors of dispersal into sites. In all cases, the best model simulated spread initiating at the most likely initial invasion of the pest rather than the centroid of the host range. Bio6 represents a fitted minimum temperature threshold for HWA mortality.

	Kernel	**ϕ**	**δ**	**α**	**Predictor(s)**	**MET (km)**	**R^2_{om}**
HWA	negative exponential	0.0020	2.48	2.93	human population (+ in) = 0.19; bio6 = -9.33°C	11.10	0.45
GM	leptokurtic	0.0046	4.60	5.14	income (- in)= 1.19	9.82	0.92
BBD	negative exponential	0.0008	1.27	1.37	NA	11.37	0.86

Table 2.2 The results of the GDK validation for both uncorrected and intercept-corrected models. All GDK models have parameter values of forested land area (+ in) = 0. 53, tree density (- out) = 15.61, human population density (+ in) = 0.16, human population density (- out) = 0.32, $\phi = 0.00054$, $\delta = 1.30$.

	α	**MET (km)**	R^2_{om}
uncorrected			
HWA	1.74	33.22	0.30
GM	1.74	41.26	0.87
BBD	1.74	110.01	0.55
intercept-corrected			
HWA	1.65	31.17	0.20
GM	2.25	8.94	0.98
BBD	3.95	10.13	0.87
starting point-corrected			
HWA	1.74	32.14	0.73
GM	1.74	18.16	0.92
BBD	1.74	1.70	0.89
starting point, intercept-corrected			
HWA	1.48	24.84	0.35
GM	1.61	2.55	0.98
BBD	1.78	1.35	0.89
starting point, intercept, climate-corrected			
HWA	1.47; bio6 = -7.64°C	1.75	0.85

Connecting statement

In Chapter 2, I built customized spread models for three invasive forest pests based on their individual year-to-year detection records, compared the predictive power of these models to the GDK, and created intermediate models that combined the GDK with simple species-specific corrections. Using the same procedure as the GDK, I built dispersal models of each of these species separately, which we call customized models. I fit these models on single-species timeseries. I also tested additional dispersal kernel shapes, initial invasion locations, and additional species-specific predictor variables. As an intermediate model type, I created semi-generalized dispersal kernel models, or SDKs. For the SDKs, I tested the inclusion of three additional layers of species-specific information that went beyond the original GDK. These did not use time series information, so they could be applied to all pest species. I found that the SDK outperformed the other two model types, and thus I was able to create robust predictions of spread for the entire pest community.

Within the SDK, I utilized a species-specific intercept. Species vary in how well the GDK predicts their spread, where some spread faster or slower. If these deviations were consistent, we could use them predictively to scale overall spread rates based on unknown factors. My strong predictive results suggested that general models, such as the Chapter 1 GDK model, could be effectively synthesized with context-specific information for single species to respond quickly to invasions. The SDK dispersal forecasts were used as inputs to Chapters 4, while Chapter 3 disentangled the factors that cause pest species to differ that result in the SDK having a species-specific intercept.

Chapter 3.

A unifying phylogenetic model of amplification and dilution effects of host biodiversity on pest establishment

Authors: Emma J. Hudgins, T. Jonathan Davies, Brian Leung

3.1 Abstract

Invasive pest species cost trillions of dollars globally, and invasion rates are only increasing. Pest managers must work to decrease the number of pests successfully establishing in order to limit the associated ecological and economic effects of these species. A key factor influencing pest secondary establishment is the species composition of the recipient host community, where recipient community diversity may have the potential to buffer against successful invasion (what is known as the dilution effect). However, there has been literature support for an opposing positive (amplification) effect of host biodiversity on pest establishment. The dilution and amplification effects have had mixed support for plant pathogens, potentially due to the conflation of the role of host diversity with sampling processes, density-dependent effects, and correlated spatial patterns of propagule pressure. We modelled whole-community United States forest pest establishment, while controlling for spatially-autocorrelated pest dispersal patterns, to examine phylogenetic factors that may predispose certain areas of the United States to higher probabilities of pest establishment. We demonstrated that when host phylogenetic diversity is measured as dissimilarity from the focal host community, and is modelled synergistically with propagule pressure, richness, and density effects, we could detect a nonlinear relationship between phylogenetic host dissimilarity and pest establishment. When hosts are closely related to focal hosts, the greater their density, the more likely a pest is to establish (amplification), and when hosts are less related to the focal host up a maximum dissimilarity, the greater their density, the less likely a pest is to establish (dilution). Beyond a threshold of relatedness, highly unrelated hosts have negligible impacts on establishment. This nonlinear relationship has not previously been demonstrated, and occurs alongside separable positive species presence effects and spatially autocorrelated pest spread. Further, these patterns are generalizable across the entire

pest community of 72 species ranging from insects to fungi. We show that this result cannot be solely attributed to the higher establishment of phylogenetic generalist pests, or general climatic factors. These results provide a more nuanced picture of the relationship between diversity and infestation, and allow us to predict sites at high risk of future pest secondary establishment. These risk predictions can be used in conjunction with secondary spread forecasts to coordinate management that can buffer against future tree mortality and economic losses.

3.2 Introduction

The number of invasions by non-indigenous forest pests is increasing worldwide due to growing travel and trade (Liebhold 2012), with an average of 2.5 previously unrecognized species establishing in the U.S. annually (Aukema et al. 2010). The cost of these invasions is borne primarily by local governments and residential property owners (Aukema et al. 2011). We have estimated that 8% of all street trees will die from 2020 to 2050 due to currently-established invasive forest pests (~5 million trees), along with 318 million community trees and 59 million residential trees, and estimate costs of 146M USD annually just in terms of tree removal and replacement costs of dead street trees (Hudgins et al., Ch.4). After the successful invasion of a new area by an invasive species, secondary invasions consist of three phases: the arrival of individuals to a new location within the invaded range, their establishment at that location, and their spread to subsequent areas (Elton 2000). While arrival is critical, species may not establish even if they succeed in reaching an area (Simberloff & Gibbons 2004). Modelling this process touches upon many fundamental ecological questions, such as the role of evolutionary history, habitat suitability, and competition in structuring communities, and the ecological consequences of preserving biodiversity.

In a previously published model based on the same data (Hudgins et al. 2019), we discovered that pest species had consistent deviations in their spread rates from general expectations. Previously, we used these deviations predictively to scale pest species-specific spread rates based on unknown factors (SDK, Hudgins et al. 2019). However, these pest-specific deviations could very well have been due to differences in secondary establishment success, which operates as a filter on invasive propagule success after secondary spread (Simberloff & Gibbons 2004). Beyond pest traits that cause overall higher or lower rates of secondary establishment, there are likely general spatial factors that impact pest establishment at a given site. Differential pest propagule pressure and preferred habitats across pest species mean that these spatial differences could cause pest-level differences in establishment, and thus different spread rates when spread and establishment are examined jointly. In this paper, we build a joint secondary spread and establishment model to explore general, site-level factors that lead to pest-level differences in secondary establishment.

A key spatial factor influencing pest secondary establishment is the species composition of the recipient host community at a given site. Biodiversity putatively governs a wide range of ecosystem functions and services (Cardinale et al. 2012; Hooper et al. 2012), including the ability to potentially buffer against human and animal disease (Young et al. 2017). The opposing dilution and amplification effects of host diversity have been studied extensively within the epidemiological, animal, and plant disease literature (Ostfeld & Keesing 2012). Dilution occurs when increased host diversity decreases the relative frequency of preferred hosts and subsequently reduces pathogen success (Gilbert et al. 2016). This can happen even when multiple host species are suitable for pathogen persistence, if pest reproductive success (transmission) varies across suitable hosts, since the less favourable hosts divert pest propagules to hosts with lower transmission success (Ostfeld & Keesing 2012). Amplification occurs when increased host diversity promotes pathogen success, for instance in pest species where suboptimal host species can act as transient habitats for pests, thereby extending their persistence in a region until they can disperse to a suitable host for reproduction (Randolph & Dobson 2012).

The effect of host biodiversity on infestation is known to have been shaped by evolutionarily processes across host phylogenetic trees. More specifically, due to the linkage between phylogeny and functional similarity, the probability of plant species being invasible by the same pest declines with evolutionary distance between them (Gilbert & Webb 2007). Rather than coevolution with a particular pest within a native range, broader elements of functional similarity appear to also govern invasibility, because this pattern has emerged for hosts not found in pest species native ranges (Parker et al. 2015). Dilution and amplification effects were originally conceptualized as impacting pathogen abundance within the epidemiological literature (Ostfeld & Keesing 2012). However, host diversity – including phylogenetic diversity – should also moderate the presence/absence of pest species and resulting pest species richness via analogous processes. Parker et al. (2015) found that sites featuring phylogenetically rare host species were less susceptible to invasion by an array of plant pest species (dilution). Conversely, Liebhold et al. (2013) recently examined the factors that predispose certain counties in the United States (US) to higher pest loads, and found that in addition to propagule pressure proxies such as human population density and the length of roads in a county, metrics such as host tree density and host species richness were positively related to pest load (amplification).

The current means of assessing the existence of dilution and amplification effects has produced inconsistent results. This may be because the ways in which diversity is measured can obscure its role in infestation. The primary sources of conflation are due to correlations between focal host presence and total host species richness, between focal host density and total host species richness of phylogenetic diversity, and between spatially-autocorrelated spread patterns and predictors of establishment.

Firstly, total host species richness may be correlated with probability of susceptible host presence, and susceptible host presence may be the key factor driving establishment rather than a direct effect of total diversity (i.e. a sampling effect). This pattern need not reflect of some direct ecological effect of high diversity on establishment. Along these lines, parasite load follows the latitudinal biodiversity gradient globally (Hechinger & Lafferty 2005).

A second, contrasting relationship may exist between high total host phylogenetic diversity or host species richness and reduced density of susceptible host species. This could produce a negative correlation between local diversity and establishment (a dilution effect) for pests with density-dependent infestation patterns (likely the majority of invasive plant pest species, Tobin et al. 2011). Again, this process is not governed by a direct link between biodiversity and infestation (i.e., if a diverse patch instead possessed only two species, but the same density of susceptible hosts, it would have the same probability of infestation), and is instead governed between the simpler link between host density and pest establishment. Conversely, a high density of non-susceptible hosts could interfere with infestation through the more classical dilution mechanism. Thus, not all tree density is equal, and models should ideally distinguish between susceptible and non-susceptible host densities (ideally on a continuum), and the effects that each may have.

When diversity is instead assessed as dissimilarity of a recipient community from a preferred or focal host, dilution effects have been observed. Correlational studies consistently show lower single-pest invasion success in mixed forests compared to monocultures of a preferred host (Jactel & Brockerhoff 2007; Haas et al. 2011). However, we note that these studies are also subject to a confounding focal host density correlation. Experiments have confirmed that for many plant pathogens, higher host phylogenetic dissimilarity (measured as greater phylogenetic distance from a species' preferred host) is associated with lower invasibility (Gilbert & Webb 2007; Parker et al. 2015). Support for the dilution effect in the plant pathogen literature has led to the promotion of the so-called buffering role of host biodiversity against pests (Cardinale et al. 2012; Young et al. 2017), with proposed mechanisms of greater dispersal interference, disruptions of host chemical signals, and the presence of more natural enemies (Cappucino et al. 1998; Jactel et al. 2001; Quayle et al. 2003).

Thirdly, the potential for pest establishment depends critically on the propagule pressure reaching a site. Existing models for the diversity-establishment relationship have failed to control for the spatial signal of pest dispersal (Parker et al. 2015; Guo et al. 2019), and hence may simply be correlated with pest entry sites or sites of high human traffic. The incorporation of an establishment model within a species-specific, spatial spread model could thus further help elucidate the true mechanisms underlying pest establishment.

The parameterization of a semi-mechanistic model of pest infestation that contains separate parameters for tree species richness, each tree species' volume, and each tree species' phylogenetic divergence from a pest's focal host community, that together interact to determine pest establishment after controlling for spread patterns, would allow us to disentangle the major mechanisms governing the secondary establishment of all invasive forest pests across the US. We hypothesized that when host phylogenetic diversity is modelled in concert with propagule pressure, host richness, and host density effects, we would be able to detect a separable phylogenetic host relatedness effect on pest establishment. We predicted that we would observe an amplification effect (higher probabilities of pest establishment) due to greater densities of closely-related host species, and a dilution effect (lower probabilities of pest establishment) due to greater densities of distantly-related host species.

3.3 Methods

3.3.1 Data sources

Data were obtained for all economically damaging invasive forest pests in the US, which consist of 72 economically damaging insect and fungal pathogen species and 294 of their host tree species (Aukema et al. 2010; Liebhold et al. 2013; Table S3.1.1). Spread model parameters were obtained from an existing spatial model of whole-community US pest spread, the GDK (Hudgins et al. 2017). Host tree distributional information came from the Forest Inventory and Analysis Program (FIA, Miles et al. 2001), which accounts only for tree species in forested areas. We standardized county-level pest and host tree data to a 50x50km grid to coincide with the scale of the spread model. A pest was considered successfully established within a cell if it was found in any county that made up the grid cell, and total host volume (m^3 of tree biomass) within a county was assigned proportionally to the area a county occupied within each grid cell, therefore assuming an even distribution of trees within each county.

3.3.2 Phylogenetic analyses

The host phylogenetic tree was created by inputting the host species list into Nix (http://phylodiversity.net/nix/), which creates plant taxonomies by querying the ITIS taxonomic database (Bigsby et al. 2006). The Nix output was then entered into Phylomatic v3 (http://www. phylodiversity.net/phylomatic/, Webb & Donaghue 2007) to create a phylogenetic tree in Newick format based on the taxonomy using the Zanne et al. (2014) molecular phylogeny for seed plants. Phylogenetic information was found for all 294 host tree species (Appendix S3.2).

3.3.3 Establishment model

We wished to create a single model for the establishment of invasive species that brought together previously studied mechanisms. We began by deriving an integrative model that simultaneously included the three major factors highlighted in the existing literature (host species richness, density, and phylogenetic divergence), which could result in relations between host diversity and pest establishment. We tested this model against simplified special cases and competing structures in order to determine our best hypothesis for the mechanisms driving pest establishment. Later, output of this establishment-only model was inputted into a previously published pest spread model (the General Dispersal Kernel or GDK model, Hudgins et al. 2017; 2019) as an offset to predicted propagule pressure at each timestep to create the best integrative joint model for secondary establishment and spread.

In formulating our integrative establishment model, we wished to recapture the most likely mechanisms for both amplification and dilution emerging from the synthesis of the previous literature. That is, an amplification effect of closely related species, and a dilution effect of distantly related species, as a function of their density. This could be captured through a term that allowed additional trees of closely related species to increase establishment probabilities, while additional trees of unrelated species decreased establishment probabilities. Standard GLM formulations of site-level suitability would have conflated all host density, or would have required a binary choice between hosts and non-hosts. In contrast, a more process-based formulation could help to distinguish hosts that would amplify establishment with their density, from those that would dilute establishment, along a continuum. The formulation of amplification and dilution as a smooth continuum was critical for our integrative framework, as it allowed us to understand the split within the literature as being due to a focus on either end of this spectrum. We predicted that increased suitable host density would have a positive effect that increased with proximity to focal host species, potentially levelling off for species with many highly susceptible hosts. In contrast, increased unsuitable host density was predicted to have a negative effect that increased with dissimilarity from focal hosts, potentially becoming negligible beyond some level of dissimilarity for entirely non-susceptible hosts (Figure 3.1a-d, Table 3.1a). Beyond these mechanisms, alternative findings in the literature, which we believed were merely correlates of this mechanism, could emerge as special cases, such as the sufficiency of focal host presence (Parker et al. 2015), density (Guo et al. 2019) or species richness (Liebhold et al. 2013) to explain pest infestation patterns (Figure 3.1e-g; Table 3.1b).

3.3.4 Mathematical formulation

While simpler generalized linear models linking diversity and establishment are possible, we chose a more process-based formulation for our model that operated at the tree species level at each site. We believe this choice helps us better elucidate the true process of establishment, since it operates at the level of host trees. We modelled pest establishment based on principles of mass action that underly foundational epidemiology (Wilson & Worcester 1945). According to mass action, infestation increases with contact rates between hosts and pests as a function of their population sizes (proxied by host tree volume and expected pest propagule pressure, respectively), and is a random process. This formulation implies independence across pest species. This was a fairly reasonable assumption, as there are a very large number of trees at each invaded site, and the few pest species that share focal hosts only rarely overlap in their distributions across space and time (Aukema et al. 2010; 2011). The resulting probability of pest establishment from this integrative model was then combined with spread predictions within the GDK architecture. Our integrative joint model predicted spread and establishment simultaneously by fitting a rescaling factor for the GDK-predicted relative propagule pressure of each pest at each site based on fitted establishment model output. We used only relative propagule pressure in this analysis and estimates of tree volume. As such, while the integrative joint model is proportionally reflective of the process occurring at the individual propagule level, parameters should not be interpreted as those relating to individual pests and trees.

We related the probability of a site being invasible to the volume of trees of each species and the phylogenetic dissimilarity of each host tree species to a particular pest's focal host community. For each pest (*i*) and host (*t*) species combination, we determined the minimum pairwise phylogenetic distance between each US tree species and the entirety of a given pest species' known community of US focal hosts ($\mathrm{minpd}_{i,t}$, Aukema et al. 2010). This amounted to taking the minimum of all possible pairwise combinations of a particular pest's focal hosts and a given tree species. In the case of focal host presence, this distance was zero. To control for the positive relationship between the number of focal host species of a particular pest and the portion of the phylogenetic tree spanned (Tucker et al. 2017), we transformed these minimum pairwise distances into z scores via a null model ($\mathrm{minpd}_{z,i,t}$). In this null model, we produced 10,000 random focal host assemblages of the same size (number of host species) from the set of host tree species that had at least one occurrence within each pest species' known host range based on FIA. We then calculated the minimum pairwise distance of these random draws to that pest's focal host community. We took the mean and standard deviation of the 10,000 random draws and used these to standardize our observed pairwise distance estimates ($minpd_{zi,t}$=($minpd_{obs,i,t}$-mean($minpd_{null,i,t}$))/σ($minpd_{null,i,t}$)). Species whose hosts are less phylogenetically clustered (phylogenetic generalists) possess a lower mean and maximum minpd than specialists, and therefore have lower-magnitude $minpd_z$ values (i.e., focal hosts of generalists and specialists both have raw minpd values of zero, but these are rescaled to more negative $minpd_{z,i,j}$ values for specialists than generalists). This behaviour is consistent with our expectation that the dilution and amplification effects will be the strongest for specialist species (Gilbert et al. 2016; Guo et al. 2019).

The species-specific probability of a single pest propagule of species *i* establishing at a given site *j* was modelled as:

$$p_{estab_{i,j}} = 1 - a_1 e^{-z_{i,j}} \tag{3.1}$$

Where a_1 is an intercept term corresponding to the mean probability of non-establishment across all sites, and $z_{i,j}$ is the relative probability of establishment of site *j* for pest species *i* based on the recipient host community, calculated based on the contribution of all host species to establishment:

$$z_{i,j} = \sum_t z_{t_{i,j}} \tag{3.2}$$

$$z_{t_{i,j}} = \begin{cases} a_2 + \left(V_{t,j}{}^{(c_1 + c_2 s_{i,t} + c_3 s_{i,t}{}^2)}\right), & V_{t,j} > 0 \\ 0, & V_{t,j} = 0 \end{cases} \tag{3.3}$$

Where $V_{t,j}$ is the tree volume of a particular host tree species *t* at site *j*, and $s_{i,t}$ is a $minpd_{z,i,t}$ term for a given host/pest-species combination, calculated as:

$$s_{i,t} = \frac{1}{1+e^{-minpd_z}} \tag{3.4}$$

This logit scaling allowed susceptibility to have an influence ranging between 0 and 1, and improved identifiability and fit of our model relative to other formulations. Since our grid size is constant, volume and density are proportionally equivalent in these models. The constant a_2 is added based on presence of each given tree species at a site. When a_2<0, negative density dependence can cause tree species presence to have a more negative impact on pest establishment than tree species absence ($z_{t_{i,j}} < 0$) for some maximum volume $V_{t,j}{}^{(c_1+c_2 s_{i,t}+c_3 s_{i,t}{}^2)} < -a_2$, though we note that a positive effect of species presence ($z_{t_{i,j}}$>0) is possible for any species with a volume that satisfies $V_{t,j}{}^{(c_1+c_2 s_{i,t}+c_3 s_{i,t}{}^2)} > -a_2$.

The *c* terms acted as shape parameters to allow for nonlinear relationships with tree density (c_1) and phylogenetic relatedness (c_2, c_3) (Fig. 3.1). In this equation, the term $z_{t_{i,j}}$ can be conceptualized as an 'effective volume' of host trees for a given pest. We predicted that closely related tree species would exhibit positive density dependence (high effective tree volume), while distantly related species would exhibit negative density dependence (low effective tree volume). In the case of $c_2 > 0$, $c_3 \geq 0$, higher tree volume and higher susceptibility values increase the effective tree volume, while volume of lower-susceptibility trees is converted to lower or even negative effective tree volume (Fig 3.1a-b).

Since phylogeny is a proxy for functional similarity, there may be limits to the impact a host species has on invasibility if it is highly dissimilar to the focal host community. Alternatively, generalist pests may tolerate all hosts above some minimum relatedness. These effects can be captured in the second-order term (c_3), which allows for density dependence to have differential strength for closely-related hosts compared to distantly related hosts (Fig 3.1b-d). In addition to an accelerating positive density dependence as relatedness increases (Fig 3.1b), positive density dependence may level off at some maximum relatedness beyond which all hosts are similarly susceptible (Fig 3.1c), or highly unrelated species may contribute negligibly to invasibility compared to less distantly-related hosts that may divert more propagules from focal hosts (Fig 3.1d). The evidence of non-linearity was tested empirically when analyzing the importance of model terms (see below). We bounded this equation between 0 and 1 by forcing p_{estab} values above and below this range to 0.0001 and 0.9999 respectively, to ensure the outcome could be represented as a probability.

The overall likelihood across all pest species and sites was:

$$L(\theta|y) \propto p(y|\theta) \propto \prod_i \prod_{j\in k} p_{estab_{i,k_i}} \prod_{j\in l}(1 - p_{estab_{i,k_i}}) \qquad (3.5)$$

Where θ are the model parameters, and y are binomial distributional data of all pests i, including presence sites k_i and absence sites l_i. The calculation of a single likelihood meant that pests with greater host ranges contributed more strongly (which was reasonable, because we had more distributional information through which we could assess establishment patterns for these species), and the use of species-independent parameters constrained all relationships to be equivalent across species.

The integrative establishment model was fit via maximum likelihood through R's *optim* function (R Core Team 2020). $V_{t,j}$ was converted to 10000m^{-3} units to aid comparison of relative parameter influence. The significance of model terms was analyzed by comparing simplified models in order to examine the importance of density, richness, propagule pressure, and phylogenetic diversity via Likelihood Ratio Tests (Table 3.2). Models were also compared in terms of their percent difference in deviance explained in comparison to an intercept-only model (null deviance), and the relative importance of terms was examined in a Type III test (Zar 1999).

We fit the integrative establishment model parameters separately from the spread model, assessed their ability to capture pest distributional patterns without controlling for spread, and then incorporated the establishment model predictions into the spread model containing its previously fitted parameters (Hudgins et al. 2017; 2019) through an offset term to determine the explanatory power of the integrative joint model.

The spread model originally formulated relative propagule pressure dynamics at each 5-year timestep as:

$$PP_{i,j,c+1} = (PP_{i,j,c} - \sum_m T_{i,j,m} PP_{i,j,c} + \sum_k T_{i,k} PP_{i,k,c})\,\delta \tag{3.6}$$

The relative propagule pressure (PP) of pest i in cell j at timestep c+1 was equal to the relative propagule pressure at time c, minus dispersal (T) to all cells m, plus dispersal from all cells k, multiplied by the growth rate (δ=1.30*).* Cells were considered 'presences' capable of being a source of propagules when they were above a threshold population size (ϕ = 0.00054) with a maximum relative propagule pressure in a cell of 1.

The original spread model was fit by restricting potential spread to the focal host range of each pest species. However, we removed this restriction, because the goal of the current analysis was to explicitly model the role of host diversity, richness, and density in impacting the establishment process. We assumed that our previously-fitted model parameters were reflective of the general mechanism of spread. Establishment thus acted as a second filter on pest presence, determining reproductive success following propagule arrival. In our integrative joint model, we rescaled the relative propagule pressure (PP) of each pest species i at site j by the establishment probability at that site at each time step:

$$PP_{i,j,c+1} = (PP_{i,j,c} - \sum_m T_{i,j,m} X_{i,j,c} + \sum_k T_{i,k} X_{i,k,c})\,\delta * (B_0 + B_1 * p_{estab_{i,j}}) \tag{3.7}$$

B_0 was an intercept term to offset over/underprediction in p_{estab} when applied outside of the focal host range, and B_1 was a slope term for the impact of the integrative establishment model. We used the GDK's fitting metric, MET (Aslan & Zech 2005, Hudgins et al. 2017) to fit B_0 and B_1, and evaluate the improvement of incorporating the integrative establishment model into the integrative joint model. We optimized based on MET rather than a likelihood due to the binary nature of the output of the GDK, which is not amenable to classical likelihood approaches. We also present our previously-published pseudo-R^2 metric, as a more intuitive descriptive measure of spatial variation explained (R^2_{om}, Hudgins et al. 2019). None of the standard optimization schemes can guarantee global optimality for this type of multimodal problem over a reasonable time window, and many stochastic approaches can be very computationally intensive, but steps can be taken to avoid local minima (Xiang et al. 2013). To verify we achieved model convergence, we repeated our optimization with our updated parameter set until the outputted MET score was constant across iterations.

3.3.5 Special case models

As noted above, the establishment model structure has a series of nested special case models (Table 3.1b). The simplest of these is a null model where trees have no impact, $p_{estab_{i,j}} = 1 - a_1$. If only richness impacted establishment, an intercept would suffice, such that z_{t_j}=a_2. Another simple case is one where all trees are equivalent in their impact on establishment, such that the effective trees term for each tree species is z_{t_j}=$a_2 + {V_{t,j}}^{c_1}$. In contrast, if only host trees impacted establishment (no dilution), we would see a steep negative linear impact of minpd$_Z$, and no impact of tree presence (a_2, c_1=0). In addition to these special cases, the examination of additional factors requires only the addition of a similarly formulated term to those included in the model. Any additional tree species-specific factor can be added to the z_{t_j} component, any site-specific factor can be added to z_j outside the species-specific summation, and any pest species-specific factor can be added to the intercept a_1.To ensure our model's parameters could be reliably identified, we performed theoretic simulations where we assessed identifiability by fitting our model to simulated data and comparing predicted and simulated (true) parameter values (Appendix S3.3).

3.4 Results

3.4.1 Integrative establishment model

The impact of phylogenetic diversity within the integrative establishment model was as expected from first principles: The functional form was a parabola similar to Fig. 3.1d, where more related species had positive density-dependent effects on the number of effective trees, while more unrelated species had negative density-dependent effects (Table 3.2, Fig. 3.2). The non-linear relatedness term contributed substantially to model fit based on Type III tests (Table 3.2), indicating phylogeny had a saturating impact on dilution below a threshold of relatedness. Interestingly, species presence had a baseline positive effect across all species ($z_{t_{i,j}} > 0$ even as $V_{t,j} \rightarrow 0$), indicating that sites with higher species richness have greater establishment than less diverse sites when closely-related host volume is high and unrelated host volume is low. In this model, tree species presence has a more negative effect on pest presence than tree species absence ($z_{t_{i,j}} < 0$) for tree volumes above $(-a_2)^{\left(\frac{1}{c_1+c_2 s_{i,t}+c_3 s_{i,t}{}^2}\right)}$(blue and purple regions, Fig. 3.2). At the parabola's vertex (susceptibility ~0.1625), this maximum effective volume is 6 423 m^3/km^2. As susceptibility approaches 0, this value is 20 649 m^3/km^2, and all tree volume begins to have a positive density-dependent effect at a susceptibility of 0.42 (yellow region, Fig. 3.2).

This model explained 6.21% of the deviance in pest distributions across all species compared to an intercept-only model before being incorporated into the integrative joint model (Table 3.2). Based on theoretic analyses, we have confidence in our derived ‘maximum effective trees’ values, the overall signs of effects, and the shape of fitted relationships such as Fig. 3.2 (Appendix S3.3).

3.4.2 Special case models

In addition to the intercept-only null model, we assessed the fit of some additional nested null model structures (Table 3.1b). A model where only richness impacted establishment ($z_{i,j} = a_2$) had 2.34% deviance explained. This model had a very slight positive effect of species richness ($a_2 = 0.0051$). A model where all tree volume contributed equally to establishment ($z_{t_{i,j}} = a_2 + {V_{t,j}}^{c_1}$) had 2.41% deviance. In this model, tree presence had a near-zero positive effect ($z_{t_{i,j}} > 0$ even as $V_{t,j} \rightarrow 0$) and density dependence was overall slightly positive ($c_1 = 0.00058$). The deviance explained by this model implies that phylogeny is responsible for the majority of predictive power of the integrative establishment model (61% of the overall 6.23% deviance explained). These models had findings consistent with previous analyses of the same dataset (Liebhold et al. 2013, Guo et al. 2019, Fig. 3.3).

3.4.3 Spread model synthesis

Examination of the spatial residuals of the integrative establishment and spread-only models showed clear opposing spatial structure (Fig. 3.4a-b), indicating that a synthesis of the two models could result in improvements in fit. We found that integrative establishment model inclusion within the spread model (the integrative joint model) improved the fitting metric (MET score) by 14.9%, and improved the % spatial variation explained (R^2_{om}) by 7.5%. The fitted intercept shifted spread-only model predictions downward to account for overall overprediction when not restricting to focal host ranges (B_0=0.93), and the integrative establishment model probability had a positive effect (B_1=3.08). The residuals of the integrative joint model showed decreases in the northeast and interior US, but continued to demonstrate spatial patterning with a clear East-West regionality (Fig. 3.4c).

3.5 Discussion

3.5.1 Integrative establishment model

We have shown how dilution and amplification effects can be unified in a single model by weighting host density by phylogenetic dissimilarity. Our results suggest that, rather than community structure being governed primarily by dilution or amplification, both dilution and amplification occur at differing degrees of host relatedness. This general, nonlinear relationship between phylogenetic dissimilarity and establishment substantially improved pest distributional predictions beyond a spread-only model (improvement in R^2_{om} of the integrative joint model vs. spread model alone =7.5%). After controlling for spread patterns, pest establishment is highest in areas with a high number and high volume of tree species that are highly related to a pest's focal host community ($s \sim 1$). Pest establishment is lowest at sites with high volumes of unrelated hosts ($0<s<0.42$, purple and blue regions, Fig. 3.2), with a peak negative impact at $s=0.1625$ (vertex of Fig. 3.2). At the same time, species presence always has a positive effect for any tree species as its volume tends to zero, indicating that up to some threshold volume, the presence of any additional tree species at a site is beneficial.

Higher species richness could be indicative of the presence of diverse microclimates for a large number of species of all kinds (the "diversity begets diversity" hypothesis, Fridley et al. 2007; Hechinger & Lafferty 2005), or that habitats are not specialized enough to support natural enemies of pest species compared to sites with only focal hosts. These beneficial effects could be overtaken by negative density dependence in cases of higher tree volume of less-related species due to conventional dilution mechanisms *sensu* Gilbert & Parker (2016). Other mechanisms for negative density dependence include higher-level trophic effects, such as a greater diversity of food sources for natural enemies of pests. In contrast, sites with a low richness and a low volume of highly related hosts may indicate a strong impact of biotic filtering at a given site, which may coincide with a harsher climate for pest establishment (Kraft & Ackerly 2014).

3.5.2 Comparison with previous work

In a recent paper using the same dataset, Guo et al. (2019) found that pest richness was highest in regions with moderate levels of host diversity, with an underlying positive correlation between pest richness and focal host richness, compared to a triangular negative relationship between pest diversity and non-focal host tree diversity. All pests and hosts were examined together, so it was difficult to distinguish whether these patterns are emergent properties at the level of pest richness, or whether they operated on a single-pest level. Additionally, this type of analysis does not allow for the separation of the impact of host density from the role of phylogenetic diversity in pest establishment, nor does it account for spatial autocorrelation due to pest dispersal.

On the surface, our findings appear to conflict with the Guo et al. model of pest species richness (2019). However, we would have found the same patterns with richness in our analysis had we not examined density concurrently, since intermediate richness sites contain the highest focal host volumes, which coincide with the greatest pest species richness (Fig. 3.3). In contrast, we found that there was a potential for the presence of any additional tree species to have a positive effect on establishment up to some maximum volume. Within our integrative framework, we can attribute the nonlinearity previously deemed to be due to host species richness to phylogenetically-mediated density dependence.

We demonstrated a nonlinear impact of relatedness on establishment, where maximum dilution occurs at a nonzero level of relatedness (s=0.1625), beyond which dilution becomes less extreme (purple region, Fig. 3.2). Analogous nonlinearities have been uncovered in several related systems. These include a hump-shaped relationship between host-specific disease mortality and divergence times from focal hosts (Farrell et al. 2019), and a hump-shaped relationship between the probability of high economic pest impacts and divergence times between native range hosts and invasive range hosts (Mech et al. 2020). In our case, we hypothesize that dilution is most important when there is some functional similarity between host species, and that entirely unrelated hosts may be less likely to divert propagules.

3.5.3 Alternative mechanisms

As we mentioned in the introduction, our model can easily be extended with additional pest, host, or site-specific parameters. We formulated several model extensions to explore competing hypotheses for the results obtained, including phylogenetic generalism, hotspots of climatic suitability, and regional differences based on forest type (Appendix S3.4). We found some support for higher establishment rates for generalist pests, and some evidence of differences in invasibility between angiosperms and gymnosperms. We note that none of these additional mechanisms could account for the observed nonlinear impact of phylogenetic dissimilarity.

3.5.4 Limitations and future directions

We acknowledge that there are other possible functional forms for the establishment process, but we chose this particular structure to ensure that our models were nested, i.e. that when parameters were insignificant, the model structure reduced to a simplified form of the overall model (for instance, when establishment is driven entirely by richness, c_1,c_2,c_3,=0). We also argue that our formulation of the density term is much more process-based than a traditional density dependence term, which treats all tree species equally. Our use of minpd assumes that all identified focal host species are equally capable of supporting the pest species. However, substantial uncertainty exists regarding host quality within this dataset. We tested an alternative metric, mean pairwise distance (mpd_z, Tucker et al. 2017), and found that the mpd model was less predictive (deviance explained = 3.41%).

Our analysis is at the 50x50km scale, while previous work has spanned forest plot to country scales (Gilbert & Webb 2007, Guo et al. 2019). This scale allowed us to model establishment at the same scale as our spread model. However, we acknowledge that different relationships to host relatedness and density may exist at smaller spatial scales.

We did not fit the spread and establishment model parameters simultaneously, and instead relied on a fitted spread and integrative establishment model parameters as input into the integrative joint model, and fit only an offset. This meant that some factors important for establishment could have been misattributed within the spread model (e.g. the MET score/ R^2_{om} of the spread model could be in part due to collinear factors linked to establishment such as host volume or phylogenetic dissimilarity), and vice versa. This misattribution should have limited the impact of the integrative establishment model's inclusion within the integrative joint model, and therefore should have decreased our power. We showed that incorporating the integrative establishment model within the GDK architecture substantially improved pest distributional predictions beyond a spread-only model (improvement in MET and R^2_{om} of the integrative joint model vs. spread model alone =14.9%; 7.5%). We attempted to perform simultaneous fitting of both processes, but the resulting model was highly computationally intensive, and suffered from severe lack of identifiability of predictors of spread versus establishment.

This analysis was conducted on the known set of US (invasive range) focal hosts of these pest species. However, the process of spillover is typically modelled in relation to host communities within the native range (where the pest evolved). We know of only a few gymnosperm pest species where this set of species has been characterized (Mech et al. 2020), but believe that testing whether distance from this community produces a better-fitting model is an important extension of the present work.

3.5.5 Conclusion

To limit the grave consequences of invasive pest species, we must understand the factors that increase their establishment success in new environments. While recipient community diversity has been studied extensively as one of these factors, previous work has been unable to distinguish the multiple mechanisms that combine to link host prevalence and relatedness to pest establishment. These include host species richness, density dependence, the link between evolutionary relatedness and establishment success, and the confounding spatially-autocorrelated patterns of propagule pressure. In this analysis of whole-community US forest pest establishment, we separated these four processes and detected a novel, nonlinear relationship between phylogenetic host dissimilarity and pest establishment. We found that density-dependent amplification occurs when hosts are phylogenetically closely related, and density-dependent dilution occurs when hosts are phylogenetically distant. This result cannot be explained solely by a greater ease of generalist pests to establish, but appears to be driven by climatic or other host biotic factors beyond the scope of this analysis. This general pattern emerged across all 72 invasive forest pests in the US, thereby highlighting the importance of considering evolutionary history when attempting to understand the occurrence of invasive species, and providing a more nuanced, macroecological picture of the role host diversity plays on pest infestation.

3.6 References

Aukema, J. E., Leung, B., Kovacs, K., Chivers, C., Britton, K. O., Englin, J., ... *et al*. (2011). Economic impacts of non-native forest insects in the continental United States. *PLoS One*, 6(9).

Aukema, J. E., McCullough, D. G., Von Holle, B., Liebhold, A. M., Britton, K., & Frankel, S. J. (2010). Historical accumulation of nonindigenous forest pests in the continental United States. *BioScience*, 60(11), 886-897.

Bigsby, F. A., Ruggerio, M. A., Wilson, K. L., Cachuela-Palacio, M., Kimani, S. W., Roskov, Y., ... *et al*. (2006). *Species 2000 & ITIS Catalogue of Life, Annual Checklist*.

Cappucino, N., Lavertu, D., Bergeron, Y. & Regniere, J. (1998). Spruce budworm impact, abundance and parasitism rate in a patchy landscape. *Oecologia*, 114, 236–242.

Cardinale, B. J., Duffy, J. E., Gonzalez, A., Hooper, D. U., Perrings, C., Venail, P., … *et al*. (2012). Biodiversity loss and its impact on humanity. *Nature,* 486(7401), 59-67.

Desurmont, G. A., Donoghue, M. J., Clement, W. L., & Agrawal, A. A. (2011). Evolutionary history predicts plant defense against an invasive pest. *Proceedings of the National Academy of Sciences,* 108(17), 7070-7074.

Elton, C. S. (2000). *The ecology of invasions by animals and plants*, 2. University of Chicago Press, Chicago, United States.

Farrell, M. J., & Davies, T. J. (2019). Disease mortality in domesticated animals is predicted by host evolutionary relationships. *Proceedings of the National Academy of Sciences*, 116(16), 7911-7915.

Fridley, J. D., Stachowicz, J. J., Naeem, S., Sax, D. F., Seabloom, E. W., Smith, M. D., *et al*. (2007). The invasion paradox: reconciling pattern and process in species invasions. *Ecology*, 88(1), 3-17.

Gilbert, G. S., & Parker, I. M. (2016). The evolutionary ecology of plant disease: A phylogenetic perspective. *Annual Review of Phytopathology*, 54, 549-578.

Gilbert, G. S., & Webb, C. O. (2007). Phylogenetic signal in plant pathogen-host range. *Proceedings of the National Academy of Sciences,* 104, 4979-4983.

Guo, Q., Fei, S., Potter, K. M., Liebhold, A. M., & Wen, J. (2019). Tree diversity regulates forest pest invasion. *Proceedings of the National Academy of Sciences*, 116(15), 7382-7386.

Haas, S. E., Hooten, M. B., Rizzo, D. M., & Meentemeyer, R. K. (2011). Forest species diversity reduces disease risk in a generalist plant pathogen invasion. *Ecology Letters*, 14(11), 1108-1116.

Hechinger, R. F., & Lafferty, K. D. (2005). Host diversity begets parasite diversity: bird final hosts and trematodes in snail intermediate hosts. *Proceedings of the Royal Society of London, Series B: Biological Sciences*, 272(1567), 1059-1066.

Hooper, D. U., Adair, E. C., Cardinale, B. J., Byrnes, J. E., Hungate, B. A., Matulich, K. L., … *et al*. *(*2012). A global synthesis reveals biodiversity loss as a major driver of ecosystem change. *Nature*, 486(7401), 105-108.

Hudgins, E. J., Liebhold, A. M., & Leung, B. (2017). Predicting the spread of all invasive forest pests in the United States. Ecology letters, 20(4), 426-435.

Hudgins, E. J., Liebhold, A. M., & Leung, B. (2018). Corrigendum for Hudgins et al. (2017) https://doi.org/10.1111/ele.12741. Ecology letters, 21(11), 1752-1754.

Hudgins, E. J., Liebhold, A. M., & Leung, B. (2019). Comparing generalized and customized spread models for nonnative forest pests. *Ecological Applications*, 30(1), e01988.

Jactel, H., & Brockerhoff, E. G. (2007). Tree diversity reduces herbivory by forest insects. *Ecology Letters,* 10(9), 835-848.

Jactel, H., Van Halder, I., Menassieu, P., Zhang, Q.H. & Schlyter, F. (2001). Non-host volatiles disrupt the response of the stenographer bark beetle, *Ips sexdentatus* (Coleoptera: Scolytidae), to pheromone baited traps and maritime pine logs. *Integrated Pest Management Review,* 6, 197–207.

Koch, F. H., Ambrose, M. J., Yemshanov, D., Wiseman, P. E., & Cowett, F. D. (2018). Modeling urban distributions of host trees for invasive forest insects in the eastern and central USA: A three-step approach using field inventory data. *Forest Ecology and Management*, 417, 222-236.

Kraft, N. J., & Ackerly, D. D. (2014). Assembly of plant communities. *Ecology and the Environment*, 8, 67-88.

Liebhold, A. M. (2012). Forest pest management in a changing world. *International Journal of Pest Management*, 58(3), 289-295.

Liebhold, A. M., McCullough, D.G., Blackburn, L. M., Frankel, S. J., Von Holle, B. & Aukema, J. E. (2013). A highly aggregated geographical distribution of forest pest invasions in the USA. *Diversity and Distributions,* 19, 1208-1216.

Losos, J. B. (2008). Phylogenetic niche conservatism, phylogenetic signal and the relationship between phylogenetic relatedness and ecological similarity among species. *Ecology Letters*, 11(10), 995-1003.

Mech, A. M., Thomas, K. A., Marsico, T. D., Herms, D. A., Allen, C. R., Ayres, M. P., ... & Liebhold, A. M. (2019). Evolutionary history predicts high-impact invasions by herbivorous insects. *Ecology and Evolution*, 9(21), 12216-12230.

Miles, P.D., Brand, G.J., Alerich, C.L., Bednar, L.R., Woudenberg, S.W., … *et al*. (2001) *The forest inventory and analysis database: database description and users manual version 1.0*. General Technical Report NC-218, North Central Research Station, USDA Forest *2.0*. Service, St. Paul, MN.

Ostfeld, R. S., & Keesing, F. (2012). Effects of host diversity on infectious disease. *Annual Review of Ecology, Evolutions, and Systematics*, 43, 157-182.

Parker, I. M., Saunders, M., Bontrager, M., Weitz, A. P., Hendricks, R., Magarey, R., Suiter, K. … *et al*. (2015). Phylogenetic structure and host abundance drive disease pressure in communities. *Nature*, 520, 542-544.

Quayle, D., Régnière, J., Cappucino, N. & Dupont, A. (2003). Forest composition, host population density, and parasitism of spruce budworm *Choristoneura fumiferana* eggs *by Trichogramma minutum*. *Entomologia Experimentalis et Applicata*, 107, 215–227.

Randolph, S. E., & Dobson, A. D. M. (2012). Pangloss revisited: a critique of the dilution effect and the biodiversity-buffers-disease paradigm. *Parasitology*, 139(07), 847-863.

R Core Team. (2020). R: A language and environment for statistical computing.

Simberloff, D., & Gibbons, L. (2004). Now you see them, now you don't!–population crashes of established introduced species. *Biological Invasions*, *6*(2), 161-172.

Tobin, P. C., Blackburn, L. M., Fleischer, S. J., & Robert, E. A. (2011). Population ecology considerations for monitoring and managing biological invasions. *GIS Applications in Agriculture, Volume Three: Invasive Species*, 29.

Tucker, C. M., Cadotte, M. W., Carvalho, S. B., Davies, T. J., Ferrier, S., Fritz, S. A., ... *et al*. (2017). A guide to phylogenetic metrics for conservation, community ecology and macroecology. *Biological Reviews*, *92*(2), 698-715.

Webb, C. O., & Donoghue, M. J. (2005). Phylomatic: tree assembly for applied phylogenetics. *Molecular Ecology Resources*, 5(1), 181-183.

Wilson, E. B., & Worcester, J. (1945). The law of mass action in epidemiology. *Proceedings of the National Academy of Sciences of the United States of America*, 31(1), 24.

Xiang, Y., Gubian, S., Suomela, B., & Hoeng, J. (2013). Generalized Simulated Annealing for Global Optimization: The GenSA Package. *R Journal*, *5*(1).

Young, H. S., Parker, I. M., Gilbert, G. S., Guerra, A. S., & Nunn, C. L. (2017). Introduced

Species, Disease Ecology, and Biodiversity–Disease Relationships. *Trends in Ecology and Evolution*, 32(1), 41-54.

Zanne, A. E., Tank, D. C., Cornwell, W. K., Eastman, J. M., Smith, S. A., FitzJohn, R. G, McGlinn, D.J., … *et al. (*2014). Three keys to the radiation of angiosperms into freezing environments. *Nature*, 506(7486), 89-92.

3.7 Figures and Tables

3.7.1 Figures

Figure 3.1 Potential relationships between host tree relatedness (s) and the effect of host density on establishment probabilities ($V_{t,i}$ exponent), where blue indicates dilution and yellow indicates amplification across all plots. Hypothesized mechanisms (Table 3.1a): **a.** linear amplification for closely related species and linear dilution for distantly related species ($c_2>0$, $c_3=0$) **b.** nonlinear amplification for closely related species and nonlinear dilution for distantly related species, ($c_2>0$, $c_3>0$) **c.** nonlinear amplification for closely related species peaking at some maximum relatedness (green), and nonlinear dilution for distantly related species ($c_2>0$,$c_3<0$) **d.** nonlinear dilution for distantly related species, with a minimum at some minimum functional relatedness (purple), and nonlinear amplification for closely related species ($c_2<0$,$c_3>0$). Alternative mechanisms to yield previously published results (Table 3.1b): **e.** Host species richness mediated amplification ($a_2>0$) and dilution ($a_2<0$) (no effect of volume or phylogeny), **f.** Total host volume mediated amplification (no effect of phylogeny)**, g.** Focal host volume mediated amplification.

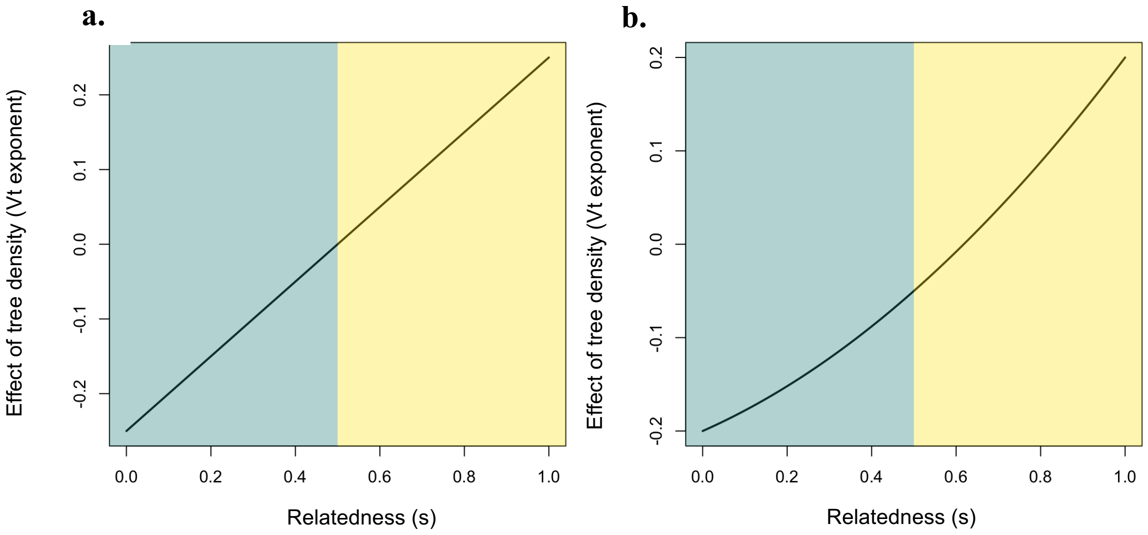

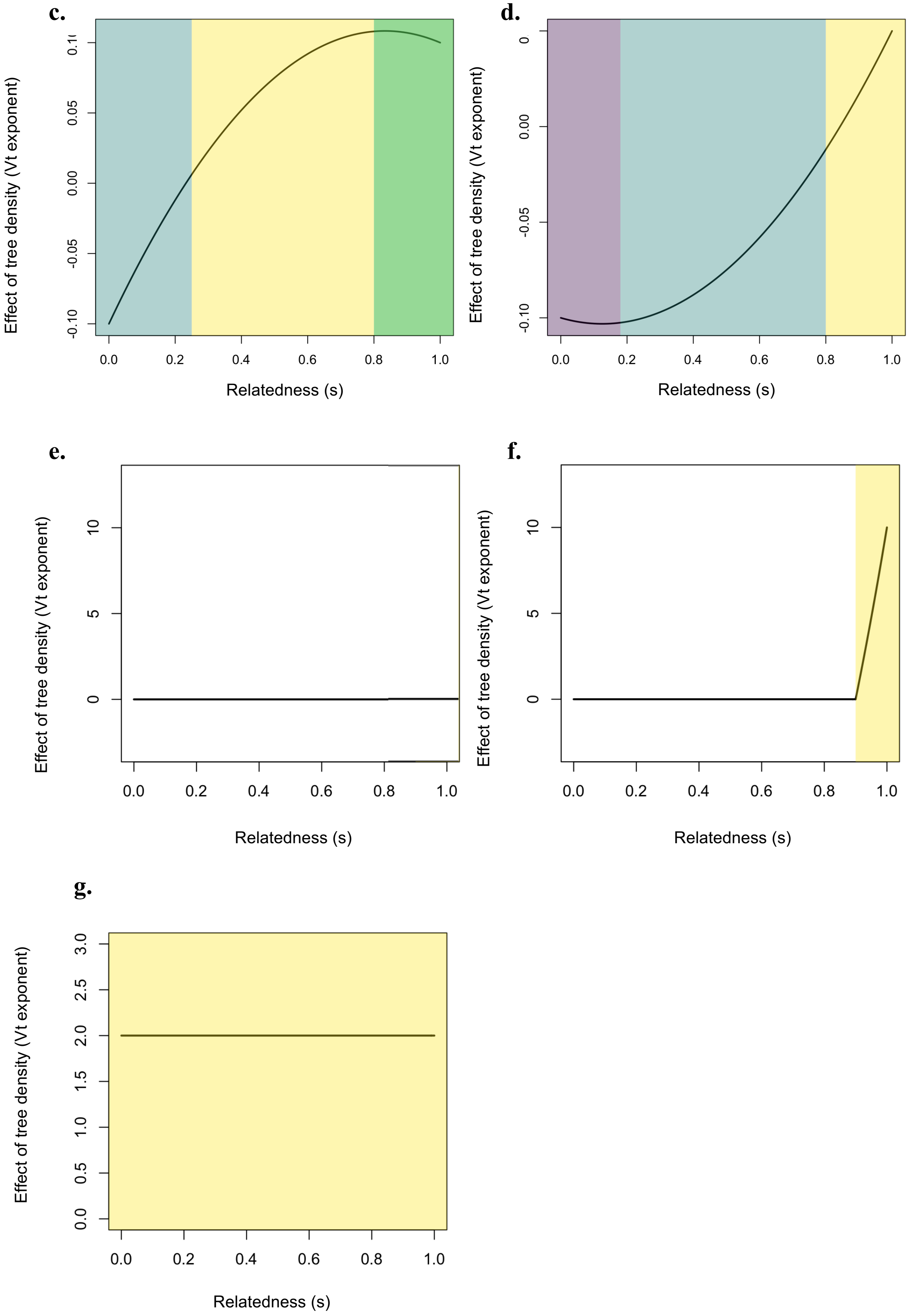
c.
d.
e.
f.
g.
Effect of tree density (Vt exponent)
Relatedness (s)
0.1
0.05
0.00
-0.05
-0.10
0
0.00
-0.05
-0.10
10
5
0
3.0
2.5
2.0
1.5
1.0
0.5
0.0
0.0
0.2
0.4
0.6
0.8
1.0

Figure 3.2 Fitted relationship between the relatedness (s) of trees of a given species *t* to each pest *i* and the effect of increased density of tree species *t* at site *j* ($V_{t,i}$ exponent) in the integrative establishment model. Tree volume contributes positively to establishment for closely related hosts (yellow), while it contributes negatively for distantly related hosts (blue), levelling-off and even slightly increasing for very unrelated hosts (purple), consistent with phylogenetically-based dilution.

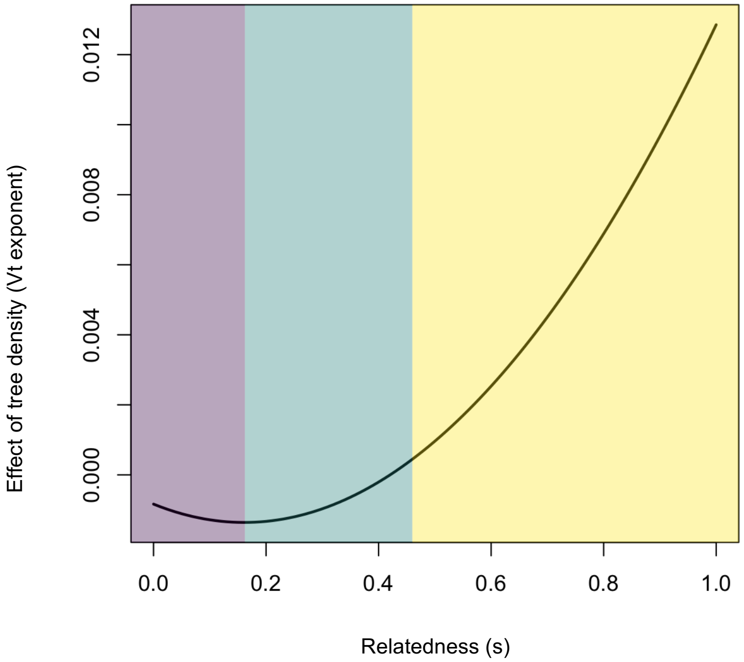

Figure 3.3 Relationship between alternative model proxies (see Table 3.1b) and pest infestation levels, including: **a.** Pest species richness and total host species richness, **b.** Pest species richness and log(total host volume), **c.** Pest species richness and log(focal host volume), and **d.** Host species richness and log(focal host volume).

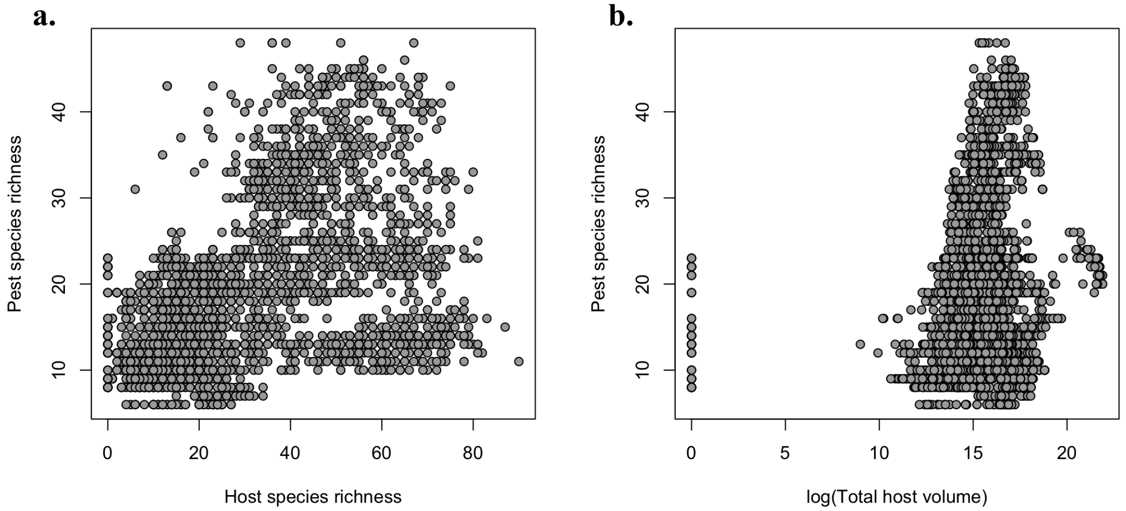

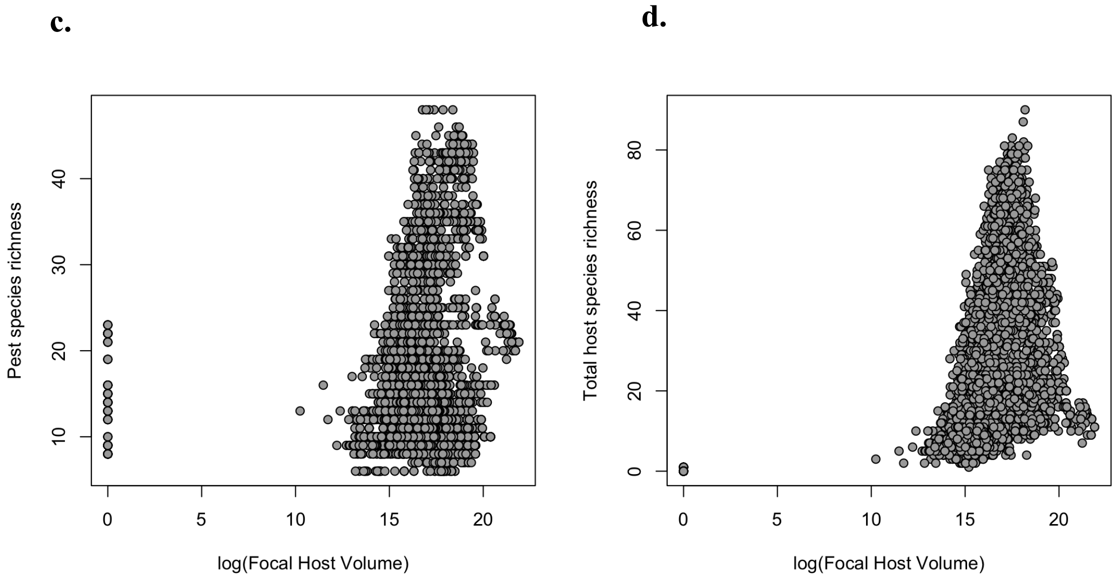

Figure 3.4 Spatial pattern of model residuals, for the spread (**a**) and establishment (**b**) models. Clear opposing patterns are present, indicating a likely benefit with their synthesis. The integrative joint model residuals are shown in (**c**), indicating some persistent spatial patterning, particularly in terms of East-West regionality.

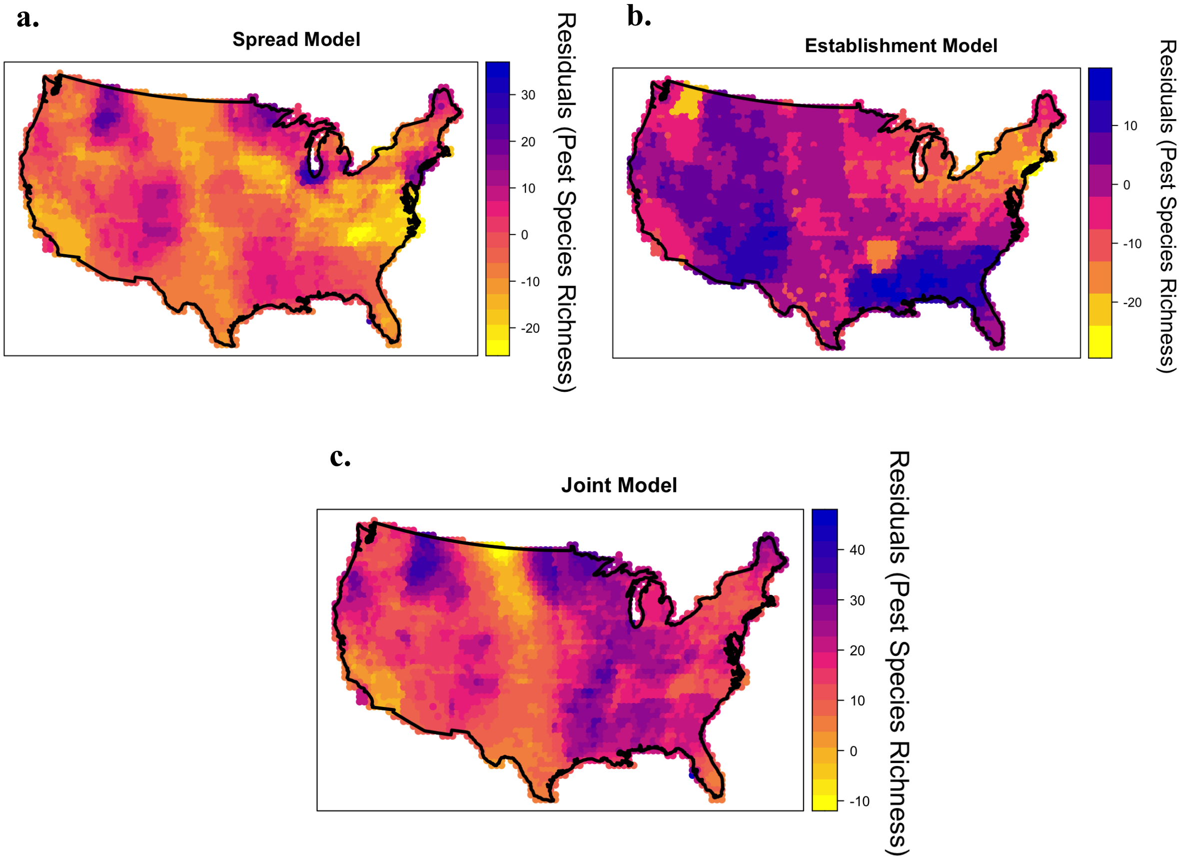

3.7.2 Tables

Table 3.1 Hypothesized relationships between predictor variables and probability of establishment when modelled simultaneously (**a**), and alternative model comparisons (**b**).

a. Integrative model	Term in model	Predicted sign	Predicted relationship with (s)
Focal host density	$z_{t,i,j}$ when $s \approx 1$	+ (amplification)	Fig 3.1a-d
Susceptible host density	$z_{t,i,j}$ as $s \rightarrow 1$	+ (amplification)	
Non-Susceptible host density	$z_{t,I,j}$ as $s \rightarrow 0$	- (dilution)	
b. Alternative models			
Total host species richness only	$z_{t,i,j} = a_2$ $(c_1, c_2, c_3 = 0)$	+ (Liebhold et al. 2013; Guo et al. 2019), or – (Jactel & Brockerhoff 2007; Haas et al. 2011)	Fig. 3.1e
Total host volume only	$z_{t,i,j} = a_2 + V_{t,i,j}$ $(c_2, c_3 = 0)$	+ (Liebhold et al. 2013)	Fig 3.1f
Focal host volume only	$z_{t,i,j} \approx 0$ when $s < 1$ $(c_2 >> 0; c_3 >> 0)$	+ (Liebhold et al. 2013)	Fig 3.1g

Table 3.2. Establishment model results. Significance is examined via Type III Likelihood Ratio Tests (comparing the full model to a reduced model without a given parameter). The overall model log-likelihood was 123809.60, while the null (a_1 only) model likelihood was 132000.23, and overall deviance explained was 6.21%. The last column presents the proportional change in deviance explained for the reduced model.

Parameter	Coefficient	Δ LL	χ^2	p-value	Δ Deviance
c_1	-0.00083	-137.90	275.80	<2e-16	0.10%
c_2	-0.0065	-450.90	901.80	<2e-16	0.34%
c_3	0.020	-1534.70	3069.40	<2e-16	1.16%
a_1	0.89	-4297.78	8595.56	<2e-16	3.26%
a_2	-0.997	-3518.50	7037.00	<2e-16	2.67%

Connecting statement

From the comparison of general and semi-generalized spread models from Chapters 1 and 2, we know that pest species have different spread rates. Rather than summarizing this in an intercept term as in the SDK of Chapter 2, I wanted to tease apart the mechanisms allowing some pests to have greater secondary establishment success than others. Biologists can spend years producing a precise model for the establishment of one species using their idiosyncratic characteristics, but again, more general models allow for early detection and rapid management responses. I focused on the quality of the host range of each species, in terms of the amount and types of hosts present, and asked whether there are general spatial predictors of forest pest secondary establishment.

This general, integrative establishment model was similar in structure to the GDK of Chapter 1 and the urban the tree distributional models of Chapter 4, in that it grouped the general factors responsible for secondary establishment into broad categories: pest traits, host traits, and site traits. These broad groupings are analogous to the pest traits, habitat traits, and propagule pressure proxy variable groupings used to fit the GDK, and the municipal, climatic, and total tree variable groupings used in the Chapter 4 urban tree distributional models.

Chapter 4.

Estimating damage to urban trees from invasive forest pests in the United States

Authors: Emma J. Hudgins, Frank H. Koch, Mark J. Ambrose, Brian Leung

4.1 Abstract

Economic assessments of the impacts of non-native species inform and incentivize cost-effective spending, and should be based on the best available data and most rigorous analysis possible. Urban trees have been identified as the main target of economic damages due to invasive forest pests in the United States, but analyses have been limited due to a paucity of urban tree data and lack of spread and mortality estimates for most forest pest species. We combined new estimates of the tree population in roughly 30,000 US communities, estimates of future tree exposure by incorporating recent species-specific spread predictions for 57 pest species, estimates of host tree death due to pest exposure, and a simple model of management behaviours to produce a spatiotemporally resolved estimate of future damages. We estimate that 8% of all street trees will die from 2020 to 2050 due to invasive forest pests (~5 million trees), along with 318 million community trees and 59 million residential trees. "Mortality hotspot cities" facing the greatest tree mortality are predominantly in the Midwest and include Minneapolis-St. Paul, MN and Milwaukee, WI, though other major cities such as New York City, NY and Seattle, WA will also see major mortality. These patterns are driven by ash (*Fraxinus spp*.) mortality caused by emerald ash borer (*Agrilus planipennis*). We predict that future annualized management costs will range between $84M and $225M USD for street trees alone within our most likely mortality model. Street trees account for only 6.8% of all urban trees, and thus the total urban tree costs could be an order of magnitude larger (~$1.6B annually). We identify two key sources of uncertainty, which greatly affect cost estimates: the magnitude of "mortality debt", which is the temporal lag between when a pest initially infests a community and when it reaches its asymptotic mortality level there; and pest management practices beyond street tree removal and replacement. Fortunately, the former is well characterized for the dominant source of damages

(emerald ash borer), but the latter must be better understood in order to fully understand future costs to US municipalities.

4.2 Introduction

Previous analyses suggest that urban trees are likely to be the dominant component of damages due to forest insect pests (Aukema et al. 2011). Urban trees tend to include highly susceptible species like ash (*Fraxinus spp*.) that have been decimated in recent years by pests such as emerald ash borer (EAB, *Agrilus planipennis,* Kovacs et al. 2010), and dead and dying urban trees pose an immediate threat to resident safety, and thus require management (Klein et al. 2019). On the other hand, within the United States (US), non-harvested forested areas have minimal pest management, apart from coordinated spray programs for particularly damaging species such as European gypsy moth (*Lymantria dispar*). Further, areas marked for timber harvest can reduce economic damages due to pest infestation through substitution and salvage logging (Holmes et al. 2009).

Moreover, the importance of urban forests is only expected to grow. Across the world, more people are moving to cities, and while urbanization is already very high in the US (82% in 2018), it has not yet saturated (World Bank, http://data.worldbank.org, UN DESA, http://population.un.org). At the same time, there has been a push for urban 'greening' (i.e., increasing urban forest canopy), both for environmental benefits, as well as to improve urban dwellers' wellbeing. Urban trees perform many important ecosystem services, including reducing the heat island effect of cities and lowering cooling costs (Norton et al. 2015), buffering against flooding, increasing air quality, carbon sequestration, improving citizens' mental and physical health outcomes, and creating important habitat for other urban species and species using cities as movement corridors (van den Berg et al. 2010; Roy et al. 2012). It is thus critical to understand how pests may affect urban trees.

Many factors influence how damaging a given invasive pest species will be. Pest traits such as the dominant method by which they attack their host (known as their feeding guild) can be important determinants of the extent of their damage (Aukema et al. 2010). However, while the life histories of these species can differ, they are known to be transported at large scales by humans (Hulme et al. 2009), potentially in analogous patterns across entire pathways (Hudgins et al. 2017), and it is their combined, cumulative impacts that we wish to capture. In addition to life history differences, pests vary in terms of their host range size, how far they have already spread and will spread into the future, and in terms of how deadly they are for their host species. Forest pest management must balance the costs of managing these pests with the likely benefit to investing in the management of each, and thus the variability in their impacts should be examined to prioritize future management. Further, under the hypothesis of analogous pathway-level anthropogenic dispersal, the creation of a pathway-level damage estimate is a demonstration of the severity of the pest community associated with anthropogenic secondary spread as a whole, and therefore the extent to which it is important to limit future spread via these pathways (e.g. through quarantines, highway checkpoints to limit firewood movement). Moreover, since many of these pests enter the US through analogous mechanisms, this estimate can motivate policies to limit entry risk (Leung et al. 2014). Past estimates of forest pest damage have been important in providing support for phytosanitary measures such as ISPM15 (IPPC 2002), a wood packing material treatment protocol, whose adoption is growing worldwide (Leung et al. 2014).

The previous pathway-level estimate for the cumulative cost of all US forest pests was performed a decade ago, and had substantial data limitations (Aukema et al. 2011). This was the best analysis possible given the data available at the time. However, it was limited to dispersal estimations for three highly damaging invaders, and cost estimates for two host tree genera from a handful of communities. Since then, contemporary advances in characterizing pest-induced mortality, host prevalence, and pest spread have occurred. It is feasible and timely to revisit forest insect pests' effects on urban trees.

Recent generalized dispersal models (Hudgins et al. 2017; Hudgins et al. 2019) can be employed to project pest spread across the United States over the next 30 years for all invasive forest pest species known to cause non-negligible economic impacts (which we define as the pest community associated with anthropogenic secondary spread). However, the impact of pest spread into different areas is unequal, and depends on the types of urban trees encountered. Koch et al. (2018) have created an extensive database of urban trees across the US from the amalgamation of hundreds of community inventories. This will allow pest spread to be matched to their urban host distributions. Additionally, mortality estimates can now be derived from Potter et al. (2019), who created a database of the top five threatening pests to each host tree species in the United States and quantified these threats on a Likert scale. Combined, these new data sources and models allow the best current estimate of the extent and locations of damage due to forest pest invasions.

In this paper, we synthesized four subcomponent models of forest pest invasions: 1) a model of whole community pest spread, 2) a model for the distribution of all urban street tree host genera across all US communities, 3) a model of host mortality in response to pest-specific infestation for all urban host tree species, and 4) a simple model of the human management response to dead host trees. Through their synthesis, we provide the best current estimate of the damage to street trees, including explicit estimates for all known invasive forest pests across all major insect guilds. Given the continued migration of people to urban centers, and the growing importance of urban trees, this analysis provides a tool to understand the potential for losses of urban trees due to forest insect pests and to motivate policy to limit these losses.

4.3 Methods

We have provided a conceptual diagram of our methodology in Figure 4.1 in order to clarify how our four subcomponent models connect to produce damage estimates. We recommend readers refer to it throughout this section.

4.3.1 Pest dispersal forecasts

We modelled spread using the Semi-Generalized Dispersal Kernel (SDK, Hudgins et al 2019). This is a spatially explicit, negative exponential dispersal kernel model that can account for additional spatial predictors in source and recipient sites. The SDK builds from the Generalized Dispersal Kernel (GDK, Hudgins et al. 2017) as a starting point, using human population density, forested land area and tree density in source and destination sites as moderators of spread. The SDK combines up to three species-specific corrections for each species to maximize predictive ability: 1) a species-specific intercept term, 2) information on a pest's likely initial invasion location, and 3) niche-related limitations when evidenced in the literature (Hudgins et al. 2019). The SDK was applied to all 72 pests believed to cause some damage from Aukema et al. (2011).

We synthesized SDK (Hudgins et al. 2019) projections from 2020 through 2050 with models predicting urban host genus distributions (see below). We note that the SDK model was fit to natural forests rather than urban trees. However, given the strong predictive ability of the published dispersal model without urban host information (Hudgins et al. 2019), we assumed that spread was driven by the invasion of forested areas, while damages were driven by spillover into urban areas.

4.3.2 Street tree models

Our fitting set consisted of 653 street tree databases for US communities where street tree inventory data had been collected and were available for use in this type of analysis (Fig. S4.1.1, Koch et al. 2018). These authors used the inventory data to model basal area (BA) of three of the most common urban tree genera (*Fraxinus, Acer,* and *Quercus)*. We extended this and estimated the number of trees of all genera (not just the top three), and also modelled diameter at breast height (DBH) for trees within each genus, as treatment costs are dependent on number and diameter of trees (Aukema et al. 2011). We split trees into three diameter classes (small = 0-30cm, medium = 31-60cm, large >60cm). We first fit models for the total tree abundance of all species by diameter class, and then used these total tree models to predict genus-specific tree abundance within each diameter class. Street tree inventory data are not always reliably reported to the species level across municipalities, and some species are so rare in street tree inventories that it would have been very difficult to develop robust species-level models, so we limited our examination to the genus level. Since some pests cannot invade all host trees in a genus, we had to estimate the fraction of invasible tree species within each host genus for each pest-host combination. We did so by estimating the species-level breakdown of each genus based on their average relative proportions across our 653 inventoried communities, and assuming this distribution was representative across the US.

We modelled the total abundance of street trees in a community using boosted regression trees (*gbm.step* within R package *dismo,* Hijmans et al. 2017) relating the total tree abundance within a DBH size class to community-specific predictors, employing environmental variables from WORLDCLIM (Fick & Hijmans 2017) and community characteristics used in Koch et al. (2018), and sourced largely from the National Land Cover Database (NLCD, Homer et al. 2015) and the US Census and the American Community Survey (US Census Bureau 2015) (Table S4.1.1). We hypothesized that the age and wealth of a community would influence the types and sizes of trees planted there. In our model, median home value and mean year of construction (at the block-group level) as well as median household income (at the county level) were used as proxies of the age of the urban tree community and the community budget for street trees. We also tested the use of Poisson GAM models, but high levels of concurvity (the GAM equivalent of multicollinearity, Amodio et al. 2014) amongst predictors and lower predictive performance indicated Poisson GAMs were an inferior modelling structure for estimating total abundance.

Next, we estimated the abundance of street trees within each genus, using the same climatic and demographic factors as the total tree abundance model as well as the total tree abundance model output as predictors (Fig. 4.1). We compared two methods and chose the best one for each genus based on R^2: 1) Zero-inflated Poisson GAMs, or 2) Boosted Regression Trees (BRT, *gbm.step* within the *dismo* package, Hijmans et al. 2017). For BRT, we modeled tree presence/absence, followed by tree abundance given presence (using logarithmically-scaled tree abundance and back-transforming when predicting), and then combining the two models. The number of trees of genus i in size class j at a particular site k was:

$$trees_{i,j,k} = c_{i,j,k} * pred_{exist,i,j,k} * pred_{number,i,j,k} \tag{4.1}$$

$$c_{i,j,k} = \frac{1}{\sum_k (pred_{exist,i,j,k} * pred_{number,i,j,k}) / \sum_k obs_{number,i,j,k}} \tag{4.2}$$

This process is similar to that underlying the zero-inflated Poisson (ziP) model (Lambert 1992), but its functional form is less constrained, in that it is unnecessary to link the parameters of the binary and continuous components of the model. A standard ziP model always produces output that sums to the observed counts (Lambert 1992), but because the regression tree model is built in two independent parts that need not combine to sum to observations, we added a rescaling step (eqn 4.2). We removed all highly correlated variables ($r > 0.8$) prior to fitting, and refit GAMs until maximum estimated worst-case concurvity was below 0.8 (*concurvity* function within *mgcv,* Wood (2012)).

We compared BRT and GAM models that were fit to all genera simultaneously (general BRT/GAM models using genus-specific intercept terms) with models that were fit to each genus separately (customized BRT/GAM models) (Fig. 4.1). Predictive power could be higher when modelling all genera together if the genera respond similarly to predictors. Conversely, power could be higher for individually fitted genera where environmental and community characteristic relationships are idiosyncratic and where the sample size is sufficient. We chose the model that produced the strongest relationship for each genus (again via R^2). We used these models to predict urban tree distributions throughout the contiguous US. Alaska and Hawaii were removed to match the spatial extent of pest spread predictions, and because urban trees are likely quite different in these areas compared to the contiguous US.

To assess fit, we calculated R^2 values that were relative to the 1:1 line (i.e, a normalized mean squared error, R^2_{MSE}), which more correctly measures deviations between observations (y) and predictions ($\hat{y}$).

$$R^2_{MSE} = 1 - \frac{\Sigma(y-\hat{y})^2}{\Sigma(y-\bar{y})^2} \tag{4.3}$$

We removed New York City from the fitting set as it was likely to be a high leverage observation and could have significantly changed the resulting models due to it possessing a markedly different street tree genus composition. Both the GAM and BRT models were fitted using their built-in cross-validation algorithms for parameter estimation, and can therefore tolerate occasional outliers with minimal effect on their parameter estimates (though we have less evidence that other outliers would have changed model parameters for cities other than New York City). Given the higher data requirements of GAMs, they were not considered in cases of limited single-genus data (i.e., when only a few cities contained that genus).

4.3.3 Host mortality model

We ranked the severity of a given pest infestation on a particular host using a scale based on observed long-term percent mortality (defined in Potter et al. 2019). We assumed that this database reflected pest-induced mortality over and above natural tree mortality. We added two additional categories to this scale to represent pest species missing from their database that were still considered pests on a particular host within the Aukema et al. (2011) dataset. The lowest-impact pest-host combinations were those featuring pests reported as 'low impact' in Aukema et al. (2011). These accounted for most known combinations. The second lowest category featured 'intermediate impact' pest species from Aukema et al. (2011) that did not appear as threats to a given known host in the Potter et al. (2019) database. We assumed that, were these species quantified by Potter et al. (2019), their associated severities would be lower than the lowest category within the authors' ranking scheme. All other pest-host combinations were assigned to the same categories as in Potter et al. (2019). Pest frequency within severity categories was normalized across the sum of their known hosts so that each pest had equal impact on the frequency distribution (i.e., frequency summed to 1 for each pest). For instance, if a pest had 3 hosts, and had severities of 3, 5, and 9 on each host, we would give them a frequency of 1/3 under each bin. We fit a beta distribution to the frequency distribution of pests in each of these categories using Stan (Carpenter et al. 2017), a program and language for efficient Bayesian estimation. We chose to fit a beta distribution because proportional mortality ranged between 0 and 1. Additionally, we fit the upper limit of the two lowest mortality categories and the lower limit of the highest category. We did this because these categories did not have quantified bounds, but could be ranked relative to others. We used the posterior mean as the expected mortality for a pest in each severity category, rather than the simple midpoint of the range of each category.

Forest pests were grouped into four feeding guilds based on the predominant mode in which they damage their host trees (Aukema et al. 2010). Foliage feeders included insects that feed on leaf or needle tissue. Sap feeders included all species that consume sap, including scale insects and gall-forming species. Borers included species that feed on phloem, cambium, or xylem. Pathogens included species of fungi (e.g. chestnut blight, *Cryphonectria parasitica*) and disease complexes (e.g. beech scale, *Cryptococcus fagisuga*, and beech bark disease, *Neonectria faginata* and *N. ditissima*). Upon examination of the severity category distribution within each guild, we found that for 3 of the 4 feeding guilds, the logic from Aukema et al. (2011) appeared to hold: most species were innocuous but a small number caused high mortality (Appendix S4). In contrast, while several invasive pathogens were mentioned in Potter et al. (2019), pathogens are only reliably reported when they produce noticeable (i.e. intermediate) impacts (Aukema et al. 2011). Further, while many of the pathogens listed in Potter et al. (2019) have already killed the majority of their hosts (e.g., chestnut blight fungus, *Cryphonectria parasitica),* some pathogens, such as laurel wilt disease (*Raffaelea lauricola*), are presently killing a large number of trees in forested areas (Fei et al. 2019). To avoid mischaracterizing their impacts, we removed pathogens from the remainder of our analysis.

Samples were taken from the posterior beta distribution of expected mortality within each pest severity category and assigned to the corresponding pest/host combinations in order to determine the long-range (asymptotic) tree mortality for each host tree species due to invasion by each pest species.

4.3.4 Mortality debt

We define the term ‘mortality debt’ as the time period between a pest initiating damage within a community and reaching its estimated asymptotic host mortality within that community. While we had estimates of the asymptotic proportional mortality of host trees (Potter et al. 2019), we had no information on the rate by which trees reach this plateau. Previous estimates have ranged from 5 to 100 years (Aukema et al. 2011; Pugh 2010), so we analyzed three scenarios within this range (10, 50, 100 years). To account for what is currently known about the mortality dynamics of pests within each of the feeding guilds, we also examined scenarios based on our best guess of the duration of mortality debt across pest feeding guilds. EAB is estimated to kill the majority of its susceptible hosts in the first decade following infestation (Knight et al. 2013), while maximum mortality is estimated to take closer to 100 years for hemlock woolly adelgid (Aukema et al. 2011), so we used the 10 and 100-year scenarios for borers and sap-feeders, respectively. A recent publication examining mortality rates in forested areas suggested that European gypsy moth has a mortality rate intermediate between borers and sap-feeders, so we set defoliators at 50-years (Fei et al. 2019). For simplicity, we assumed mortality increased by a constant fraction over time until reaching its maximum and levelling off. For example, in the 50 year mortality debt scenario, if a pest's maximum host mortality was defined as 90%, mortality would increase by 9% at each 5-year timestep for 10 timesteps until 90% mortality had been reached.

4.3.5 Species-specific cost estimates

As a final layer that allowed us to move from mortality estimates to cost estimates, we made several assumptions about the management response to street tree mortality. Because preventative behaviour is much harder to estimate, we estimated what we believe is the minimal management response required: only dead trees are managed, and they are managed by removal and replacement. This does not account for additional preventative cutting or any non-cutting management such as spraying or soil drenching with pesticides. We assumed that cutting was a one-time 100% effective treatment against pests. In other words, newly planted trees were assumed to be of different species and thus not susceptible to the same pest species that killed the previous trees. We assumed a 2% discount rate for future damages (Aukema et al. 2011), and also assumed that infestations were independent. In other words, invasion by one pest was assumed to not interfere with invasion by another. This is likely a fair assumption, as there is minimal host sharing across pest species, and pest species each infest only a small proportion of hosts at a given time interval, so there is minimal potential for species interactions (Aukema et al. 2010). We assumed the same per-tree cost estimates for cutting and replacing dead trees as in

Aukema et al. (2011), where the cost of cutting increases nonlinearly with size class. If we assume that street trees are always under the jurisdiction of local governments, the cost of removal and replacement of each tree is US$450 for small trees, US$600 for medium trees, and US$1200 for large trees (these costs jump to an estimated US$600, US$800, and US$1500 for homeowners). We reported all costs incurred from 2020 to 2050 in 2019 US dollars based on a 2% discount rate relative to these baseline costs. Since these baseline per-tree management costs came from a 2011 publication, we converted them to 2019 USD via the consumer price index, which amounted to an inflation of 13.65% (World Bank, https://data.worldbank.org), though we note that the present-day costs of per-tree removal may have declined with advances in technology. Once all subcomponent models had been parameterized, we synthesized the urban tree estimates, pest spread estimates, host mortality estimates, and management responses to produce cost estimates (Fig. 4.1).

4.3.6 Whole-community costs

We summed the damages from 2020 to 2050 to obtain a total discounted cost for this 30-year window. We then obtained annualized costs by calculating an annuity over the 30-year time horizon using the following equation:

$$Annualized\ damage = D\frac{\sum_{time=min}^{max} Costs_{time}}{(1-(1+D)^{max-min})} \qquad (4.4)$$

Where D is the discount rate (2%). Using these forecasts, we extended the concept of cost-curves from Aukema et al. (2011), which were based on frequencies of occurrences of low and intermediate damaging pests, and explicit economic estimates of three poster pests. To parameterize the cost-curves in this manuscript, rather than just 3 poster pests, we estimated street tree costs for all 60 intermediate-impact pest species across the 3 major insect feeding guilds, in addition to frequencies of low-impact species. The summed area under each guild-specific curve can be interpreted as the estimate of the total annualized cost of all invasive forest pests in the US to street trees. Since our curves were missing only low-impact species, the total cost estimated with these approaches is not appreciably different from a simple sum of the costs of the non-missing (57 intermediate) species reported in text, but we included these analyses to allow for the prediction of the costs of novel invaders from each guild (Appendix S4.4).

4.3.7 Uncertainty and sensitivity

Once a pest was predicted to infest an area, we imposed a 10-year initial lag phase between pest arrival at a site and the initial onset of damage (Hochberg and Weis 2001; Liebhold and Tobin 2008), and then began increasing the host mortality following our mortality debt scenario to the asymptotic level (defined by the host mortality model). We assessed uncertainty in the cost curve functional form using Bayesian model averaging (Wintle et al. 2003) and in pest-specific host mortality rates by sampling from the outputted posterior beta distribution for the asymptotic mortality of each host species due to each pest species. We also used sensitivity analysis to explore the effect of different mortality debt scenarios, including 1) our best guess scenario, 2) setting all guilds to 10, 50, or 100-year debts, and 3) varying each guild separately while holding the other two guilds at their best guess scenario.

4.3.8 Theoretical validation

While our host distribution models were based on standard modelling approaches (e.g. GAM), we wished to test the theoretical validity of the non-standard, Bayesian components of our framework (mortality estimates and cost curves). See Appendix S4.4 for details of our theoretic analyses.

4.3.9 Mortality and potential costs to non-street trees

We built a model for whole-community trees from the dataset of 56 communities where genus-level estimates were reported, subtracted predicted street trees from this whole community estimate, and apportioned the remaining trees into residential and non-residential (community) trees based on their average fractions across all sites where land type breakdowns were provided (32 municipalities). Given the roughness of these predictions, we caution against overinterpretation of these results, particularly once translated into costs.

4.4 Results

4.4.1 Street tree models

Total tree abundance models were moderately predictive with some outliers (Fig. S4.2.1, fitted R^2 for small trees = 0.78, medium trees = 0.58 large trees= 0.42). Removing the outliers changed the fitted R^2 to 0.76 for small trees, 0.76 for medium trees, and 0.58 for large trees. Both demographic and environmental predictors were important in predicting total trees, with human population size, ecological province, and community area emerging as top predictors across size classes, mean year of home construction emerging as predictive for medium and large trees and community canopy cover for large trees (Table S4.2.1).

The total tree abundance models were used as inputs to the genus-level models, which were then used to predict abundances for each host tree genus. Our genus-level model fits were strong, but became slightly weaker for rare genus and size class combinations (Fig. 4.2, overall R^2 for all genera of small trees = 0.93, medium trees = 0.93, large trees = 0.92). Within each genus, the best combined model fits were generally strong (Table S4.2.5, mean R^2=0.76, σ=0.16 for small trees, mean R^2=0.78, σ=0.14 for medium trees, mean R^2=0.78, σ=0.17 for large trees). While relationships were variable across genera, the genera that were fit most poorly did not make up a large proportion of predicted trees, and none were below $R^2 = 0.25$ (Fig. S4.2.2). Some genera were very rare within our inventoried communities at a given size class, and therefore had insufficient data to fit their genus-specific models. In these cases, R^2 is reported as NA in Table S4.2.6.

The optimal genus-level method (global BRT, global GAM, customized BRT, or customized GAM, Fig. 4.1) differed across genera depending on diameter class, prevalence of genera, and whether presence/absence or tree abundance was the response variable (Tables S4.2.2-4). Across diameter classes, a general GAM for presence was most frequently selected when the number of predicted trees and the number of sites with trees present for that genus were high, indicating that the presence of common genera is driven by the same environmental and social variables. When predicting tree abundance, given presence, more common genera tended to be fit better by customized BRT or GAM models, indicating more idiosyncratic relationships to predictor variables at the level of tree quantity for ubiquitous genera. Where the number of total predicted trees and sites was not as high, small and medium size classes tended to be predicted best by a global BRT for both tree presence and abundance, while large trees tended to be fit best by a customized GAM for presence, followed by a global BRT for tree abundance. It appears that even in cases of data scarcity, genus-specific predictors of presence/absence can be detected for some rare genera. However, for tree abundance, rarer genera are better fit by general models, potentially due to their increased statistical power (Fig. S4.2.3).

According to our models, across the US, the population of small street trees is mostly made up of *Acer* and *Quercus*, with substantial *Fraxinus* (Fig. S4.2.4). Medium trees are again mostly *Acer*, but with a large number of *Eucalyptus* and *Fraxinus*. The largest street trees are the most evenly split across genera, but dominated by *Acer* and *Quercus*. When we compared our fitting set (653 communities) to our extrapolations of tree distributions across all communities in the US (~30 000 communities), small tree predictions remained relatively close to the inventoried distribution. Conversely, medium trees were predicted to have a much higher proportion of *Eucalyptus* than in the fitting set (we note these were predicted almost entirely in California). Similarly, we predicted a much smaller proportion of medium-sized *Quercus* than in the fitting set, and a much smaller proportion of large-sized *Ulmus*. These discrepancies are likely due to tree community differences in the southern US, where we had very few tree inventories, compared to the northern communities that comprised the majority of our data.

4.4.2 Host tree exposure

We synthesized the previous two modelling steps (Fig. 4.3a-b), intersecting pest spread forecasts with predicted tree distributions, to create forecasts of tree exposure. We define exposure as the sum of predicted pest density of each pest species, multiplied by their predicted host tree abundance in each community. Predicted street tree exposure across all tree types from 2020 to 2050 is generally high in the eastern US, and only sporadically high across the western US (Fig. 4.3c). Predicted street tree exposure is highest among *Acer* (12.0M)*, Quercus* (4.1M)*,* and *Pinus spp*. (2.0M), and the greatest number of trees are predicted to become exposed to Japanese beetle (*Popillia japonica*, 9.9M), gypsy moth (5.2M), and Asiatic oak weevil (*Cyrtepistomus castaneus*, 4.7M). Among residential and community trees, exposure is greatest among *Acer, Quercus* and *Prunus spp*. (1.2B, 985M, 668M, respectively), and most frequently predicted pest encounters are with Japanese beetle, gypsy moth and winter moth (*Operophtera brumata*) (1.8B, 1.1B, 447M).

4.4.3 Host mortality model

The best-fitting mortality model had the majority of its posterior probability density in the very low bins, and the majority of the posterior density at the low end of severity within each bin (Fig. 4.4, full results in Appendix S4.4). Thus, mortality risk was predicted to be much lower than if the midpoint of each bin had been taken as the expected risk.

4.4.4 Street tree mortality

In our best-guess scenario (i.e., 10-year scenario for borers, 50-year scenario for defoliators, 100-year scenario for sap feeders), we estimated a loss of 5-12% of street trees by 2050, but the most extreme scenarios led to projected losses upwards of 67% (Table 4.1). Over time, predicted street tree death varied by an order of magnitude based on the mortality debt scenario, with shorter debts leading to lower total mortality between now and 2050 (Table 4.1). This sensitivity was driven largely by the borer guild, as demonstrated by the sensitivity of mortality estimates to their mortality debt scenarios ("Vary Borers" row, Table 4.1). Spatially, future damages will be primarily borne in the Northeast and Midwest, driven by EAB spread (Fig. 4.3d). The top ten "mortality hotspot cities", where projected mortality is in the range of 20-100,000 street trees, include Minneapolis/St. Paul/Bloomington, MN; Milwaukee, WI; Indianapolis, IN; Chicago/Aurora, IL; and Columbus, OH. These cities have large amounts of *Fraxinus* predicted to have been in the path of recent EAB spread, leading to high mortality. Cities predicted to have high mortality outside of the Midwest include New York City, NY and Seattle, WA. These are cities with high numbers of street trees and high human populations, which attract EAB propagules within our spread model. The states most impacted by street tree mortality match these patterns, where the highest mortality is in Minnesota, Ohio, and Illinois.

4.4.5 Costs

We estimated annualized street tree costs across all guilds to be between $84-225M USD per year in our best guess scenario (mean = $146M, Fig. 4.5). The total cost associated with street tree mortality in hotspot cities was estimated at $170M from 2020 to 2050, with $48M in Minneapolis alone. Over time, street tree damages varied by an order of magnitude based on mortality debt scenario, because of the mortality patterns described in the preceding section (Fig. 4.6). Given the dominance of borers in total costs, our best guess indicates that the impact of mortality debt will more closely match the 10-year scenario (red line, Fig. 4.6). We also see that longer mortality debt leads to a smoother cost curve, or costs that do not vary much due to temporal variability in pest spread. In particular, the SDK predicts that EAB will spread to regions with lower urban ash from 2020 to 2025. Communities in these regions will not experience the same magnitude of street tree mortality as communities invaded previously by EAB. These spread patterns explain the cost fluctuations in the shortest mortality debt scenario in Fig. 4.6.

The ranking of feeding guild severity was relatively robust across mortality debt scenarios, in spite of the potential for differences due to the interaction of pest-specific spread and mortality debt dynamics. Borers were predicted to be the most damaging feeding guild ($80M-$846M mean annualized street tree damages across scenarios), and EAB was consistently the top threat. Predicted costs were lowest in our 10-year mortality debt scenario. Defoliators were predicted to be the second most damaging guild in short (10-year) and mid-range (50-year) scenarios (means = $11M and $5M), but had lower damages than defoliators in long-range (100-year) scenarios (mean = $5M). Defoliators had a 1-2 order of magnitude lower cost than wood-boring species, but again showed consistency in top threats within the guild, with Japanese beetle and European gypsy moth topping the list. The sap-feeding group had the second highest costs in the long scenario (mean = $12M USD), but lower relative costs to defoliators in the shorter scenarios (means= $3M). Unsurprisingly, hemlock woolly adelgid (*Cryptococcus fagisuga*) was the top sap feeder threat, and estimated damages from calico scale (*Eulecanium cerasorum*) were also notable. Total costs were only notably sensitive to borer mortality debt scenario misspecification (Table 4.1), which is promising, given our certainty of the shorter scenario for EAB.

4.4.6 Predicted mortality and potential costs to non-street trees

Mean mortality for community trees in the best guess scenario was 4.6% (318M trees), and mean mortality for residential trees was 4.2% (59M trees) (Table S4.5.1). If we assume that non-street trees will be managed in the same way as street trees (i.e., removal and replacement), this mortality would incur an estimated annualized cost of $1.2B for community trees and $290M for residential trees.

4.5 Discussion

Urban trees represent the most substantial sector of economic damages for forest pests (Aukema et al. 2011), yet until recently, data did not exist on the urban distribution of host trees (Koch et al. 2019), the spread of pest species (Hudgins et al. 2019), nor the mortality risk for hosts due to different pests (Potter et al. 2019). Furthermore, previous impact estimates did not break down these impacts into predicted mortality by tree genus and land type (residential, community, street), but we showed that projected tree deaths are incredibly striking. Our analyses show that, based on the best available information, pests could kill 5-12% of all street trees, 59M residential trees, and 318M community trees by 2050, owing in large part to *Fraxinus* mortality due to EAB. Borers are projected to be by far the most damaging feeding guild, followed by defoliators and sap feeders. For street trees, we estimate that management of dead trees will cost between 74-198M USD annually. Given previous assumptions about treatment from Aukema et al., the management costs of non-street trees are potentially twice as high as previous estimates (but see

Limitations). Our integrative analysis provides the best estimate of future spatio-temporal mortality for trees in all land types, both asymptotically and for the period of 2020 to 2050, as well as robust spatiotemporal cost projections for street trees, and highlights the information needed to better characterize the latter across land types.

4.5.1 Comparison to previous work

We found that both demographic and environmental predictors were important in determining street tree distributions, including human population size, ecological province, community area, mean year of home construction and community canopy. In comparison, Koch et al. (2018) also found canopy cover and area to be highly predictive of total community basal area in their models. However, these authors did not find housing or human population variables to be predictive, but instead found latitude and longitude to be predictive. Given that their analysis was restricted to three genera in the eastern and central US, it may have been easier to capture larger climatic patterns in the distribution of these trees in these areas, and latitude and longitude act might have served as surrogates for other factors in their restricted area of analysis.

Our projected urban tree costs have greater resolution compared to Aukema et al. (2011), and thus provide the best current estimate of urban costs. The previous cost estimate was for all urban trees, including street and non-street trees. This analysis separated trees into residential and non-residential types (grouping street trees in the latter). Cost differences compared to this analysis can be explained largely by saturating spread patterns across pest species, and greater resolution in *Fraxinus spp*. distributions. We estimate annualized costs for non-residential trees to be slightly below the Aukema et al. (2011) estimate (\$1.2B versus \$2.0B). Our estimate of residential tree costs is less than one third of the Aukema estimate ($290M vs. $1.1B). Both of these estimates are lower because of a decreased predicted impact of defoliators and sap feeders relative to borers, and due to lower rates of *Fraxinus* exposure to EAB, particularly in residential areas. While this previous analysis was limited to cost estimates, our approach also allows the spatiotemporal examination of tree exposure and tree mortality at the level of individual tree genera and causal pest species.

4.5.2 Spatial Considerations

Spatially, total damages will occur mostly in the Northeast and Midwest, and while these are areas with both high host diversity (Liebhold et al. 2013) and high current and future pest load (Hudgins et al. 2019), the pattern of damage is distinct from either of these. Our predictions span less of New England than pest load predictions, and span less far south than regions of high host diversity. Damages cannot be predicted simply by examining either host or pest distributional forecasts because they depend instead on the intersection of these two elements and subsequent mortality dynamics. We predict the greatest tree exposure in the eastern US, which translates to the highest risk close to the leading edge of present-day EAB distributions when synthesized with mortality estimates, particularly in areas predicted to have high *Fraxinus* densities. At the level of individual cities, many of the highest-risk communities are highly populated and along the EAB leading edge (e.g., Minneapolis-St. Paul, MN), but we see high risk in major urban centers with large urban tree communities containing *Fraxinus* even outside of this region (e.g., Seattle, WA).

4.5.3 Temporal Considerations

These cost and mortality estimates vary substantially based on dynamics of host mortality following initial pest invasion, in particular due to the duration and functional form of mortality debt. Thankfully, the guild (borers) and species (EAB) whose impact on total community costs is most sensitive to correct specification of the mortality debt dynamics is the one for whom we are most confident. Several publications have demonstrated near-complete decimation of ash stands in the decade following EAB infestation (Kovacs et al. 2010; Knight et al. 2013; Fei et al. 2019). Furthermore, since total tree mortality is asymptotically equivalent across all mortality debt regimes, if other feeding guilds possessed 10-year mortality debt regimes, we should have been able to detect a rapid die-off of their hosts as they spread, similarly to what we found for EAB (albeit scaled by their maximum mortality rates). This was not the case.

Our temporal results show an analogous effect to other 'debt' dynamics in ecology, where communities pay the price in the present for impacts that began in the past as a result of time lags. One such example is extinction debt, where fragmentation's effects on biodiversity occur with a time lag (Vellend et al. 2006). More closely related to mortality debt is invasion debt, where the long-term ecological consequences of invasive species are only realized after a lag due to introduction, establishment, spread, and/or impact dynamics (Bennett et al. 2013; Rouget et al. 2016), where it can be understood as one mechanism behind a time lag in long-term impact.

Based both on economic processes of temporal discounting, and the slowing of the spread of existing invaders as they saturate their communities, we see a decreasing trend in the economic impacts of these invaders over the next 30 years. This implies that the window of opportunity for preventing damages due to these pests is closing, and rapid responses to immediate threats to municipalities are needed to avoid the worst anticipated future damages. It is, however, important to keep in mind that this analysis does not account for the costs of novel invaders that may begin to cause impacts within this time window. Since our estimate is limited by our knowledge of the invasion dynamics and impacts of pests that have already completed primary establishment, forecasting subsequent primary establishment and resulting secondary impacts of novel invaders is a key complementary analysis.

4.5.4 Limitations

The aim of this paper was to provide the best estimate of expected future damages (over a 30-year time horizon) due to each invasive forest pest across 30,000 US communities at the level of their individual host tree genera. We chose to explore several aspects of uncertainty in this analysis, but did not exhaustively examine potential sources of variation in the damage projections, including 1) future climatic variability, 2) spread model uncertainty, 3) host distributional model uncertainty, 4) variability in management behaviour, 5) asymptotic mortality misestimation, and 6) mortality debt model misspecification. In Table 4.2, we have categorized the relative level of uncertainty across land types associated with the different impact metrics reported in this paper. The table includes all of the elements from the above list impacting each of these categories. All impact metrics are sensitive to climatic variability, as well as a correctly-specified pest spread and tree distributional models. While the pest spread model accounts for climate change as it is predicted to impact invasive pest spread through forests, we acknowledge that climate change could alter urban pest and host distributions, as well as host susceptibility and mortality risk following pest invasion in ways we cannot capture within this framework. In the current climate our pest spread model is demonstrably predictive and consistent across land types, but we are more confident in our urban tree models for street trees than residential and community trees, as we were able to draw on a much larger fitting dataset for these, so all impact metrics have greater uncertainty for residential and community trees. Our most robust impact metric is predicted focal host exposure to each pest, since it is only sensitive to pest spread and urban tree distributional models. Asymptotic mortality refers to the maximum mortality predicted from our mortality model that can be attributed to forecasted pest spread from 2020 to 2050. This mortality would be reached eventually in any mortality debt scenario, and relies on accurate mortality estimates from our Bayesian approach. Specifying a time-window of 2020 to 2050 for impacts make the final two metrics (mortality and cost 2020 to 2050) more sensitive to the correct mortality debt model, but we know that the more uncertain pest species in terms of mortality debt scenario contribute less substantially to cost estimates. As such, we are relatively confident in all mortality estimates reported for 2020 to 2050 across all three land types. In addition to these sources of uncertainty, management responses cause additional uncertainty when translating from mortality within a given time range and cost within that range. These behaviours are most certain for street tree management, moderately uncertain for residential tree management, and most uncertain for community tree management (Table 4.2, see below).

We caution against grouping all non-residential trees together when calculating costs as in the analysis of Aukema et al. (2011), because management behaviour likely differs substantially between highly valuable street trees and other trees (e.g., trees in parks, wooded areas, and commercial developments). These trees are likely at a lower priority for removal, and even within these other uses, management may differ. For example, dead trees may be left standing in wooded areas, but that is less likely in heavily used public parks where such trees would be hazardous to park users. Though we report rough cost estimates for the cases where these other trees are managed analogously to street trees (all dead trees are removed, taking into account that homeowners must pay more for tree treatment compared to municipalities who can benefit from economies of scale, Aukema et al. 2011), we believe this is likely an overestimate, because responsibility and behaviour is likely far more variable. Indeed, this may be a particularly severe overestimate for non-residential community trees, as management jurisdictions may be ambiguous for these trees, and many may not put people at risk (e.g., trees deep in wooded areas of parks or in industrial areas). While homeowners are likely to respond more frequently to dead trees, residential management is likely still to be more variable than street tree management. For instance, residential trees will likely be cut and replaced if the risk of them falling on a home is very high, but could be ignored otherwise. This decision is likely to vary with things like lot size and household income. Nonetheless, the sheer number of projected deaths of non-street trees likely means they will contribute substantially to future costs. On average across communities where land type data are reported (Koch et al. 2018, n=61), street trees make up 6.8% of urban trees (though we note that this is likely an underestimate for cities in areas that are naturally grasslands or deserts), so the total cost of forest pests depends a great deal on how these other land types are treated. Based on our estimates, we note that non-street trees have the potential to lead to damages two orders of magnitude higher than those of street trees.

We note that all known host genera for invasive forest pests were present in at least one community within our fitting set (Aukema et al. 2010). However, there are clear spatial biases in our records (Fig. S4.1.1). The majority of the communities in our fitting set are in the northern US and California. Our data spanned 32 states, but include relatively few communities in the southern US. It is possible that the regions we were missing have different relationships with the modelled predictor variables, but we were limited to the data available. Nonetheless, our data spanned a variety of climates (plant hardiness zones 3-11, Daly et al. 2012) and our communities ranged widely in population size (70 people – 8.6M people), which likely indicates a variety of potential tree assemblages.

We note that the database upon which we built our mortality models (Potter et al. 2019) is based partly on expert elicitation. It is therefore subject both to a high degree of imprecision and a potential bias toward overestimation of pest risk from forestry experts who have witnessed low-probability events (Skjong & Wentworth 2001). Fei et al. (2019) recently published empirical mortality rates for a subset of these pest species based on forested area data (Forest Inventory and Analysis program, (FIA), Miles et al. 2001), which were reported relative to background forested host mortality, and included estimates for some pathogens. Had we included pathogens in our analysis, we could have underestimated the mortality rate for deadly pathogens such as laurel wilt disease compared to these authors (Fei et al. 2019). However, mortality rates in forested stands may not align well with urban host mortality risk for these pest species. Nonetheless, the characterization of future pathogen-induced urban tree impacts is an important area of complementary analysis given the potential for high mortality rates. Background tree mortality was also not accounted for in our models, which may have killed some exposed hosts before the pests could cause impacts. This is especially true in the longer time-horizon mortality debt models, since natural mortality probabilities are likely high on the scale of 100 years. Since the majority of projected damage is due to shorter-term dynamics, background mortality should offset only a small fraction of future pest-induced tree mortality in the next 30 years.

For street trees, this cost estimate is arguably a lower bound, since it only examines the cutting of dead trees. In cities such as Chicago (https://www.chicago.gov/city/en/depts/streets.html), trees are being preventatively treated for EAB, and similar schemes exist in many US cities. As such, preventative behaviour is a key additional cost that is worth exploring in subsequent expansions of this framework. Additionally, there was a time lag between tree inventory data collection and this tree mortality analysis for many cities, particularly in the Midwest (Koch et al. 2018). While this lag is useful for not obscuring potential contemporary tree mortality, many of the cities where we predicted high losses from EAB might already have felt some of these losses and/or have started proactively removing ash by the time of this publication. Another missing cost is the cost of novel invaders that will enter the US between 2020 and 2050. While we show the dominance of borers within currently-established forest pests, future damages may shift to other feeding guilds, for instance with the anticipated arrival of the Asian gypsy moth (*Lymantria dispar var. asiatica*) (Hajek & Tobin 2009).

4.5.5 Conclusion

In order to make the most effective pest management decisions, policymakers and managers require information on the most likely spatiotemporal pattern of future pest damages. Further, in the absence of cost information, the degree of devastation caused by invasive species can easily be brushed aside. We have created a framework to estimate urban tree damages across all US invasive forest pests in roughly 30 000 US communities. We have shown that these pests have the potential to kill a substantial fraction of street trees and hundreds of millions of urban trees in the next 30 years, and that these deaths could correspond to total damages on the order of tens of billions of dollars, where the majority will be paid by urban centers in the Midwest due to EAB-induced ash mortality. While these are rough estimates subject to varying levels of uncertainty, they illustrate the gravity of pest infestations in urban areas, particularly in terms of street tree mortality and management costs. The creation of fine scale spatiotemporal cost estimates also allows for the prioritization of future management efforts, for instance in identifying tree mortality hotspots. This approach can allow for predictive impact modelling for future invaders, thereby allowing managers to be better prepared for future threats.

4.6 References

Amodio, S., Aria, M., & D'Ambrosio, A. (2014). On concurvity in nonlinear and nonparametric regression models. *Statistica*, *74*(1), 85-98.

Aukema, J. E., Leung, B., Kovacs, K., Chivers, C., Britton, K. O., Englin, J., ... *et al*. (2011). Economic impacts of non-native forest insects in the continental United States. *PLoS One,* 6(9).

Aukema, J. E., McCullough, D. G., Von Holle, B., Liebhold, A. M., Britton, K., & Frankel, S. J. (2010). Historical accumulation of nonindigenous forest pests in the continental United States. *BioScience*, 60(11), 886-897.

Bennett, J. R., Vellend, M., Lilley, P. L., Cornwell, W. K., & Arcese, P. (2013). Abundance, rarity and invasion debt among exotic species in a patchy ecosystem. *Biological*

Invasions, 15(3), 707-716.

Carpenter, B., Gelman, A., Hoffman, M. D., Lee, D., Goodrich, B., Betancourt, M., ... *et al*. (2017). Stan: A probabilistic programming language. *Journal of Statistical Software*, 76(1).

Daly, C., Widrlechner, M. P., Halbleib, M. D., Smith, J. I., & Gibson, W. P. (2012). Development of a new USDA plant hardiness zone map for the United States. *Journal of Applied Meteorology and Climatology*, *51*(2), 242-264.

Essl, F., Lenzner, B., Courchamp, F., Dullinger, S., Jeschke, J. M., Kühn, I., ... & Seebens, H. (2019). Introducing AlienScenarios: a project to develop scenarios and models of biological invasions for the 21 st century. *NeoBiota*, 45, 1-17.

Fei, S., Morin, R. S., Oswalt, C. M., & Liebhold, A. M. (2019). Biomass losses resulting from insect and disease invasions in US forests. *Proceedings of the National Academy of Sciences*, 116(35), 17371-17376.

Fick, S. E., & Hijmans, R. J. (2017). WorldClim 2: new 1-km spatial resolution climate surfaces for global land areas. *International Journal of Climatology*, 37(12), 4302-4315.

Hajek, A. E., & Tobin, P. C. (2009). North American eradications of Asian and European gypsy moth. In *Use of microbes for control and eradication of invasive arthropods* (pp. 71-89). Springer, Dordrecht.

Hijmans, R. J., Phillips, S., Leathwick, J., Elith, J., & Hijmans, M. R. J. (2017). Package 'dismo'. *Circles*, 9(1), 1-68.

Hochberg, M.E., & Weis, A.E. (2001). Ecology: bagging the lag. *Nature* 409, 992–93.

Homer, C.G., Dewitz, J.A., Yang, L., Jin, S., Danielson, P., Xian, G., … *et al*. (2015.)

Completion of the 2011 National Land Cover Database for the conterminous United States – representing a decade of land cover change information. *Photogrammatic Engineering and Remote Sensing,* 81, 345–354.

Hudgins, E. J., Liebhold, A. M., & Leung, B. (2017). Predicting the spread of all invasive forest pests in the United States. Ecology letters, 20(4), 426-435.

Hudgins, E. J., Liebhold, A. M., & Leung, B. (2020). Comparing generalized and customized spread models for nonnative forest pests. *Ecological Applications*, 30(1), e01988.

Hulme, P. E. (2009). Trade, transport and trouble: managing invasive species pathways in an era of globalization. *Journal of Applied Ecology*, *46*(1), 10-18.

IPPC (International Plant Protection Convention). 2002. *International standards for phytosanitary measures*. Rome, Italy: FAO. www.fao.org/docrep/009/a0450e/a0450e00.htm. Viewed 12 May 2020.

Klein, R.W., Koeser, A.K., Hauer, R.J., Hansen, G., & Escobedo, F.J. (2019). Risk assessment and risk perception of trees: a review of literature relating to arboriculture and urban forestry. *Arboriculture & Urban Forestry,* 45(1), 26-38.

Knight, K. S., Brown, J. P., & Long, R. P. (2013). Factors affecting the survival of ash (*Fraxinus spp*.) trees infested by emerald ash borer (*Agrilus planipennis*). *Biological Invasions*, 15(2), 371-383.

Koch, F. H., Ambrose, M. J., Yemshanov, D., Wiseman, P. E., & Cowett, F. D. (2018). Modeling urban distributions of host trees for invasive forest insects in the eastern and central USA: A three-step approach using field inventory data. *Forest Ecology and Management*, 417, 222-236.

Kovacs, K. F., Haight, R. G., McCullough, D. G., Mercader, R. J., Siegert, N. W., & Liebhold,

A. M. (2010). Cost of potential emerald ash borer damage in US communities, 2009–2019. *Ecological Economics*, 69(3), 569-578.

Lambert, D. (1992). Zero-inflated Poisson regression, with an application to defects in manufacturing. *Technometrics*, *34*(1), 1-14.

Leung, B., Hudgins, E. J., Potapova, A., & Ruiz-Jaen, M. C. (2019). A new baseline for countrywide α-diversity and species distributions: illustration using> 6,000 plant species in Panama. *Ecological Applications*, 29(3), e01866.

Liebhold, A.M., & Tobin, P.C. (2008). Population ecology of insect invasions and their management. *Annual Review of Entomology,* 53, 387–408.

Miles, P.D., Brand, G.J., Alerich, C.L., Bednar, L.R., Woudenberg, S.W., Glover, J.F. … *et al*. (2001). *The forest inventory and analysis database: database description and users manual version 1.0*. General Technical Report NC-218, North Central Research Station, USDA Forest Service, St. Paul, MN.

Norton, B. A., Coutts, A. M., Livesley, S. J., Harris, R. J., Hunter, A. M., & Williams, N. S. (2015). Planning for cooler cities: A framework to prioritise green infrastructure to mitigate high temperatures in urban landscapes. *Landscape and Urban Planning*, 134, 127-138.

Potter, K. M., Escanferla, M. E., Jetton, R. M., & Man, G. (2019). Important insect and disease threats to United States tree species and geographic patterns of their potential impacts. *Forests*, 10(4), 304.

Pugh, S.A. (2010). *Michigan's forest resources, 2008*. Research Note NRS-50. Newtown Square, PA: U.S. Forest Service, Northern Research Station. 4 pp.

Rouget, M., Robertson, M. P., Wilson, J. R., Hui, C., Essl, F., Renteria, J. L., & Richardson, D.

M. (2016). Invasion debt–quantifying future biological invasions. *Diversity and Distributions*, 22(4), 445-456.

Roy, S., Byrne, J., & Pickering, C. (2012). A systematic quantitative review of urban tree benefits, costs, and assessment methods across cities in different climatic zones. *Urban Forestry & Urban Greening*, 11(4), 351-363.

Skjong, R., & Wentworth, B. H. (2001, January). Expert judgment and risk perception. In *The Eleventh International Offshore and Polar Engineering Conference*. International Society of Offshore and Polar Engineers.

Van den Berg, A. E., Maas, J., Verheij, R. A., & Groenewegen, P. P. (2010). Green space as a buffer between stressful life events and health. *Social science & medicine*, 70(8), 1203-1210.

Vellend, M., Verheyen, K., Jacquemyn, H., Kolb, A., Van Calster, H., Peterken, G., & Hermy, M. (2006). Extinction debt of forest plants persists for more than a century following habitat fragmentation. *Ecology*, *87*(3), 542-548.

Wintle, B.A., McCarthy, M.A., Volinsky, C.T., Kavanagh, R.P. (2003). The Use of Bayesian Model Averaging to Better Represent Uncertainty in Ecological Models. Conservation Biol 17**:** 1579-1590.

Wood, S. (2012). *mgcv: Mixed GAM Computation Vehicle with GCV/AIC/REML smoothness estimation*. R package.

4.7 Figures and Tables

4.7.1 Figures

Figure 4.1 Schematic representation of the four subcomponent models we combined to produce refined damage estimates to street trees from invasive US forest pests. Methodology is represented within braces, where GAM= Generalized Additive Model, and BRT= Boosted Regression Tree. The spread model predictions correspond to SDK forecasts from Hudgins et al (2019).

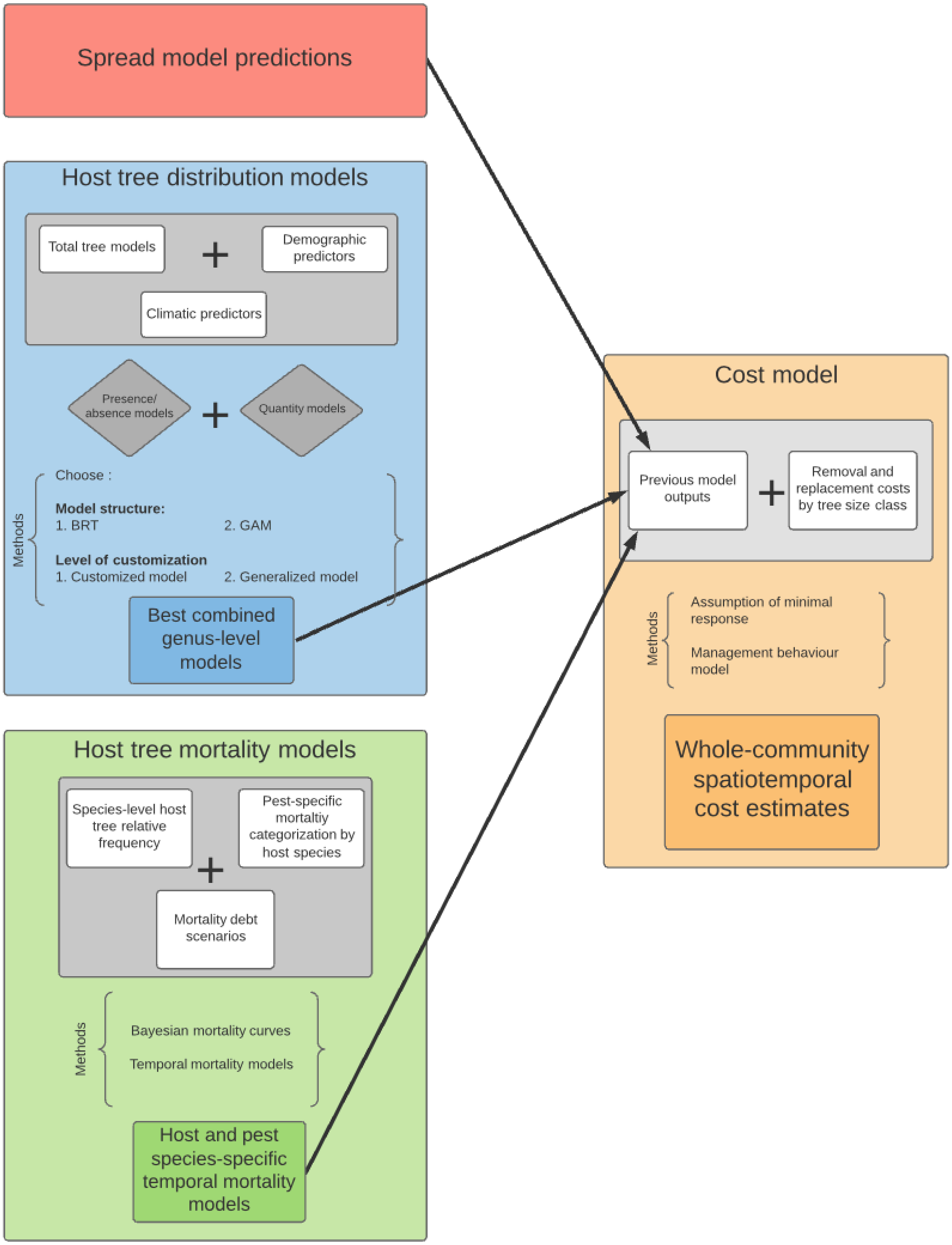
Spread model predictions
Host tree distribution models
Total tree models
+
Demographic predictors
Climatic predictors
Presence/ absence models
+
Quantity models
Methods
Choose :
Model structure:
1. BRT
2. GAM
Level of customization
1. Customized model
2. Generalized model
Best combined genus-level models
Host tree mortality models
Species-level host tree relative frequency
+
Pest-specific mortaltiy categorization by host species
Mortality debt scenarios
Methods
Bayesian mortality curves
Temporal mortality models
Host and pest species-specific temporal mortality models
Cost model
Previous model outputs
+
Removal and replacement costs by tree size class
Methods
Assumption of minimal response
Management behaviour model
Whole-community spatiotemporal cost estimates

Figure 4.2 Fit of the genus-specific host tree models across all genera and size classes.

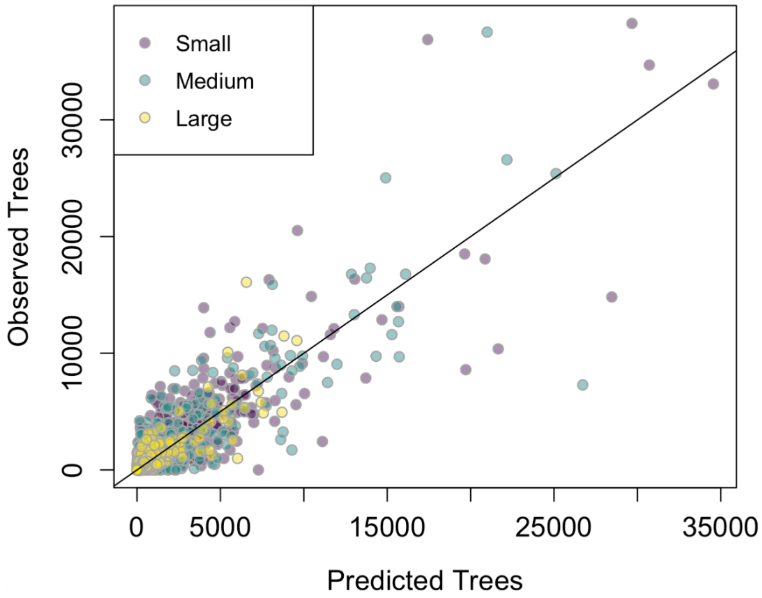

Figure 4.3 Model outputs for the first three subcomponent models, including **a.** predicted street tree abundance, **b.** predicted new pest invasions, **c.** predicted street tree exposure levels (number of focal host tree + pest species interactions) from 2020 to 2050, and finally **d.** Predicted total tree mortality from 2020 to 2050 in the best guess mortality debt scenario across space. Top ten most impacted cities are shown in terms of total tree mortality 2020 to 2050 (A =Minneapolis/St. Paul/Bloomington; MN, B=Milwaukee, WI; C=New York City, NY; D=Indianapolis, IN; E=Columbus, OH; F=Chicago/Aurora, IL; G=Seattle, WA).

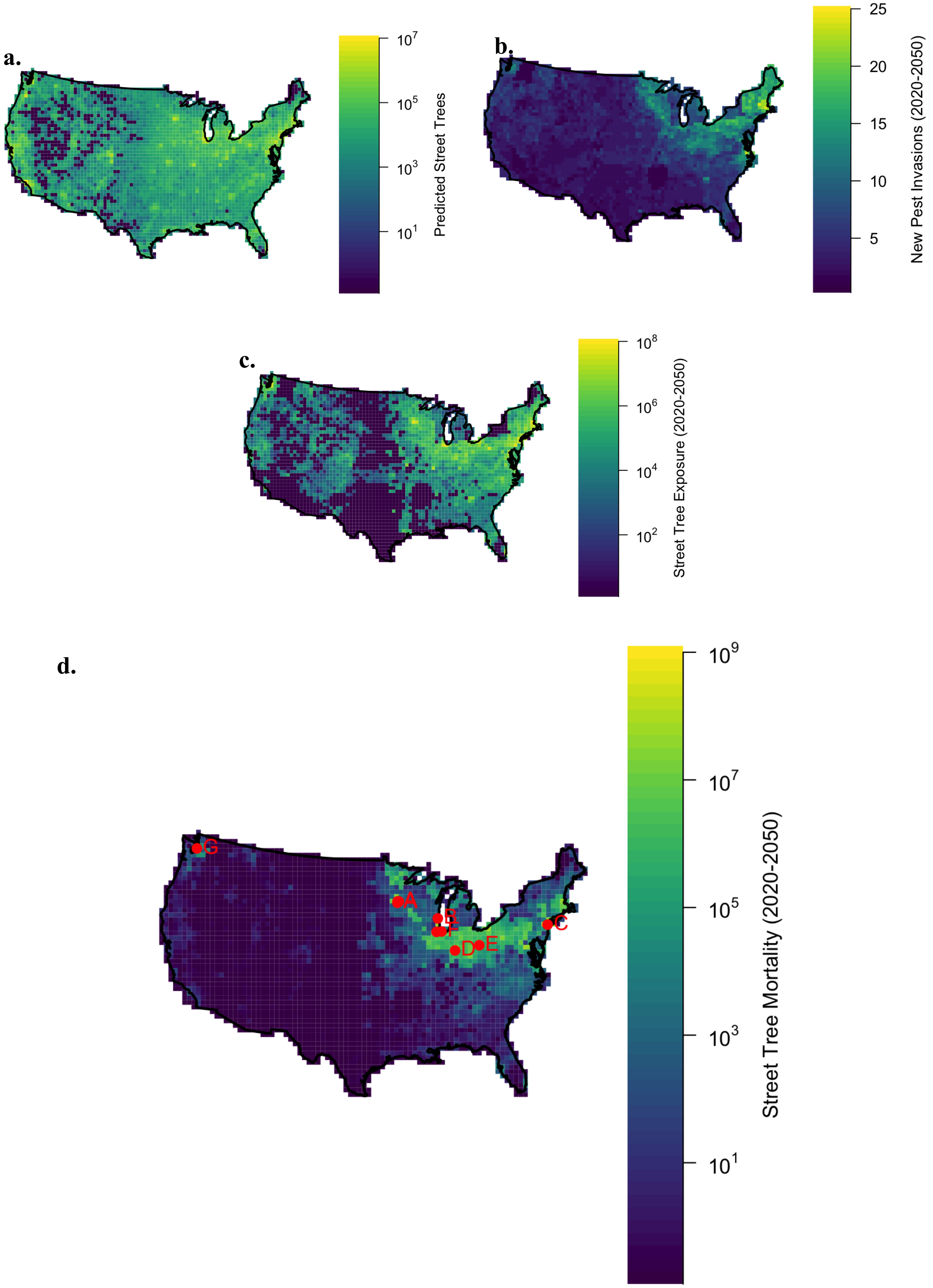
a.
10^7
10^5
10^3
10^1
Predicted Street Trees
b.
25
20
15
10
5
New Pest Invasions (2020-2050)
c.
10^8
10^6
10^4
10^2
Street Tree Exposure (2020-2050)
d.
G
A
B
F
C
D
E
10^9
10^7
10^5
10^3
10^1
Street Tree Mortality (2020-2050)

Figure 4.4 Posterior distribution for the beta model of host mortality due to pests within each severity category. 95% Bayesian credible intervals are shown in grey, and the posterior median is shown in black. Coloured bins represent severity categories extended from Potter et al. (2019).

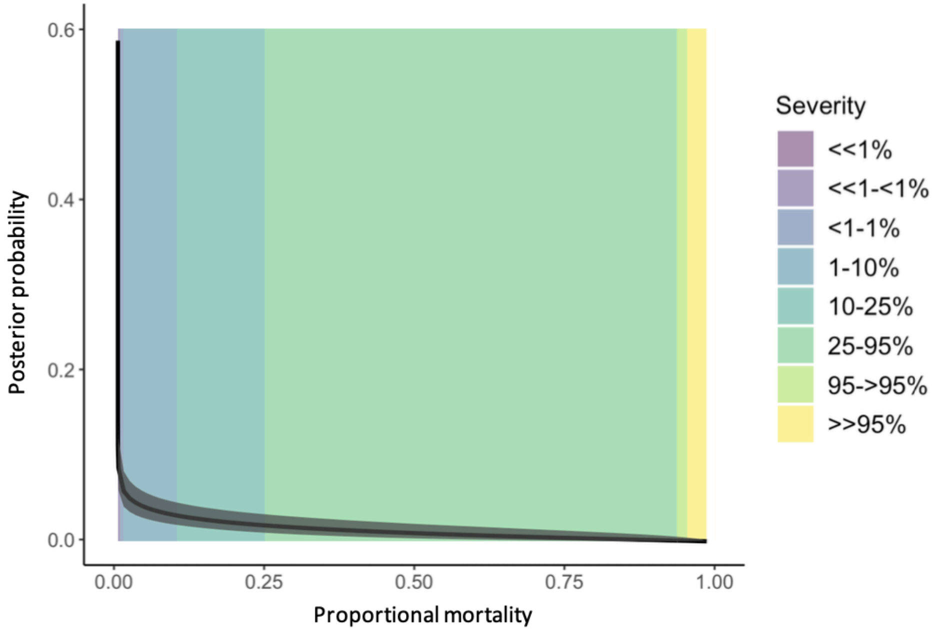

Figure 4.5 Predicted annualized costs for the best guess mortality debt scenario, with 95% Bayesian credible intervals shown in yellow and the posterior mean shown in red (146M USD).

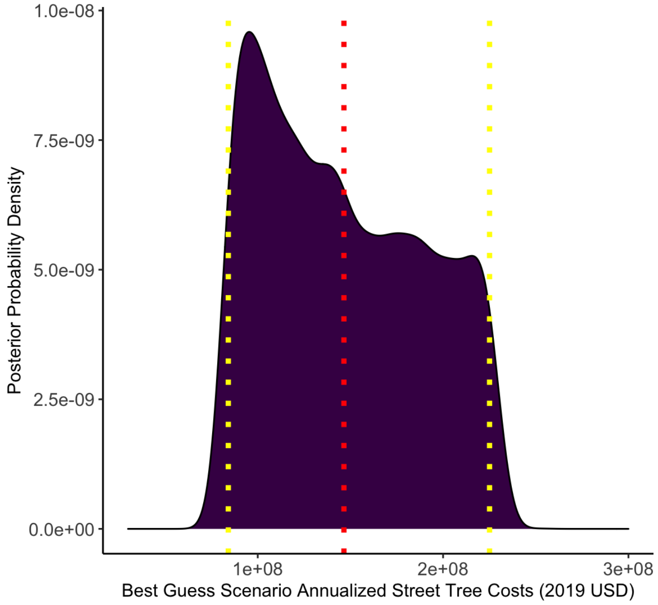

Figure 4.6 Depiction of the influence of mortality debt on temporal cost patterns. Predicted costs 2020 to 2050 for the 10 year (yellow), 50 year (teal), and 100 year (purple) mortality debt scenarios with a 10 year initial invasion lag. The best guess predictions are shown as a dashed red line. Costs are presented in 5-year increments in accordance with the timestep length within our spread model.

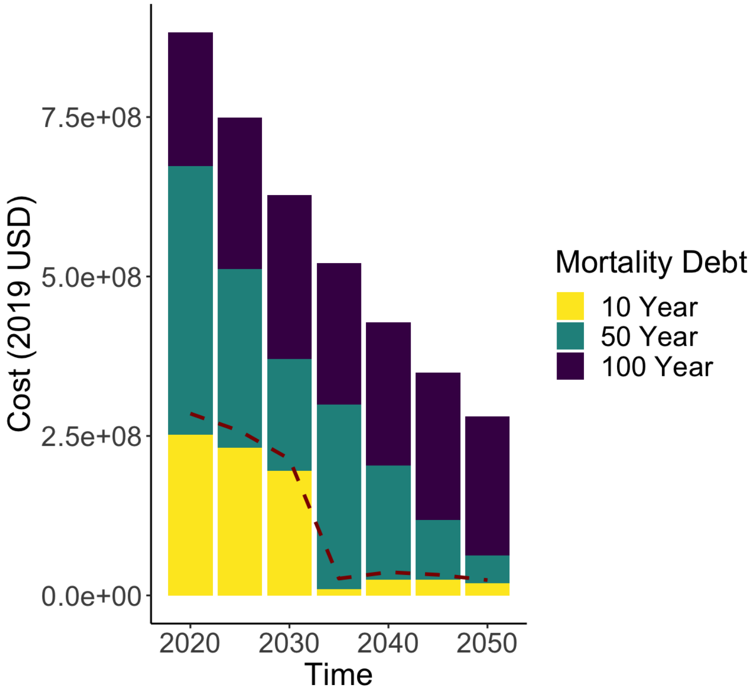

4.7.2 Tables

Table 4.1 Predicted annualized cost (in 2019 USD) and tree mortality across invasion scenarios from 2020 to 2050 across all 57 species. "Best Guess" indicates the scenario with expert-elicited mortality debt durations by guild, "Vary" scenarios hold all guilds but the focal guild constant at their best guess scenario, and "All" fix all three guilds at a given mortality debt duration. Mean mortality for best guess = 7.8%, 59M trees, 146M USD annualized (3.3B over the next 30 years).

Mortality Debt Scenario	Annualized Cost (millions 2019 USD)		Tree Mortality (millions)		Percent Mortality	
	lower 95% CI	upper 95% CI	lower 95% CI	upper 95% CI	lower 95% CI	upper 95% CI
Best Guess	84.1	225	2.72	7.26	4.5%	12.0%
Vary Borers	84.4	846	2.62	38.8	4.4%	64.3%
Vary Defoliators	80.4	218	2.49	6.96	4.1%	11.5%

Vary Sap-Feeders	80.5	212	2.50	6.70	4.1%	11.1%
All 10	82.7	218	2.51	6.69	4.1%	11.1%
All 50	16.2	446	7.47	20.6	12.4%	34.0%
All 100	32.4	897	14.8	41.1	24.42%	67.82%

Table 4.2 Visual representation of the sources of uncertainty and their relative quantification across impact types, where redder hues indicate greater uncertainty. Sources of uncertainty include 1) future climatic variability, 2) spread model uncertainty, 3) host distributional model uncertainty, 4) asymptotic mortality misestimation, 5) mortality debt model misspecification, 6) variability in management behaviour.

Tree Type	**Dimension of Impact**			
	Exposure[1,2,3]	Mortality (Asymptotic)[1,2,3,4]	Mortality (2020-2050)[1,2,3,4,5]	Cost (2020-2050)[1,2,3,4,5,6]
Residential	🟨	🟧	🟧	🟥
Community	🟨	🟧	🟧	🟥
Street	🟨	🟨	🟧	🟧

Connecting statement

In Chapter 4, I moved from a more purely ecological focus to an impact focus, and created estimates of damages to urban trees due to the three major US insect forest pest feeding guilds. In spite of the applied focus, these projections remained heavily informed by ecological models, including projections of pest distributions from the SDK, and newly-developed models of host tree distributions and host tree mortality due to each pest species.

In this chapter, I combined 4 subcomponent models to produce cost estimates: first, a model for urban trees, second, the SDK predictions from Chapter 2, third, a model of host death given pest exposure, and finally, some simple assumptions about the human response to tree infestation. The first three model components were major advances compared to the previous work. I moved from assuming all cities had the same tree distribution, to spatial resolution at the city level for urban trees, and from 3 point estimates for pest spread and host mortality due to each pest, to different estimates for each pest. This improvement was possible due to high resolution spatiotemporal spread predictions from Chapter 2.

This framework demonstrated how general models that leverage the increased predictability of invasions at a macroecological scale due to anthropogenic replacement can be used to create higher resolution predictions of managerial interest. I was able to use these general models to move from rough estimates of damage with no spatiotemporal resolution, to species, host tree, city, and time-specific predictions of pest damage for each pest species.

General Discussion

5.1 Introduction

The primary goal of this thesis was to identify largescale generalities across species invasions in the secondary invasion process, in order to uncover new macroecological rules governing invasive community ecology, as well as to advance predictive pest management. In Chapter 1, I built a general spread model for US invasive forest pests. In Chapter 2, I contrasted this general model with more complex single-species models, and derived an intermediate-complexity model that leveraged the benefits of both customization and anthropogenically-induced generalities. Chapter 3, I moved from spread to the establishment phase within secondary invasions, and built a general, integrative establishment model to uncover the nuanced relationship between host biodiversity and secondary invasion success. Finally, in Chapter 4, I built an impact framework from a suite of predictive ecological and economic models in order to determine the extent of future damage to urban trees from invasive forest pests.

5.2 Main findings

Currently, most predictions of species invasions use species-specific models (Muirhead et al. 2006; Carrasco et al. 2010, Gagnon et al. 2015). In Chapter 1, I showed that a common dispersal kernel can capture much of the variation in pest extent across all known damaging forest pests in the US, thereby showing support for novel macroecological rules governing pest invasions.

Further, my GDK model advances predictive invasion biology through its ability to forecast the spread of new invaders using only a point of likely introduction and knowledge of their host species. I hypothesized that the generalities uncovered were due to anthropogenic replacement, where humans transport species analogously across the entire community of forest pest species.

Within Chapter 2, I explored the value of using the GDK as a basic structure upon which to build models, adding context-specific information where it was known within the SDK. Given that spread models have previously been parameterized using the same time-series data as the customized models, and that these were found to be weaker than the SDK, I demonstrated that even models using the best available data may not produce highly predictive forecasts. On the other hand, it appears that a model employing snapshots of whole-community pest distributions, a species' known initial invasion location, and when necessary, its known niche limitations, can outperform the best-fitting customized model. My Chapter 2 forecasts suggested future invasions will be even more aggregated in space, and that urban centers and areas of high forest cover and high tree density appear to be general attractors for all pests.

In Chapter 3, I performed an analysis of whole-community US forest pest secondary establishment, where I was able to separate the role of host density, species richness, and the spatially-autocorrelated spread process from the role of host evolutionary history. Within this framework, I was able to detect a novel, nonlinear relationship between phylogenetic host dissimilarity and pest establishment, where density-dependent amplification occurs for closely related hosts, density-dependent dilution occurs for more distantly related hosts, and very distantly related hosts have negligible effects. These patterns occur in part due to the greater ease of generalist pests to establish, but appear to also be driven by climatic or other biotic factors beyond host community composition. This general pattern emerged across all 72 invasive forest pests in the US. This finding highlighted the importance of considering evolutionary history when attempting to understand the occurrence of invasive species, and provided a more nuanced, macroecological picture of the role host diversity plays on pest infestation.

Within Chapter 4, I demonstrated that various sources of partial information, including pest distributional predictions from Chapter 2, can be synthesized in order to produce finer scale spatiotemporal predictions of future pest impacts. This estimate was a major increase in accuracy compared to the previous analysis, which relied on 3 single-species estimates and the assumption that host trees are distributed uniformly across the US based on estimates from a handful of cities (Aukema et al. 2011). My analyses show that US invasive forest pests will likely kill hundreds of millions of urban trees in the next 30 years, and that managing dead street trees alone will cost $146M USD annually. The cities facing the greatest tree mortality are predominantly in the Midwest, and mortality patterns are driven by emerald ash borer induced ash mortality. Street trees account for only 6.8% of all urban trees, meaning the total urban tree costs could be an order of magnitude larger (~$1.6B annually). Therefore, management behaviour for non-street trees must be better understood in order to fully understand future costs to US municipalities.

5.3 Implications

5.3.1 Ecological implications

This thesis has examined generalities that emerge at large scales across species invasions from the ecological to the applied. These analyses have provided support for the theory that humans are allowing for invasive species distributions, and thus their associated damages, to become broadly predictable across contexts. A fundamental aspect of ecology, and for any branch of scientific theory, is a search for general theories that can be applied broadly without many case-specific modifications. The fit of the GDK in Chapter 1 was extremely strong, in spite of having very few predictor variables, indicating consistency in the spread process of a diversity of pests at large scales. In Chapter 2, I performed the first known comparison of general and species-specific ecological spread models' predictive abilities. My results suggested that general models can be effectively synthesized with context-specific information to respond quickly to invasions. In Chapter 3, I simultaneously modelled the many processes involved in pest establishment and detected a novel, nonlinear relationship between phylogenetic host dissimilarity and pest establishment, which was generalizable across all species in the pest community, analogous to the generalizability of the spread process. This thesis has thus provided support for general rules governing invasive pest spread and establishment by being able to make predictions across species, time and space using common models and frameworks.

This work advances the literature on invasive spread models by providing a more process-based framework to understand long-distance dispersal that still builds from its foundations in reaction-diffusion (Skellam et al. 1951). The original population ecology models for invasive spread predict isotropic spread (Shigesada et al. 1995; Neubert & Parker 2004; Skarpaas & Shea 2007). These models are not spatially-explicit, and do not allow for the flexibility of including additional spatial predictors of dispersal. More contemporary models have allowed for the incorporation of spatial factors, but are quite distinct from travelling wave formulations of invasive spread (e.g. gravity models, Gertzen et al. 2011; Potapov et al. 2011). Given the more continuous nature of forests, the parameterization of a smoother dispersal kernel is likely more appropriate than a gravity model formulation. However, the use of the basic structure of the dispersal kernel formulation, augmented by the inclusion of spatial predictors, allows us to balance the benefits of continuous spread without relying on the assumption that it is isotropic.

Throughout this thesis, I have demonstrated support for my anthropogenic replacement hypothesis, where humans are making systems easier to predict at large scales, and have used this to my advantage to create higher resolution forecasts of future pest establishment, spread, and associated damage for forest pests. While the Chapter 3 integrative establishment model parameters are not explicitly linked with human influence, the majority of variation in pest establishment patterns could have been explained by anthropogenically mediated pest spread as captured through the GDK alone. Thus, I showed that this signal must be accounted for when assessing the role of additional predictors of establishment. Across chapters, I have used general models that borrow power across contexts to help overcome limited data, whether this was with the GDK and SDK, the general establishment model, or the urban tree and host mortality components of my economic analysis. Along the way, I have uncovered a more nuanced role of host biodiversity on forest pest infestation.

5.3.2 Management implications

The general macroecological rules uncovered with the GDK, SDK and establishment models also have considerable applied value in allowing potential new pest threats to be predicted and management to be planned before they have even established in a region. The frameworks produced throughout this thesis have immediate value to forest managers. They can be used to motivate and direct the effective allocation of government funding for invasive species surveillance and management by delineating areas of high future risk and associated potential economic losses if preventative measures are not taken.

In order to make the most effective pest management decisions, policymakers and managers require information on the most likely spatiotemporal pattern of future pest damages. Further, in the absence of cost information, the degree of devastation caused by invasive species can easily be brushed aside. Based on recent advances and my own previous work, I was able create a more accurate, better resolved picture of future spatiotemporal damages across the entire insect pest community. I have shown that these pests will likely kill ~8% of existing street trees by 2050, and could have total damages on the order of tens of billions of dollars. While these are rough estimates subject to many sources of uncertainty, they illustrate the gravity of pest infestations in urban areas. The creation of finescale spatiotemporal cost estimates also allows for the prioritization of future management efforts, for instance through the delineation of so-called "mortality hotspot cities", and can allow for predictive impact modelling for future invaders, thereby allowing managers to be better prepared for future threats.

The cost curves I was able to produce as a result of the Chapter 4 framework can be synthesized with pathway level risk analyses for future pest entry in order to forecast future pathway level risk for entire suites of pest species. Further, for invaders known to be on the horizon such as the Asian gypsy moth (*Lymantria dispar var. asiatica*, Gray 2017), the submodels can be used to predict future spread and subsequent impact trajectories given different initial introduction sites. The integration of this framework within a spatial prioritization tool (i.e. allowing future damage trajectories to vary with the imposition of policies such as quarantines) would also allow policymakers to determine key sites for limiting future damages due to the entire pest community.

5.4 Limitations

As I showed in Chapter 2 , there is substantial uncertainty in future pest distributions and damages even with our best current models, given available data. Intuitively, such uncertainty will commonly occur, and I argue that invasive species models should be validated using temporal data withheld from fitting, where possible. I chose to explore several additional aspects of uncertainty in this thesis, including variability across climate and population growth scenarios, uncertainty in true host mortality rates, and across mortality debt scenarios, but have not been exhaustive. As I showed in Table 4.2, one of the most challenging sources of data scarcity is a lack of understanding of the human response to pest infestation. I am fairly confident in my mortality and cost estimate methodology for US urban trees given the scenario that only dead trees are managed. However, a large amount of uncertainty exists surrounding how non-street trees will be managed, particularly for community trees, and surrounding the extent of preventative management behaviour across all land types.

My models employed only two of the many alternative climate and population growth scenarios. Further, my models were based on current and historical conditions. Climate change could alter environmental suitability either due to its direct influence on the invading species or indirectly via effects on hosts and other species (Hellmann et al. 2008, Appendix S2.3). Fortunately, the SDK and urban tree distributional frameworks can easily parameterize any type of spatial limitation for any pest species or host genus, and can thus incorporate future knowledge of pest distributional thresholds.

I was also necessarily limited in the model structures examined for these four thesis chapters. I believe that I have made the best choices for the underlying mechanisms being studied, and have chosen structures that are modular and thus can easily incorporate additional components. One less positive aspect of modularity is the non-independence between the spread and establishment models of Chapters 1 and 3. I relied on a fitted establishment model as input into the spread model, and did not refit spread model parameters beyond a scaling factor when creating the Chapter 3 integrative joint model. This means that some factors important for spread could have been misattributed to the establishment model, and vice versa. This would have limited their detectability in the integrative joint model, and therefore diminish their predicted importance. As such, the 14.9% improvement to the spread model through the incorporation of the integrative establishment model is likely an underestimate of its importance.

Another limitation that made relationships difficult to detect is an overall paucity of data across the models within this thesis. The opportunistic nature of data collection can also lead to biases in the types of data examined. In Chapter 2, I fit customized models to only three species, because these were the only species with available time series, which happened to be some of the most damaging pest species in the overall dataset. In Chapter 4, the subset of inventoried host communities was also a biased set of US urban areas. It is possible that the missing regions and species have different relationships with the modelled predictor variables. This could have produced models with higher or lower predictive performance, but I was limited to the data available. On the other hand, I have used the inherent data scarcity to my advantage by showcasing the ability to augment predictive ability with general models via the SDK, general urban tree distributional models, and the general establishment model.

5.5 Future directions

My existing models are fit to all economically-damaging United States invasive forest pests, but a logical next step would be to extend these models into Canada with the aid of Canadian government researchers. Natural Resources Canada's Canadian Forest Service possesses Canadian tree inventory data, and the Canadian Food Inspection Agency houses a database of nationwide pest surveillance efforts, both of which would be highly useful in this extension. Key challenges to producing a Canadian analog to this framework will be the predominantly East-West traffic patterns of human dispersal within Canada, and a lower resolution of forest inventory data relative to the US.

Over the course of my PhD, I focused on descriptive models of invasions across species at large scales, including models of establishment and dispersal, as well as descriptive analyses of future pest damages. I did not explore the role of alternative management scenarios. I intend to move from a descriptive to a prescriptive perspective in future work, and use model projections of pest distributions according to future treatment and quarantine scenarios to determine optimal management strategies. My existing models of pest distributions, host tree distributions, and subsequent host tree mortality could be used directly as inputs to the optimization schemes created (Chadès et al. 2017). The economic analyses from Chapter 4 could then be updated according to different future management scenarios to determine how quarantines and treatment regimens would impact future pest dispersal and subsequent tree mortality and economic loss. Additionally, value of information analyses could incorporate the uncertainties uncovered in the pest distributional models from Chapter 2 in order to determine the relative benefit of increasing surveillance to more accurately delineate pest distributions, versus allocating budgets toward active quarantine and treatment (Bennett et al. 2018). These analyses will help determine whether humans are not only allowing for invasion risk to become more predictable, but also creating situations where the optimal treatment, quarantine and/or surveillance actions are also consistent across forest pest species, space, and time. Conventional approaches to optimize management utilize simplified invasion models that cannot capture hubs of human transport such as cities, and therefore may misestimate the effects of management (Sharov et al. 2002). Further, imperfect monitoring means that true pest distributions are uncertain. While increased surveillance reduces uncertainty, the benefit of correctly delineating distributions must be weighed against the cost of waiting for better information.

In the future, I plan to create a mathematical framework for the optimal control of forest pest invasions that balances the roles of surveillance and management. I hypothesize that there are generalities in the best management strategies, and in the budgetary balance between management and surveillance across species. Further, I hypothesize that accounting for spatial spread alters optimal strategies compared to conventional approaches. To explore these hypotheses, I will overlay a decision theoretical model that assesses the effects of potential management decisions on sub-models of pest dispersal, host tree distributions, and host mortality to determine the set of management actions that minimizes economic losses. I will also conduct a value of information analysis to determine the ideal balance between taking action and reducing uncertainty through increased surveillance. To explore the existence of largescale generalities, optimizations will be examined for common spatiotemporal patterning, and the objective function will be calculated based on heuristics derived from these common patterns to determine a suite of nearly optimal responses. These rules of thumb will be summarized in an online tool where managers can provide information on their pests and regions of interest as well as their management options and budgets to receive control recommendations.

5.6 Conclusion

This thesis has achieved its goal of uncovering largescale generalities across species invasions. These generalities can be explained by anthropogenic replacement, where the dominant role of humans means that many of the drivers of invasive species establishment, spread, and associated damages are common among species. Generalized predictive models, especially when augmented with simple context-specific information, can actually outperform models containing idiosyncratic data fit separately, due to increases in predictive power from anthropogenic generalities. These generalities extend from the secondary spread to the secondary establishment process, and can be used to uncover broad relationships between host biodiversity and pest success, where host density, relatedness, and species richness all combine to determine the likelihood of pest establishment. The generalities uncovered in the factors governing present and future pest distributions can also be used to create high-resolution forecasts of future spatiotemporal damages of the entire pest community to urban trees. I project future mortality of urban trees on the order of hundreds of millions in the next 30 years, and annualized damages of $146M USD for the management of dead street trees alone. Moving from a descriptive to a prescriptive lens, predictions from these models can act as inputs to invasive species control programs, and I plan to use them in subsequent work to develop general heuristics for effective pest management.

References

Aukema, J. E., Leung, B., Kovacs, K., Chivers, C., Britton, K. O., Englin, J., ... *et al*. (2011). Economic impacts of non-native forest insects in the continental United States. *PLoS One*, 6(9).

Aylor, D. E. (1990). The role of intermittent wind in the dispersal of fungal pathogens. *Annual Review of Phytopathology,* 28(1), 73-92.

Bennett, J. R., Maxwell, S. L., Martin, A. E., Chadès, I., Fahrig, L., & Gilbert, B. (2018). When to monitor and when to act: Value of information theory for multiple management units and limited budgets. *Journal of Applied Ecology*, *55*(5), 2102-2113.

Bradie, J., Chivers, C., & Leung, B. (2013). Importing risk: quantifying the propagule pressure–establishment relationship at the pathway level. *Diversity and Distributions*, 19(8), 1020-1030.

Bradie, J., & Leung, B. (2015). Pathway-level models to predict non-indigenous species establishment using propagule pressure, environmental tolerance and trait data. *Journal of Applied Ecology*, 52(1), 100-109.

Bradshaw, C. J., Leroy, B., Bellard, C., Roiz, D., Albert, C., Fournier, A., ... *et al*. (2016). Massive yet grossly underestimated global costs of invasive insects. *Nature communications*, *7*(1), 1-8.

Brown, J. H. (1999). Macroecology: progress and prospect. *Oikos*, 3-14.

Cadotte, M. W., Murray, B. R., & Lovett-Doust, J. (2006). Ecological patterns and biological invasions: using regional species inventories in macroecology. *Biological Invasions*, 8(4), 809-821.

Cardinale, B. J., Duffy, J. E., Gonzalez, A., Hooper, D. U., Perrings, C., Venail, P., … *et al*. (2012). Biodiversity loss and its impact on humanity. *Nature,* 486(7401), 59-67.

Carrasco, L. R., Mumford, J. D., MacLeod, A., Harwood, T., Grabenweger, G., Leach, *et al*. (2010). Unveiling human-assisted dispersal mechanisms in invasive alien insects: integration of spatial stochastic simulation and phenology models. *Ecol. Model*., 221(17), 2068-2075.

CBD. (2006). *Global Biodiversity Outlook 2*. Secretariat of the Convention on Biological Diversity, Montreal, 81 + vii pages.

Chadès, I., Nicol, S., Rout, T. M., Péron, M., Dujardin, Y., Pichancourt, J. B., ... *et al*. (2017). Optimization methods to solve adaptive management problems. *Theoretical Ecology*, *10*(1), 1-20.

Crutzen, P. J. (2006). The "anthropocene". In Earth system science in the anthropocene (pp. 13-18). Springer, Berlin, Heidelberg.

Drake, J. M., & Lodge, D. M. (2004). Global hot spots of biological invasions: evaluating options for ballast–water management. *Proceedings of the Royal Society of London. Series B: Biological Sciences*, 271(1539), 575-580.

Elton, C. S. (2000). *The ecology of invasions by animals and plants*, 2. University of Chicago Press, Chicago, United States.

Essl, F., Lenzner, B., Courchamp, F., Dullinger, S., Jeschke, J. M., Kühn, I., ... *et al.* (2019). Introducing AlienScenarios: a project to develop scenarios and models of biological invasions for the 21 st century. *NeoBiota*, 45, 1-17.

Gagnon, K., Peacock, S. J., Jin, Y., & Lewis, M. A. (2015). Modelling the spread of the invasive alga *Codium fragile* driven by long-distance dispersal of buoyant propagules. *Ecological Modelling*, 316, 111-121.

Gertzen, E., Leung, B. & Yan, N. (2011). Propagule pressure, Allee effects and the probability of establishment of an invasive species (*Bythotrephes longimanus*). *Ecosphere*, 2, 1-17.

Gilbert, G. S., & Webb, C. O. (2007). Phylogenetic signal in plant pathogen-host range. *Proceedings of the National Academy of Sciences,* 104, 4979-4983.

Gilbert, M., Grégoire, J. C., Freise, J. F., & Heitland, W. (2004). Long-distance dispersal and human population density allow the prediction of invasive patterns in the horse chestnut leafminer *Cameraria ohridella*. *Journal of Animal Ecology*, 73(3), 459-468.

Gray, D. R. (2017). Risk analysis of the invasion pathway of the Asian gypsy moth: a known forest invader. *Biological Invasions*, 19(11), 3259-3272.

Haack, R. A. (2006). Exotic bark-and wood-boring Coleoptera in the United States: recent establishments and interceptions. *Canadian Journal of Forest Research,* 36(2), 269-288.

Haas, S. E., Hooten, M. B., Rizzo, D. M., & Meentemeyer, R. K. (2011). Forest species diversity reduces disease risk in a generalist plant pathogen invasion. *Ecology Letters*, 14(11), 1108-1116.

Hechinger, R. F., & Lafferty, K. D. (2005). Host diversity begets parasite diversity: bird final hosts and trematodes in snail intermediate hosts. *Proceedings of the Royal Society of London. Series B: Biological Sciences*, 272(1567), 1059-1066.

Hellmann, J. J., Byers, J. E., Bierwagen, B. G., & Dukes, J. S. (2008). Five potential consequences of climate change for invasive species. *Conservation Biology*, 22(3), 534-543.

Hooper, D. U., Adair, E. C., Cardinale, B. J., Byrnes, J. E., Hungate, B. A., Matulich, K. L., *et al*. (2012). A global synthesis reveals biodiversity loss as a major driver of ecosystem change. *Nature*, 486(7401), 105-108.

Hudgins, E. J., Liebhold, A. M., & Leung, B. (2017). Predicting the spread of all invasive forest pests in the United States. *Ecology Letters*, 20(4), 426-435.

Hudgins, E. J., Liebhold, A. M., & Leung, B. (2020). Comparing generalized and customized spread models for nonnative forest pests. *Ecological Applications*, 30(1), e01988.

IPPC (International Plant Protection Convention). 2002. *International standards for phytosanitary measures*. Rome, Italy: FAO. www.fao.org/docrep/009/a0450e/a0450e00.htm. Viewed 12 May 2020.

Jactel, H., & Brockerhoff, E. G. (2007). Tree diversity reduces herbivory by forest insects. *Ecology Letters,* 10(9), 835-848.

Kelly, N. E., Wantola, K., Weisz, E., & Yan, N. D. (2013). Recreational boats as a vector of secondary spread for aquatic invasive species and native crustacean zooplankton. *Biological Invasions*, 15(3), 509-519.

Kovacs, K. F., Haight, R. G., McCullough, D. G., Mercader, R. J., Siegert, N. W., & Liebhold, A. M. (2010). Cost of potential emerald ash borer damage in US communities, 2009–2019. *Ecological Economics*, 69(3), 569-578.

Leung, B., Hudgins, E. J., Potapova, A., & Ruiz-Jaen, M. C. (2019). A new baseline for countrywide α-diversity and species distributions: illustration using> 6,000 plant species in Panama. *Ecological Applications*, 29(3), e01866.

Leung, B., Roura-Pascual, N., Bacher, S., Heikkilä, J., Brotons, L., Burgman, M. A, … *et al.* (2012). TEASIng apart alien species risk assessments: a framework for best practices. *Ecology Letters, 15*(12), 1475-1493.

Leung, B., Springborn, M. R., Turner, J. A., & Brockerhoff, E. G. (2014). Pathway-level risk analysis: the net present value of an invasive species policy in the US. *Frontiers in Ecology and the Environment,* 12(5), 273-279.

Liebhold, A. M. (2012). Forest pest management in a changing world. *International Journal of Pest Management*, *58*(3), 289-295.

Liebhold, A. M., Halverson, J. A., & Elmes, G. A. (1992). Gypsy moth invasion in North America: a quantitative analysis. *Journal of Biogeography*, 19(5),513-520.

Lockwood, J. L., Cassey, P., & Blackburn, T. (2005). The role of propagule pressure in explaining species invasions. *Trends Ecol. Evol.,* 20(5), 223-228.

Lodge, D. M., Williams, S., MacIsaac, H. J., Hayes, K. R., Leung, B., Reichard, S., … *et al.* (2006). Biological invasions: recommendations for US policy and management. *Ecological Applications*, 16(6), 2035-2054.

Lovett, G. M., Weiss, M., Liebhold, A. M., Holmes, T. P., Leung, B., Lambert, K. F., … *et al.* (2016). Nonnative forest insects and pathogens in the United States: Impacts and policy options. *Ecological Applications,* 26, 1437-1455.

Muirhead, J. R., Leung, B., Overdijk, C., Kelly, D. W., Nandakumar, K., Marchant, K. R., … *et al.* (2006). Modelling local and long-distance dispersal of invasive emerald ash borer *Agrilus planipennis* (Coleoptera) in North America. *Diversity and Distributions,* 12(1), 71-79.

Neubert, M. G., & Parker, I. M. (2004). Projecting rates of spread for invasive species. *Risk Anal*. 24(4), 817-831.

Parker, I. M., Simberloff, D., Lonsdale, W. M., Goodell, K., Wonham, M., Kareiva, P. M., ... *et al*. (1999). Impact: toward a framework for understanding the ecological effects of invaders. *Biological Invasions*, *1*(1), 3-19.

Potapov, A., Muirhead, J., Yan, N., Lele, S. & Lewis, M. (2011). Models of lake invasibility by *Bythotrephes longimanus*, a non-indigenous zooplankton. *Biological Invasions,* 13, 2459-2476.

Potter, K. M., Escanferla, M. E., Jetton, R. M., & Man, G. (2019). Important insect and disease threats to United States tree species and geographic patterns of their potential impacts. *Forests*, 10(4), 304.

Ricciardi, A., & Cohen, J. (2007). The invasiveness of an introduced species does not predict its impact. *Biological Invasions*, *9*(3), 309-315.

Sardain, A., Sardain, E., & Leung, B. (2019). Global forecasts of shipping traffic and biological invasions to 2050. *Nature Sustainability*, 2(4), 274-282.

Seebens, H., Blackburn, T. M., Dyer, E. E., Genovesi, P., Hulme, P. E., Jeschke, J. M., ... *et al*. (2017). No saturation in the accumulation of alien species worldwide. *Nature Communications*, 8(1), 1-9.

Seebens, H., Gastner, M. T., Blasius, B., & Courchamp, F. (2013). The risk of marine bioinvasion caused by global shipping. *Ecology Letters,* 16(6), 782-790.

Shigesada, N., Kawasaki, K. & Y. Takeda. (1995). Modeling stratified diffusion in biological invasions. *American Naturalist,* 146(2), 229-251.

Sharov, A. A., Leonard, D., Liebhold, A. M., Roberts, E. A., & Dickerson, W. (2002). "Slow the spread": a national program to contain the gypsy moth. *Journal of Forestry* 100(5), 30-36.

Simberloff, D., & Gibbons, L. (2004). Now you see them, now you don't!–population crashes of established introduced species. *Biological Invasions*, 6(2), 161-172.

Skarpaas, O., & Shea, K. (2007). Dispersal patterns, dispersal mechanisms, and invasion wave speeds for invasive thistles. *American Naturalist,* 170(3), 421-430.

Skellam, J.G. (1951). Random dispersal in theoretical populations. *Biometrika* 38, 196-218.

Steffen, W., Broadgate, W., Deutsch, L., Gaffney, O., & Ludwig, C. (2015). The trajectory of the Anthropocene: the great acceleration. *The Anthropocene Review*, 2(1), 81-98.

Taylor, R. A. J., Bauer, L. S., Poland, T. M., & Windell, K. N. (2010). Flight performance of *Agrilus planipennis* (Coleoptera: Buprestidae) on a flight mill and in free flight. *Journal of Insect Behaviour,* 23(2), 128-148.

Tisseuil, C., Gryspeirt, A., Lancelot, R., Pioz, M., Liebhold, A.M., & Gilbert, M. (2015). Evaluating methods to quantify spatial variation in the velocity of biological invasions. *Ecography,* 39, 409-418.

Vilà, M., & Hulme, P. E. (Eds.). (2017). *Impact of biological invasions on ecosystem services* (Vol. 12). Cham: Springer.

Walter, J. A., Johnson, D. M., Tobin, P. C., & Haynes, K. J. (2015). Population cycles produce periodic range boundary pulses. *Ecography*, 38(12), 1200-1211.

Young, H. S., Parker, I. M., Gilbert, G. S., Guerra, A. S., & Nunn, C. L. (2017). Introduced Species, Disease Ecology, and Biodiversity–Disease Relationships. *Trends in Ecology and Evolution,* 32(1), 41-54.

Appendices

Appendix S1. Appendices for Chapter 1

Appendix S1.1 Corrigendum for Chapter 1

Corrigendum for *Hudgins et al*. (2017) DOI: 10.1111/ele.12741

Authors: Emma J. Hudgins, Andrew M. Liebhold, and Brian Leung

First published 08 February 2017

Predicting the spread of all invasive forest pests in the United States

Volume 20 Issue 4, 426-435, Article first published online: 08 February 2017

Corrigendum

This dispersal model was originally fit to 64 pest species, where we limited each pest's dispersal to areas within their known host range by matching a list of host information for each pest to tree attributes within each grid cell.

We have discovered an error in the processing of our input data for the host trees of three forest pests: *Anoplophora glabripennis*, *Cronartium ribicola*, and *Ophiostoma novo-ulmi*. Some possible hosts of these pests were not considered in our analysis as published due to a string-parsing error in data pre-processing, affecting both the possible invasible counties, as well as the host range centroid from which spread originated in our analyses for these three species. The list of host species included in our original Dryad publication remains accurate, but the data's host density tab is now inaccurate (though calculable from the other data present).

Further, we discovered that the Forest Service data on pest presence recorded one erroneous presence of gypsy moth in Floyd Co., Virginia. The species was only recorded in this county in 2012, so it should have been listed as absent in our analyses. This affected one cell of our Dryad grid (ID 4627 in *dryad_griddata* should show 0 for GM_pres).

We apologize for these two errors, and have refit the model with these two updates. In refitting the model, we found that *Anoplophora glabripennis* (Asian longhorned beetle, ALB) became a strong outlier (Figure S1.1.1), but that the model was able to fit the other 63 species.

We believe our model's inability to predict the distribution of ALB is because it has not actually successfully invaded forested areas (it is still under eradication in N. America), while its potential invasible range spans the entire US due to its breadth of suitable hosts. All detected ALB populations occur in rural or semi-rural areas, and most of them have already been successfully extirpated (Trotter & Hull-Sanders 2015). The erroneous restriction of this species' host range in the previous version of our model masked the mismatch between its very small observed distribution and immense potential distribution.

While we were not able to fit ALB, removal of this data point retained (and marginally improved) the good fits previously found for the remaining 63 species. Accuracy changed from 68.00% to 67.49% and R^2_{MSE} changed from 67.94% to 68.70% in the constant model, indicating that dispersal is still fairly consistent across locations and species. Our final model includes the same explanatory variables as before with the same signs (updated Table 1.1). However, once the confounding effect of the outlier ALB was removed, two additional terms exceeded our threshold of improved fit and were added to the GDK, such that our final model included the following 4 terms: Forested Land Area (increasing dispersal into sites, *old*), Tree Density (reducing dispersal out of sites, *new*), Human Population Density (2 terms: increasing dispersal into sites, *old*, and reducing dispersal out of sites, *new*).

While these 2 additional factors will be of interest for prediction, the other main conclusions of the manuscript remain similar: 1) invasive pest dispersal is influenced by the extent of forested habitat and the presence of humans, but still contains no pest life history trait variables, and 2) our updated general model remains highly predictive, with roughly equivalent accuracy (73.85% vs. 73.91%), and a 3.03% improvement in R^2_{MSE} (0.7774 vs. 0.7471). However, the new GDK parameters result in a 21.14% improvement in MET for these 63 species (47.45 km vs. 60.17 km per species), indicating substantially better spatial concordance between predicted and observed distributions.

Researchers intending to make use of the Dryad data should note these changes. The updated data and scripts are available at: github.com/emmajhudgins/Hudgins-et-al.-2017--ELE--corrigendum. As Figures 1.2, 1.3, 1.4, S1.1.6 and have also changed, we include the updated versions here (see Chapter 1 main text).

Figure S1.1.1 Distribution of MET scores for the published parameter set applied to the updated data (black), and the optimal parameter set applied to the updated data (green) when *Anoplophora glabripennis* (Asian longhorned beetle, ALB) is included in fitting (circled). The old parameters lead to low MET scores for all species but ALB, and the new parameter set acts to reduce this species' MET score, though it still remains much higher than all other species.

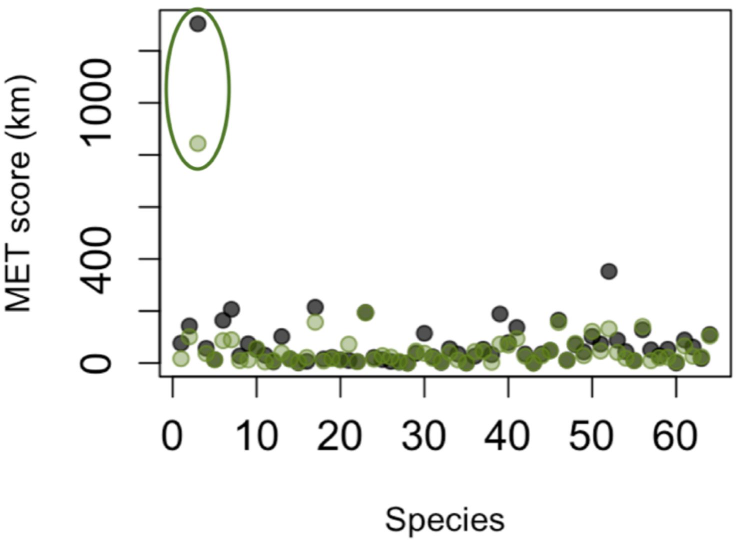

References

Trotter, R. T., & Hull-Sanders, H. M. (2015). Quantifying dispersal of the Asian longhorned beetle (*Anoplophora glabripennis*, Coleoptera) with incomplete data and behavioral knowledge. *Biological invasions,* 17(12), 3359-3369.

Appendix S1.2 Pest body size data

Table S1.2.1 Pest body size data (maximum adult length in milimetres) and associated sources (applicable only for non-pathogens).

Latin Name	Common Name	Pathogen (yes=1/no =0)	Maximum adult length (mm)	Source
Acantholyda erythrocephala	Pine False Webworm	0	12.7	D. Allen 1998. Pine False Webworm - potential threat to NY's white pine. NY Forest Owner. Http://www.dec.state.ny.us/website/dlf/privland/linkspag.html
Adelges abietis	Eastern Spruce Gall Adelgid	0	3	Canadian Journal of Arthropod Identification: Common nursery & landscape pests of Ontario http://dkbdigitaldesigns.com/clm/species/adelges_abietis
Adelges piceae	Balsam Woolly Adelgid	0	1.2	http://www.cabi.org/isc/datasheet/3268
Adelges tsugae	Hemlock Woolly Adelgid	0	0.74	http://www.cabi.org/isc/datasheet/3270
Agrilus planipennis	Emerald Ash Borer	0	14	http://www.agr.gc.ca/eng/science-and-innovation/agricultural-practices/agroforestry/diseases-and-pests/emerald-ash-borer/?id=1367251084402
Anarsia lineatella	Peach Twig Borer	0	12.7	D. Alston. 2007. Peach Twig Borer (Anarsia lineatella). Utah Pests Fact Sheet. Utah State University Extension and Utah Plant Pest Diagnostic Laboratory. ENT-36-07. Http://www.utah pests.usu.edu
Anoplophora glabripennis	Asian Longhorned Beetle	0	35	http://www.agr.gc.ca/eng/science-and-innovation/agricultural-practices/agroforestry/diseases-and-pests/asian-long-horned-beetle/?id=1366991673596
Aonidiella aurantii	California Red Scale	0	2	http://www.cabi.org/isc/datasheet/5849
Asterolecanium variolosum	Golden Oak Scale	0	2.286	T.J. Swiecki and E.A. Bernhardt. 2006. A field guide to insects and diseases of California oaks. USDA FS. Pacific Southwest Research Station General Technical Report, PSW-GTR-197.
Callidellum rufipenne	Japanese Cedar Longhorn Beetle	0	13	http://www.cabi.org/isc/datasheet/10631

Carulaspis juniperi	Juniper Scale	0	1.524	G.A. Hoover. 2002.Entomological Notes: Juniper Scale. College of Agriculture Sciences, Cooperative Extension, Department of Entomology, Penn State. http://ento.psu.edu/extension/factsheets/pdf/juniperscale.pdf
Ceratocystis fagacearum	Oak Wilt	1	NA	NA
Coleophora laricella	Larch Casebearer	0	6	http://www.agr.gc.ca/eng/science-and-innovation/agricultural-practices/agroforestry/diseases-and-pests/larch-casebearer/?id=1367260079294
Contarinia baeri	European Pine Needle Midge	0	1.7	http://www.cfs.nrcan.gc.ca/pubwarehouse/pdfs/29720.pdf
Cronartium ribicola	White Pine Blister Rust	1	NA	NA
Cryphonectria parasitica	Chestnut Blight	1	NA	NA
Cryptoccocus fagisuga Lind.	Beech Scale	0	1	http://www.cabi.org/isc/datasheet/15802
Cryptodiaporthe populea	Cryptodiaporthe Canker	1	NA	NA
Cryptorhynchus lapathi	Poplar and Willow Borer	0	10	http://www.agr.gc.ca/eng/science-and-innovation/agricultural-practices/agroforestry/diseases-and-pests/poplar-and-willow-borer/?id=1367421771921
Cyrtepistomus castaneus	Asiatic Oak Weevil	0	5.2	Bright, D.E. & Bouchard, P., Insects and Arachnids of Canada Series, Part 25. Coleoptera, Curculionidae, Entiminae. NRC Research Press, Ottawa, Ontario, Canada, 2008.
Diaspidiotus perniciosus	San Jose Scale	0	2.2	http://www.cabi.org/isc/datasheet/46224
Diprion similis	Introduced Pine Sawfly	0	10	http://www.cabi.org/isc/datasheet/19195
Discula destructiva	Dogwood Anthracnose	1	NA	NA
Elatobium abietinum	Green Spruce Aphid	0	1.8	http://www.cabi.org/isc/datasheet/30897
Epinotia nanana	European Spruce Needleminer	0	11.176	Craighead, Frank Cooper, ed. Insect enemies of eastern forests. No. 657. US Department of Agriculture, 1950.
Eulecanium cerasorum	Calico Scale	0	7.874	J.F. Stimmel. 1986. Calico scale, Eulecanium cerasorum (Cockerell) Homoptera: Coccidae. Regularory Horticulture 12(2):13-14. Entomology

				Circular No. 105, PA Dept. of Agriculture, Bureau of Plant Industry.
Euproctis chrysorrhoea	Browntail Moth	0	12.5	Length calculated from image of museum specimen with scale bar, property of Museum of Toulouse: https://en.wikipedia.org/wiki/Brown-tail#/media/File:Euproctis_chrysorrhoea_MHNT.CUT.2012.0.356._Les_Mathes_Male.jpg
Fenusa pusilla	Birch Leafminer	0	3.048	http://ento.psu.edu/extension/factsheets/pdf/birchLeafminer.pdf
Fenusa ulmi	Elm Leafminer	0	4.064	Alford, David V. Pests of Ornamental Trees, Shrubs and Flowers: A Colour Handbook. CRC Press, 2012.
Fiorinia externa	Elongate Hemlock Scale	0	1.016	Kosztarab, Michael. Scale insects of northeastern North America: identification, biology, and distribution. Virginia Museum of Natural History, 1996.
Glycaspis brimblecombei	Redgum Lerp Psyllid	0	6.35	Halbert SE, 2001. Pest Alert: Red gum lerp psyllid, http://www.doacs.state.fl.us/pi/enpp/ento/glycaspis.html.
Gremmeniella abietina	Scleroderris Canker	1	NA	NA
Homadaula anisocentra	Mimosa Webworm	0	17.018	Clarke, John Frederick Gates. A New Pest of Albizza in the District of Columbia (Lepidoptera: Glyphipterygidae). US Government Printing Office, 1943.
Hylastes opacus	European Bark Beetle	0	3.048	http://www.invasive.org/browse/detail.cfm?imgnum=5324031
Lachnellula willkommii	European Larch Canker	1	NA	NA
Lepidosaphes ulmi	Oystershell Scale	0	2.54	http://ento.psu.edu/extension/factsheets/oystershell-scale
Leucoma salicis	Satin Moth	0	38.1	http://www.maine.gov/dacf/mfs/forest_health/insects/satin_moth.htm
Lymantria dispar	Gypsy Moth	0	35	http://www.cabi.org/isc/datasheet/31807 ; http://animaldiversity.org/accounts/Lymantria_dispar/
Matsucoccus matsumurae	Red Pine Scale	0	4.7625	http://www.fs.usda.gov/Internet/FSE_DOCUMENTS/fsbdev2_043074.pdf
Melampsora larici-populina	Eurasian Poplar Leaf Rust	1	NA	NA
Neodiprion sertifer	European Pine Sawfly	0	8.89	Hamilton, Clyde C. "The Pine sawfly Neodiprion sertifer Geoff. and its control with concentrated lead arsenate sprays." Journal of Economic Entomology 36 (1943): 236-40.

Nuculaspis tsugae	Circular Hemlock Scale	0	2	http://www.na.fs.fed.us/spfo/pubs/pest_al/ehscale/ehscale.htm
Operophtera brumata	Winter Moth	0	29.972	Ferguson, D. C. "Pests not known to occur in the United States or of limited distribution. Winter moth Operophtera brumata (L.) Lepidoptera: Geometridae." Cooperative Plant Pest Report 3.48/52 (1978): 687-694.
Ophiostoma novo-ulmi	Dutch Elm Disease	1	NA	NA
Otiorhynchus sulcatus	Black Vine Weevil	0	11	http://www.cabi.org/isc/datasheet/38071
Phoracantha recurva	Eucalyptus Longhorned Beetle	0	29.2	http://www.cabi.org/isc/datasheet/40371
Phytophthora cinnamomi	Phytophthora Root Rot	1	NA	NA
Phytophthora lateralis	Port-Orford-Cedar Root Disease	1	NA	NA
Phytophthora ramorum	Sudden Oak Death	1	NA	NA
Plagiodera versicolora	Imported Willow Leaf Beetle	0	5	http://idl.entomology.cornell.edu/files/2013/11/Imported-Willow-Leaf-Beetle-2328m44.pdf
Popillia japonica	Japanese Beetle	0	11	http://www.cabi.org/isc/datasheet/43599
Pristiphora erichsonii	Larch Sawfly	0	8	http://www.agr.gc.ca/eng/science-and-innovation/agricultural-practices/agroforestry/diseases-and-pests/larch-sawfly/?id=1367419008793
Pristiphora geniculata	Mountain Ash Sawfly	0	7.5	Forbes, R. S., & Daviault, L. "The biology of the mountain-ash sawfly, Pristiphora geniculata (Htg.)(Hymenoptera: Tenthredinidae), in eastern Canada." The Canadian Entomologist 96(1964): 1117-1133.
Profenusa thomsoni	Ambermarked Birch Leafminer	0	4.064	http://www.entomology.ualberta.ca/searching_species_details.php?c=8&rnd=01092600&s=5778
Rhyacionia buoliana	European Pine Shoot Moth	0	10	http://www.cabi.org/isc/datasheet/23641
Scolytus multistriatus	Smaller European Elm Bark Beetle	0	3.8	http://www.fs.usda.gov/Internet/FSE_DOCUMENTS/stelprdb5347208.pdf
Sirex noctilio	Sirex Wood Wasp	0	34	http://www.cabi.org/isc/datasheet/50192

Sirococcus clavigignenti-juglandace	Butternut Canker	1	NA	NA
Taeniothrips inchesconsequens	Pear Thrips	0	1.778	http://ento.psu.edu/extension/factsheets/pear-thrips-pa
Thrips calcaratus	Introduced Basswood Thrips	0	5	http://www.na.fs.fed.us/SPFO/pubs/howtos/ht_bassthrips/ht_bassthrips.htm
Tomicus piniperda	Pine Shoot Beetle	0	4.8	http://www.cabi.org/isc/datasheet/54154
Trichiocampus viminalis	Poplar sawfly	0	8.89	de Tillesse, Veronique, et al. "Damaging poplar Insects-Internationally important species." (2015).
Venturia saliciperda	Willow Scab	1	NA	NA
Xanthogaleruca luteola	Elm Leafbeetle	0	6	http://www.cabi.org/isc/datasheet/44619

Appendix S1.3 Full description of data sources used to fit the GDK model

Term	Type	Description	Source	Citation
Intercept	NA	NA	NA	NA
Forested land (km^2)	HI	Sum of land area covered by forest	FIA	Miles, P.D., Brand, G.J., Alerich, C.L., Bednar, L.R.,Woudenberg, S.W., Glover, J.F. et al. 2001. The forest inventory and analysis database: database description and users manual version 1.0. General Technical Report NC-218, North Central Research Station, USDA Forest Service, St. Paul, MN.
Human Population (km^{-2})	PP	Current human population density at each time step	US Census	http://www.census.gov/popest
Host Density (km^{3}km^{-2})	HI	Host tree volume for that particular pest per grid cell	FIA	Miles et al. (2001)
Host Species Count	HI	Number of tree species that are hosts of any pest present in grid cell	FIA	Miles et al. (2001)
Tree Density (m^{3}km^{-2})	HI	Total tree volume by grid cell	FIA	Miles et al. (2001)
Body Size (mm)	LH	Maximum pest body length in mm (separate intercept fit for pathogens)	Suppl. Mat. S3	NA
Continent of Origin	LH	Continent of native range	AFPE	http://www.nrs.fs.fed.us/tools/afpe/maps
Feeding Guild	LH	Fungi vs. Insects (binary variable)	Aukema et al. 2011	Aukema, J. E., Leung, B., Kovacs, K., Chivers, C., Britton, K. O., Englin, et al. (2011). Economic impacts of non-native forest insects in the continental United States. PLoS One 6:e24587.
Number of Hosts	LH	Number of host species possessed by pest	AFPE	http://www.nrs.fs.fed.us/tools/afpe/maps

Income (USD)	PP	Per capita income in 1999	US Census	http://quickfacts.census.gov/qfd/meta/long_INC910199.htm
Road Length (km)	PP	Total length of all major roads in grid cell	ArcGIS	http://www.esri.com/data/data-maps/data-and-maps-server

Appendix S1.4 Correlations among predictor variables examined in the model

Table S1.4.1 Correlations among predictor variables examined in the model, divided into predictors applied across species (**a**.) and across space (**b**.). Spatial predictors that were applied differently across time or species (human population density and host density, respectively) are presented as averages.

Pest Life History Predictors

	Guild	Continent	Number of Hosts	Body Size
Guild	1	-0.1440	-0.1314	-0.5461
Continent	-0.1440	1	0.01742	-0.1160
Number of Hosts	-0.1314	0.01742	1	0.4598
Body Size	-0.5461	-0.1160	0.4598	1

Spatial Predictors

	Average Population Density	Average Host Density	Income	Road Length	Forested Land	Host Species Count	Tree Density
Average Population Density	1.00	0.03	0.45	0.65	-0.09	0.19	0.01
Average Host Density	0.03	1.00	0.08	0.07	0.26	0.05	0.54
Income	0.45	0.08	1.00	0.42	0.02	0.09	0.11
Road Length	0.65	0.07	0.42	1.00	0.02	0.27	0.03
Forested Land	-0.09	0.26	0.02	0.02	1.00	0.25	0.21
Host Species Count	0.19	0.05	0.09	0.27	0.25	1.00	0.01
Tree Density	0.01	0.54	0.11	0.03	0.21	0.01	1.00

Appendix S1.5 Results of fitting the GDK in 5-year increments

We used 10-year increments to fit the GDK both for computational feasibility, and because our human population data from the US Census are in decadal increments. In our original GDK, the MET score of each species was inversely related to the extent of spread ($r = -0.3406$, $p = 0.0059$). This relationship is consistent with choosing a time step width that is too wide, causing species who have spread over a smaller extent to be more negatively impacted by the binning process. However, this relationship could be caused by several other factors.

In order to determine whether this relationship was caused by time step width, we have rerun our model-building procedure the using 5-year increments linearly interpolating the census data. If our MET outliers were due to binning, we would expect the effect of extent on MET to decrease at smaller bin sizes. This model included the same first three variables as our 10-year model and did not fit substantially better (Δ% overlap (5-year - 10-year model) = -1.12%, 0.82%, 0.62%, 0.75% for the first four models of increasing complexity), and had a nearly identical relationship between MET and distance of spread ($r = -0.3360$, $p = 0.0066$ for the best 3-term model). Additionally, the pattern of outliers (defined as median+1.5*interquartile range) was not substantially different, with 8/10 outliers remaining, despite the finer temporal resolution, providing strong evidence that the relationship was not due to binning.

We offer an alternative explanation. As species spread farther, they saturate their host ranges, leading to fewer possible errors in predicted presences. In contrast, smaller extents are more reflective of stochasticity and starting conditions, and our need to initiate spread at host centroids (due to absent urban tree data) could affect species with smaller extents more severely. To determine whether urban tree data could be the culprit, we examined the MET scores of species whose source locations were inside known host range versus outside, and found a significantly poorer fit for those species with source locations outside of the host range ($t_{0.05(2),62}$ = 2.793, p = 0.006988, see Fig. 1 below).

Figure S1.5.1 MET scores in kilometers for species whose estimated first establishment occurred inside the natural host range (left) versus outside the natural host range (right).

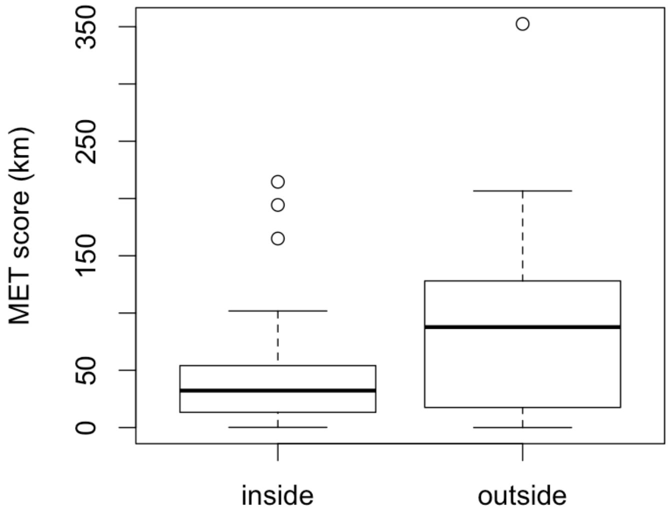

Appendix S1.6 Expanded description of metrics of fit

We used the Minimum Energy Test (MET) as our metric of model fit between predicted versus true distributions. MET compares the locational distributions of predicted versus true pest presences, and accounts for distances between predicted and true presences, which constitutes a higher information content than exact matches of presence/absence (i.e., mismatch of 50 km is better than a mismatch of 1000 km). MET was originally developed for applications in physics (Aslan & Zech 2005, Delaney *et al*. 2012). MET can be understood as a comparison of the average distance between data points within a distribution (either predicted or observed distributions) to the average distance between data points across the two distributions:

$$M = \frac{1}{n_1 n_2}\sum_{i=1}^{n_1}\sum_{j=1}^{n_2} d(L_{1,i}, L_{2,j}) - \frac{1}{2n_1^2}\sum_{i=1}^{n_1}\sum_{j=1}^{n_1} d(L_{1,i}, L_{1,j}) - \frac{1}{2n_2^2}\sum_{i=1}^{n_2}\sum_{j=1}^{n_2} d(L_{2,i}, L_{2,j}) \qquad \text{(Eqn. 1)}$$

where n_1 and n_2 are the number of occurrences observed (1) and predicted (2), respectively, d is the Euclidian distance between the locations L of occurrences. The MET score is obtained by first calculating the average distance between all occurrences from predicted versus observed distributions minus the average distance between occurrences within each distribution. If the predicted and observed distributions are identical, these quantities will be equal. As the distributions become less similar, the average distance between distributions becomes greater than within distributions. Lower MET scores represent models with better goodness-of-fit.

MET scores were minimized across species using numerical optimization (*optim*) in R (R Core Team 2015). We built our full dispersal model (GDK) using a forward selection procedure based on MET scores. Starting from the intercept-only constant dispersal model, we determined the MET score for every possible two-term model built by adding the remaining 18 terms individually to the intercept-only model. The MET score improvement between the intercept-only and each two-term model was calculated. The term producing the largest improvement was then added to the model, and forward selection repeated with higher term models, until further additions of terms did not improve the model's MET score by 5km. 5km was chosen as an arbitrary threshold to retain biological relevance.

We report two metrics of model performance. First, we compared predicted and observed locational distributions, using MET. We also report locational accuracy, which is defined as the proportion of correctly assigned presences and absences across the number of possible presence sites. As a spatial null comparison model, we also used the observed number of infested cells, but simulated randomized occurrences within the host distribution for each species (random allocation model) and took the mean MET score of 1000 simulated pest distributions for each species. As our second metric, we compared predicted ($\hat{y}$) to observed (y) range sizes, to evaluate the ability to predict the extent of invasions. We used squared deviations from the 1:1 line of ($\hat{y}$) vs. (y) as our metric of fit (i.e. mean squared error, MSE, as a proportion of the variation in observed range sizes; R^2_{MSE}):

$$R^2_{MSE} = 1 - \frac{\Sigma(y-\hat{y})^2}{\Sigma(y-\bar{y})^2} \qquad \text{Eqn. (2)}$$

This is a more conservative metric than the conventional R^2, which generates residuals from the best fitting regression line, as R^2_{MSE} forces the relationship between predicted and observed values through the 1:1 line, meaning that R^2_{MSE} will always be less than or equal to R^2. As the "null" comparison model for the extent of spread, we regressed the area occupied by all pests against the time since they were first discovered in the United States (Liebhold et al. 2013). Though a regression of pest radius and time follows more logically from the invasion literature (Skellam 1951), we wanted to keep our predictions comparable across models, and results were very similar between pest radius and pest area (within ~2% variation explained), and did not change the conclusions of this study.

References

Aslan, B. & Zech, G. (2005). New test for the multivariate two-sample problem based on the concept of minimum energy. *Journal of Statistical Computation and Simulation,* 75(2), 109-119.

Delaney, D. G., Edwards, P. K. & Leung, B. (2012). Predicting regional spread of non-native species using oceanographic models: validation and identification of gaps. *Marine Biology,* 159(2), 269-282.

Liebhold, A. M., McCullough, D.G., Blackburn, L. M., Frankel, S. J., Von Holle, B. & Aukema, J. E. (2013). A highly aggregated geographical distribution of forest pest invasions in the USA. *Diversity and Distributions,* 19, 1208-1216.

R Core Team, (2015). *R: A language and environment for statistical computing*. Vienna, Austria: R Foundation for Statistical Computing.

Skellam, J.G. (1951). Random dispersal in theoretical populations. *Biometrika* 38, 196-218.

Appendix S1.7 Model predictions across species

Observed distributions (left column) and predicted presences for constant dispersal (centre column) and GDK models (right column) for each pest species. Presences are shown in green.

Real Data Constant GDK

Wood-boring Pests

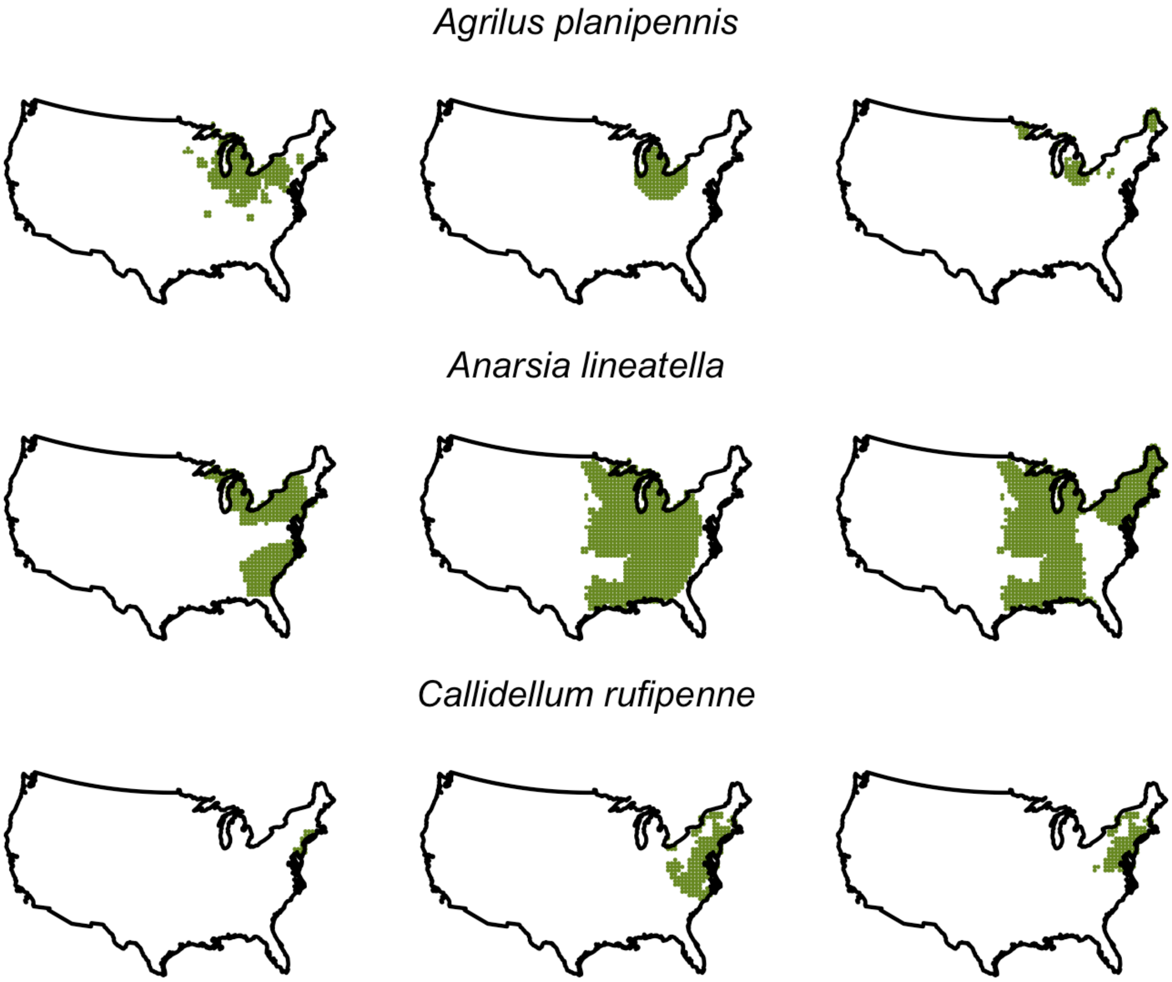

Agrilus planipennis

Anarsia lineatella

Callidellum rufipenne

Cryptorhynchus lapathi

Hylastes opacus

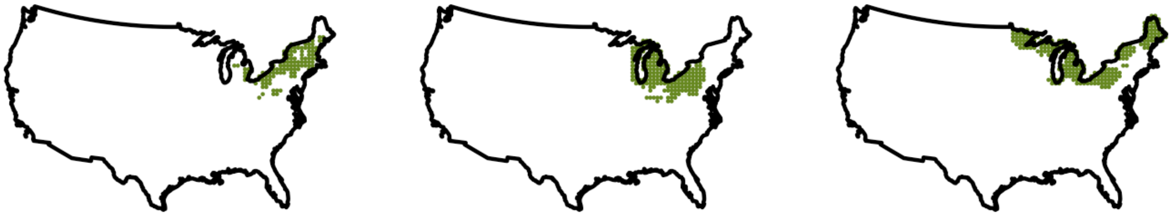

Phoracantha recurva

Scolytus multistriatus

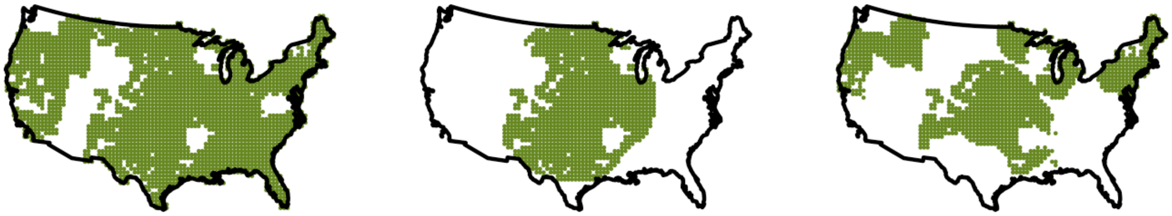

Sirex noctilio

Tomicus piniperda

Defoliating Pests

Acantholyda erythrocephala

Coleophora laricella

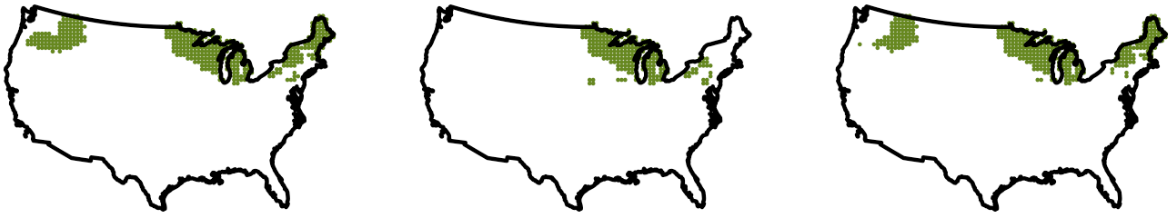

Contarinia baeri

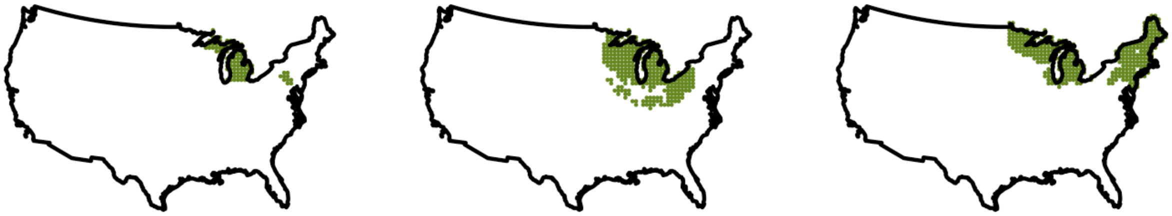

Cyrtepistomus castaneus

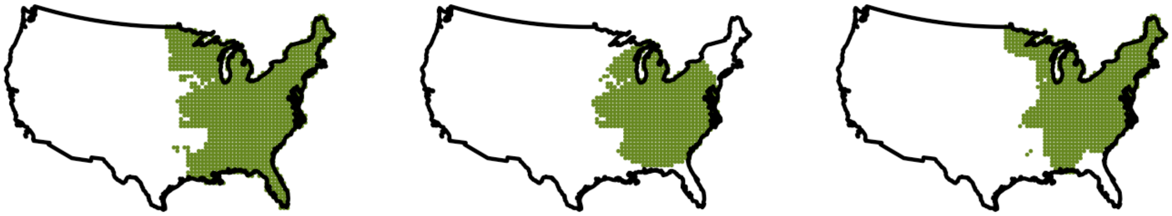

Diprion similis

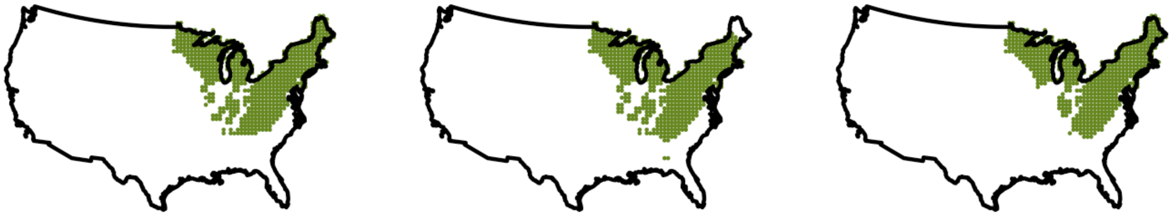

Epinotia nanana

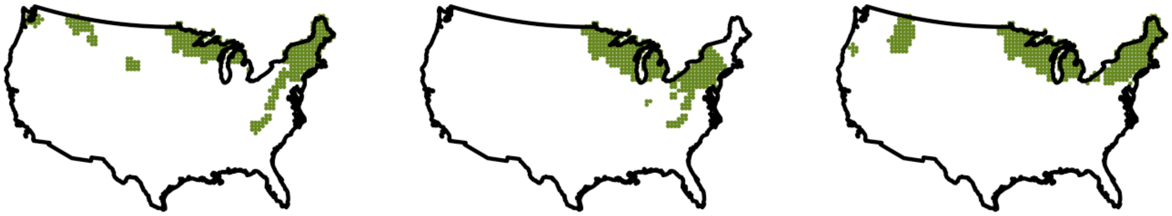

Euproctis chrysorrhoea

Fenusa pusilla

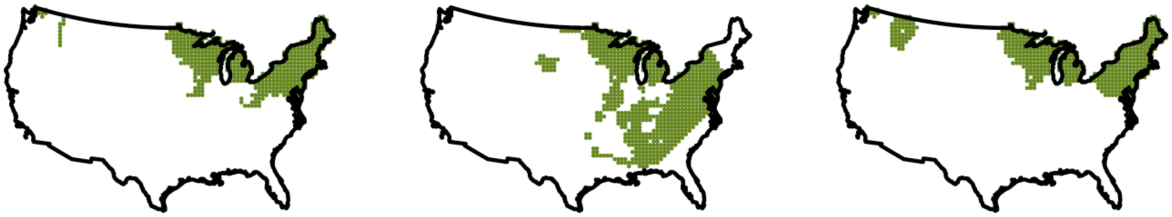

Fenusa ulmi

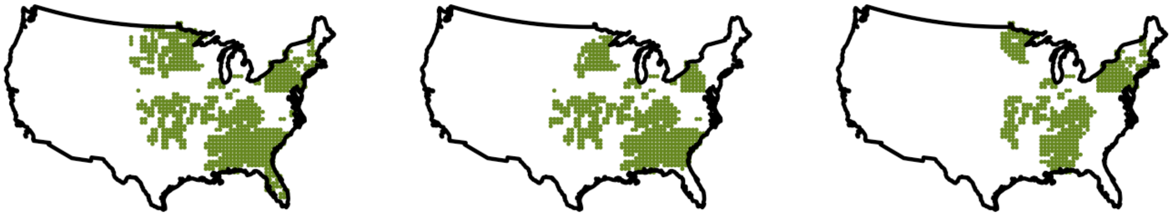

Homadaula anisocentra

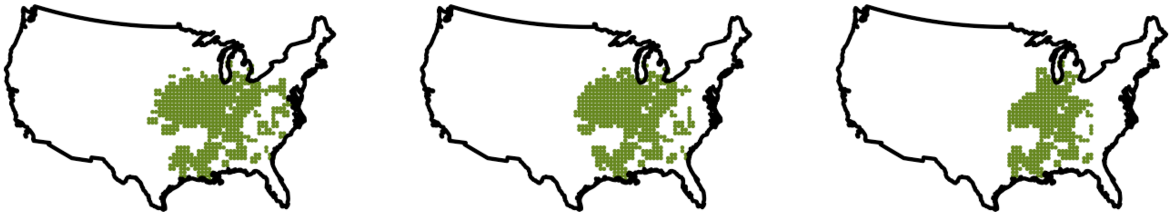

Leucoma salicis

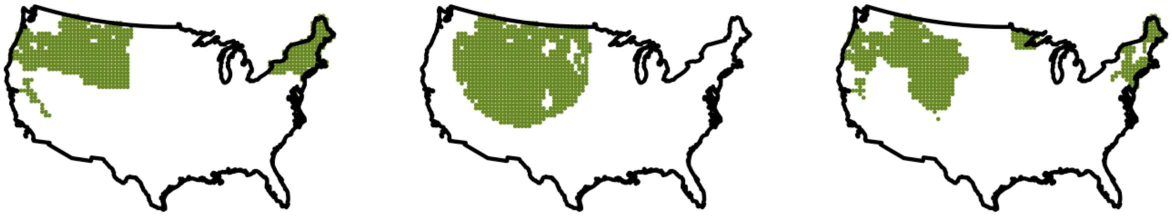

Lymantria dispar

Neodiprion sertifer

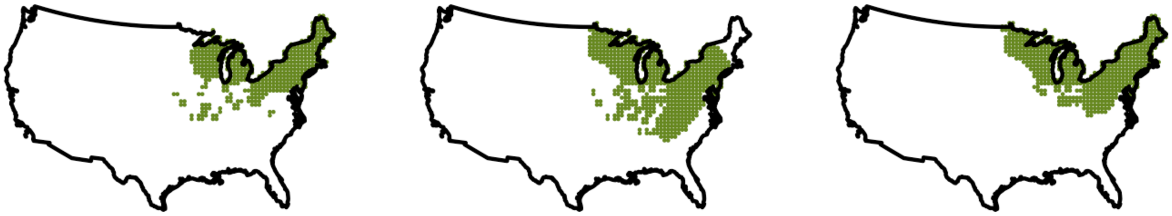

Operophtera brumata

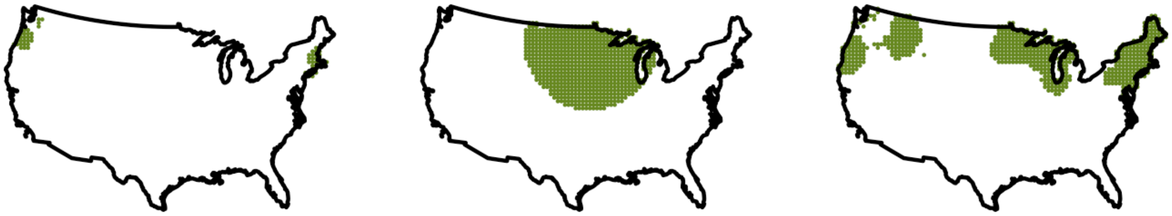

Otiorhynchus sulcatus

Plagiodera versicolora

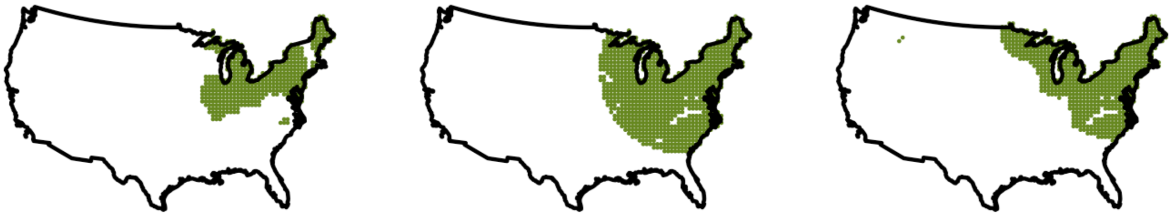

Popillia japonica

Pristiphora erichsonii

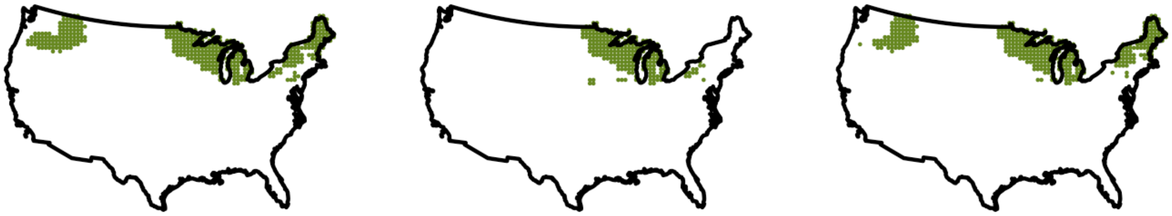

Pristiphora geniculata

Profenusa thomsoni

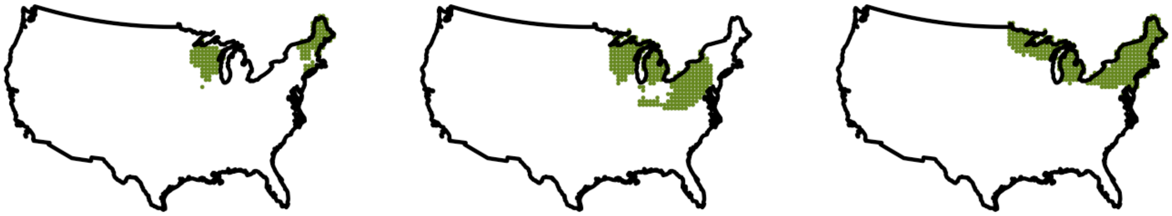

Rhyacionia buoliana

Trichiocampus viminalis

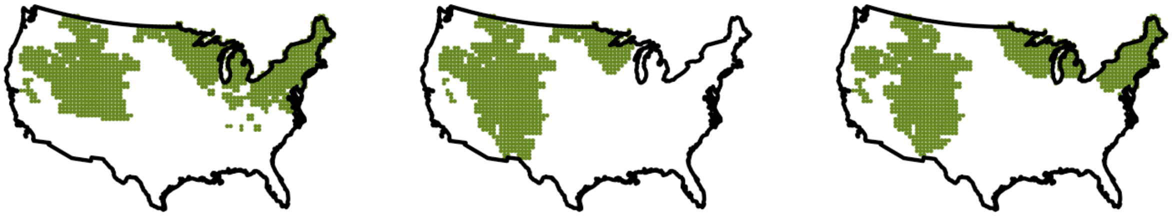

Xanthogaleruca luteola

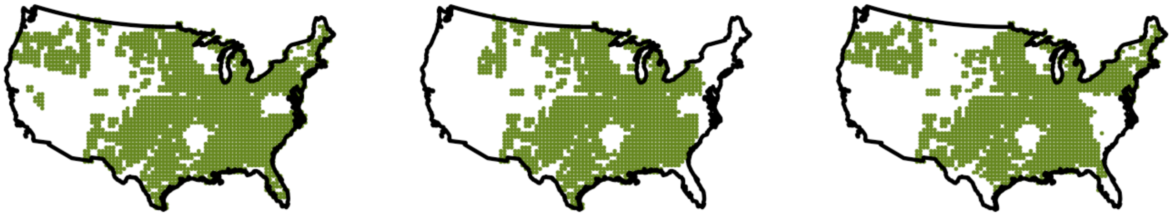

Tree Pathogens

Ceratocystis fagacearum

Cronartium ribicola

Cryphonectria parasitica

Cryptodiaporthe populea

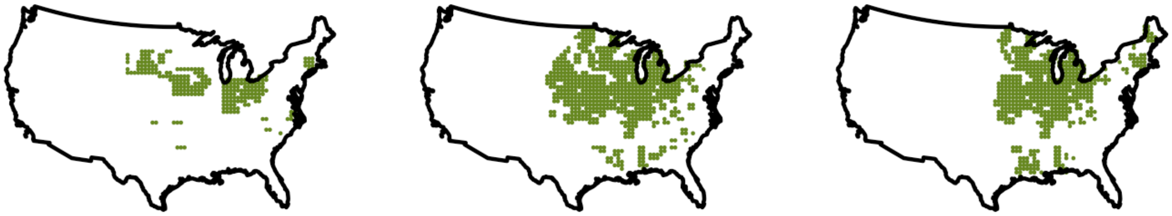

Discula destructiva

Gremmeniella abietina

Lachnellula willkommii

Melampsora larici-populina

Ophiostoma novo-ulmi

Phytophthora cinnamomi

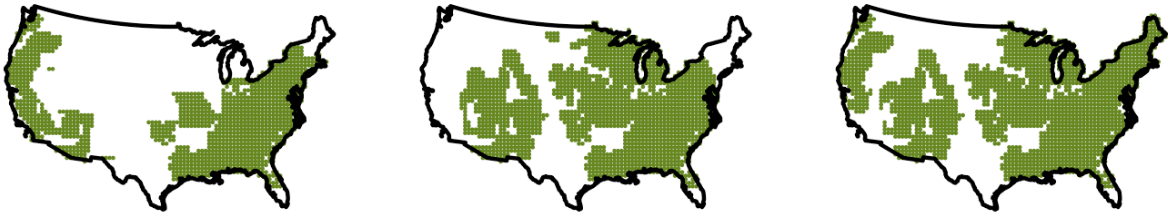

Phytophthora lateralis

Phytophthora ramorum

Sirococcus clavigignenti-juglandace

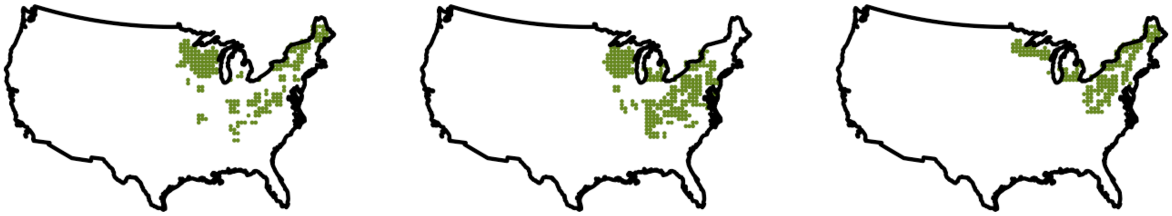

Venturia saliciperda

Sap-Feeding Pests

Adelges abietis

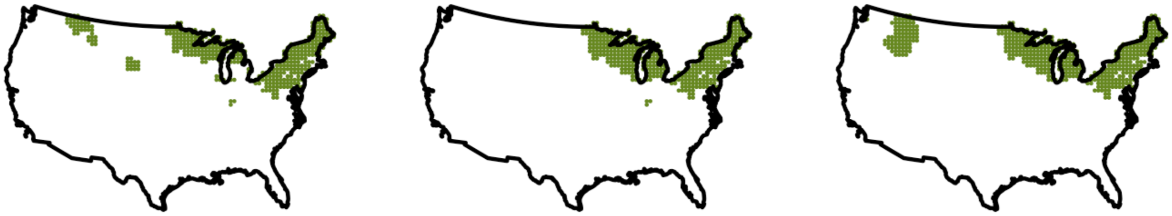

Adelges piceae

Adelges tsugae

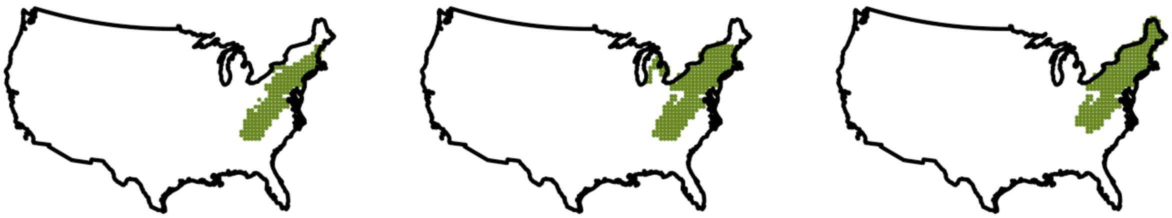

Aonidiella aurantii

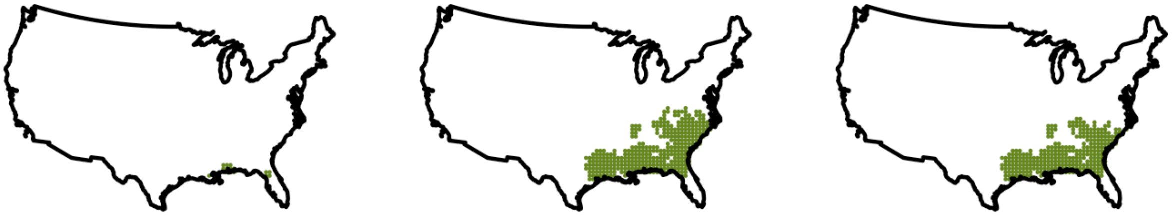

Lymantria dispar

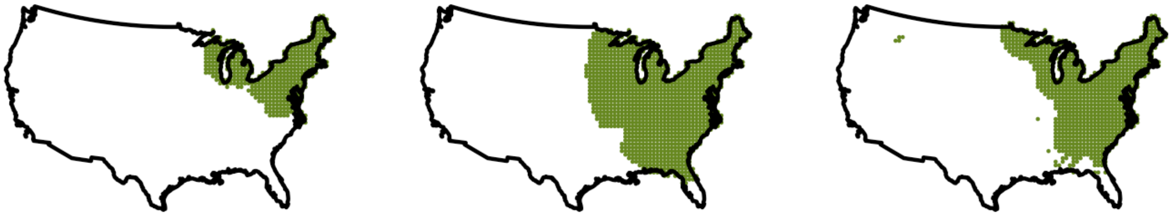

Asterolecanium variolosum

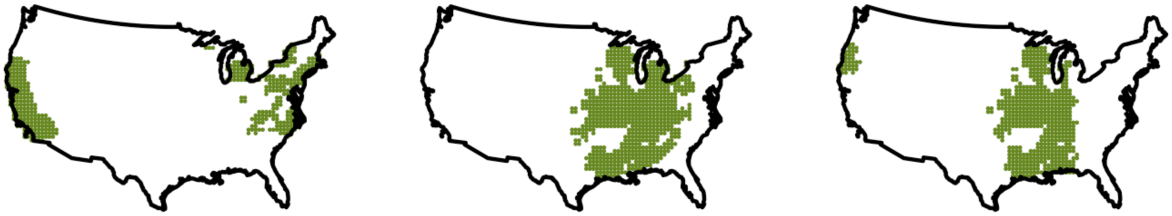

Carulaspis juniperi

Cryptoccocus fagisuga Lind.

Diaspidiotus perniciosus

Elatobium abietinum

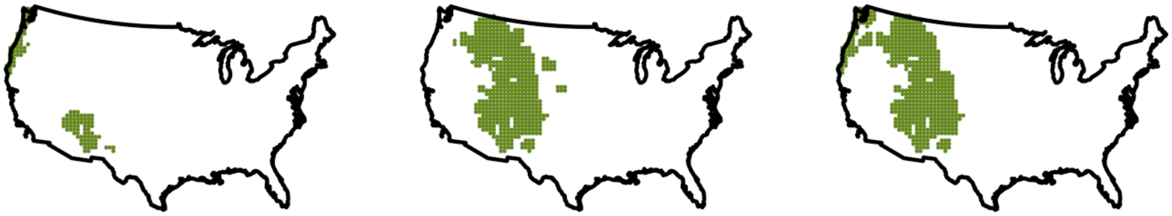

Eulecanium cerasorum

Fiorinia externa

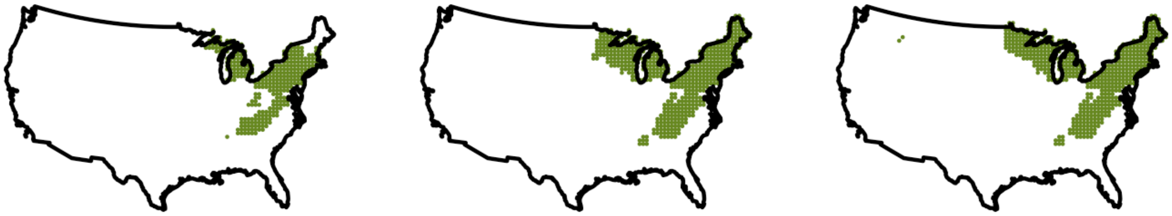

Glycaspis brimblecombei

Lepidosaphes ulmi

Matsucoccus matsumurae

Nuculaspis tsugae

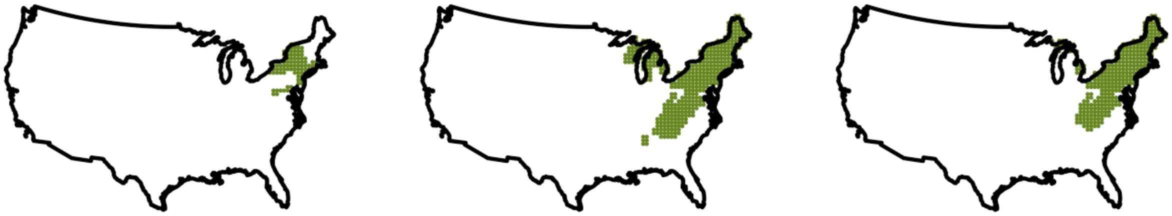

Taeniothrips inconsequens

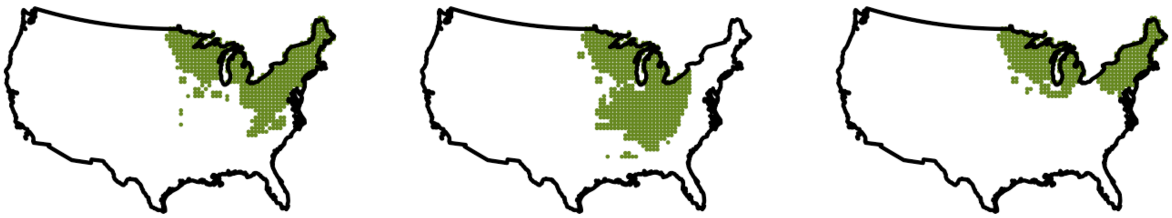

Thrips calcaratus

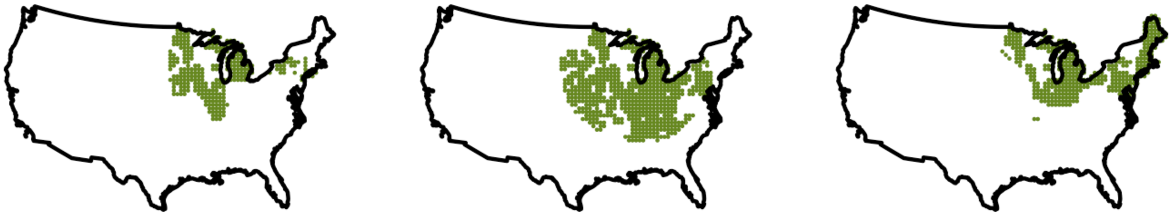

Appendix S1.8 Sensitivity analysis

Figure S1.8.1 The results of a sensitivity analysis of the two additional predictor variables kept in the GDK, including tree density (top row), fit at b1 = -0.8438, and human population density (bottom row), fit at b2 = -0.1378, with fitted values shown by red vertical lines. The sensitivity analysis was performed by holding the other GDK model parameters constant and varying b1 and b2 separately by ±1 times their fitted values to examine the resulting MET score (left column) and R^2_{MSE} values (right column). Both parameters have a fairly smooth optimization surface, as indicated by the unimodal relationship between MET and the value of the parameter evaluated. The fitted values minimize MET, indicating successful optimization, and also nearly maximize R^2_{MSE} in a smooth, unimodal way, even though it was not the metric used to fit the model. As expected, values of each parameter smaller in magnitude (closer to zero) have smaller effects on both metrics. Changes in b1 have a much larger effect on both metrics of fit than changes in b2, which follows from it entering the forward selection model first.

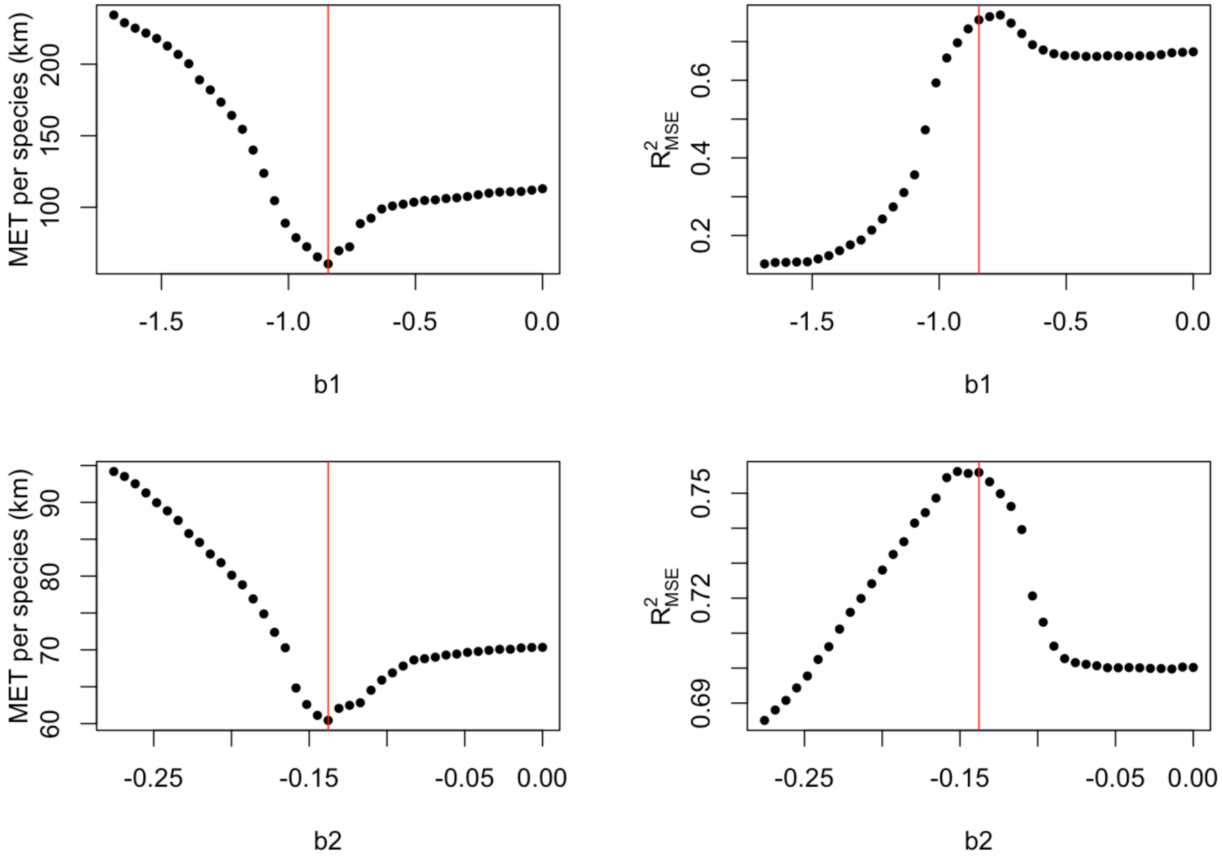

Appendix S2. Appendices for Chapter 2

Appendix S2.1 Pest list

Table S2.1.1 List of the 63 economically damaging United States invasive forest pests analyzed in this manuscript.

Common Name	Guild	Latin Name
Ambermarked Birch Leafminer	Defoliators	Profenusa thomsoni
Asiatic Oak Weevil	Defoliators	Cyrtepistomus castaneus
Balsam Woolly Adelgid	Suckers	Adelges piceae
Beech Scale	Suckers	Cryptoccocus fagisuga Lind.
Birch Leafminer	Defoliators	Fenusa pusilla
Black Vine Weevil	Defoliators	Otiorhynchus sulcatus
Browntail Moth	Defoliators	Euproctis chrysorrhoea
Butternut Canker	Pathogens	Sirococcus clavigignenti-juglandacearum
Calico Scale	Suckers	Eulecanium cerasorum
California Red Scale	Suckers	Aonidiella aurantii
Chestnut Blight	Pathogens	Cryphonectria parasitica
Circular Hemlock Scale	Suckers	Nuculaspis tsugae
Cryptodiaporthe Canker	Pathogens	Cryptodiaporthe populea
Dogwood Anthracnose	Pathogens	Discula destructiva
Dutch Elm Disease	Pathogens	Ophiostoma novo-ulmi
Eastern Spruce Gall Adelgid	Suckers	Adelges abietis
Elm Leafbeetle	Defoliators	Xanthogaleruca luteola
Elm Leafminer	Defoliators	Fenusa ulmi
Elongate Hemlock Scale	Suckers	Fiorinia externa
Emerald Ash Borer	Borers	Agrilus planipennis
Eucalyptus Longhorned Beetle	Borers	Phoracantha recurva
Eurasian Poplar Leaf Rust	Pathogens	Melampsora larici-populina
European Bark Beetle	Borers	Hylastes opacus
European Larch Canker	Pathogens	Lachnellula willkommii
European Pine Needle Midge	Defoliators	Contarinia baeri
European Pine Sawfly	Defoliators	Neodiprion sertifer
European Pine Shoot Moth	Defoliators	Rhyacionia buoliana
European Spruce Needleminer	Defoliators	Epinotia nanana

Golden Oak Scale	Suckers	Asterolecanium variolosum
Green Spruce Aphid	Suckers	Elatobium abietinum
Gypsy Moth	Defoliators	Lymantria dispar
Hemlock Woolly Adelgid	Suckers	Adelges tsugae
Imported Willow Leaf Beetle	Defoliators	Plagiodera versicolora
Introduced Basswood Thrips	Suckers	Thrips calcaratus
Introduced Pine Sawfly	Defoliators	Diprion similis
Japanese Beetle	Defoliators	Popillia japonica
Japanese Cedar Longhorn Beetle	Borers	Callidellum rufipenne
Juniper Scale	Suckers	Carulaspis juniperi
Larch Casebearer	Defoliators	Coleophora laricella
Larch Sawfly	Defoliators	Pristiphora erichsonii
Mimosa Webworm	Defoliators	Homadaula anisocentra
Mountain Ash Sawfly	Defoliators	Pristiphora geniculata
Oak Wilt	Pathogens	Ceratocystis fagacearum
Oystershell Scale	Suckers	Lepidosaphes ulmi
Peach Twig Borer	Borers	Anarsia lineatella
Pear Thrips	Suckers	Taeniothrips inconsequens
Phytophthora Root Rot	Pathogens	Phytophthora cinnamomi
Pine False Webworm	Defoliators	Acantholyda erythrocephala
Pine Shoot Beetle	Borers	Tomicus piniperda
Poplar and Willow Borer	Borers	Cryptorhynchus lapathi
Poplar sawfly	Defoliators	Trichiocampus viminalis
Port-Orford-Cedar Root Disease	Pathogens	Phytophthora lateralis
Red Pine Scale	Suckers	Matsucoccus matsumurae
Redgum Lerp Psyllid	Suckers	Glycaspis brimblecombei
San Jose Scale	Suckers	Diaspidiotus perniciosus
Satin Moth	Defoliators	Leucoma salicis
Scleroderris Canker	Pathogens	Gremmeniella abietina
Sirex Wood Wasp	Borers	Sirex noctilio
Smaller European Elm Bark Beetle	Borers	Scolytus multistriatus
Sudden Oak Death	Pathogens	Phytophthora ramorum
White Pine Blister Rust	Pathogens	Cronartium ribicola
Willow Scab	Pathogens	Venturia saliciperda
Winter Moth	Defoliators	Operophtera brumata

Appendix S2.2 Parameterization of a temperature threshold for HWA spread and forecasts of temperature-limited dispersal to 2030

We explored the incorporation of an additional layer of customization into both our customized models and SDK for HWA related to well-known niche limitations. This species' spread is known to be climatically limited in the northern end of its range (Evans & Gregoire 2007; Fitzpatrick et al. 2012; Parker et al. 1998, 1999; Trotter & Shields 2009). As such, we used the bioclimatic variable "minimum temperature of the coldest month" (bio6) from BIOCLIM (www.worldclim.org) to fit the optimal temperature for HWA mortality based on MET for both the customized and GDK model for HWA. So-called 'current' WorldClim values represent temperatures from 1960-1990, so we transformed them to 2005 through interpolation, assuming they represented 1975, with the WorldClim 1.4 2050 temperature projections for NASA's GISS-ER-2 rcp2.6 and rcp8.5 scenarios sampled at 2.5 arc-minutes (taking the midpoint of the best and worst-case climate change warming scenarios). Since WorldClim does not provide estimates for older contemporary climates, we used the 'current' conditions from the beginning of pest spread until 1975.

HWA was a more complex case for SDK fitting, as all three of our additional layers of complexity (starting point, intercept and niche corrections) were needed in order to maximize predictive ability (Table 2). The intercept-corrected GDK did not produce predictive results for HWA ($R^2_{om} = 0.20$ vs $R^2_{om} = 0.30$ for the uncorrected model). Further, while the starting-point correction improved forecasts, it did not substantially improve fit until the intercept correction was also added, and this model produced a weaker forecast (53% of spatial variation explained). The model incorporating both the intercept and starting point correction and the lower temperature threshold had a fitting MET of 1.75 km (vs. 33.22 km for the uncorrected GDK).

The intercept of this model was α=1.47 and the temperature threshold was -7.64°C, and it resulted in an R^2_{om} = 0.85. This indicates that the best fitting model has faster spread (smaller intercept) which is offset by pest mortality in the north end of the range.

To explore the implications of this climatic limitation with future climate change, our forecasts of HWA spread used in the community forecast come from the model that includes the temperature threshold. We show the HWA-only results in Fig S1. While the inclusion of a temperature threshold restricts future HWA spread compared to the model without the threshold, the species continues to spread eastward and westward, and surprisingly, jump dispersal events are predicted near Detroit and Cleveland (Fig. S2.2.1b.). If we maintain the entire US at its 2005 values for minimum winter temperature, the species actually spreads farther than if we account for climate change (Fig. S2.2.1c). This is counterintuitive, as climate change is typically associated with winter warming, which would increase HWA establishment, but minimum winter temperatures are actually projected to decline in parts of the northern United States (Fig. S2.2.2), so accounting for climate change makes the threshold more restrictive over time. These results support the notion that climate change will influence future HWA distributions, though not in a necessarily expected direction (Parker et al. 1999).

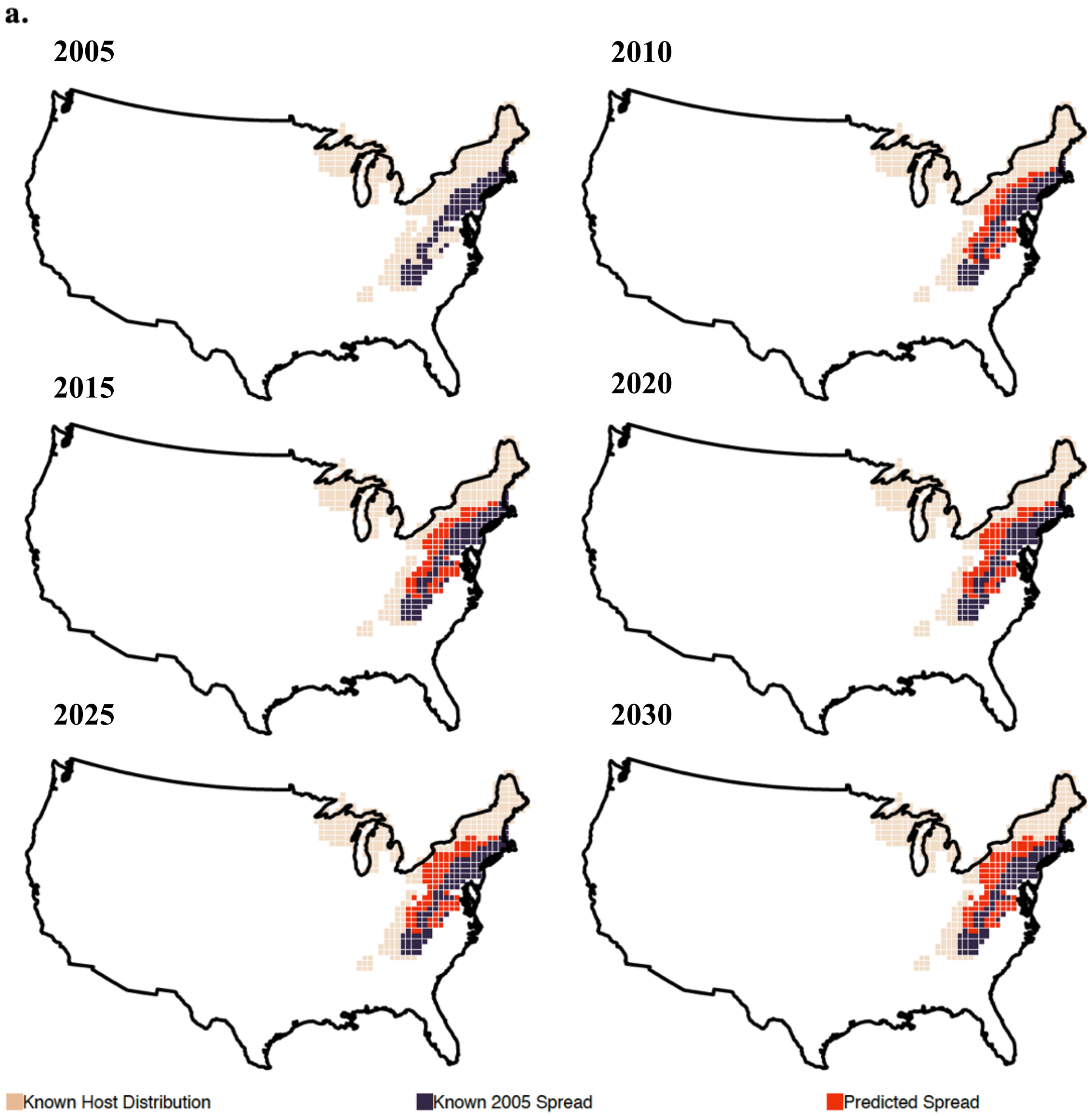
a.
2005
2010
2015
2020
2025
2030
Known Host Distribution
Known 2005 Spread
Predicted Spread

b.

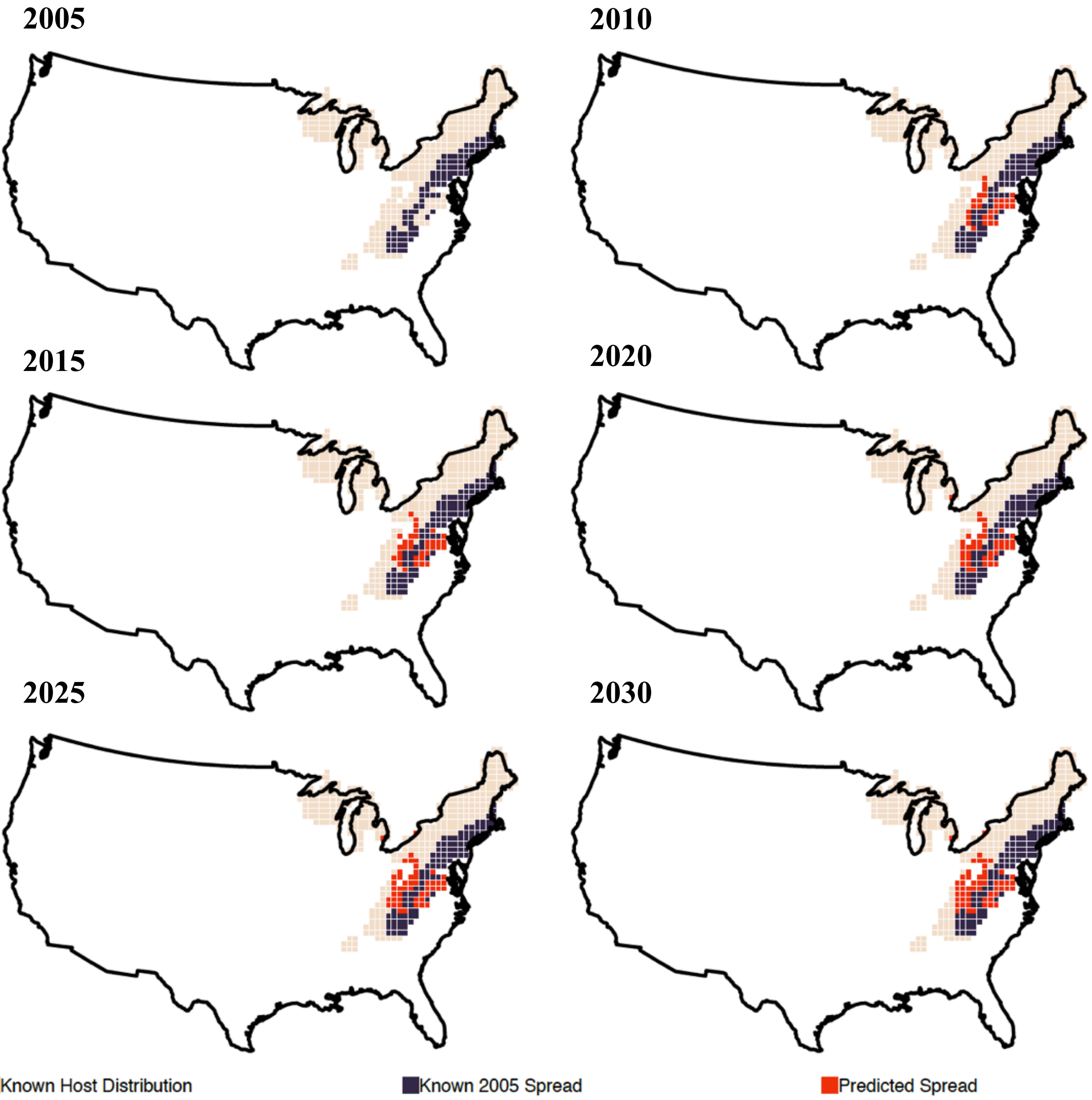
2005
2010
2015
2020
2025
2030
Known Host Distribution
Known 2005 Spread
Predicted Spread

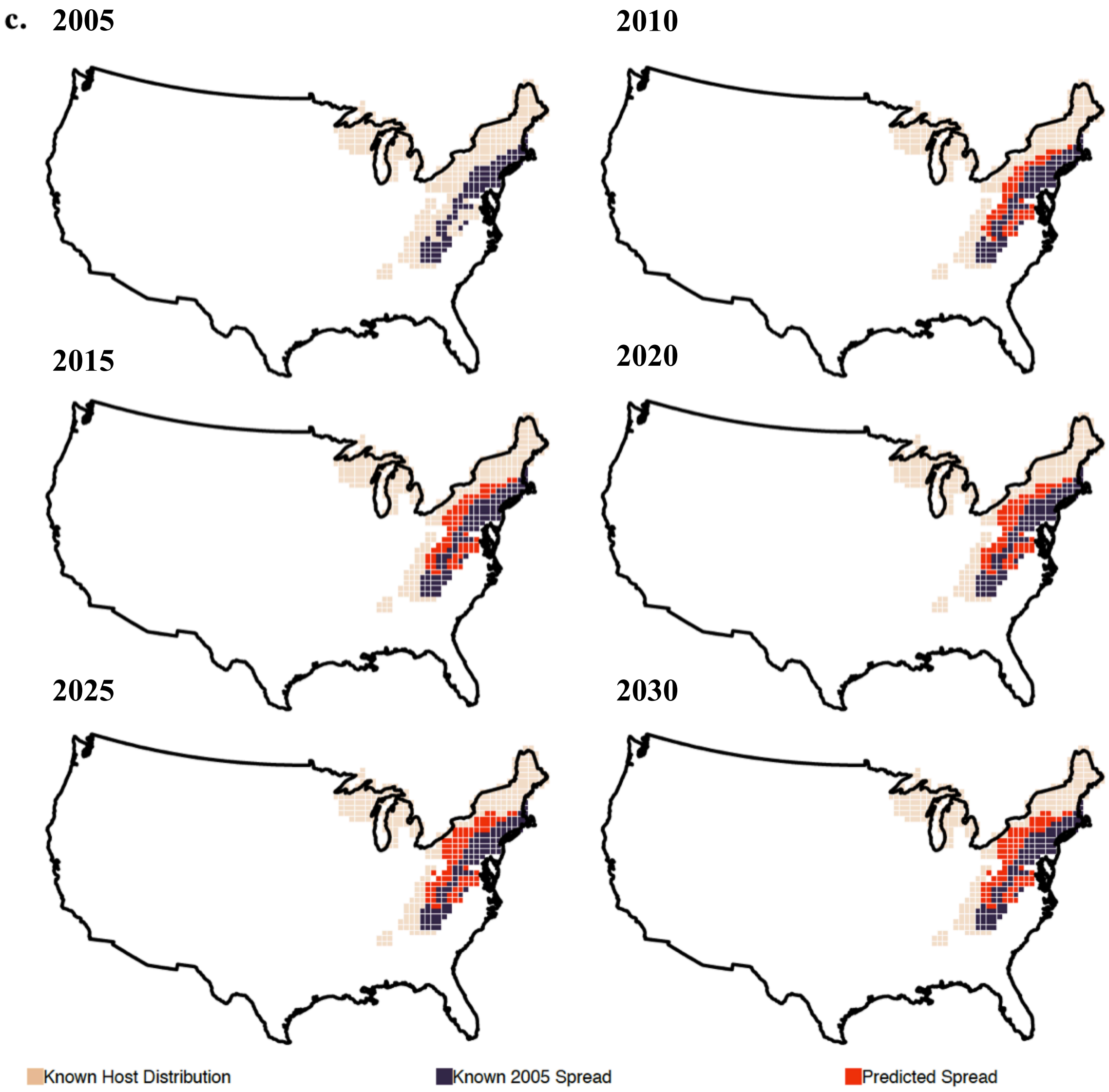

Figure S2.2.1 Forecasts for HWA spread **a.** without and **b.** with a fitted temperature threshold for pest establishment, and **c.** forecasts with a fitted temperature threshold where minimum winter temperatures are held constant at 2005 levels. Panels span from 2005-2030.

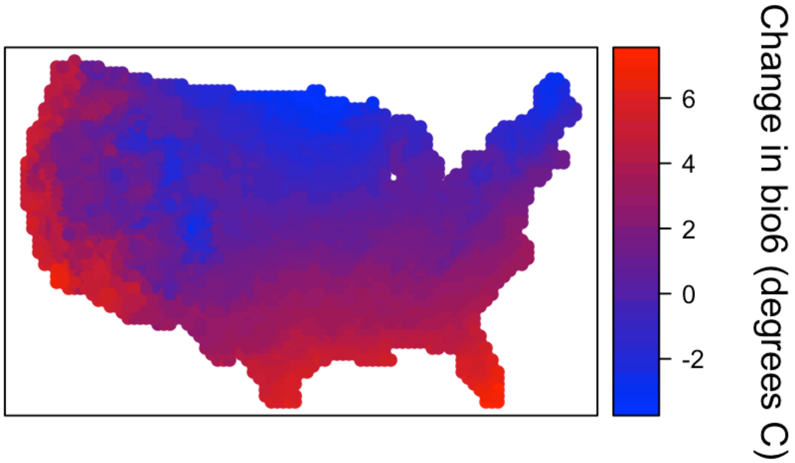

Figure S2.2.2 Projected change in minimum January temperatures (BIOCLIM variable bio6) across the United States from 2005 to 2030.

Literature Cited

Evans, A. M., & Gregoire, T. G. (2007). A geographically variable model of hemlock woolly adelgid spread. Biological Invasions, 9(4), 369-382.

Fitzpatrick, M. C., Preisser, E. L., Porter, A., Elkinton, J., & Ellison, A. M. (2012). Modeling range dynamics in heterogeneous landscapes: invasion of the hemlock woolly adelgid in eastern North America. Ecological Applications, 22(2), 472-486.

Parker, B. L., Skinner, M., Gouli, S., Ashikaga, T., & Teillon, H. B. (1998). Survival of hemlock woolly adelgid (Homoptera: Adelgidae) at low temperatures. Forest Science, 44(3), 414-420.

Parker, B. L., Skinner, M., Gouli, S., Ashikaga, T., & Teillon, H. B. (1999). Low lethal temperature for hemlock woolly adelgid (Homoptera: Adelgidae). Environmental Entomology, 28(6), 1085-1091.

Trotter III, R. T., & Shields, K. S. (2009). Variation in winter survival of the invasive hemlock woolly adelgid (Hemiptera: Adelgidae) across the eastern United States. Environmental Entomology, 38(3), 577-587.

Appendix S2.3 Derivation of relationship between alpha and diffusion constant

From Skellam et al. (1951), if one imagines a single source of propagules invading the center of some radial coordinate space, a reaction-diffusion (Gaussian) dispersal kernel can be modelled as such:

$$k(d) = \frac{1}{4\pi D} e^{-\frac{d^2}{4D}} \tag{S1}$$

Where the kernel density k is a function of the distance d from the source, and D is the diffusion coefficient. Since its original application in ecology, reaction-diffusion has been extended as a particular case of an integrodifference model – a more flexible modelling framework that has been applied extensively to invasive species dispersal (Mollison 1977; Andow et al. 1990; Neubert & Parker 2004). This Gaussian kernel is part of a family of kernels explored in Clark et al. (1998; 1999) that take the form:

$$k(d) = \frac{1}{N} e^{-\left(\frac{d}{q}\right)^c} \tag{S2}$$

Where N is a normalization constant such that all proportional densities dispersing from a given source sum to 1, q is a dispersion parameter that has units of distance, and c is a dimensionless shape parameter controlling kurtosis. Importantly, q can be thought of as the root mean squared displacement of propagules from the source, which is related to the diffusion coefficient ($q = 2\sqrt{D}$), and can be estimated empirically through mark-recapture experiments (Andow et al. 1990). In the Gaussian case originally examined, c = 2

We chose the negative exponential kernel for the GDK, as it frequently outperforms the Gaussian case and is commonly used in invasion biology (Nathan et al. 2012). In the negative exponential case of eqn. S2, c = 1 (Clark et al. 1999).

In the GDK, at the same first timestep, we have

$$k_{GDK}(d) = \frac{e^{-df(Z)}}{\sum_j e^{-df(Z)}} \tag{S3}$$

Since we also implement normalization as a means of redistributing propagules proportionally, can rewrite our equation as:

$$k_{GDK}(d) = \frac{1}{N} e^{-df(Z)} \tag{S4}$$

Where *f(z)* incorporates our predictor variables and is centered on our intercept, α, such that when all their predictors are at their mean values, the equation is as follows:

$$k_{GDK}(d) = \frac{1}{N} e^{-d\alpha} \tag{S5}$$

If we set, $q=1/\alpha$, the equation matches eqn. S2 for the negative exponential case (c = 1):

$$k_{GDK}(d) = \frac{1}{N} e^{-\left(\frac{d}{q}\right)} \tag{S6}$$

Thus, α is analogous to $1/q$, and is thus mathematically related to the diffusion constant *D* from Skellam et al. (1951).

Literature Cited

Andow, D. A., Kareiva, P. M., Levin, S. A., & Okubo, A. (1990). Spread of invading organisms. *Landscape Ecol.*, 4(2), 177-188.

Clark, J. S., Macklin, E., & Wood, L. (1998). Stages and spatial scales of recruitment limitation in southern Appalachian forests. *Ecol. Monographs*. 68, 213-235.

Clark, J. S., Silman, M., Kern, R., Macklin, E., & HilleRisLambers, J. (1999). Seed dispersal near and far: patterns across temperate and tropical forests. *Ecology*, 80(5), 1475-1494.

Mollison, D. (1977). Spatial contact models for ecological and epidemic spread. *J Roy. Stat. Soc.: B*. 39(3), 283-313.

Nathan, R., Klein, E. K., Robledo-Arnuncio, J. J., & Revilla, E. (2012). Dispersal kernels. In *Dispersal ecology and evolution* (pp. 187-210). Oxford: Oxford University Press.

Neubert, M. G., & Parker, I. M. (2004). Projecting rates of spread for invasive species. *Risk Anal*. 24(4), 817-831.

Skellam, J. G. (1951). Random dispersal in theoretical populations. *Biometrika*, *38*(1/2), 196-218.

Appendix S2.4 Theoretical behaviour of R^2_{om}.

We wished to create a metric that takes its maximum value when two distributions have the same number of points, with the proportions of the points in the correct spatial locations. If the points are proportionally arranged in space correctly, but the number of predicted points is lower or higher than the observed number, there is some penalty, and if the number of points is correct, but the spatial proportions are incorrect, there is also some penalty. Further, this penalty should be applied symmetrically, such that over- and underpredicting had the same additive distance-related penalty.

To calculate *omMSE*, we first used *optmatch* (Hansen, 2007), to perform a one to one match between our predicted and observed presence points for a given pest. Next, the leftover points caused by differences in predicted and observed range size were then used to penalize the distance score. To do this, we assigned these leftover points the mean distance between that point and all other points in the opposing distribution. This value is higher than the nearest neighbor distance for that point, so it penalizes the score. In each random draw from the host distribution, we chose a number of points with the true observed pest range size and calculated the associated *omMSE*. This null model thus creates an additional penalty for predicting the wrong range size for a given pest. We took the mean of this entire vector of distances to obtain *omMSE*.

For ease of interpretation, we converted *omMSE* to a Pseudo R^2 (R^2_{om}) by comparing the observed o*mMSE* value to a spatial null expectation, using 10,000 random draws of spatial points from the host distribution. In each random draw from the host distribution, we chose a number of points with the true observed pest range size and calculated the associated *omMSE*. This null model thus creates an additional penalty for predicting the wrong range size for a given pest.

We tested the behavior of R^2_{om} as over- or under-estimation of presences changed. Specifically, we chose the HWA distribution at 2005, which has 94 presences, and varied the predicted number of presences from 1 (underestimation) to 400 (overestimation) (Fig. S2.4.1). We also considered different patterns of overlap with the true distribution, including 100% predicted presences sampled from "true" presence locations (black points), 50% from true and 50% from random locations (blue points), and 100% from random locations (red points). As expected, the perfectly matching value has a $\mathrm{R}^2_{\mathrm{om}}$ score of 100%. Mismatched numbers of presences have an additive effect on *omMSE*, and reduce it to below-zero values at the extreme. There appears to be a roughly equivalent penalty on *omMSE* for getting the wrong range size whether or not predicted presences match observed presences (as indicated by roughly equivalent slopes). Also as expected, where predicted presences do not overlap true presences, $\mathrm{R}^2_{\mathrm{om}}$ also decreases (compare black versus blue and red lines), approaching zero, even when total number of presences matched, where predicted presences are generated randomly (red line).

Note that at non-extreme levels of mismatch, there is a symmetrical additive effect of over- and under- prediction. When predicted distributions are empty or entirely saturate the host range, *omMSE* scores are roughly equivalent. However, overprediction results in an asymptotic relationship with the maximum *omMSE*, while underprediction is more linear. This is in part because with overprediction, one eventually selects the entire observed range, even when selecting random points, whereas with underprediction, randomly selected points are more likely to all fall outside of the observed distribution. Our fitted relationships do not possess such extreme levels of mismatch (e.g., they all display positive *omMSE*), so we argue that this lack of symmetry is less relevant for our purposes.

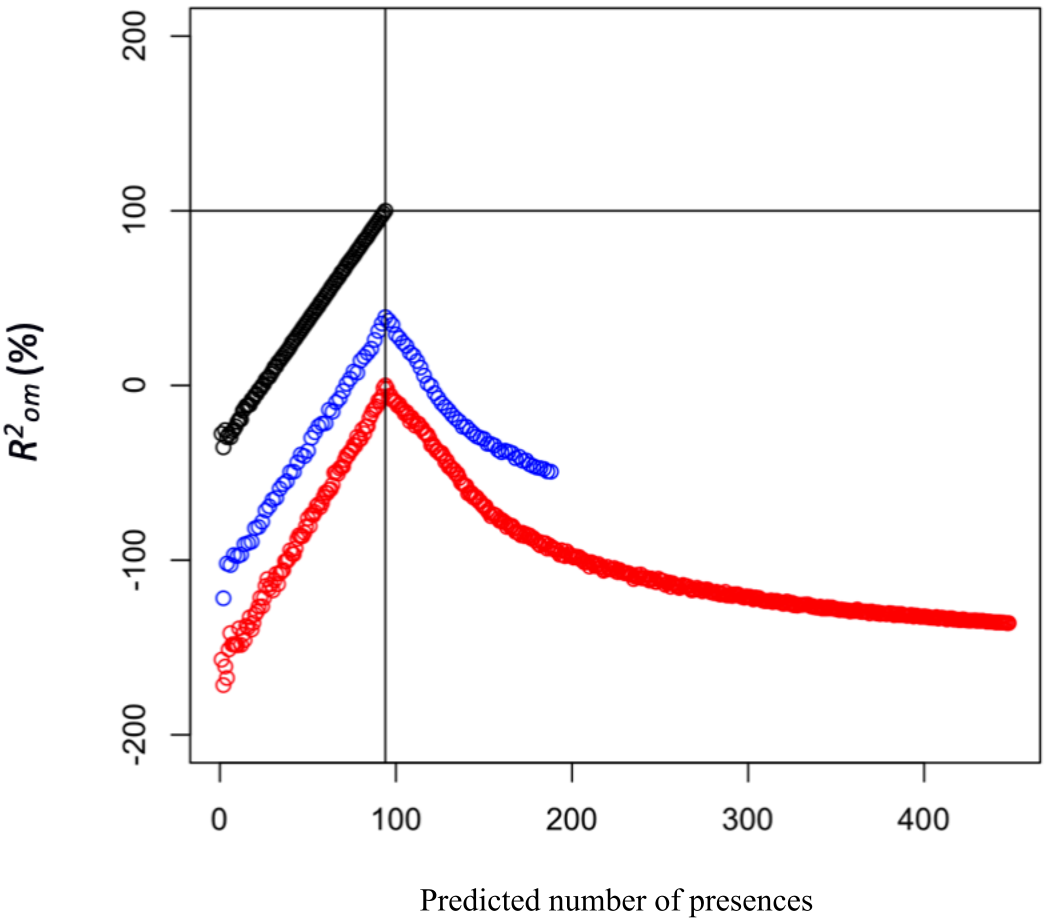

Figure S2.4.1 Theoretical behavior of *omMSE*. We show R^2_{om} for different simulated distributions in comparison to the observed HWA distribution (94 true presences), varying the predicted number of presences from 1 (underestimation) to 400 (overestimation) in each case (x-axis). We considered 3 different patterns of overlap with the true distribution 1) including 100% predicted presences sampled from "true" presence locations (black points), 50% from true and 50% from random locations (blue points), and 100% from random locations (red points). The points represent the mean of 100 Monte Carlo simulations in each case.

Appendix S2.5 SDK methodology applied to all 63 species, including further niche corrections for two species.

We used the fitted MET score applied to each individual species' snapshot of dispersal in 2005 in order to determine the SDK layers to include for each species (intercept, starting point, and niche limitation corrections where there was evidence from the literature that they were necessary. We applied the intercept correction to all species, since it was bound to lead to at least an equivalent MET score. The starting point correction is not equally reliable across species, but assessment of SDK fit can allow us to determine whether potential starting points constitute reliable data. The starting point correction improved MET scores for 21 species including GM, BBD and HWA, and was thus included in the SDK for these species. For HWA, we forecasted based on the intercept, starting point, and niche-corrected model (based on the results summarized in Table 2.2 and Appendix S2.2).

To extend our SDK methodology to all species in our dataset, we wished to correct the fits for other species known to show niche limitations: sudden oak death disease (SOD, *Phythophthora ramorum*) and balsam woolly adelgid (BWA, *Adelges piceae*). While GM is also thought to be temperature-limited, we could already explain 98% of the spatial variation in its future spread without any further corrections, so we did not assess the effect of additional parameters. Since BWA is known to be limited by cold winter temperatures in a similar fashion to HWA (Hrinkevich et al. 2016), we used the same minimum temperature of the coldest month variable to limit its spread using a minimum threshold for pest survival. For SOD, where low humidity is limiting (Meentemeyer et al. 2004), we obtained average daily relative humidity data in 2010 from the R package *GSODR* (Sparks et al. 2017), which utilizes data from the Global

Surface Summary of the Day (GSOD, https://data.noaa.gov/dataset/dataset/global-surface-summary-of-the-day-gsod/) provided by the US National Centers for Environmental Information (NCEI). Relative humidity data was collected for all weather stations within the US, and was subsequently interpolated to our 50 x 50 km grid cell centroids via inverse distance weighting (R package *gstat*, power = 2, Pebesma 2004). We modelled the effect of mean relative humidity as a minimum threshold for pest survival.

The best model for SOD that included this threshold initiated spread from our best guess of the initial invasion location in the United States, while best model for BWA initiated spread from the centroid of the host range (Table S2.5.1). Both of these updated models were used as the SDK in forecasts of whole-community dispersal.

Literature cited

Hrinkevich, K. H., Progar, R. A., & Shaw, D. C. (2016). Climate Risk Modelling of Balsam Woolly Adelgid Damage Severity in Subalpine Fir Stands of Western North America. *PLoS ONE*, 11(10), e0165094.

Meentemeyer, R., Rizzo, D., Mark, W., & Lotz, E. (2004). Mapping the risk of establishment and spread of sudden oak death in California. *For. Ecol. Manage.*, 200(1-3), 195-214.

Pebesma, E. J. (2004). Multivariable geostatistics in S: the gstat package. *Computers & Geosciences*, *30*(7), 683-691.

Sparks, A. H., Hengl, T., & Nelson, A. (2017). GSODR: Global Summary Daily Weather Data in R.

Table S2.5.1 Fits of further-corrected GDK models for sudden oak death disease (SOD, *Phythophthora ramorum*) and balsam woolly adelgid (BWA, *Adelges piceae*). The variable *bio6* represents a threshold for pest survival based on the minimum temperature of the coldest month, while *hum* represents a minimum survival threshold based on average relative humidity.

	α	**MET (km)**
uncorrected		
SOD	1.74	53.70

BWA	1.74	67.98
intercept-corrected		
SOD	1.65	36.60
BWA	1.77	67.73
starting-point corrected		
SOD	1.74	19.36
BWA	1.74	1273.36
starting point and intercept-corrected		
SOD	2.31	12.33
BWA	0.07	75.46
intercept, temperature-corrected		
BWA	1.77; bio6= -13.99°C	67.56
starting point, intercept, humidity-corrected		
SOD	2.39; hum= 64.33%	6.25

Appendix S2.6. Uncertainty calculations

We performed two different examinations of model uncertainty:

1) We simulated future dispersal across different future climate and human population density projections (Fig. S2.5.1). The fitted model used the midpoint between rcp2.6 and rcp8.5 scenarios for future minimum January temperature, which represent less extreme and more extreme scenarios of future climate change, respectively. In addition to this midpoint, we also examined using either of these scenarios to illustrate the range of possible climate change scenarios (though changes to January temperature only influence two species: HWA and BWA, see Appendix S2.5). Similarly, in addition to the population growth scenario presented within the manuscript, we also tested the most extreme scenarios of population growth projected from the Shared Socioeconomic Pathways (O'Neill et al. 2017), where the slowest growth represented the "Regional Rivalry" scenario and the fastest growth was with the "Fossil-fueled Development" scenario (Hauer 2019). The upper and lower bounds of these forecasts to 2030 are shown in comparison with the middle-of-the-road projection included in the main text in Fig. 3b. Interestingly, reduced population growth need not lead to reduced spread, since it has both a positive influence on dispersal into sites but also a negative influence on dispersal out of sites. Similarly, a less extreme climate change scenario may not necessarily mean less favorable conditions for HWA spread north with bio6, if it means that temperature variability is also lower (see Appendix S2.2). The minimum change scenario matches very closely with the published results, except for slightly patchier high richness areas in places like Montana, Idaho and New Mexico (regions B, K in Fig. 2.4), as well as richness patterns extending slightly further south within the northeastern United States.

The maximum change scenario leads to far higher future pest risk compared to the other scenarios, and a much greater number of distinct patches of future pest establishment. The central United States – which had very few high-richness patches, now possesses a few hotspots. Interestingly, spread is more variable within previously more continuous patches of high future richness such as northern New England, Northern Minnesota and Wisconsin (regions C, E in Fig. 2.4), leading to greater richness predicted in some parts of these regions and lower richness predicted in other parts.

2) We examined the influence of parameter uncertainty on forecasted pest richness via sensitivity analysis. We did this by randomly perturbing all fitted parameters independently by small amounts that were sufficiently extreme to result in poor fits in many cases, and selecting parameter sets within an average MET score of 5 km from the fitted values (our threshold for parameter inclusion in our model fitting process). We generated 1000 perturbed model parameter sets, of which 345 were within this threshold. The need to discard ~2/3 of the perturbed parameter sets indicates that our level of perturbation was severe enough that a range of alternative parameter values was explored, but not so severe that it did not also produce a variety of cases that fit similarly to the optimum. Each of the 345 remaining perturbed parameter sets was then used to forecast pest richness to 2030. We show the variability in these forecasts across time as ranges of predicted pest richness (maximum-minimum) in Fig S2.2. It is worth noting that uncertainty need not only increase into the future, since as sites saturate with the total number of pests that can establish, spread patterns necessarily become more deterministic. Variation increases steadily from 2010-2030, and identified 'hotspot' regions B, H, and K from Fig 2.4. show particularly high uncertainty in future richness

(likely due to variation in the importance of forests), as well as parts of Florida and the area around Atlanta, GA (likely due to variation in the importance of population). While uncertainty increases across large parts of the Western and Eastern United States, the central United States is consistently predicted to have little growth in pest richness, so variation remains low.

We then merged all sources of uncertainty to produce a combined map of variation in future pest richness at 2030 (Fig 2.5). In spite of high variability, even in the case of minimum future pest spread, the northeastern US had the greatest number of relative establishments, indicating a consistent pattern of future spatial risk in spite of uncertainty (Fig. S2.6.3). The 10 scenarios that led to the lowest future spread all came from the maximum population growth scenario and included population density terms that had been perturbed to decrease dispersal into and out of high population density sites, thereby causing pests to remain at urban centers once arriving there. The 10 scenarios that led to the highest future spread were predominantly from the middle-of-the-road scenario with overall greater pest growth rates and less preferential dispersal into high population areas, leading to more even dispersal patterns across space and higher spread velocity due to pest population growth. It thus appears that a key factors influencing the extent of future dispersal are the pattern of future human population growth and the extent to which human population will act as an attractive force keeping pests in cities.

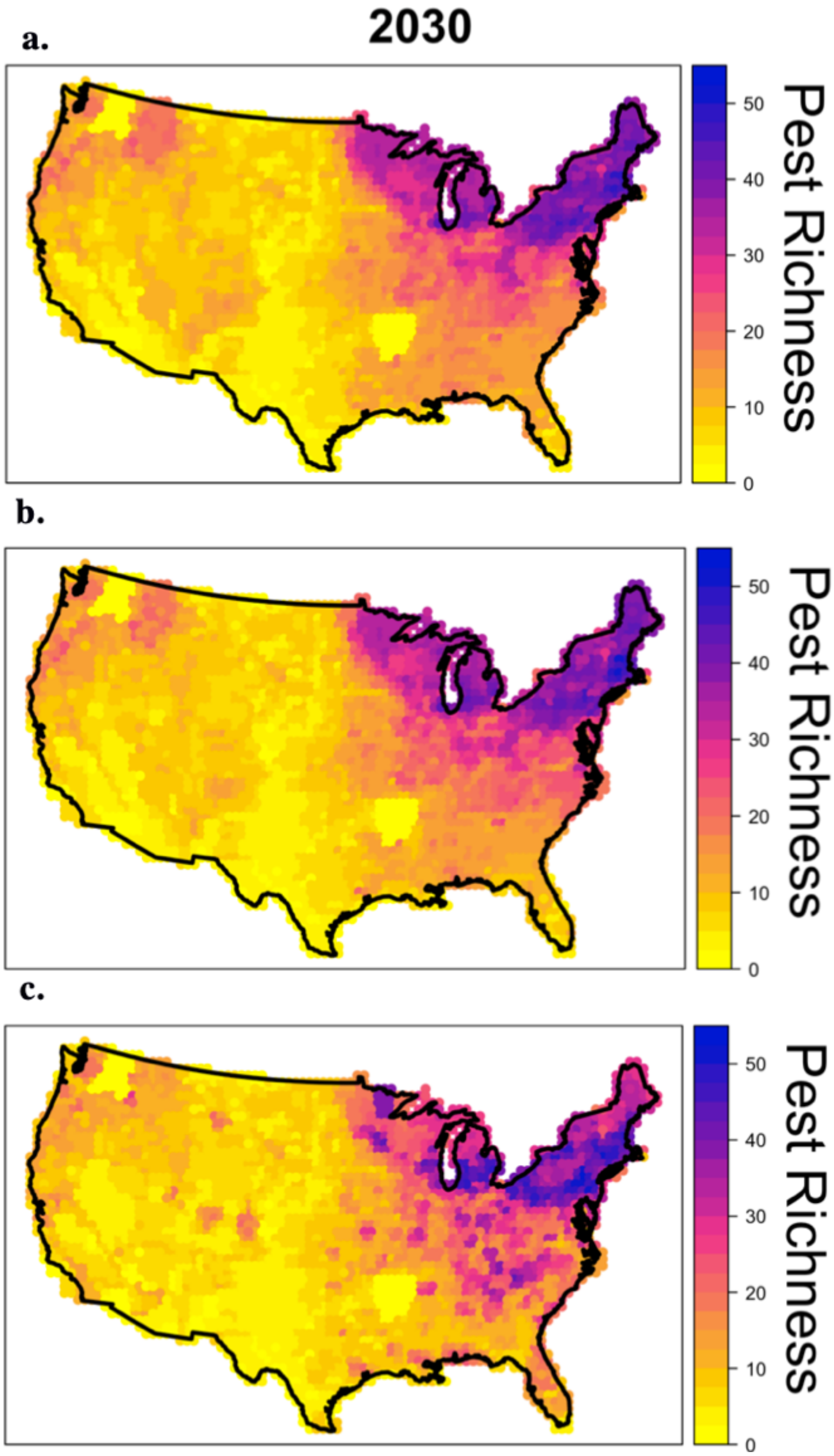

Figure S2.6.1 Projections of SDK using **a.** the ‘middle-of the road’ scenario used in text from ProximityOne **b.** A minimum change future scenario (using rcp2.6 as the climate change scenario for bio6 and SSP3 ‘Regional Rivalry’ for county-level population growth), and **c.** A maximum change future scenario (using rcp8.5 as the climate change scenario for bio6 and using SSP5 ‘Fossil-Fueled Development’ for county-level-population growth.

a.

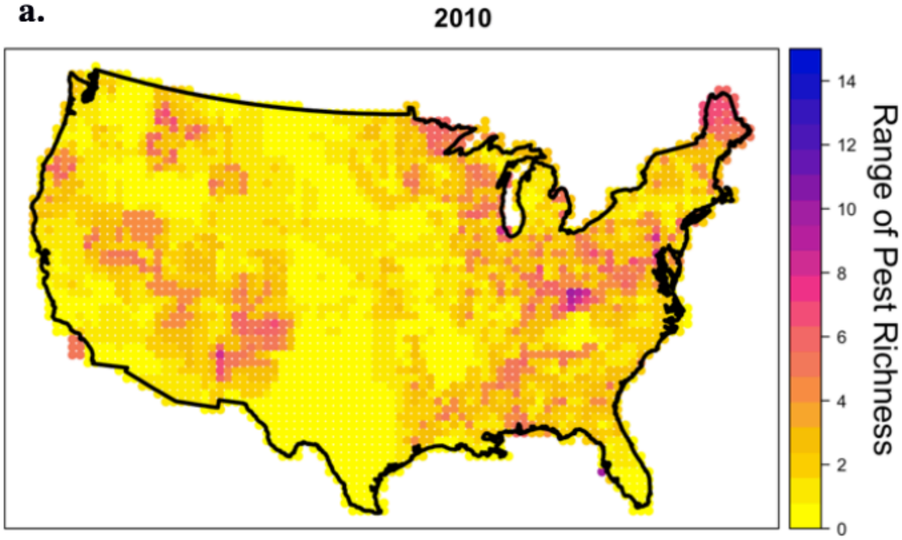
2010
Range of Pest Richness
0
2
4
6
8
10
12
14

b.

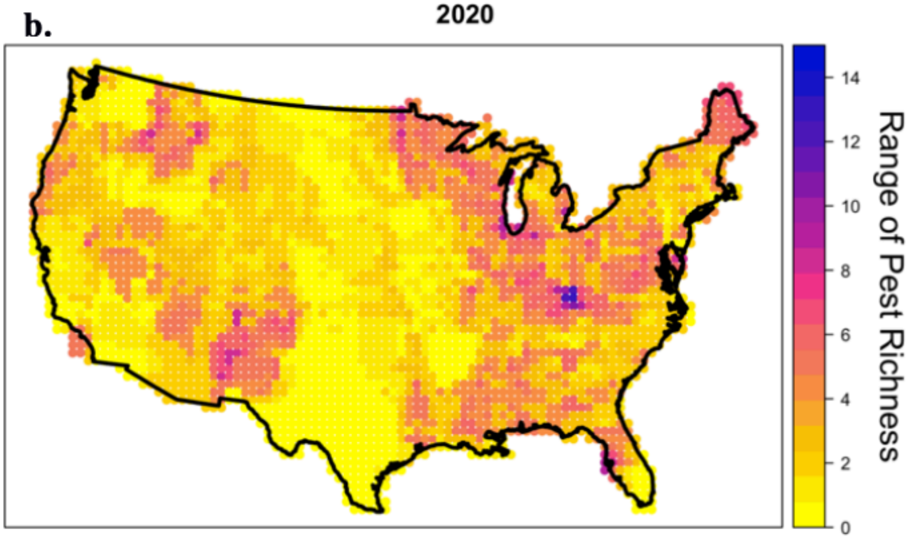
2020
Range of Pest Richness
0
2
4
6
8
10
12
14

c.

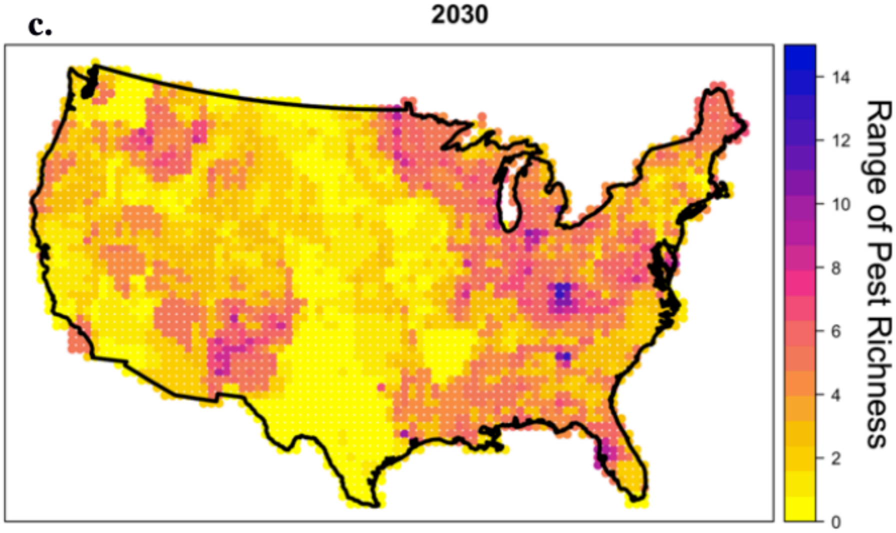
2030
Range of Pest Richness
0
2
4
6
8
10
12
14

Figure S2.6.2 Projections of SDK uncertainty (range of predicted pest richness at each site) due to parameter uncertainty at **a.** 2010, **b.** 2020, and **c.** 2030.

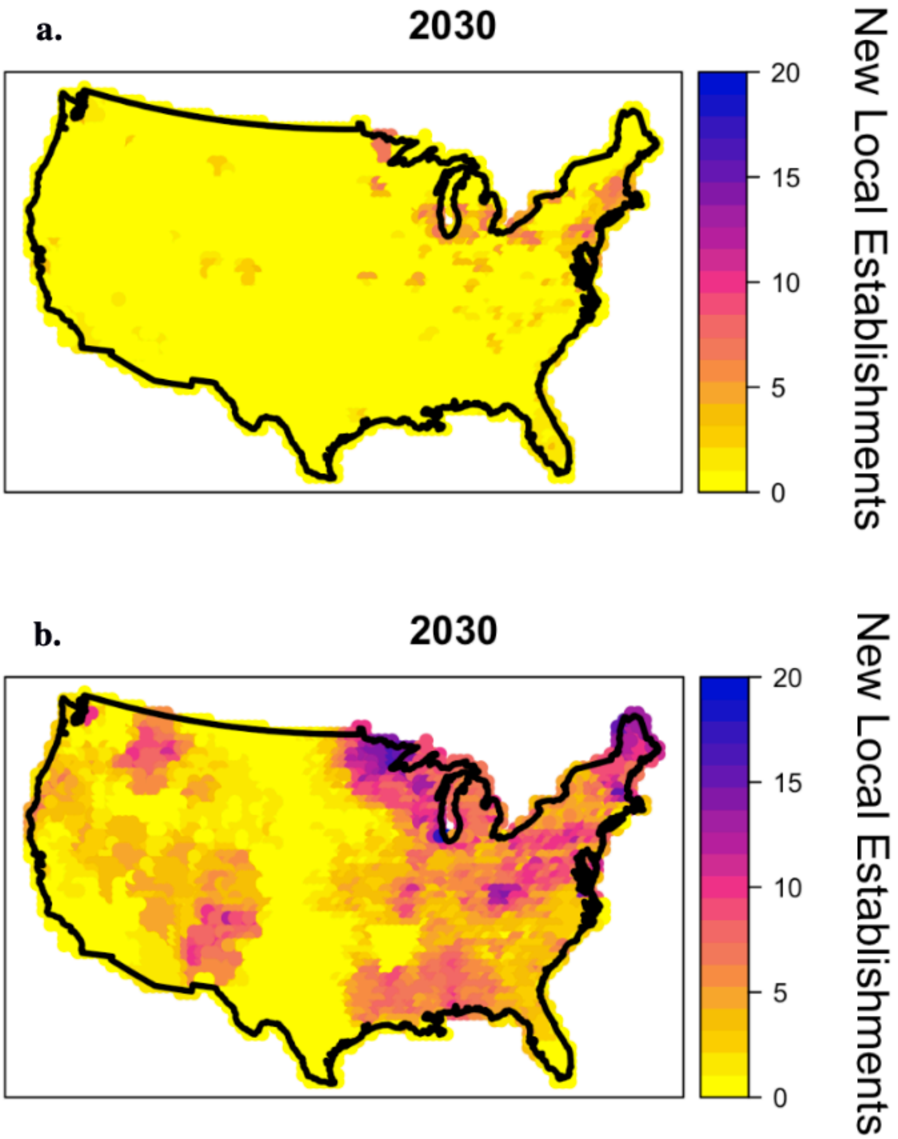

Figure S2.6.3 Extreme cases of future pest local establishment across uncertainty simulations, including the **a.** minimum spread and **b.** maximum spread scenario.

Literature Cited

Hauer, M. E. (2019). Population projections for US counties by age, sex, and race controlled to shared socioeconomic pathway. *Scientific data*, *6*, 190005.

O'Neill, B. C., Kriegler, E., Ebi, K. L., Kemp-Benedict, E., Riahi, K., Rothman, D. S., *et al*. (2017). The roads ahead: Narratives for shared socioeconomic pathways describing world futures in the 21st century. *Global Environmental Change*, *42*, 169-180.

Appendix S2.7 Distance-based residual examination as a predictor for forecasting ability

We tested whether the three species examined in this analysis were representative of the goodness-of-fit of our GDK by comparing the residuals of their spread range size (number of invaded cells) to the average misestimation across species in the uncorrected GDK. Our metric of misestimation is the log ratio of predicted and observed invaded cells, which is symmetric around 0 in the case of perfect range size predicted. We found that two out of three of these species were substantially overpredicted by the model (Table S1), with log ratios higher than the mean (49/63 species are fit better than HWA, and 44/63 species are fit better than BBD). Meanwhile, GM is fit slightly better than the average species (though worse than the median fit, as 37/63 species had fits better than GM). The ranking of these three species in terms of these residuals matches their ranking in terms of R^2_{om} for the GDK in our validation set. As such, we argue that the forecasting ability of a species can be roughly estimated by its distance-based residuals in the fitted GDK.

Table S2.7.1 GDK distance residuals for the 3 species examined compared to the average value for all fitted species. The absolute value of the log-ratio of predicted to observed invaded cells is taken so that under and overprediction have comparable effects.

	Predicted cells invaded (n_{pred})	Observed cells invaded (n_{obs})	Abs(log(n_{pred}/n_{obs}))
Mean (uncorrected GDK)			0.66
HWA	200	70	1.05
GM	692	403	0.54
BBD	433	182	0.87

Appendix S3. Appendices for Chapter 3

Appendix S3.1 Additional pests modelled in Chapters 3 and 4 (n=9)

Table S3.1.1 Names of pests added to the Chapter 3 and 4 datasets. This pest list was combined with the list in Table S2.1.1 and consists of pests who were first detected after 1999 (and thus that could not be fit in the original GDK).

Latin Name	**Common Name**
Agrilus prionurus	Soapberry Borer
Hylurgus ligniperda	Red-haired Pine Bark Beetle
Orthotomicus erosus	Mediterranean Pine Engraver Beetle
Scolytus schevyrewi	Banded Elm Bark Beetle
Enarmonia formosana	Cherry Bark Tortrix
Orchestes alni	Elm Flea Weevil
Raffaelea lauricola	Laurel Wilt Disease
Blastopsylla occidentalis	Eucalyptus Psyllid
Maconellicoccus hirsutus	Pink Hibiscus Mealybug

Appendix S3.2 Invasive range host phylogeny for United States invasive forest pests (n=294)

Figure S3.2.1 Phylogeny adapted from Zanne et al. (2014) seed plant phylogeny. All major nodes listed, branch lengths scaled to molecular branch lengths via Phylomatic v3.

Appendix S3.3 Theoretic analyses for the integrative establishment model

To ensure our model's parameters could be reliably identified, we performed theoretic simulations where we generated random relationships between diversity, richness and establishment using a variety of parameter values (Table S3.3.1). We assessed identifiability by fitting our model to these simulated data and comparing predicted and simulated (true) parameter values. We performed Latin Hypercube simulations to generate random parameter sets within a bounded range (Table S3.3.1), which we used in binomial simulation model for pest establishment that mirrored our fitting model (where resulting pest distributions were subject to stochasticity across binomial trials). We ensured that the parameter sets produced simulated data with enough variability to fit relationships by excluding theoretic results where establishment occurred in <10% or >90% of all pest-site combinations, where at least half of site-level establishment probabilities were at a bound (0.0001 or 0.9999), or where the standard deviation of probabilities of establishment was <5%. We assumed that any parameter set used to generate these results would not be identifiable due to the low variability in outcomes.

We generated 1000 random parameter sets through Latin Hypercube simulations, and retained 920 parameter sets that satisfied our variability conditions. Visual analyses of predicted vs. simulated (true) parameter sets indicated our fitting procedure had limited precision in determining exact parameter estimates (Fig. S3.31a-e, but that this misspecification had little impact on important derived model components, such as $z_{t,i,j}$, effective tree volume ($V_{t,i,j}$ exponent), or p_{estab} (Fig. S3.3.1f). Parameter estimates generally followed the 1:1 line, but it appears that many roughly equivalent parameter sets can produce the derived model components of interest (we note that centering and scaling the minpd_z term to correct for collinearity did not change these theoretical results appreciably, so we left it unscaled). Since the derived model components themselves were reliable, we have confidence in our derived ‘maximum effective trees’ values, the overall signs of effects, and the shape of fitted relationships such as Fig. 3.1.

Table S3.3.1 Latin Hypercube parameter sampling bounds. All parameters were sampled independently on a uniform distribution 1000 times. 920 parameter sets producing sufficient variability were retained to assess identifiability, uncertainty and bias.

Parameter	Minimum	Maximum
a_1	0.1	0.9
a_2	-1	-0.75
c_1	-0.5	0.5
c_2	-0.5	0.5
c_3	-0.25	0.25

Figure S3.3.1 Theoretic simulation results for the establishment model in terms of its ability to recapture model parameters (**a-e**), and derived model components (**f**), as measured by the R^2 between predicted and observed model components, where a value of 1 would indicate perfect identifiability. $V_{t,i,j}$ exponent mean=0.97, σ=0.074; $z_{t,i,j}$ mean=0.98, σ=0.072; p_{estab} mean=0.98, σ=0.019)

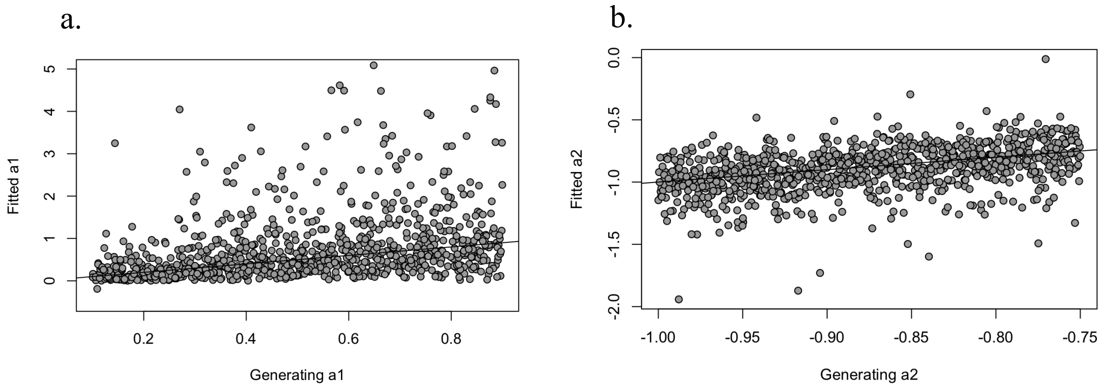

c.

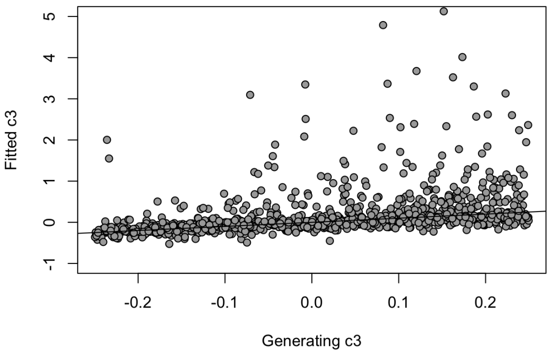
Fitted c3
5
4
3
2
1
0
-1
-0.2
-0.1
0.0
0.1
0.2
Generating c3

d.

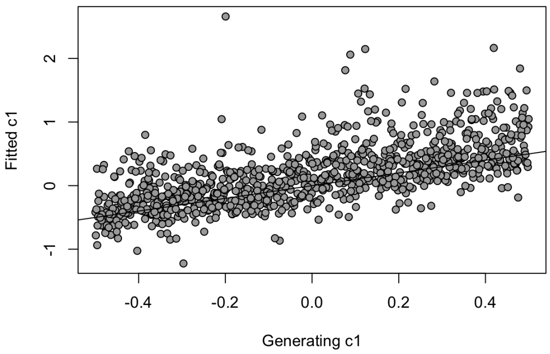
Fitted c1
2
1
0
-1
-0.4
-0.2
0.0
0.2
0.4
Generating c1

e.

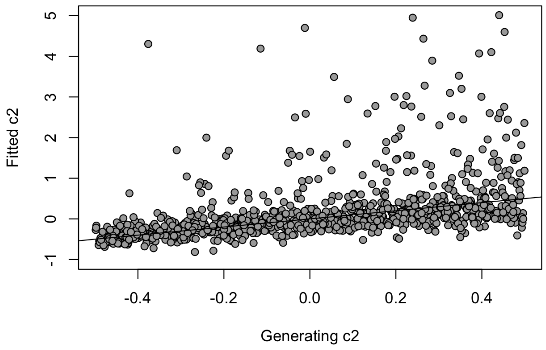
Fitted c2
5
4
3
2
1
0
-1
-0.4
-0.2
0.0
0.2
0.4
Generating c2

f.

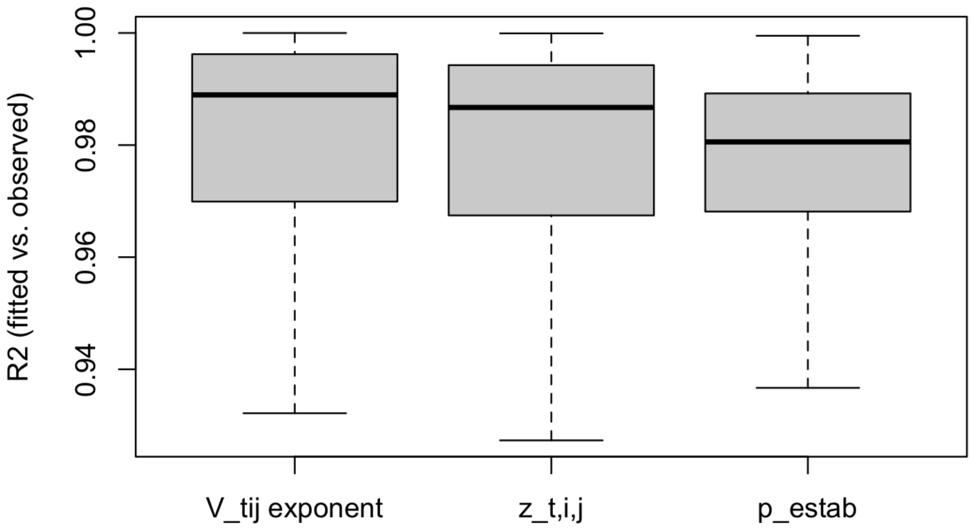
R2 (fitted vs. observed)
1.00
0.98
0.96
0.94
V_tij exponent
z_t,i,j
p_estab

Appendix S3.4 Additional mechanisms driving establishment

As we mentioned in the introduction, our model can easily be extended with additional pest, host, or site-specific parameters. We formulated several model extensions to explore competing hypotheses for the results obtained, including phylogenetic generalism, hotspots of climatic suitability, and regional differences based on forest type.

Firstly, our results could have been driven by a pest phylogenetic generalism effect, since generalist pest species have larger potential ranges (Fig. S3.4.1) and may have higher establishment rates overall. This may have upweighted high richness sites, since they are more likely to contain focal hosts of phylogenetic generalists. To test this, we fit an additional term (B_2) in our model that offset the mean probability of non-establishment (a_1) for each pest species *i* by their host breadth (root mean pairwise phylogenetic distance, Letten & Cornwell (2015))), $a'_{1,i} = a_1 + B_2\sqrt{mpd_i}$. This term had the correct sign ($B_2 = -0.0033$) in that species with greater host breadth had higher establishment overall (or lower probabilities of non-establishment). This term modestly improved fit (deviance explained = 6.74%), but the positive richness effect and phylogenetically-mediated density dependence effects remained ($a_2=-0.997, c_1=-0.00079$, $c_2=-0.0040$, $c_3=0.015$), indicating that an overall effect of phylogenetic generalism could not account for the observed patterns.

We lean toward the ‘diversity begets diversity’ hypothesis (Fridley et al. 2007) to explain the persistent relative benefit of richness. Most pest species are present in the Northeastern United States, which is also an area of high tree species richness (Liebhold et al. 2013), and may be a hotspot for both pest and tree species in terms of environmental suitability. This might indicate a lack of biotic filtering of any species at these sites. In contrast, the presence of only focal hosts at a site could indicate that this site possesses some sort of idiosyncratic quality (climatic or otherwise) that prevents many species of all kinds from surviving (Kraft & Ackerly 2014).

To examine the existence of suitability hotspots, we tested whether an additional climatic suitability metric could explain the model residuals by fitting a term for the extent of 'climatic anomaly' at each site. We used Euclidean distance from the mean climatic conditions measured across all bioclimatic variables across any host range within the United States (Fick & Hijmans 2017) as a measure of climatic anomaly. We found negligible evidence for a beneficial effect of 'moderate' environmental conditions, captured by a negative effect of increased Euclidean distance from mean climate (Δ % deviance <0.01%). Without rigorous understanding of pest environmental tolerances, this is a much more difficult mechanism to demonstrate, as specific environmental variables are likely to be important for each pest. We thus leave it as an area of future exploration for subsequent work.

The remaining spatial structure of integrative joint model residuals (Fig. 3.4c) indicates that the model lacked some additional spatially-structured factor that could dampen overprediction of establishment predominantly within the southeastern and midwestern United States. Since these patterns roughly followed differences in forest types, we tested the inclusion of an offset in the effective tree volume exponent for differences in gymnosperm and angiosperm host suitability. This term led to lower establishment on gymnosperm hosts and slightly improved establishment model fit (deviance explained = 6.23%), indicating regional differences in invasibility by forest type may be part of the remaining spatial signal.

Figure S3.4.1 Pest species phylogenetic generalism (mean pairwise distance across focal hosts) compared to the number of grid cells their focal host range spans (r = 0.64, p<0.0001). Generalist species have a greater area of potential establishment.

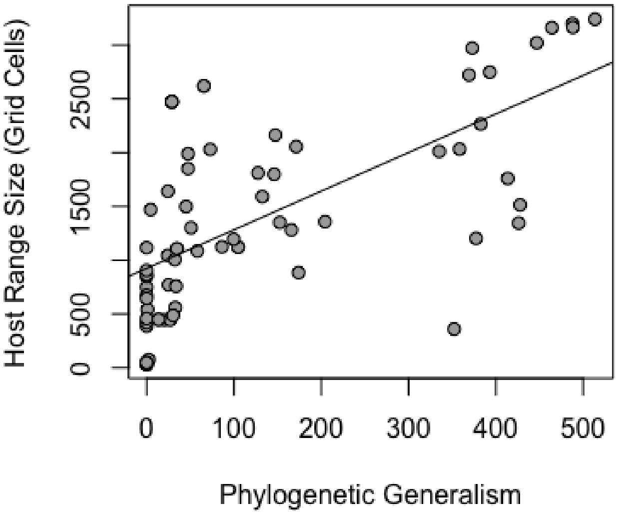

References

Fick, S. E., & Hijmans, R. J. (2017). WorldClim 2: new 1-km spatial resolution climate surfaces for global land areas. *International journal of climatology*, 37(12), 4302-4315.

Fridley, J. D., Stachowicz, J. J., Naeem, S., Sax, D. F., Seabloom, E. W., Smith, M. D., *et al*. (2007). The invasion paradox: reconciling pattern and process in species invasions. *Ecology*, 88(1), 3-17.

Kraft, N. J., & Ackerly, D. D. (2014). Assembly of plant communities. *Ecology and the Environment*, 8, 67-88.

Letten, A. D., & Cornwell, W. K. (2015). Trees, branches and (square) roots: why evolutionary relatedness is not linearly related to functional distance. *Methods in Ecology and Evolution, 6*(4), 439-444.

Liebhold, A. M., McCullough, D.G., Blackburn, L. M., Frankel, S. J., Von Holle, B. & Aukema, J. E. (2013). A highly aggregated geographical distribution of forest pest invasions in the USA. *Diversity and Distributions,* 19, 1208-1216.

Appendix S4. Appendices for Chapter 4

Appendix S4.1 Data sources for host tree models

Table S4.1.1 List of predictors used in total tree and genus-specific tree models

Predictor	**Unit**	**Description**	**Reference**
Population		2010 Census population	US Census Bureau http://www.census.gov/popest
Ecological Province		Subregions using criteria defined in the National Hierarchical Framework of Ecological Units	Cleland et al. 2007
Median number of freeze free days		Median number of days between last spring and first autumn temperature ≤0 °C	PRISM Climate Group, Oregon State University
Total road length	Log (km)	Total length of roads in community	US Geological Survey, Fort Collins Science Center; Koch et al. (2018)
Total road density	Log (km^{-1})	Length of road per square km of community area	US Geological Survey, Fort Collins Science Center; Koch et al. (2018)
Mean moisture index		Balance between precipitation and potential evapotranspiration; scaled between -1 and 1	Willmott and Feddema (1992), PRISM Climate Group, Oregon State University, Koch et al. 2018
Mean precipitation	mm	Mean annual measured precipitation	Willmott and Feddema (1992), PRISM Climate Group, Oregon State University, Koch et al. 2018,
Elevation	metres	Elevation above sea level	US Geological Survey National Elevation Dataset
Area	hectares	Community size	American Community Survey https://www.census.gov/programs-surveys/acs
Income	USD	Median household income in 1999 (County level)	US Census Bureau http://quickfacts.census.gov/qfd/meta/long_INC910199.htm
Mean Year of Home Construction	Year	Average age a home was built based on surveys from 2015	American Community Survey https://www.census.gov/programs-surveys/acs

		(block-group level)	
Median Value of Home	USD	Median value of a home in the community in 2015 (block-group level)	American Community Survey https://www.census.gov/programs-surveys/acs
bio2	°C *10	Mean Diurnal Range (Mean of monthly (max temp - min temp))	WORLDCLIM (Fick & Hijmans 2017)
bio8	°C *10	Mean Temperature of Wettest Quarter	WORLDCLIM (Fick & Hijmans 2017)
bio10	°C *10	Mean Temperature of Warmest Quarter	WORLDCLIM (Fick & Hijmans 2017)
bio11	°C *10	Mean Temperature of Coldest Quarter	WORLDCLIM (Fick & Hijmans 2017)
bio13	mm	Precipitation of Wettest Month	WORLDCLIM (Fick & Hijmans 2017)
bio15	mm^{-2}	Precipitation Seasonality (Coefficient of Variation)	WORLDCLIM (Fick & Hijmans 2017)
Distance to coast	metres		Calculated in ArcGIS with US Equidistant Conic Projection
Tree canopy cover	%	Fraction of community area covered by trees	National Land Cover Database (2011); Homer et al. (2015)
Latitude	metres		Calculated in ArcGIS with US Equidistant Conic Projection
Longitude	metres		Calculated in ArcGIS with US Equidistant Conic Projection

Figure S4.1.1 Map of the 653 inventoried street tree communities across the United States

References

Cleland, D.T., Freeouf, J.A., Keys, J.E., Jr., Nowacki, G.J., Carpenter, C.A., & McNab, W.H., 2007. *Ecological subregions: sections and subsections for the conterminous United States*. In: Sloan, A.M., (tech. ed.), 2007. Gen. Tech. Rep. WO-76D. [Map, presentation scale 1:3,500,000; colored]. Also on CD-ROM as a GIS coverage in ArcINFO format. US Department of Agriculture, Forest Service, Washington, DC.

Fick, S. E., & Hijmans, R. J. (2017). WorldClim 2: new 1-km spatial resolution climate surfaces for global land areas. *International journal of climatology*, 37(12), 4302-4315.

Homer, C.G., Dewitz, J.A., Yang, L., Jin, S., Danielson, P., Xian, G., … *et al*. (2015). Completion of the 2011 National Land Cover Database for the conterminous United States – representing a decade of land cover change information. *Photogrammatic Engineering and Remote Sensing,* 81, 345–354.

Koch, F. H., Ambrose, M. J., Yemshanov, D., Wiseman, P. E., & Cowett, F. D. (2018). Modeling urban distributions of host trees for invasive forest insects in the eastern and central USA: A three-step approach using field inventory data. *Forest ecology and management*, 417, 222-236.

Miles, P.D., Brand, G.J., Alerich, C.L., Bednar, L.R., Woudenberg, S.W., Glover, J.F. … *et al.* (2001). *The forest inventory and analysis database: database description and users manual version 1.0.* General Technical Report NC-218, North Central Research Station, USDA Forest Service, St. Paul, MN.

Appendix S4.2 Host distribution model: detailed results

Total tree abundance models

Figure S4.2.1 Fits of the total tree abundance models to small, medium, and large trees across all 653 communities

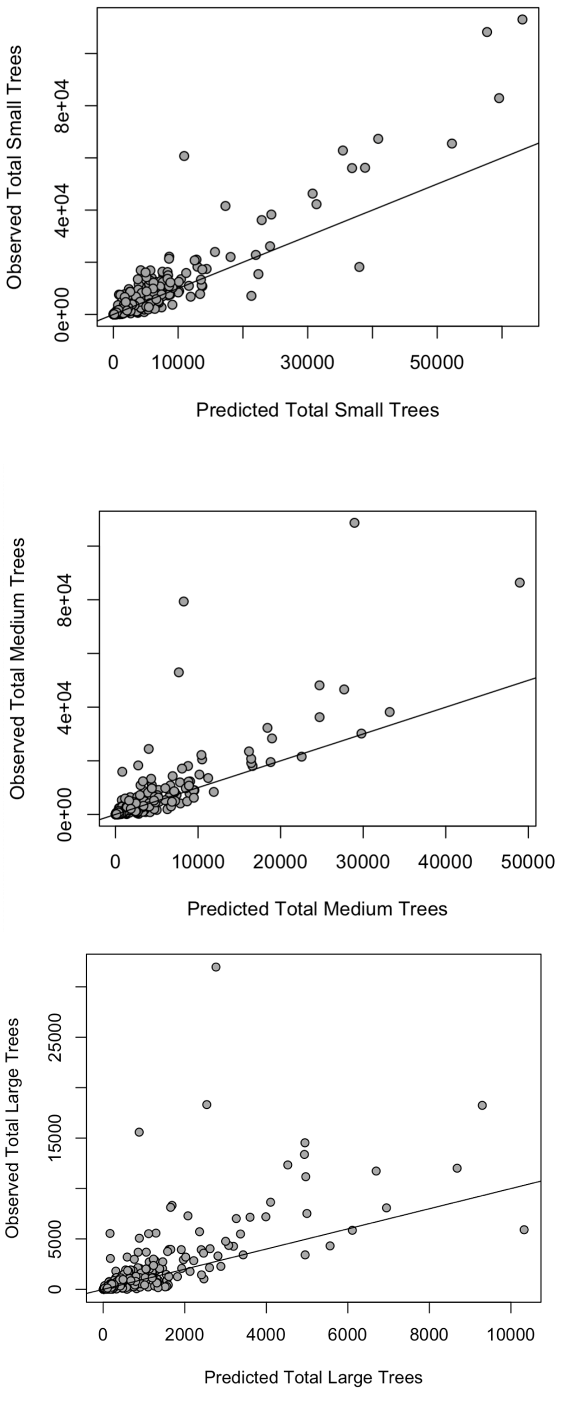

Table S4.2.1 Results of total tree abundance models (a. small, b. medium, c. large). Models were fit via boosted regression trees, so relationships with predictors are not strictly positive or negative, but the overall shape of the relationship is summarized in the 'general sign' column.

a. Small trees

Predictor	**Relative Influence**	**General Sign**
Population	55	+
Area	4.5	+
Ecological province	10.9	NA
bio10	2.8	-
Mean home value	2.7	+
Income	2.2	+
Mean year of home construction	1.5	-
Mean precipitation	1.2	+
Road density	1.2	-
Others	<1	

b. Medium Trees

Predictor	**Relative Influence**	**General Sign**
Population	58.6	+
Ecological province	13.5	NA
Area	6.3	+
Mean year of home construction	5.8	-
bio10	2.0	hump-shaped
Income	1.8	+
Road length	1.6	-
Mean number of freeze free days	1.4	+
Road density	1.3	-
bio11	1.2	-
Mean home value	1.2	+
Others	<1	

c. Large trees

Predictor	**Relative Influence**	**General sign**
Population	43	+
Mean year of home construction	13.8	-

Ecological province	13	NA
Area	6.6	+
Tree canopy cover	6.5	+
Mean number of freeze free days	3.8	+
bio11	3.4	+
Road length	1.2	-
Mean precipitation	1.1	hump-shaped
Income	1	+
Others	<1	

Genus-specific models

Figure S4.2.2 Inverse relationship between the rarity of a genus (defined as the predicted total number of trees of a particular size class) and the fit of the best single-genus model.

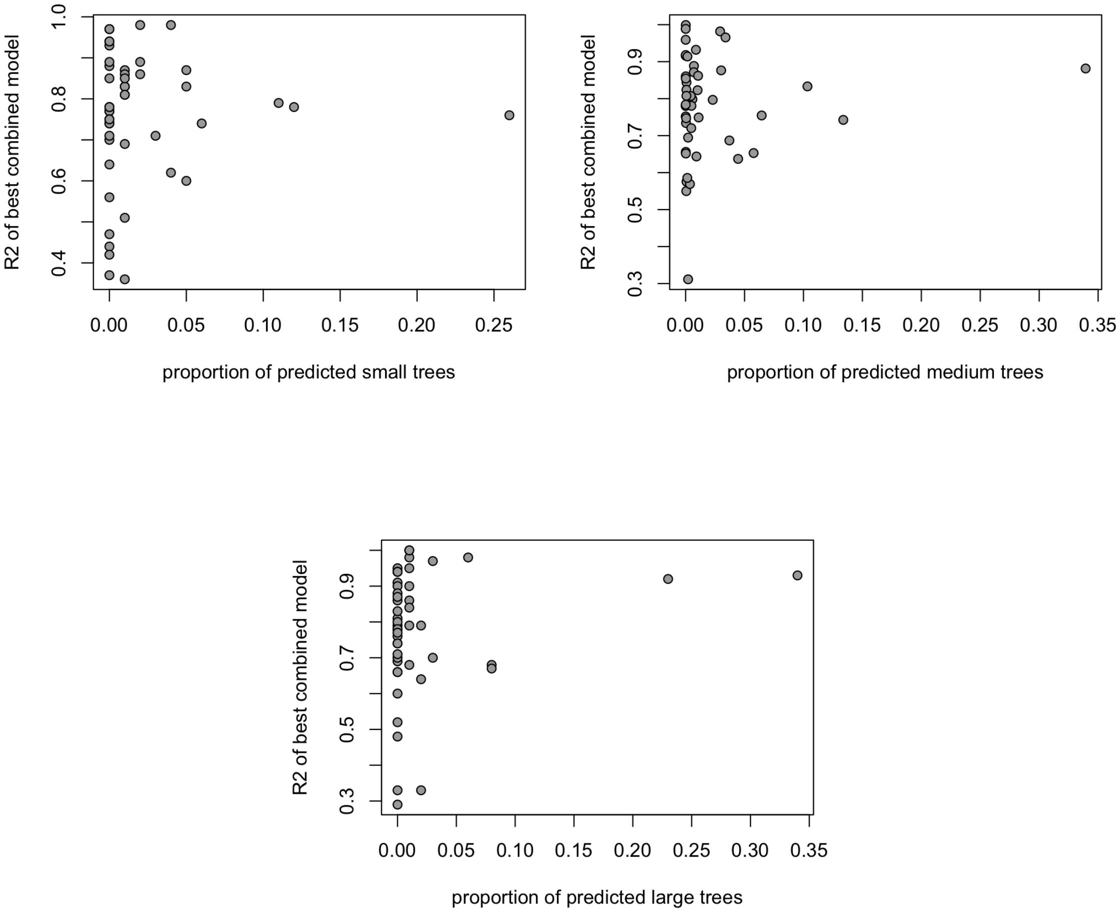

Table S4.2.2 Model selection results for small tree genus-specific models: **a.** overall combinations and **b.** individual models for presence and number of trees. "SEP" as a prefix indicates a separate model fit to a given genus, whereas no prefix indicates a global model fit to all genera.

a.

Model types	**Frequency**	**Proportion**
BRT/BRT	15	0.31
GAM/GAM	0	0
SEPBRT/SEPBRT	1	0.02
SEPGAM/SEPGAM	0	0
GAM/BRT	1	0.02
GAM/SEPGAM	0	0
GAM/SEPBRT	1	0.02
BRT/GAM	0	0
BRT/SEPGAM	12	0.25
BRT/SEPBRT	2	0.04
SEPGAM/GAM	0	0
SEPGAM/BRT	3	0.06
SEPGAM/SEPBRT	0	0
SEPBRT/GAM	0	0
SEPBRT/BRT	10	0.21
SEPBRT/SEPGAM	3	0.06

b.

Model type	**Tree presence model count**	**Tree presence model proportion**	**Tree abundance model count**	**Tree abundance model proportion**
BRT	29	0.60	29	0.60
GAM	2	0.04	0	0
SEPBRT	14	0.29	4	0.08
SEPGAM	3	0.06	15	0.31

Table S4.2.3 Model selection results for medium tree genus-specific models: **a.** overall combinations and **b.** individual models for presence and number of trees. "SEP" as a prefix indicates a separate model fit to a given genus, whereas no prefix indicates a global model fit to all genera.

a.

Model types	**Frequency**	**Proportion**
BRT/BRT	10	0.21

GAM/GAM	0	0
SEPBRT/SEPBRT	0	0
SEPGAM/SEPGAM	4	0.08
GAM/BRT	1	0.02
GAM/SEPGAM	2	0.04
GAM/SEPBRT	0	0
BRT/GAM	0	0
BRT/SEPGAM	11	0.23
BRT/SEPBRT	1	0.02
SEPGAM/GAM	0	0
SEPGAM/BRT	3	0.06
SEPGAM/SEPBRT	0	0
SEPBRT/GAM	0	0
SEPBRT/BRT	15	0.31
SEPBRT/SEPGAM	1	0.02

b.

Model type	**Tree presence model count**	**Tree presence model proportion**	**Tree abundance model count**	**Tree abundance model proportion**
BRT	22	0.46	29	0.60
GAM	3	0.06	0	0
SEPBRT	16	0.33	1	0.02
SEPGAM	7	0.15	18	0.38

Table S4.2.4 Model selection results for large tree genus-specific models: **a.** overall combinations and **b.** individual models for presence and number of trees. “SEP” as a prefix indicates a separate model fit to a given genus, whereas no prefix indicates a global model fit to all genera.

a.

Model types	**Frequency**	**Proportion**
BRT/BRT	3	0.0625
GAM/GAM	0	0
SEPBRT/SEPBRT	3	0.0625
SEPGAM/SEPGAM	5	0.10416667
GAM/BRT	3	0.0625
GAM/SEPGAM	0	0
GAM/SEPBRT	0	0

BRT/GAM	0	0
BRT/SEPGAM	2	0.04166667
BRT/SEPBRT	2	0.04166667
SEPGAM/GAM	1	0.02083333
SEPGAM/BRT	13	0.27083333
SEPGAM/SEPBRT	2	0.04166667
SEPBRT/GAM	0	0
SEPBRT/BRT	14	0.29166667
SEPBRT/SEPGAM	0	0

b.

Model type	**Tree presence model count**	**Tree presence model proportion**	**Tree abundance model count**	**Tree abundance model proportion**
BRT	7	0.15	33	0.69
GAM	3	0.06	1	0.02
SEPBRT	17	0.35	7	0.15
SEPGAM	21	0.44	7	0.15

Figure S4.2.3 Relationship between genus rarity (in terms of the number of sites where present and the predicted proportion of total trees) and the single-genus model selected across size classes. For small tree presence/absence, more GAMs and SEPGAMs are selected with more sites, while more GAMs are selected with more predicted trees. For small tree number, more SEPGAMs are selected with more sites, while more SEPBRTs are selected with more predicted trees. For medium tree presence/absence, fewer SEPBRTs are selected with fewer sites, while more BRTs and GAMs are selected with more predicted trees. For medium tree number, more SEPGAMs are selected for more sites, while more SEPBRTs are selected for more predicted trees. For large tree presence/absence, fewer GAMs are selected for fewer sites. For large tree number, more SEPBRTs are selected with more sites, and more SEPGAMs are selected with more predicted trees.

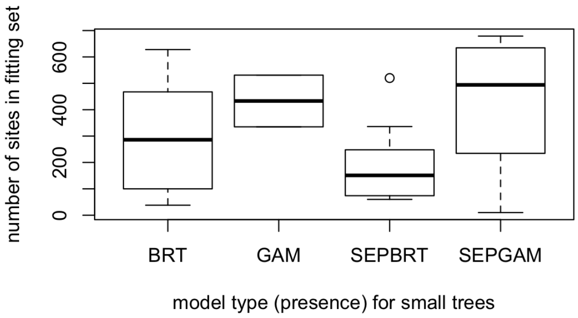
number of sites in fitting set
0
200
400
600
BRT
GAM
SEPBRT
SEPGAM
model type (presence) for small trees

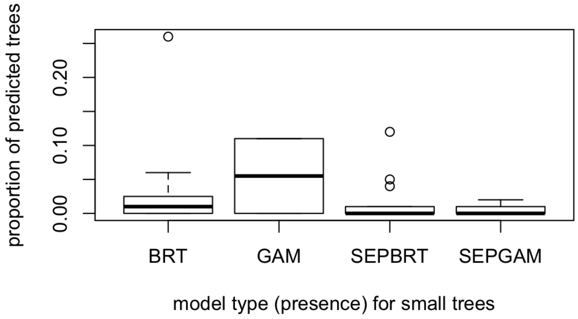
proportion of predicted trees
0.00
0.10
0.20
BRT
GAM
SEPBRT
SEPGAM
model type (presence) for small trees

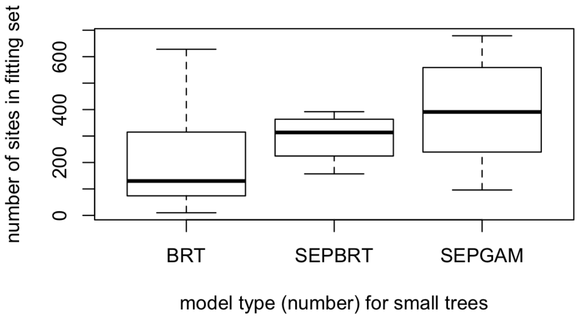
number of sites in fitting set
0
200
400
600
BRT
SEPBRT
SEPGAM
model type (number) for small trees

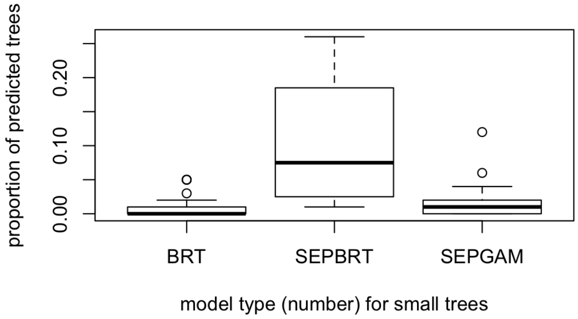
proportion of predicted trees
0.00
0.10
0.20
BRT
SEPBRT
SEPGAM
model type (number) for small trees

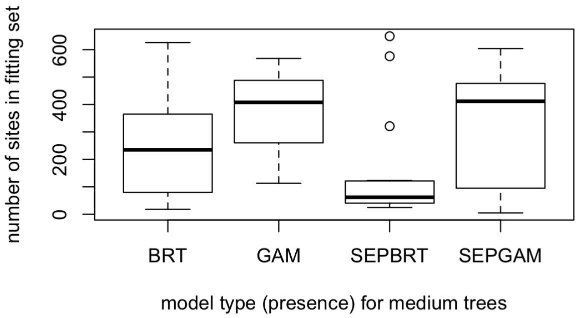
number of sites in fitting set
0
200
400
600
BRT
GAM
SEPBRT
SEPGAM
model type (presence) for medium trees

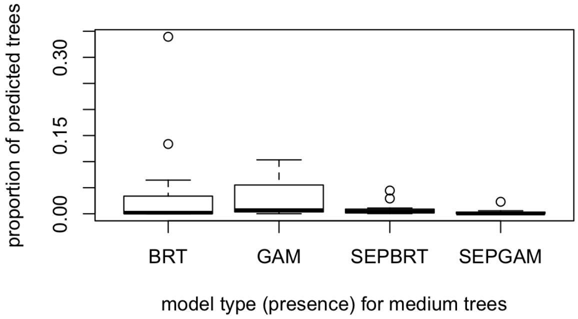
proportion of predicted trees
0.00
0.15
0.30
BRT
GAM
SEPBRT
SEPGAM
model type (presence) for medium trees

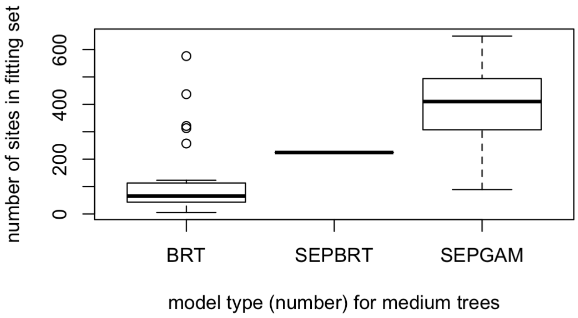
number of sites in fitting set
0
200
400
600
BRT
SEPBRT
SEPGAM
model type (number) for medium trees

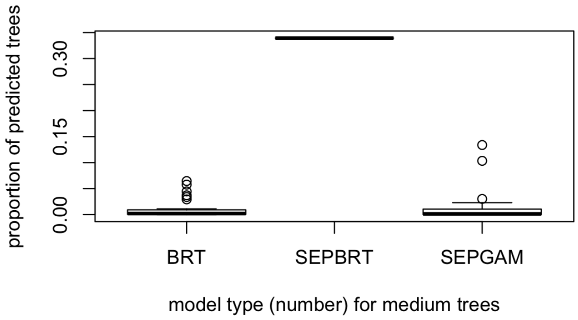
proportion of predicted trees
0.00
0.15
0.30
BRT
SEPBRT
SEPGAM
model type (number) for medium trees

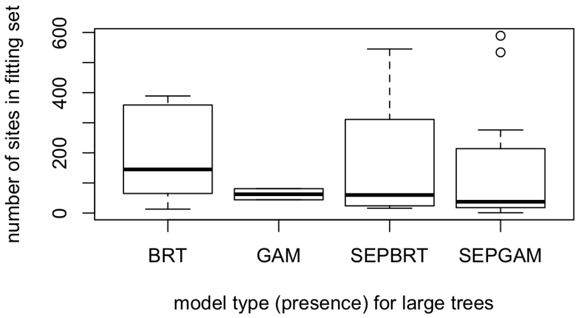
number of sites in fitting set
0
200
400
600
BRT
GAM
SEPBRT
SEPGAM
model type (presence) for large trees

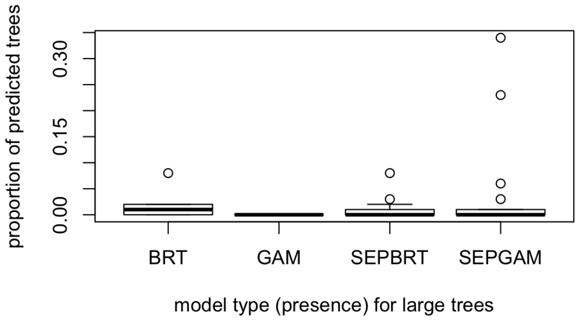
proportion of predicted trees
0.00
0.15
0.30
BRT
GAM
SEPBRT
SEPGAM
model type (presence) for large trees

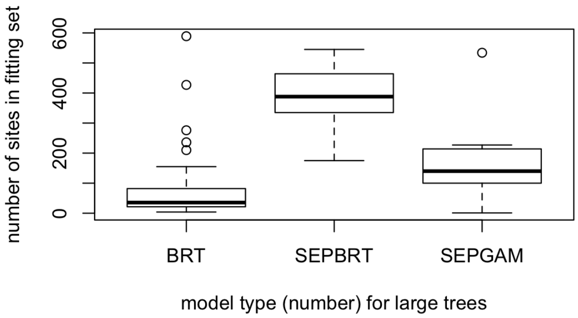
number of sites in fitting set
0
200
400
600
BRT
SEPBRT
SEPGAM
model type (number) for large trees

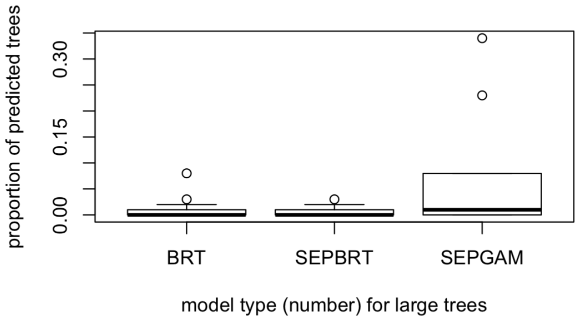
proportion of predicted trees
0.00
0.15
0.30
BRT
SEPBRT
SEPGAM
model type (number) for large trees

Figure S4.2.4 Breakdown of both fitted (**a-c**) and extrapolated (**d-f**) small, medium and large tree abundance from the genus-specific models

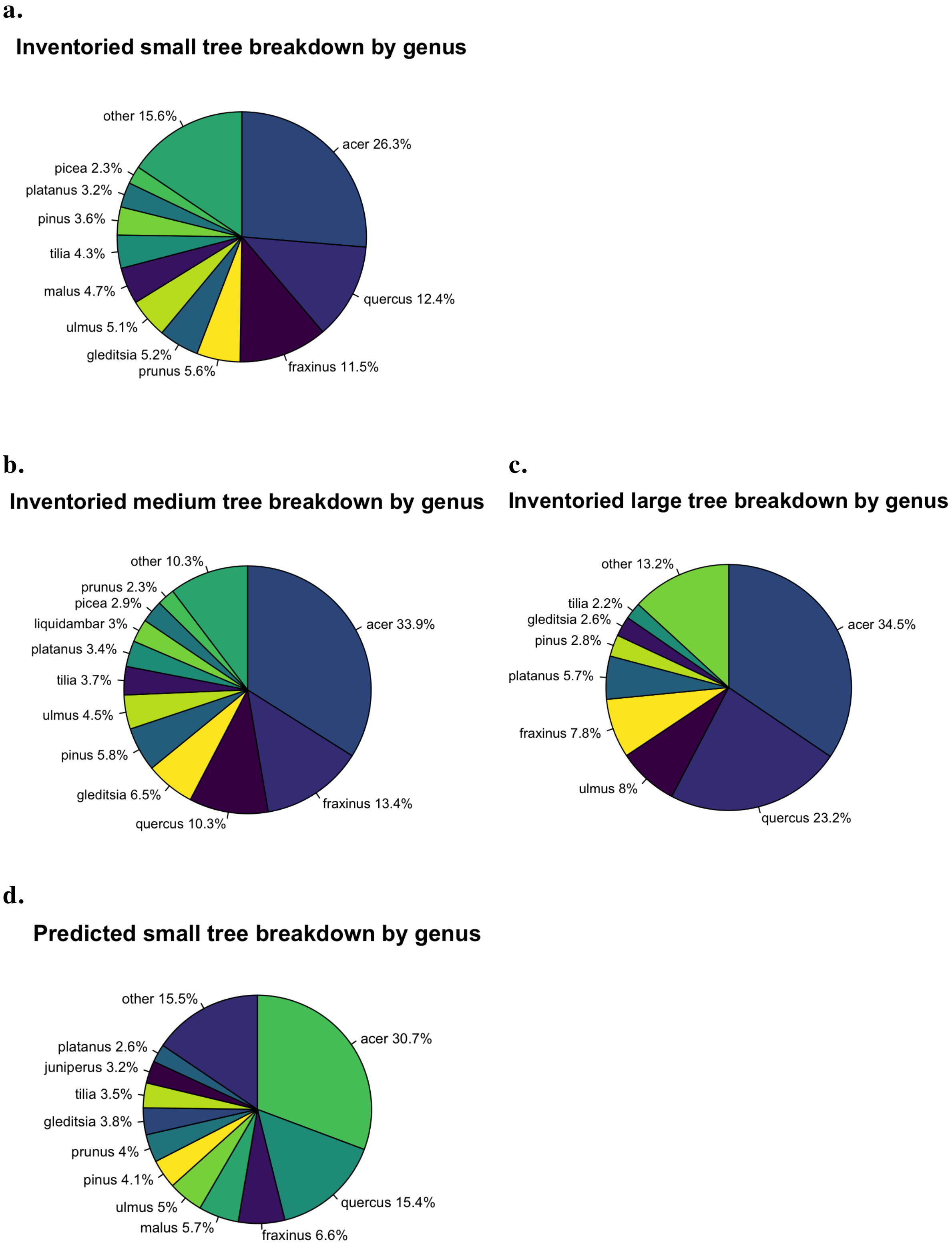

e.

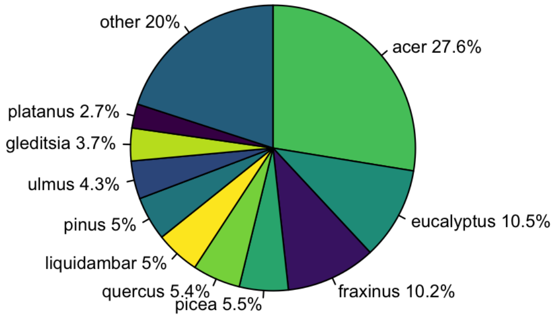
Predicted medium tree breakdown by genus

f.

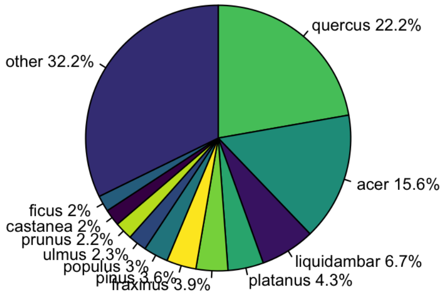
Predicted large tree breakdown by genus

Table S4.2.5 Strength of predictive ability across all single-genus tree models, with the selected best-fitting tree presence/absence and tree number model components shown for each (SEP indicates a model fit with genus-specific terms).

Genus	**R^2 (small)**	**Presence model (small)**	**Abundance model (small)**	**R^2 (medium)**	**Presence model (medium)**	**Abundance model (medium)**	**R^2 (large)**	**Abundance model (large)**	**Abundance model (large)**
Abies	0.70	BRT	BRT	0.78	SEPBRT	BRT	0.68	SEPGAM	BRT
Acacia	0.37	BRT	BRT	0.78	BRT	BRT	0.94	SEPGAM	BRT
Acer	0.76	BRT	BRT	0.81	SEPBRT	SEPGAM	0.71	SEPGAM	BRT
Aesculus	0.74	BRT	BRT	0.82	BRT	SEPGAM	0.98	BRT	BRT
Amelanchier	0.87	BRT	BRT	0.31	SEPBRT	BRT	0.29	SEPBRT	BRT
Arbutus	0.85	BRT	BRT	0.81	SEPBRT	BRT	0.999	SEPGAM	BRT
Betula	0.86	SEPGAM	SEPGAM	0.86	BRT	SEPGAM	0.90	BRT	SEPGAM
Castanea	0.77	BRT	BRT	0.75	BRT	BRT	0.97	SEPGAM	BRT
Chamaecyparis	0.77	BRT	BRT	0.98	SEPBRT	BRT	0.90	SEPBRT	BRT
Cinnamomum	0.83	BRT	BRT	0.75	SEPBRT	BRT	0.87	GAM	BRT
Citrus	0.88	BRT	BRT	0.59	SEPBRT	BRT	0.94	SEPGAM	BRT
Cornus	0.81	BRT	BRT	0.99	BRT	BRT	0.48	SEPBRT	BRT
Cotinus	0.71	SEPGAM	SEPGAM	0.57	BRT	BRT	0.999	SEPGAM	SEPGAM
Crataegus	0.83	BRT	BRT	0.92	GAM	BRT	0.91	SEPBRT	BRT
Cupressus	0.75	BRT	BRT	0.69	BRT	BRT	0.79	SEPBRT	BRT
Elaeagnus	0.78	BRT	BRT	0.96	BRT	SEPGAM	0.77	SEPGAM	BRT
Eucalyptus	0.64	BRT	BRT	0.85	BRT	SEPGAM	0.70	GAM	BRT
Fagus	0.78	BRT	BRT	0.65	BRT	SEPGAM	0.74	SEPBRT	BRT
Ficus	0.97	BRT	BRT	0.78	SEPGAM	BRT	0.88	BRT	BRT
Fraxinus	0.79	SEPBRT	SEPBRT	0.82	BRT	SEPGAM	0.78	SEPBRT	SEPBRT
Gleditsia	0.83	SEPBRT	SEPBRT	0.86	BRT	SEPGAM	0.83	SEPBRT	SEPBRT
Ilex	0.81	BRT	BRT	0.55	BRT	BRT	0.52	SEPBRT	BRT
Juglans	0.44	SEPGAM	SEPGAM	0.91	SEPBRT	BRT	0.80	SEPGAM	SEPGAM
Juniperus	0.85	SEPGAM	SEPGAM	0.83	GAM	SEPGAM	0.92	SEPGAM	SEPGAM

Larix	0.74	BRT	BRT	0.64	SEPBRT	BRT	0.67	SEPBRT	BRT
Liquidambar	0.89	SEPGAM	SEPGAM	0.74	BRT	SEPGAM	0.68	BRT	SEPGAM
Liriodendron	0.51	SEPBRT	SEPBRT	0.65	BRT	BRT	0.70	SEPBRT	SEPBRT
Maclura	0.47	BRT	BRT	0.72	SEPBRT	BRT	0.79	SEPGAM	BRT
Magnolia	0.86	SEPGAM	SEPGAM	0.88	BRT	SEPBRT	0.93	SEPGAM	SEPGAM
Malus	0.87	BRT	BRT	0.80	SEPGAM	SEPGAM	0.84	BRT	BRT
Morus	0.69	BRT	BRT	0.75	BRT	SEPGAM	0.76	SEPGAM	BRT
Ostrya	0.42	BRT	BRT	0.64	SEPBRT	BRT	0.33	BRT	BRT
Persea	0.93	BRT	BRT	0.81	SEPBRT	BRT	0.74	SEPGAM	BRT
Picea	0.98	BRT	BRT	0.92	SEPGAM	SEPGAM	0.86	SEPGAM	BRT
Pinus	0.62	SEPBRT	SEPBRT	0.87	GAM	SEPGAM	0.66	BRT	SEPBRT
Platanus	0.71	SEPBRT	SEPBRT	0.88	BRT	SEPGAM	0.64	BRT	SEPBRT
Populus	0.36	BRT	BRT	0.80	SEPGAM	SEPGAM	0.95	SEPBRT	BRT
Prunus	0.74	SEPGAM	SEPGAM	0.97	BRT	BRT	0.98	SEPGAM	SEPGAM
Pseudotsuga	0.97	BRT	BRT	0.89	SEPBRT	BRT	0.95	SEPGAM	BRT
Quercus	0.78	SEPGAM	SEPGAM	0.73	SEPBRT	BRT	0.81	SEPGAM	SEPGAM
Salix	0.94	BRT	BRT	0.81	BRT	BRT	0.69	SEPBRT	BRT
Sapindus	0.94	SEPGAM	SEPGAM	0.999	SEPGAM	BRT	0.94	SEPGAM	SEPGAM
Sassafras	0.56	BRT	BRT	0.58	SEPBRT	BRT	0.66	SEPGAM	BRT
Sorbus	0.75	BRT	BRT	0.93	SEPBRT	BRT	0.86	BRT	BRT
Taxus	0.89	BRT	BRT	0.66	BRT	BRT	0.33	SEPGAM	BRT
Tilia	0.98	SEPBRT	SEPBRT	0.69	BRT	SEPGAM	0.78	BRT	SEPBRT
Tsuga	0.78	BRT	BRT	0.75	SEPGAM	BRT	0.6	SEPGAM	BRT
Ulmus	0.60	SEPBRT	SEPBRT	0.84	SEPGAM	SEPGAM	0.79	SEPBRT	SEPBRT

Table S4.2.6 The strength of model fit across all 16 possible model combinations for each host tree genus. "SEP" as a prefix indicates a separate model fit to a given genus, whereas the lack of such a prefix indicates a global model fit to all genera. Some genera were very rare within our inventoried communities at a given size class, and therefore their genus-specific models did not have sufficient data to be fit. R^2 is reported as NA in these cases.
https://www.dropbox.com/s/c1048q8imtweaik/tableS2.4.6.xlsx?dl=0 *(hosted online because table is very large)*

Appendix S4.3 Pest spread forecasts 2020-2050

Figure S4.3.1 Predicted pest richness in the mid-range climate scenario from 2020 to 2050, with newly occurring local establishments plotted in the last panel.

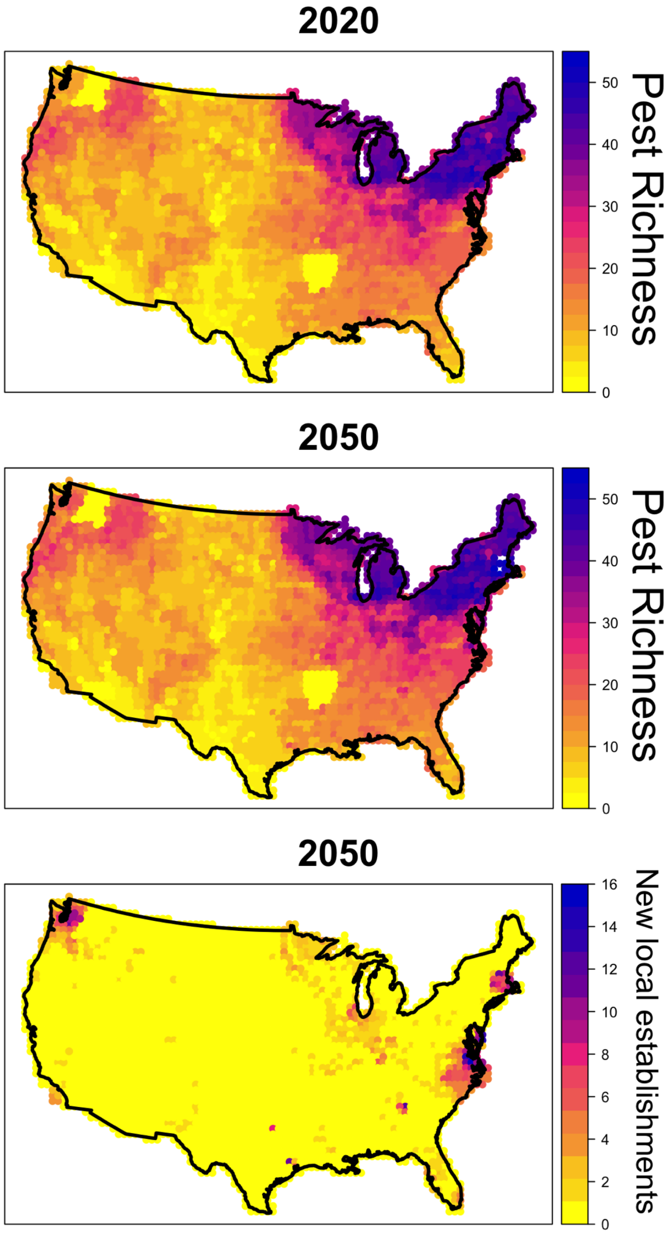

Appendix S4.4 Summary of Bayesian theoretic analyses

To ensure our resulting mortality and cost curves were identifiable and had unbiased parameters, we tested their ability to fit to simulated mortality and cost data using theoretical simulations. In our theoretic analyses, we tested a series of parameter values for five curve families (the beta family for the mortality curves and gamma, lognormal, Weibull, and Pareto families for the cost curves), and chose the least biased priors for each distribution from these. Across all Bayesian models, we used 4 Stan chains with 10000 burn-in iterations and 10000 sampling iterations. Bias and identifiability were examined through theoretic simulations using P-P plots (Leung & Steele 2013). We tested whether the chains achieved high coverage of the posterior distribution by checking effective sample size (N_{eff}, where an N_{eff} of 10% of the iterations suggests unbiased sampling) and tested for chain convergence with the Gelman-Rubin diagnostic (R_{hat}), using a threshold of 1.1, via the R package *shinystan* (Gabry et al. 2019).

A note on prior choices

We tested uniform, Jeffreys, reference, and other simple prior formulations (e.g. inverse prior) and chose the least biased priors for each distribution from these. The Jeffreys prior is defined as: $\pi(\theta) = \sqrt{Det(I(\theta))}$, where $I(\theta)$ is the Fisher information matrix. Jeffreys (1961) developed the prior as a parameterization-invariant alternative to the uniform prior. The reference prior (Bernardo 1979) can produce similar properties and sometimes has better behaviour. However, some of these formulations are very difficult to compute, and so simpler formulations such as the inverse were substituted when theoretic analyses showed they behaved well.

Mortality model

We fit a beta distribution to our host severity frequency distribution. The beta distribution is described by two free parameters, a and b:

$$proportional\ mortality \sim Beta(a, b)$$

We chose priors for a and b based on theoretical simulations, where we drew 1000 random a and b parameters via Latin hypercube sampling (Table S4.4.1) and subsequently sampled from each of these beta distributions to produce 100 severity estimates to use as data to fit our Bayesian models. To assess bias, we examined the resulting P-P plots for each model (Leung & Steele 2013). P-P plots allow for the checking of bias and uncertainty in the posterior distribution by plotting the percentiles of the posterior distribution under which the true parameters lie. The percentiles should follow the 1:1 line in a purely unbiased model. Deviations from the line can indicate over- or underestimation, as well as over- or under-prediction of uncertainty. We found that the best-behaved P-P plots corresponded to a prior of $\frac{1}{\sqrt{ab}}$ for the model (Yang & Berger, *unpubl. manuscript*), though they still resulted in slight overestimation (Fig. S4.4.1).

We performed posterior checks on our fitted Stan model through *shinystan* (Gabry 2015 to determine whether a tractable model could be estimated using uncertain, sequential bounds and no point mortality estimates. Our fitted model generated no warnings for the standard posterior checks (i.e., effective sample size N_{eff}, Gelman-Rubin diagnostic R_{hat}).

Mortality model results

The host mortality distribution groups pest-host combinations into a series of sequential bins based on severity (Fig. 4.4, Potter et al. 2019). The two lowest bins have uncertain upper bounds, and the highest bin has an uncertain lower bound. Our model thus included the relative frequencies of species within each bin as data, and we fit parameters for the beta distribution shape and scale, as well as for the bounds of the two lowest bins and the highest bin. We assumed that the mortality categories did not overlap and that mortality increased in severity, such that these bins could be assigned sequentially. The likelihood was the sum of the integrals under the associated probability density functions for different beta parameter sets and threshold values, making the log likelihood:

$$LL = A_{spp}(log \int_{i=0}^{AT} p\,(i\,|a,b)) + B_{spp}(log \int_{i=AT}^{BT} p\,(i\,|a,b)) + C_{spp}(log \int_{i=BT}^{0.01} p\,(i\,|a,b))$$

$$+ D_{spp}(log \int_{i=0.01}^{0.1} p\,(i\,|a,b)))) + E_{spp}(log \int_{i=0.1}^{0.25} p\,(i\,|a,b))))$$

$$+ F_{spp}(log \int_{i=0.25}^{0.95} p\,(i\,|a,b)))) + G_{spp}(log \int_{i=0.95}^{GT} p\,(i\,|a,b))))$$

$$+ H_{spp}(log \int_{i=GT}^{1.0} p\,(i\,|a,b))$$

Where the letters *A-H* correspond to the binned severity categories listed in Fig. S4.4.2 and *i* is the proportional mortality. The posterior can then calculated via:

$$p(a,b|y) \propto p(a,b)p(y|a,b)$$

$$\propto -\log(a) - \log(b) + A_{spp}(log \int_{i=0}^{AT} p\,(i\,|a,b)) + B_{spp}(log \int_{i=AT}^{BT} p\,(i\,|a,b))$$

$$+ C_{spp}(log \int_{i=BT}^{0.01} p\,(i\,|a,b)) + D_{spp}(log \int_{i=0.01}^{0.1} p\,(i\,|a,b))))$$

$$+ E_{spp}(log \int_{i=0.1}^{0.25} p\,(i\,|a,b)))) + F_{spp}(log \int_{i=0.25}^{0.95} p\,(i\,|a,b))))$$

$$+ G_{spp}(log \int_{i=0.95}^{GT} p\,(i\,|a,b)))) + H_{spp}(log \int_{GT}^{1.0} p\,(i\,|a,b))$$

Table S4.4.1 Latin hypercube sampling parameters. 1000 samples were taken for each parameter over a uniform distribution.

parameter	**minimum**	**maximum**
beta a	0.00001	1.00001
beta b	0.01	2.01

Table S4.4.2 Posterior distributions of the parameters of the beta distribution (a and b), the three fitted thresholds for severity categories (AT, BT, GT), and of the proportional mortality within each severity category (A-H).

	Posterior mean	**Posterior median**	**Lower 95% Bayesian CI**	**Upper 95% Bayesian CI**
a	0.013	0.0127	0.00833	0.0191
b	0.988	0.938	0.474	1.793
AT	0.0000211	0.00000795	1.16E-07	0.000125
BT	0.00427	0.00424	0.00161	0.00719
GT	0.969	0.967	0.952	0.9922
A	6.28E-06	4.36E-10	5.80E-33	7.32E-05
B	0.000267	0.000228	5.25E-05	0.000684
C	0.00327	0.00239	0.000389	0.00929
D	0.0403	0.0331	0.0107	0.0943
E	0.164	0.159	0.0245	0.103
F	0.555	0.527	0.26	0.93
G	0.964	0.963	0.951	0.983
H	0.99	0.991	0.972	0.9998

Figure S4.4.1 PP-plots for the Latin hypercube sampling of our beta distribution model. Both parameters are slightly overestimated by the model, as evidenced by the positive deviation from the 1:1 line.

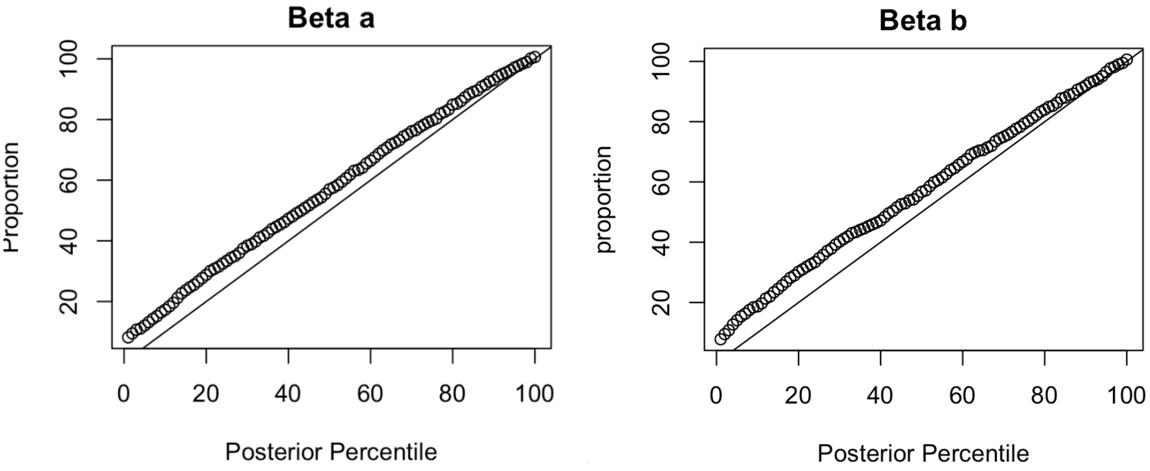

Figure S4.4.2 Posterior distributions for the proportional mortality of pests in each severity category A=<<0.01, B = <0.01, C= 1-10%, D= 10-25%, E=25-95%, F=95-99%, G=99->99%, H= >99%-100%. These were sampled from to produce projections of host mortality due to each pest species across mortality debt and invasion lag scenarios.

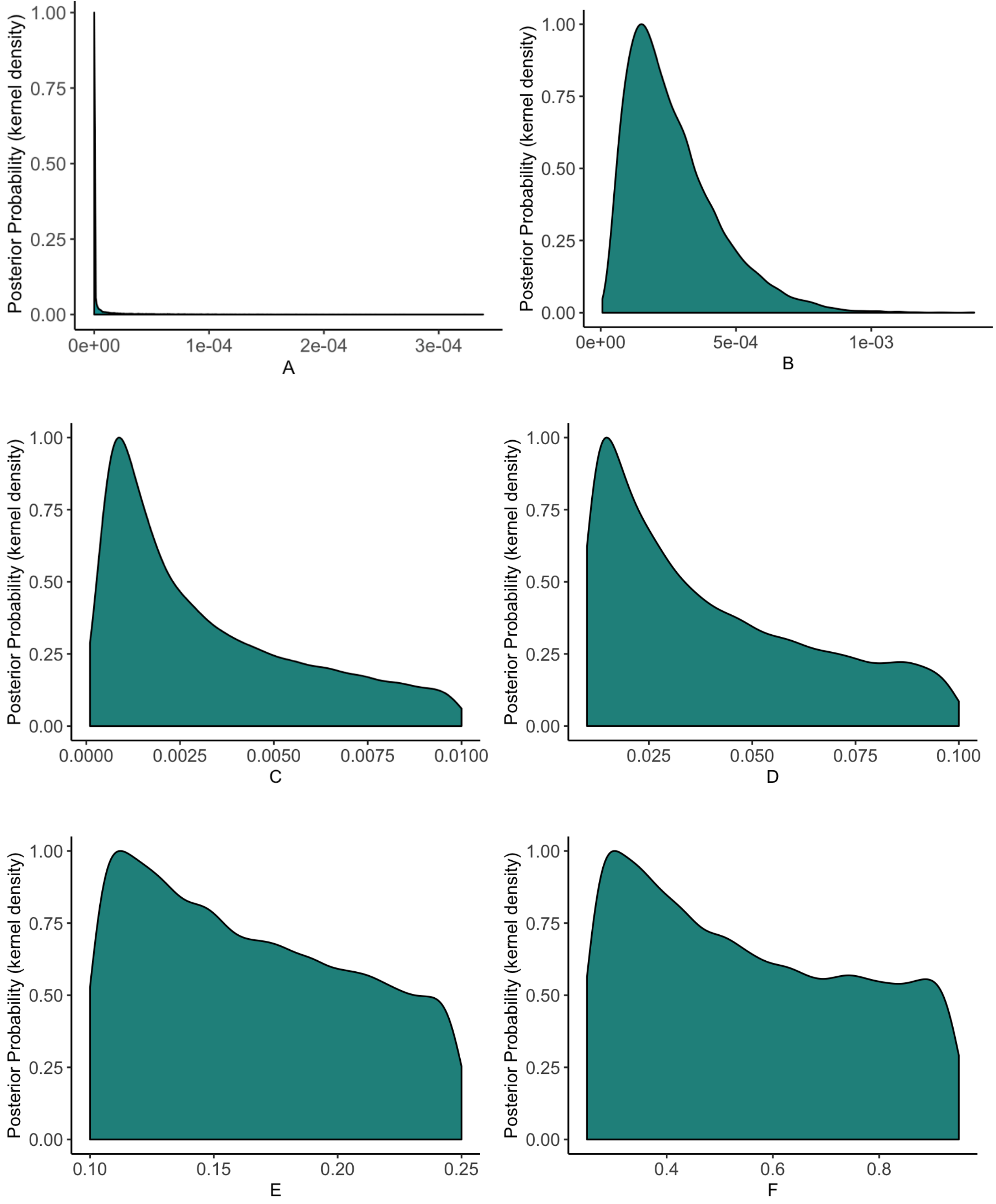

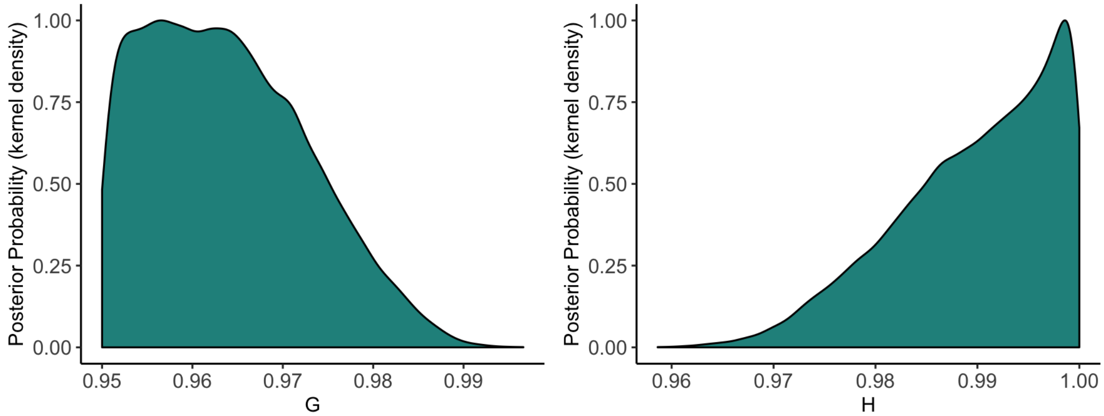

Cost curves

We tested four curve families in this analysis:

Gamma:

$$Cost \sim Gamma(shape, scale)$$

Weibull:

$$Cost \sim Weibull(shape, scale)$$

Lognormal:

$$Cost \sim LogNormal(\mu, \sigma)$$

Pareto:

$$Cost \sim Pareto(y_{min}, \alpha)$$

Each curve family fits two free parameters, which we call shape and scale above, but are alternatively called μ and σ in the lognormal model, y_{min} and α in the Pareto model.

We tested whether binned information could be combined with point estimates (as in the case of our point cost data combined with a bin of low impact invaders). In each of the 1000 Latin hypercube iterations, we took 100 samples from a gamma, Weibull, Pareto, and lognormal distribution with a range of values of these free parameters (Table S4.4.3). We kept the full cost information for half of these datapoints at random. We used the lowest and highest of these datapoints as the lowest and highest thresholds of cost in the model, and used the 80th and 95th percentile of the maximum observed cost to group the other datapoints. We then assigned the remaining species to low-, medium-, and high-cost bins based on where they fell relative to these thresholds. This is an even lower level of information than what we used in the cost curves fitted to the observed data (we have point estimates for all species apart from those below the lowest cost estimate), so we argue it is an even stronger demonstration of our approach. The likelihood of the model then became the sum of the likelihoods of the point cost estimates, plus the integrals under the various bins of the curve multiplied by the relative frequency of cost points under these curves for the species with only binned information, making our general log likelihood across the 4 curve families:

$$LL = \sum_{y} \log\left(p(y\,|shape, scale)\right) + L_{spp}\left(log \int_{i=LT}^{MT} p\,(i\,|shape, scale)\right)$$
$$+ M_{spp}\left(log \int_{j=MT}^{HT} p\,(j\,|shape, scale)\right) + H_{spp}\left(log \int_{k=HT}^{PPT} p\,(k\,|shape, scale)\right)$$

Where y are the point cost estimates and L_{spp}, M_{spp} and H_{spp} are the number of species in the low, medium, and high impact categories where we lacked point cost data.

We used the inverse prior for the scale and the uniform prior for the shape parameter in all models, though it is only the true Jeffreys prior for the lognormal and Pareto models. The Jeffreys and reference priors for the gamma and Weibull distirbutions are highly complex, and did not appear to lead to improvements over using the inverse prior, so we chose the latter in these cases, though the results are slightly biased to overestimation (Fig. S4.4.3). The overall posterior is thus:

$$p(shape, scape|y, Lspp, Mspp, Hspp)$$

$$\propto p(shape, scale)p(y, Lspp, Mspp, Hspp|shape, scale)$$

$$\propto -\log(scale) + \sum_{y} \log\left(p(y\ |shape, scale)\right)$$

$$+ L_{spp}(log \int_{i=LT}^{MT} p\ (i\ |shape, scale)) + M_{spp}(log \int_{j=MT}^{HT} p\ (j\ |shape, scale))$$

$$+ H_{spp}(log \int_{k=HT}^{PPT} p\ (k\ |shape, scale))$$

We found fairly good detectability of the appropriate curve family and of parameter estimates even in this data-poor situation (Fig. S4.4.3). Pareto distributions were the easiest to distinguish, and both Pareto and lognormal families produced unbiased parameter estimates based on P-P plots (Fig. S4.4.3, Table S4.4.3). Gamma distributions were the most difficult to distinguish, and parameters were slightly biased toward overestimation. Weibull shape parameters were also slightly overestimated. Weibull and gamma families were frequently confused with one another. While these results indicate that sole reliance on a single curve may lead to misestimation of mortality, this is partly assuaged by model averaging across the curve families.

Further, through *shinystan*, we found that all of our fitted models passed the recommended posterior checks.

Table S4.4.3 Latin hypercube protocol for cost curves. 1000 parameter sets were sampled from a uniform distribution in each case.

Parameter	Minimum	Maximum
gamma shape	1	11
gamma scale	0.001	1.001
weibull shape	0.5	5.5
weibull scale	0.1	5.1
log-normal mu	0.01	5.01
log-normal sigma	0.1	1.0001

pareto shape	0.1	1.1
pareto scale	1	11

Table S4.4.4 Theoretic simulation results for the proportion of simulations where the correct curve family (the simulated curve family from which the data were generated) had the strongest support (assessed via maximum likelihood).

	Predicted distribution			
True Distribution	Gamma	Weibull	Log-Normal	Pareto
Gamma	0.494	0.252	0.253	0
Weibull	0.212	0.763	0.025	0
Log-Normal	0.077	0.071	0.851	0.001
Pareto	0	0	0	1

Figure S4.4.3 P-P plots for the four cost curve families. A 1:1 relationship indicates unbiased posterior distributions, while a positive deviation from the line indicates parameter overestimation.

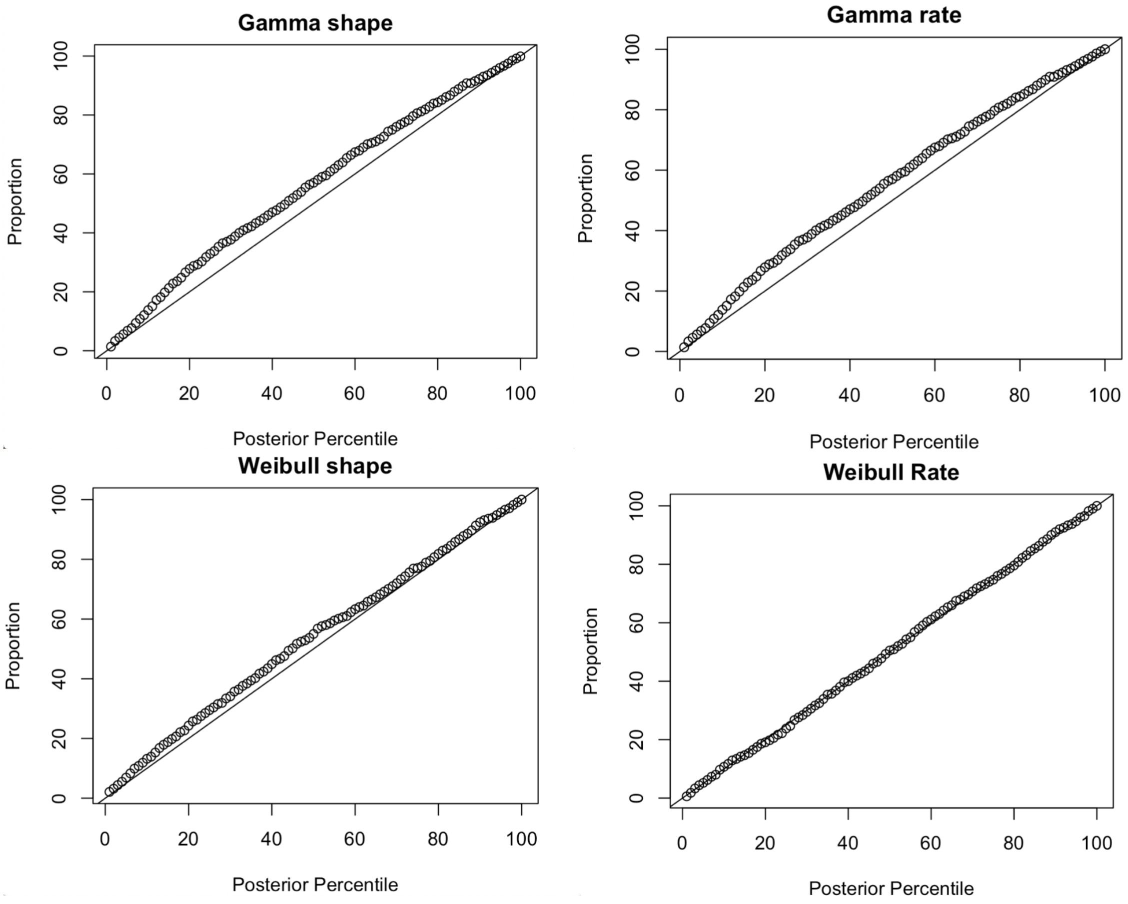

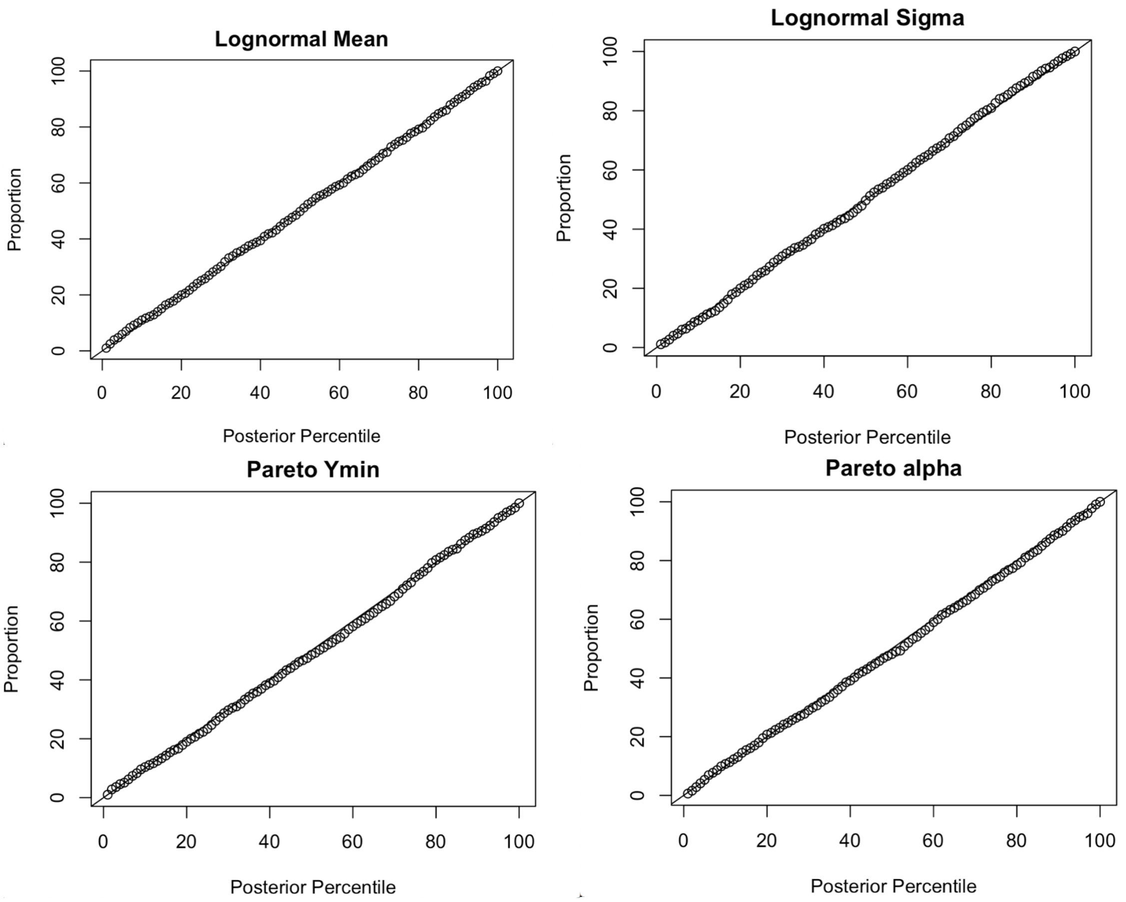

Cost curve extrapolation

While these curves have negligible impacts on the total current cost of each feeding guild, they can be used predictively to forecast the risk of any new pest. For example, the probability of there being a new invader as bad as the worst pest in each guild can be calculated as the area under the cost curve more extreme than the most damaging pest (Table S4.4.5). In order to fit cost curves, we removed any pests whose damages were predicted to be 0 in the given cost scenario, as this would lead to intractable Stan models. This resulted in the removal of one species from the borer guild (Peach Twig Borer; *Anarsia lineatella*), and one from the defoliator guild (Mimosa Webworm; *Homadaula anisocentra*). Probabilities of new high impact invaders are fairly low for all guilds, with sap feeders showing a slight increased risk relative to borers and defoliators (1.2% vs. 0.3% and 0.5%, respectively). The posterior distributions for all guilds in terms of the probability of a new high impact pest all appear very similar (Table S4.4.5), though the most likely curve family is variable across guilds. The Weibull family is the best fit for wood borers, while the gamma family is best for sap feeders and defoliators. Borers show some support for the Pareto model, sap feeders show some support for Weibull, and Defoliators show almost no support for other curve families. Pareto has some support for borers, while lognormal has the least support across guilds.

Since Weibull and gamma families were difficult to correctly identify, we tested the sensitivity of p(new) to model misspecification by assigning all of the model weight attributed to these two families to either one or the other (Table S4.4.6). We found that this misspecification had little impact on borer risk, but led to order of magnitude risk decreases for sap feeders and increases for defoliators, though we note that in the latter case, >99.9% of the support was in favour of the gamma model.

Table S4.4.5 Posterior probabilities of new high impact invaders (p(new)) and the relative support (model weight) for each of the cost curve families across the three feeding guilds.

Guild	Mean p(new)	Lower 95% CI p(new)	Upper 95% CI p(new)	Gamma weight	Weibull weight	Lognormal weight	Pareto weight
Borers	0.0028	0.00040	0.0087	0.003	0.27	0.44	0.28
Sap Feeders	0.012	0.00096	0.054	0.80	0.19	<0.0001	0.01
Defoliators	0.0049	0.000079	0.023	0.999	<0.001	<0.0001	<0.0001

Table S4.4.6 Sensitivity of posterior probabilities of new high impact invaders (p(new)) to Gamma/Weibull misspecification.

Guild	Mean p(new) Gamma	Lower 95% CI p(new) Gamma	Upper 95% CI p(new) Gamma	Mean p(new) Weibull	Lower 95% CI p(new) Weibull	Upper 95% CI p(new) Weibull
Borers	0.0045	0.00050	0.018	0.0024	0.00030	0.018

Sap Feeders	0.0033	0.000055	0.017	0.013	0.000044	0.065
Defoliators	0.0049	0.000074	0.023	0.028	0.00032	0.094

Figure S4.4.4 Posterior distributions of cost curves fit to the three feeding guilds, as well as posterior probabilities of a new high-impact pest (i.e., as damaging as the most damaging pest already present) within each guild: a-b. wood borers, c-d. sap feeders, e-f. defoliators.

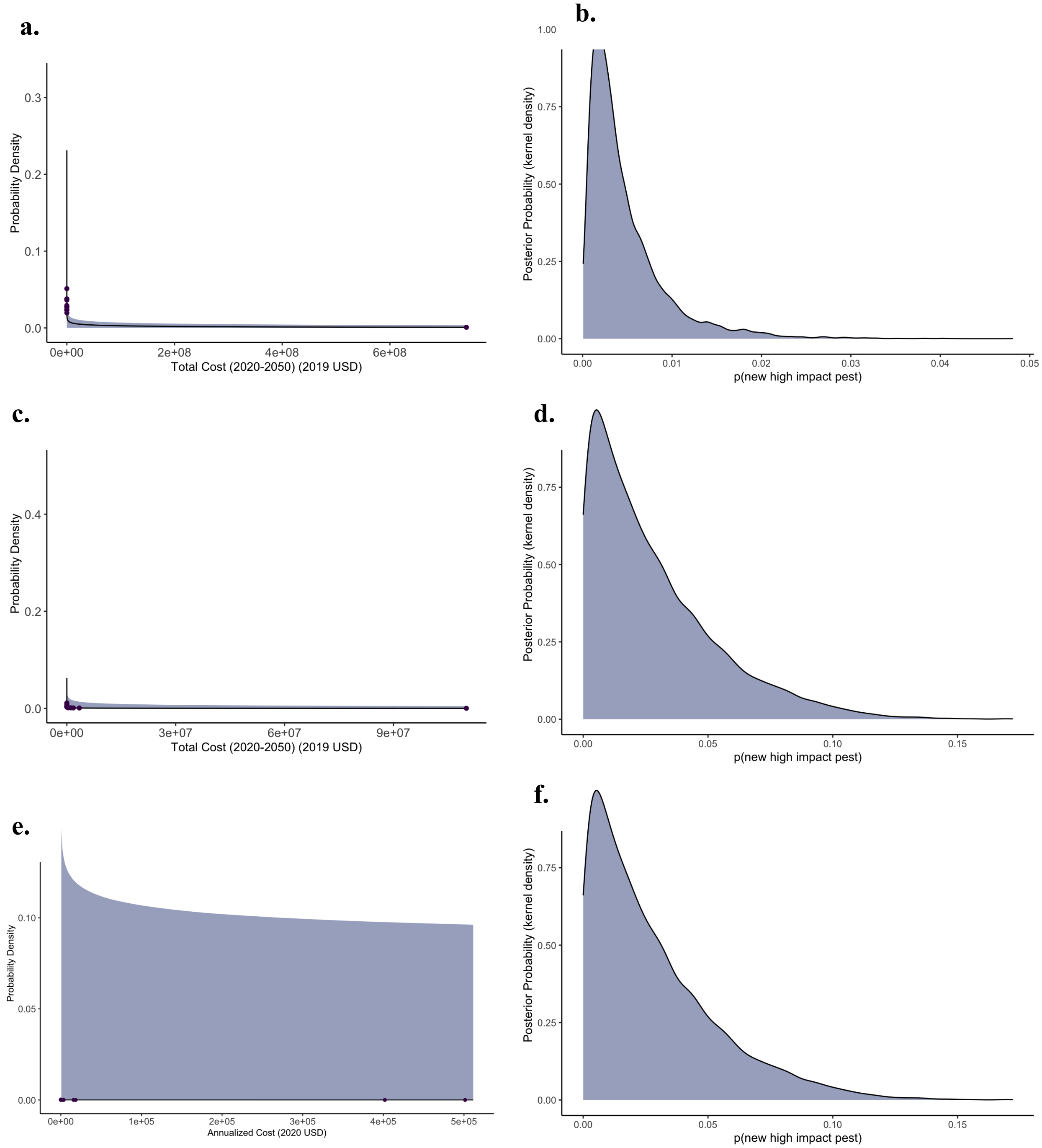

References

Bernardo, J. M. (1979). Reference posterior distributions for Bayesian inference. *Journal of the* Royal Statistical Society: Series B (Methodological), 41(2), 113-128.

Gabry, J. (2015). Shinystan: interactive visual and numerical diagnostics and posterior analysis for Bayesian models. *R package Version 2*.

Jeffreys, H. (1961) *Theory of Probability.* London: Oxford Unviversity Press.

Leung, B., & Steele, R. J. (2013). The value of a datum–how little data do we need for a quantitative risk analysis?. *Diversity and Distributions*, 19(5-6), 617-628.

Appendix S4.5 Predicted tree mortality and associated costs across invasion lag and mortality debt scenarios for street, residential, and non-street community trees

Table S4.5.1 Predicted tree mortality and annualized costs across land types and scenarios. These costs are only for tree removal and replacement for dead trees, and do not consider non-treatment costs such as property value losses as examined in Aukema et al. (2011) or any ecosystem services losses. Community trees are defined as all urban trees apart from street trees (e.g. parks, industrial areas etc.), while residential trees are the responsibility of homeowners and are on their properties. Mean mortality for community trees in the best guess scenario was 4.6% (318M trees), with an estimated annualized management cost of 1.16B USD (26B from 2020 to 2050), and mean mortality for residential trees was 4.2% (59M trees), corresponding to an annualized estimated management cost of 290M USD (6.5B from 2020 to 2050).

Land Type		Annualized Cost (millions 2019 USD)		Tree Mortality (millions)		Total tree abundance	Percent mortality	
	Mortality Debt	lower 95% CI	upper 95% CI	lower 95% CI	upper 95% CI		upper 95% CI	lower 95% CI
Community								
	Best Guess	608	2130	165	510	7000	2.4%	7.3%
	All 10	208	866	156	452	7000	2.2%	6.5%
	All 50	1300	3790	73.6	219	7000	1.1%	3.1%
	All 100	1260	3880	833	2610	7000	11.9%	37.3%
	Vary Borers	263	36200	87.2	2400	7000	1.3%	34.2%
	Vary Defoliators	236	1810	145	497	7000	2.1%	7.1%
	Vary Sap-Feeders	2310	1210	139	424	7000	2.0%	6.1%
Residential	Best Guess	151	535	30.7	95.3	1400	2.2%	6.8%
	All 10	50.8	216	28.9	84.2	1400	2.1%	6.0%
	All 50	317	927	13.6	40.8	1400	1.0%	2.9%
	All 100	3050	9460	154	484	1400	11.0%	34.7%
	Vary Borers	64.4	8820	16.2	445	1400	1.2%	31.8%
	Vary Defoliators	57.8	454	26.9	92.9	1400	1.9%	6.6%
	Vary Sap-Feeders	56.6	300	25.7	78.7	1400	1.8%	5.6%